Geoff Dougherty

Pattern Recognition and Classification

An Introduction

EXTRA MATERIALS extras.springer.com

Springer

Pattern Recognition and Classification

Geoff Dougherty

Pattern Recognition and Classification

An Introduction

Springer

Geoff Dougherty
Applied Physics and Medical Imaging
California State University, Channel Islands
Camarillo, CA, USA

Please note that additional material for this book can be downloaded from
http://extras.springer.com

ISBN 978-1-4614-5322-2 ISBN 978-1-4614-5323-9 (eBook)
DOI 10.1007/978-1-4614-5323-9
Springer New York Heidelberg Dordrecht London

Library of Congress Control Number: 2012949108

Preface

The use of pattern recognition and classification is fundamental to many of the automated electronic systems in use today. Its applications range from military defense to medical diagnosis, from biometrics to machine learning, from bioinformatics to home entertainment, and more. However, despite the existence of a number of notable books in the field, the subject remains very challenging, especially for the beginner.

We have found that the current textbooks are not completely satisfactory for our students, who are primarily computer science students but also include students from mathematics and physics backgrounds and those from industry. Their mathematical and computer backgrounds are considerably varied, but they all want to understand and absorb the core concepts with a minimal time investment to the point where they can use and adapt them to problems in their own fields. Texts with extensive mathematical or statistical prerequisites were daunting and unappealing to them. Our students complained of "not seeing the wood for the trees," which is rather ironic for textbooks in pattern recognition. It is crucial for newcomers to the field to be introduced to the key concepts at a basic level in an ordered, logical fashion, so that they appreciate the "big picture"; they can then handle progressively more detail, building on prior knowledge, without being overwhelmed. Too often our students have dipped into various textbooks to sample different approaches but have ended up confused by the different terminologies in use.

We have noticed that the majority of our students are very comfortable with and respond well to visual learning, building on their often limited entry knowledge, but focusing on key concepts illustrated by practical examples and exercises. We believe that a more visual presentation and the inclusion of worked examples promote a greater understanding and insight and appeal to a wider audience.

This book began as notes and lecture slides for a senior undergraduate course and a graduate course in Pattern Recognition at California State University Channel Islands (CSUCI). Over time it grew and approached its current form, which has been class tested over several years at CSUCI. It is suitable for a wide range of students at the advanced undergraduate or graduate level. It assumes only a modest background in statistics and mathematics, with the necessary additional material integrated into the text so that the book is essentially self-contained.

The book is suitable both for individual study and for classroom use for students in physics, computer science, computer engineering, electronic engineering, biomedical engineering, and applied mathematics taking senior undergraduate and graduate courses in pattern recognition and machine learning. It presents a comprehensive introduction to the core concepts that must be understood in order to make independent contributions to the field. It is designed to be accessible to newcomers from varied backgrounds, but it will also be useful to researchers and professionals in image and signal processing and analysis, and in computer vision. The goal is to present the fundamental concepts of supervised and unsupervised classification in an informal, rather than axiomatic, treatment so that the reader can quickly acquire the necessary background for applying the concepts to real problems. A final chapter indicates some useful and accessible projects which may be undertaken.

We use ImageJ (http://rsbweb.nih.gov/ij/) and the related distribution, Fiji (http://fiji.sc/wiki/index.php/Fiji) in the early stages of image exploration and analysis, because of its intuitive interface and ease of use. We then tend to move on to MATLAB for its extensive capabilities in manipulating matrices and its image processing and statistics toolboxes. We recommend using an attractive GUI called DipImage (from http://www.diplib.org/download) to avoid much of the command line typing when manipulating images. There are also classification toolboxes available for MATLAB, such as Classification Toolbox (http://www.wiley.com/WileyCDA/Section/id-105036.html) which requires a password obtainable from the associated computer manual) and PRTools (http://www.prtools.org/download.html). We use the Classification Toolbox in Chap. 8 and recommend it highly for its intuitive GUI. Some of our students have explored Weka, a collection of machine learning algorithms for solving data mining problems implemented in Java and open sourced (http://www.cs.waikato.ac.nz/ml/weka/index_downloading.html).

There are a number of additional resources, which can be downloaded from the companion Web site for this book at http://extras.springer.com/, including several useful Excel files and data files. Lecturers who adopt the book can also obtain access to the end-of-chapter exercises.

In spite of our best efforts at proofreading, it is still possible that some typos may have survived. Please notify me if you find any.

I have very much enjoyed writing this book; I hope you enjoy reading it!

Camarillo, CA Geoff Dougherty

Acknowledgments

I would like to thank my colleague Matthew Wiers for many useful conversations and for helping with several of the Excel files bundled with the book. And thanks to all my previous students for their feedback on the courses which eventually led to this book; especially to Brandon Ausmus, Elisabeth Perkins, Michelle Moeller, Charles Walden, Shawn Richardson, and Ray Alfano.

I am grateful to Chris Coughlin at Springer for his support and encouragement throughout the process of writing the book and to various anonymous reviewers who have critiqued the manuscript and trialed it with their classes. Special thanks go to my wife Hajijah and family (Daniel, Adeline, and Nadia) for their patience and support, and to my parents, Maud and Harry (who passed away in 2009), without whom this would never have happened.

Contents

Chapter 1
Introduction

1.1 Overview

Humans are good at recognizing objects (or *patterns*, to use the generic term). We are so good that we take this ability for granted, and find it difficult to analyze the steps in the process. It is generally easy to distinguish the sound of a human voice, from that of a violin; a handwritten numeral "3," from an "8"; and the aroma of a rose, from that of an onion. Every day, we recognize faces around us, but we do it unconsciously and because we cannot explain our expertise, we find it difficult to write a computer program to do the same. Each person's face is a pattern composed of a particular combination of structures (eyes, nose, mouth, ...) located in certain positions on the face. By analyzing sample images of faces, a program should be able to capture the pattern specific to a face and identify (or *recognize*) it as a face (as a member of a category or class we already know); this would be *pattern recognition*. There may be several categories (or classes) and we have to sort (or classify) a particular face into a certain category (or *class*); hence the term *classification*. Note that in *pattern recognition*, the term pattern is interpreted widely and does not necessarily imply a repetition; it is used to include all objects that we might want to classify, e.g., apples (or oranges), speech waveforms, and fingerprints.

A class is a collection of objects that are similar, but not necessarily identical, and which is distinguishable from other classes. Figure 1.1 illustrates the difference between classification where the classes are known beforehand and classification where classes are created after inspecting the objects.

Interest in pattern recognition and classification has grown due to emerging applications, which are not only challenging but also computationally demanding. These applications include:

- Data mining (sifting through a large volume of data to extract a small amount of relevant and useful information, e.g., fraud detection, financial forecasting, and credit scoring)

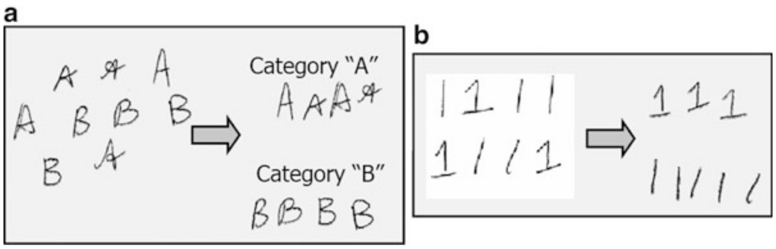

Fig. 1.1 Classification when the classes are (**a**) known and (**b**) unknown beforehand

- Biometrics (personal identification based on physical attributes of the face, iris, fingerprints, etc.)
- Machine vision (e.g., automated visual inspection in an assembly line)
- Character recognition [e.g., automatic mail sorting by zip code, automated check scanners at ATMs (automated teller machines)]
- Document recognition (e.g., recognize whether an e-mail is spam or not, based on the message header and content)
- Computer-aided diagnosis [e.g., helping doctors make diagnostic decisions based on interpreting medical data such as mammographic images, ultrasound images, electrocardiograms (ECGs), and electroencephalograms (EEGs)]
- Medical imaging [e.g., classifying cells as malignant or benign based on the results of magnetic resonance imaging (MRI) scans, or classify different emotional and cognitive states from the images of brain activity in functional MRI]
- Speech recognition (e.g., helping handicapped patients to control machines)
- Bioinformatics (e.g., DNA sequence analysis to detect genes related to particular diseases)
- Remote sensing (e.g., land use and crop yield)
- Astronomy (classifying galaxies based on their shapes; or automated searches such as the Search for Extra-Terrestrial Intelligence (SETI) which analyzes radio telescope data in an attempt to locate signals that might be artificial in origin)

The methods used have been developed in various fields, often independently. In statistics, going from particular observations to general descriptions is called inference, learning [i.e., using example (training) data] is called estimation, and classification is known as discriminant analysis (McLachlan 1992). In engineering, classification is called pattern recognition and the approach is nonparametric and much more empirical (Duda et al. 2001). Other approaches have their origins in machine learning (Alpaydin 2010), artificial intelligence (Russell and Norvig 2002), artificial neural networks (Bishop 2006), and data mining (Han and Kamber 2006). We will incorporate techniques from these different emphases to give a more unified treatment (Fig. 1.2).

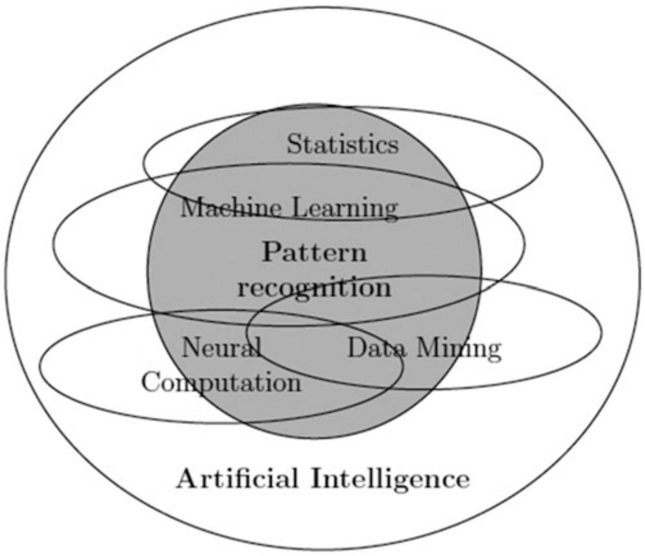

Fig. 1.2 Pattern recognition and related fields

1.2 Classification

Classification is often the final step in a general process (Fig. 1.3). It involves sorting objects into separate classes. In the case of an image, the acquired image is segmented to isolate different objects from each other and from the background, and the different objects are *labeled*. A typical pattern recognition system contains a sensor, a preprocessing mechanism (prior to segmentation), a feature extraction mechanism, a set of examples (*training data*) already classified (post-processing), and a classification algorithm. The *feature extraction* step reduces the data by measuring certain characteristic properties or *features* (such as size, shape, and texture) of the labeled objects. These features (or, more precisely, the values of these features) are then passed to a *classifier* that evaluates the evidence presented and makes a decision regarding the class each object should be assigned, depending on whether the values of its features fall inside or outside the tolerance of that class. This process is used, for example, in classifying lesions as benign or malignant.

The quality of the acquired image depends on the resolution, sensitivity, bandwidth and signal-to-noise ratio of the imaging system. Pre-processing steps such as image enhancement (e.g., brightness adjustment, contrast enhancement, image averaging, frequency domain filtering, edge enhancement) and image restoration (e.g., photometric correction, inverse filtering, Wiener filtering) may be required prior to segmentation, which is often a challenging process. Typically enhancement will precede restoration. Often these are performed sequentially, but more sophisticated tasks will require feedback i.e., advanced processing steps will pass parameters back to preceding steps so that the processing includes a number of iterative loops.

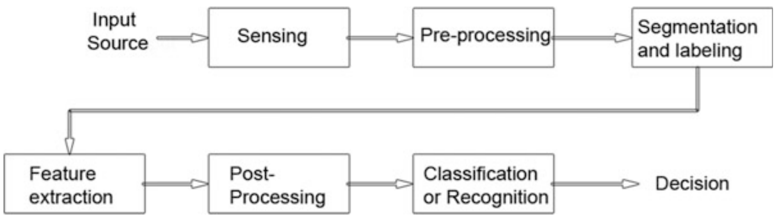

Fig. 1.3 A general classification system

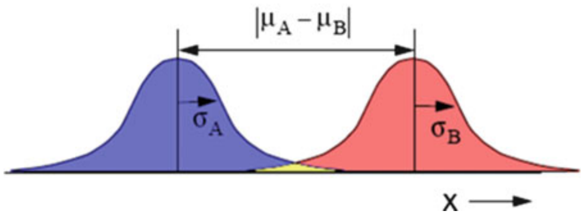

Fig. 1.4 A good feature, *x*, measured for two different classes (*blue* and *red*) should have small intra-class variations and large inter-class variations

The quality of the features is related to their ability to discriminate examples from different classes. Examples from the same class should have similar feature values, while examples from different classes should have different feature values, i.e., good features should have small intra-class variations and large inter-class variations (Fig. 1.4). The measured features can be transformed or mapped into an alternative feature space, to produce better features, before being sent to the classifier.

We have assumed that the features are continuous (i.e., quantitative), but they could be categorical or non-metric (i.e., qualitative) instead, which is often the case in data mining. Categorical features can either be nominal (i.e., unordered, e.g., zip codes, employee ID, gender) or ordinal [i.e., ordered, e.g., street numbers, grades, degree of satisfaction (very bad, bad, OK, good, very good)]. There is some ability to move data from one type to another, e.g., continuous data could be discretized into ordinal data, and ordinal data could be assigned integer numbers (although they would lack many of the properties of real numbers, and should be treated more like symbols). The preferred features are always the most informative (and, therefore in this context, the most discriminating). Given a choice, scientific applications will generally prefer continuous data since more operations can be performed on them (e.g., mean and standard deviation). With categorical data, there may be doubts as to whether all relevant categories have been accounted for, or they may evolve with time.

Humans are adept at recognizing objects within an image, using size, shape, color, and other visual clues. They can do this despite the fact that the objects may appear from different viewpoints and under different lighting conditions, have

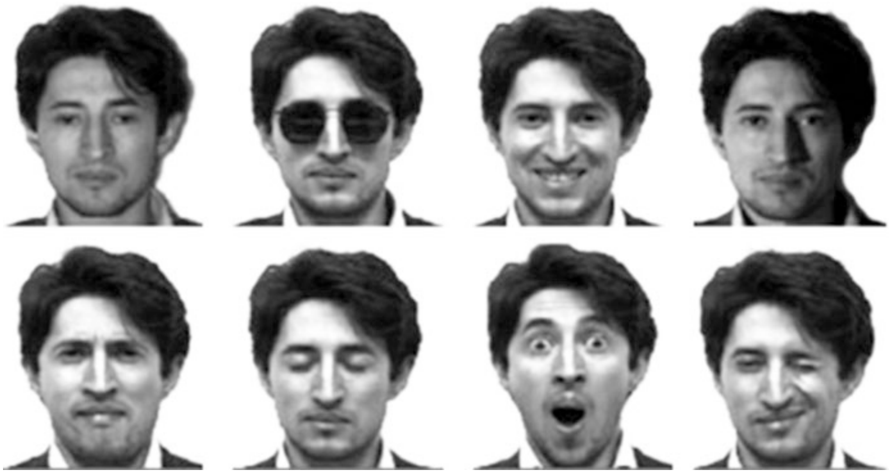

Fig. 1.5 Face recognition needs to be able to handle different expressions, lighting, and occlusions

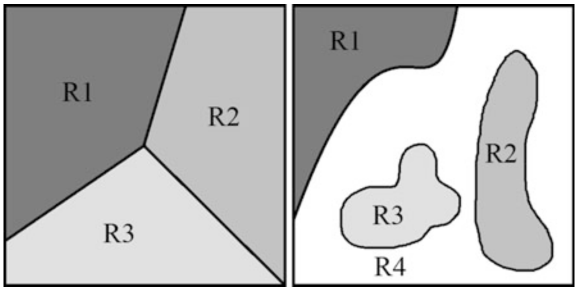

Fig. 1.6 Classes mapped as decision regions, with decision boundaries

different sizes, or be rotated. We can even recognize them when they are partially obstructed from view (Fig. 1.5). These tasks are challenging for machine vision systems in general.

The goal of the classifier is to classify new data (test data) to one of the classes, characterized by a decision region. The borders between decision regions are called decision boundaries (Fig. 1.6).

Classification techniques can be divided into two broad areas: *statistical* or *structural* (or *syntactic*) techniques, with a third area that borrows from both, sometimes called *cognitive methods*, which include *neural networks* and *genetic algorithms*. The first area deals with objects or patterns that have an underlying and quantifiable statistical basis for their generation and are described by quantitative features such as length, area, and texture. The second area deals with objects best described by qualitative features describing structural or syntactic relationships inherent in the object. Statistical classification methods are more popular than structural methods; cognitive methods have gained popularity over the last decade or so. The models are not necessarily independent and hybrid systems involving multiple classifiers are increasingly common (Fu 1983).

1.3 Organization of the Book

In Chap. 2, we will look at the classification process in detail and the different approaches to it, and will look at a few examples of classification tasks. In Chap. 3, we will look at non-metric methods such as decision trees; and in Chap. 4, we will consider probability theory, leading to Bayes' Rule and the roots of statistical pattern recognition. Chapter 5 considers supervised learning—and examples of both parametric and non-parametric learning. We will look at different ways to evaluate the performance of classifiers in Chap. 5. Chapter 6 considers the curse of dimensionality and how to keep the number of features to a useful minimum. Chapter 7 considers unsupervised learning techniques, and Chap. 8 looks at ways to evaluate the performance of the various classifiers. Chapter 9 will consider stochastic methods, and Chap. 10 will discuss some interesting classification problems.

By judiciously avoiding some of the details, the material can be covered in a single semester. Alternatively, fully featured (!!) and with a healthy dose of exercises/applications and some project work, it would form the basis for two semesters of work. The independent reader, on the other hand, can follow the material at his or her own pace and should find sufficient amusement for a few months! Enjoy, and happy studying!

1.4 Exercises

1. List a number of applications of classification, additional to those mentioned in the text.
2. Consider the data of four adults, indicating their weight (actually, their mass) and their health status. Devise a simple classifier that can properly classify all four patterns.

Weight (kg)	Class label
50	Unhealthy
60	Healthy
70	Healthy
80	Unhealthy

How is a fifth adult of weight 76 kg classified using this classifier?

3. Consider the following items bought in a supermarket and some of their characteristics:

Item no.	Cost ($)	Volume (cm^3)	Color	Class label
1	20	6	Blue	Inexpensive
2	50	8	Blue	Inexpensive
3	90	10	Blue	Inexpensive
4	100	20	Red	Expensive
5	160	25	Red	Expensive
6	180	30	Red	Expensive

   Which of the three features (cost, volume and color) is the best classifier?
4. Consider the problem of classifying objects into circles and ellipses. How would you classify such objects?

References

Alpaydin, E.: Introduction to Machine learning, 2nd edn. MIT Press, Cambridge (2010)

Bishop, C.M.: Neural Networks for Pattern Recognition. Oxford University Press, Oxford (2006)

Duda, R.O., Hart, P.E., Stork, D.G.: Pattern Classification, 2nd edn. Wiley, New York (2001)

Fu, K.S.: A step towards unification of syntactic and statistical pattern recognition. IEEE Trans. Pattern Anal. Mach. Intell. **5**, 200–205 (1983)

Han, J., Kamber, M.: Data Mining: Concepts and Techniques, 2nd edn. Morgan Kaufmann, San Francisco (2006)

McLachlan, G.J.: Discriminant Analysis and Statistical Pattern Recognition. Wiley, New York (1992)

Russell, S., Norvig, P.: Artificial Intelligence: A Modern Approach, 2nd edn. Prentice Hall, New York (2002)

Chapter 2
Classification

2.1 The Classification Process

A general classification system, without feedback between stages, is shown in Fig. 2.1.

The *sensing/acquisition* stage uses a transducer such as a camera or a microphone. The acquired signal (e.g., an image) must be of sufficient quality that distinguishing "features" can be adequately measured. This will depend on the characteristics of the transducer, but for a camera this would include the following: its resolution, dynamic range, sensitivity, distortion, signal-to-noise ratio, whether focused or not, etc.

Pre-processing is often used to condition the image for segmentation. For example, smoothing of the image (e.g., by convolution with a Gaussian mask) mitigates the confounding effect of noise on segmentation by thresholding (since the random fluctuations comprising noise can result in pixels being shifted across a threshold and being misclassified). Pre-processing with a median mask effectively removes shot (i.e., salt-and-pepper) noise. Removal of a variable background brightness and histogram equalization are often used to ensure even illumination.

Depending on the circumstances, we may have to handle missing data (Batista and Monard 2003), and detect and handle outlier data (Hodge and Austin 2004).

Segmentation partitions an image into regions that are meaningful for a particular task—the *foreground*, comprising the objects of interest, and the *background*, everything else. There are two major approaches—region-based methods, in which similarities are detected, and boundary-based methods, in which discontinuities (edges) are detected and linked to form continuous boundaries around regions.

Region-based methods find connected regions based on some similarity of the pixels within them. The most basic feature in defining the regions is image gray level or brightness, but other features such as color or texture can also be used. However, if we require that the pixels in a region be very similar, we may over-segment the image, and if we allow too much dissimilarity we may merge what should be separate objects. The goal is to find regions that correspond to objects as humans see them, which is not an easy goal.

DOI 10.1007/978-1-4614-5323-9_2, © Springer Science+Business Media New York 2013

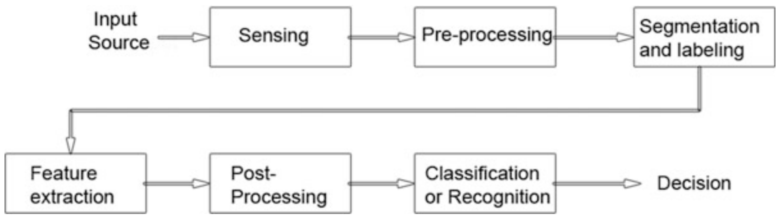

Fig. 2.1 A general classification process

Region-based methods include thresholding [either using a global or a locally adaptive threshold; optimal thresholding (e.g., Otsu, isodata, or maximum entropy thresholding)]. If this results in overlapping objects, thresholding of the distance transform of the image or using the watershed algorithm can help to separate them. Other region-based methods include region growing (a bottom-up approach using "seed" pixels) and split-and-merge (a top-down quadtree-based approach).

Boundary-based methods tend to use either an edge detector (e.g., the Canny detector) and edge linking to link any breaks in the edges, or boundary tracking to form continuous boundaries. Alternatively, an active contour (or snake) can be used; this is a controlled continuity contour which elastically snaps around and encloses a target object by locking on to its edges.

Segmentation provides a simplified, binary image that separates objects of interest (foreground) from the background, while retaining their shape and size for later measurement. The foreground pixels are set to "1" (white), and the background pixels set to "0" (black). It is often desirable to label the objects in the image with discrete numbers. Connected components labeling scans the segmented, binary image and groups its pixels into components based on pixel connectivity, i.e., all pixels in a connected component share similar pixel values and are in some way connected with each other. Once all groups have been determined, each pixel is labeled with a number (1, 2, 3, . . .), according to the component to which it was assigned, and these numbers can be looked up as gray levels or colors for display (Fig. 2.2).

One obvious result of labeling is that the objects in an image can be readily counted. More generally, the labeled binary objects can be used to *mask* the original image to isolate each (grayscale) object but retain its original pixel values so that its properties or features can be measured separately. Masking can be performed in several different ways. The binary mask can be used in an overlay, or alpha channel, in the display hardware to prevent pixels from being displayed. It is also possible to use the mask to modify the stored image. This can be achieved either by multiplying the grayscale image by the binary mask or by bit-wise ANDing the original image with the binary mask. Isolating features, which can then be measured independently, are the basis of *region-of-interest (RoI) processing*.

Post-processing of the segmented image can be used to prepare it for feature extraction. For example, partial objects can be removed from around the periphery of the image (e.g., Fig. 2.2e), disconnected objects can be merged, objects smaller or larger than certain limits can be removed, or holes in the objects or background can be filled by morphological opening or closing.

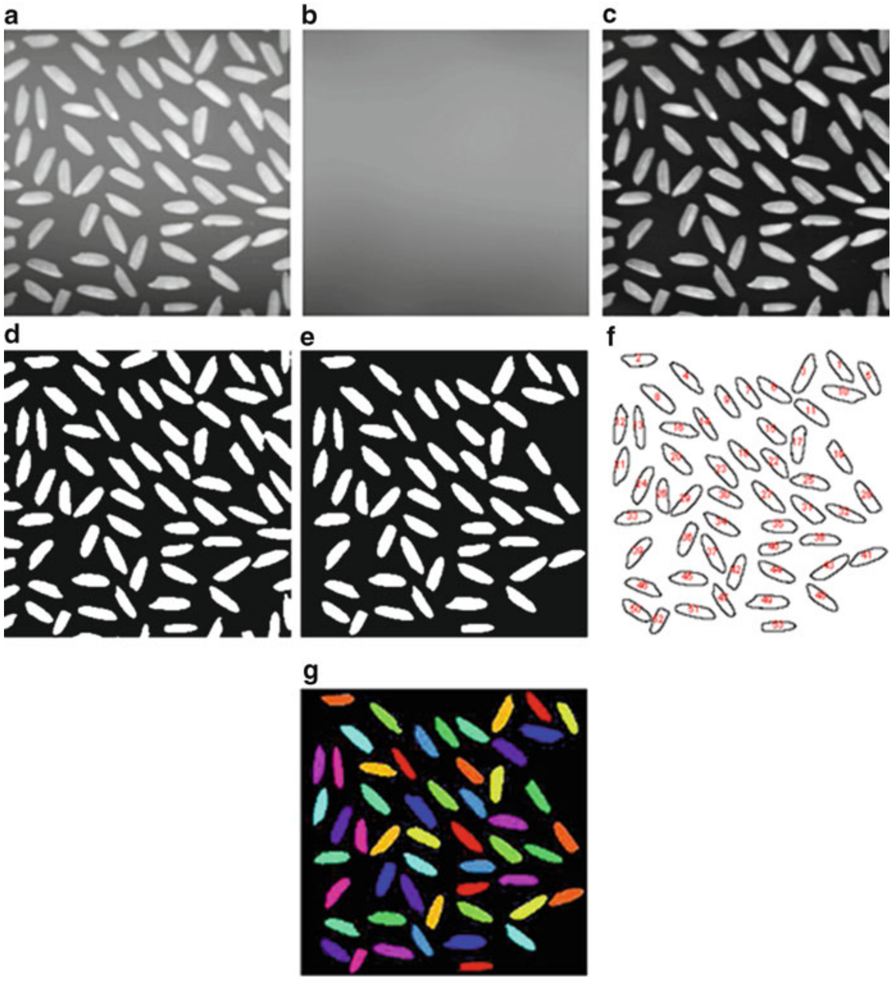

Fig. 2.2 (**a**) Original image, (**b**) variable background [from blurring (**a**)], (**c**) improved image [=(**a**) − (**b**)], (**d**) segmented image [Otsu thresholding of (**c**)], (**e**) partial objects removed from (**d**), (**f**) labeled components image, (**g**) *color-coded* labeled components image

2.2 Features

The next stage is *feature extraction*. Features are characteristic properties of the objects whose value should be similar for objects in a particular class, and different from the values for objects in another class (or from the background). Features may be continuous (i.e., with numerical values) or categorical (i.e., with labeled values). Examples of continuous variables would be length, area, and texture. Categorical features are either ordinal [where the order of the labeling is meaningful (e.g., class standing, military rank, level of satisfaction)] or nominal [where the ordering is not

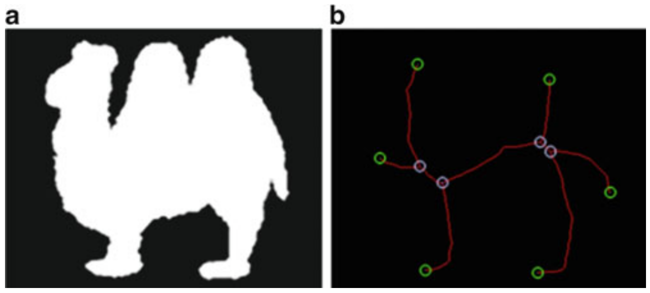

Fig. 2.3 (**a**) Image and (**b**) its skeleton (*red*), with its branch points (*white*) and end points (*green*) *circled*

meaningful (e.g., name, zip code, department)]. The choice of appropriate features depends on the particular image and the application at hand. However, they should be:

- *Robust* (i.e., they should normally be invariant to translation, orientation (rotation), scale, and illumination and well-designed features will be at least partially invariant to the presence of noise and artifacts; this may require some pre-processing of the image)
- *Discriminating* (i.e., the range of values for objects in different classes should be different and preferably be well separated and non-overlapping)
- *Reliable* (i.e., all objects of the same class should have similar values)
- *Independent* (i.e., uncorrelated; as a counter-example, length and area are correlated and it would be wasteful to consider both as separate features)

Features are higher level representations of structure and shape. Structural features include:

- Measurements obtainable from the gray-level histogram of an object (using region-of-interest processing), such as its mean pixel value (grayness or color) and its standard deviation, its contrast, and its entropy
- The texture of an object, using either statistical moments of the gray-level histogram of the object or its fractal dimension

Shape features include:

- The size or area, A, of an object, obtained directly from the number of pixels comprising each object, and its perimeter, P (obtained from its chain code)
- Its circularity (a ratio of perimeter^2 to area, or area to perimeter^2 (or a scaled version, such as $4\pi A/P^2$))
- Its aspect ratio (i.e., the ratio of the feret diameters, given by placing a bounding box around the object)
- Its skeleton or medial axis transform, or points within it such as branch points and end points, which can be obtained by counting the number of neighboring pixels on the skeleton (viz., 3 and 1, respectively) (e.g., Fig. 2.3)

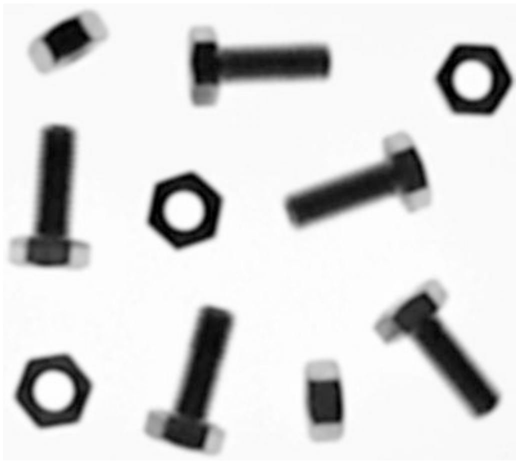
Fig. 2.4 Image containing nuts and bolts

- The Euler number: the number of connected components (i.e., objects) minus the number of holes in the image
- Statistical moments of the boundary (1D) or area (2D): the (m, n)th moment of a 2D discrete function, $f(x, y)$, such as a digital image with $M \times N$ pixels is defined as

$$m_{mn} = \sum_{x=1}^{M} \sum_{y=1}^{N} x^m y^n f(x, y) \tag{2.1}$$

where m_{00} is the sum of the pixels of an image: for a binary image, it is equal to its area. The *centroid*, or *center of gravity*, of the image, (μ_x, μ_y), is given by $(m_{10}/m_{00}, m_{01}/m_{00})$. The central moments (viz., taken about the mean) are given by

$$\mu_{mn} = \sum_{x=1}^{M} \sum_{y=1}^{N} (x - \mu_x)^m (y - \mu_y)^n f(x, y) \tag{2.2}$$

where μ_{20} and μ_{02} are the variances of x and y, respectively, and μ_{02} is the covariance between x and y. The *covariance matrix*, C or cov(x, y), is

$$C = \begin{bmatrix} \mu_{20} & \mu_{11} \\ \mu_{11} & \mu_{02} \end{bmatrix} \tag{2.3}$$

from which shape features can be computed.

The reader should consider what features would separate out the nuts (some face-on and some edge-on) and the bolts in Fig. 2.4.

A *feature vector*, **x**, is a vector containing the measured features, $x_1, x_2, \ldots, x_n$

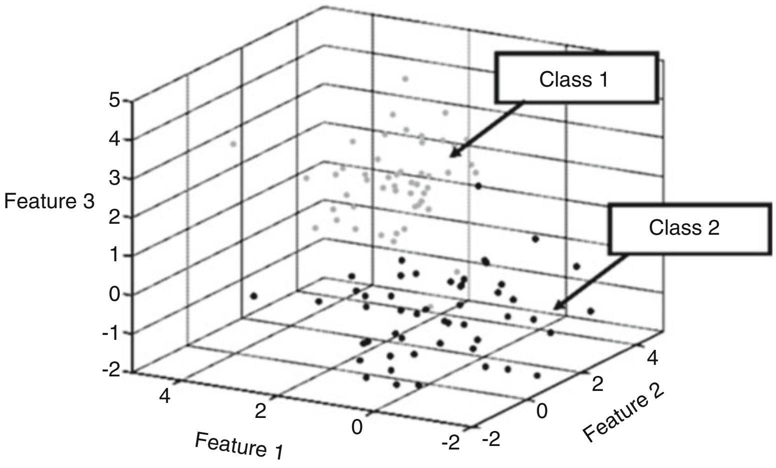

Fig. 2.5 Three-dimensional feature space containing two classes of features, class 1 (in *gray*) and class 2 (in *black*)

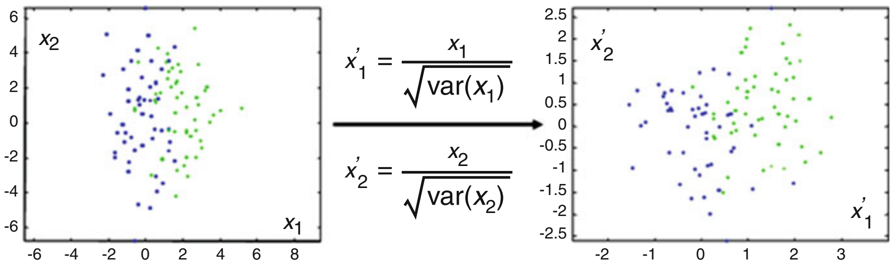

Fig. 2.6 Scaling of features

$$x = \begin{matrix} x_1 \\ x_2 \\ \cdot \\ \cdot \\ x_n \end{matrix} \tag{2.4}$$

for a particular object. The feature vectors can be plotted as points in *feature space* (Fig. 2.5). For n features, the feature space is n-dimensional with each feature constituting a dimension. Objects from the same class should cluster together in feature space (reliability), and be well separated from different classes (discriminating). In classification, our goal is to assign each feature vector to one of the set of classes $\{\omega_i\}$.

If the different features have different scales, it would be prudent to normalize each by its standard deviation (Fig. 2.6).

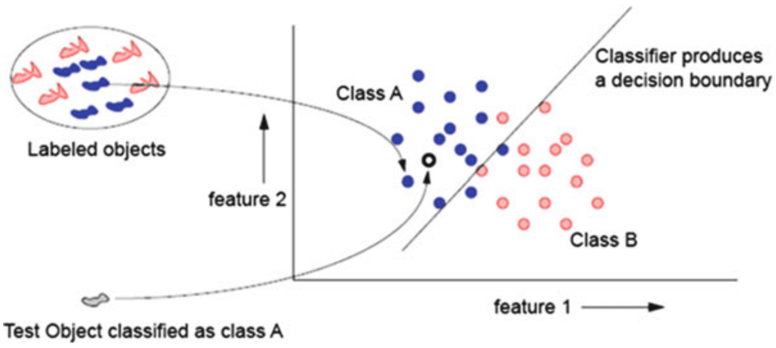

Fig. 2.7 Linear classification, using labeled training sets and two features, results in a linear decision boundary

The *classification* stage assigns objects to certain categories (or classes) based on the feature information. How many features should we measure? And which are the best? The problem is that the more we measure the higher is the dimension of feature space, and the more complicated the classification will become (not to mention the added requirements for computation time and storage). This is referred to as the "curse of dimensionality." In our search for a simple, yet efficient, classifier we are frequently drawn to using the minimum number of "good" features that will be sufficient to do the classification adequately (for which we need a measure of the performance of the classifier) for a particular problem. This follows the heuristic principle known traditionally as Occam's razor (viz., the simplest solution is the best) or referred to as KISS (Keep It Simple, Stupid) in more contemporary language; while it may not be true in all situations, we will adopt a natural bias towards simplicity.

The prudent approach is to err on the side of measuring more features per object than that might be necessary, and then reduce the number of features by either (1) *feature selection*—choosing the most informative subset of features, and removing as many irrelevant and redundant features as possible (Yu and Liu 2004) or (2) *feature extraction*—combining the existing feature set into a smaller set of new, more informative features (Markovitch and Rosenstein 2002). The most well-known feature extraction method is *Principal Component Analysis* (*PCA*), which we will consider fully in Chap. 6.

One paradigm for classification is the *learning from examples* approach. If a sample of labeled objects (called the *training set*) is randomly selected, and their feature vectors plotted in feature space, then it may be possible to build a classifier which separates the two (or more) classes adequately using a decision boundary or decision surface. A linear classifier results in a decision surface which is a hyperplane (Fig. 2.7). Again, the decision boundary should be as simple as possible, consistent with doing an adequate job of classifying. The use of a labeled training set, in which it is known to which class the sample objects belong, constitutes *supervised learning*.

2.3 Training and Learning

A typical classification problem comprises the following task: given example (or instance) objects typical of a number of classes (the *training set*), and classify other objects (the *test set*) into one of these classes. Features need to be identified such that the in-class variations are less than the between-class variations.

If the classes to which the objects belong are known, the process is called *supervised* learning, and if they are unknown, in which case the most appropriate classes must be found, it is called *unsupervised* learning. With unsupervised learning, the hope is to discover the unknown, but useful, classes of items (Jain et al. 2000).

The process of using data to determine the best set of features for a classifier is known as *training* the classifier. The most effective methods for training classifiers involve learning from examples. A performance metric for a set of features, based on the classification errors it produces, should be calculated in order to evaluate the usefulness of the features.

Learning (aka machine learning or artificial intelligence) refers to some form of adaptation of the classification algorithm to achieve a better response, i.e., to reduce the classification error on a set of training data. This would involve feedback to earlier steps in the process in an iterative manner until some desired level of accuracy is achieved. Ideally this would result in a monotonically increasing performance (Fig. 2.8), although this is often difficult to achieve.

In reinforcement learning (Barto and Sutton 1997), the output of the system is a sequence of actions to best reach the goal. The machine learning program must discover the best sequence of actions to take to yield the best reward. A robot

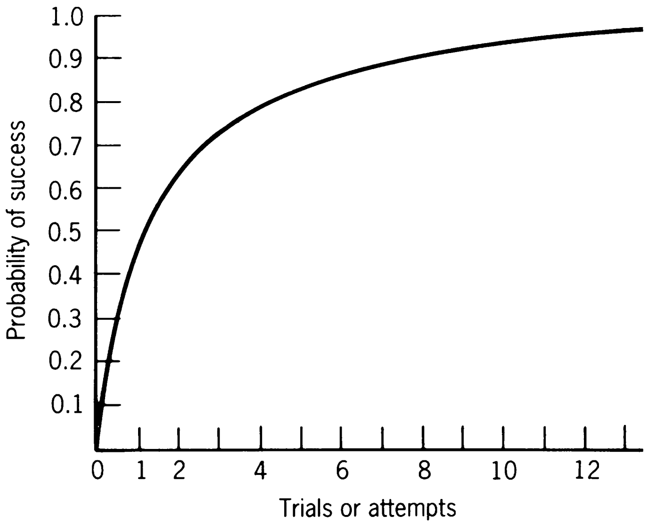

Fig. 2.8 Idealized learning curve

navigating in an environment in search of a particular location is an example of reinforcement learning. After a number of trials, it should learn the correct sequence of moves to reach the location as quickly as possible without hitting any of the obstacles. A task may require multiple agents to interact to accomplish a common goal, such as with a team of robots playing soccer.

2.4 Supervised Learning and Algorithm Selection

Supervised learning is an inductive reasoning process, whereby a set of rules are learned from instances (examples in a training set) and a classifier algorithm is chosen or created that can apply these rules successfully to new instances. The process of applying supervised learning to a real-world problem is outlined in Fig. 2.9.

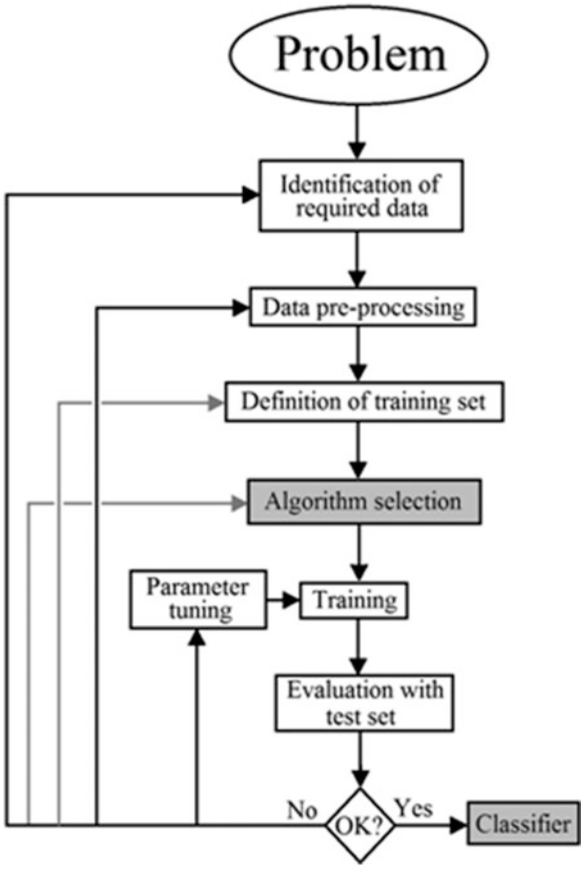

Fig. 2.9 The process of supervised learning

The choice of which specific learning algorithm to use is a critical step. We should choose an algorithm, apply it to a training set, and then evaluate it before adopting it for general use. The evaluation is most often based on prediction accuracy, i.e., the percentage of correct prediction divided by the total number of predictions. There are at least three techniques which are used to calculate the accuracy of a classifier

1. Split the training set by using two-thirds for training and the other third for estimating performance.
2. Divide the training set into mutually exclusive and equal-sized subsets and for each subset, train the classifier on the union of all the other subsets. The average of the error rate of each subset is then an estimate of the error rate of the classifier. This is known as *cross-validation*.
3. *Leave-one-out validation* is a special case of cross-validation, with all test subsets consisting of a single instance. This type of validation is, of course, more expensive computationally, but useful when the most accurate estimate of a classifier's error rate is required.

We will consider ways to estimate the performance and accuracy of classifiers in Chap. 8.

2.5 Approaches to Classification

There are a variety of approaches to classification:

1. Statistical approaches (Chaps. 4 and 5) are characterized by their reliance on an explicit underlying probability model. The features are extracted from the input data (object) and are used to assign each object (described by a feature vector) to one of the labeled classes. The decision boundaries are determined by the probability distributions of the objects belonging to each class, which must either be specified or learned. A priori probabilities (i.e., probabilities before measurement—described by probability density functions) are converted into *a posteriori* (or class-/measurement-conditioned probabilities) probabilities (i.e., probabilities after measurement). Bayesian networks (e.g., Jensen 1996) are the most well-known representative of statistical learning algorithms.

   In a discriminant analysis-based approach, a parametric form of the decision boundary (e.g., linear or quadratic) is specified, and then the best decision boundary of this form is found based on the classification of training objects. Such boundaries can be constructed using, for example, a mean squared error criterion.

   In maximum entropy techniques, the overriding principle is that when nothing is known, the distribution should be as uniform as possible, i.e., have maximal entropy. Labeled training data are used to derive a set of constraints for

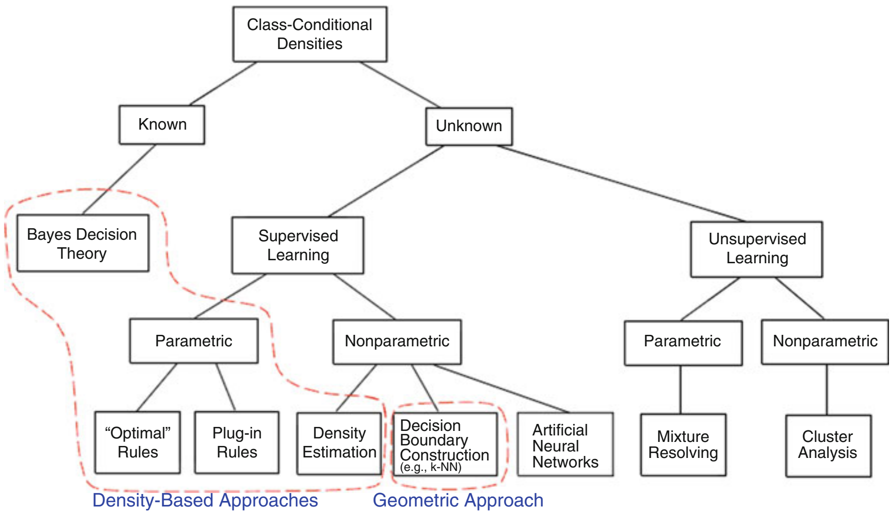

Fig. 2.10 Various approaches in statistical pattern recognition

the model that characterizes the class-specific expectations for the distribution (Csiszar 1996).

Instance-based learning algorithms are lazy-learning algorithms (Mitchell 1997), so-called because they delay the induction or generalization process until classification is performed. Lazy-learning algorithms (Aha 1998; De Mantaras and Armengol 1998) require less computation time during the training phase than eager-learning algorithms (such as Bayesian networks, decision trees, or neural networks) but more computation time during the classification process. One of the most straightforward instance-based learning algorithms is the *nearest neighbor* algorithm.

The relationship between a number of statistical pattern recognition methods is shown in Fig. 2.10. Moving from top to bottom and left to right, less information is available and as a result, the difficulty of classification increases.

2. Nonmetric approaches (Chap. 3): decision trees, syntactic (or grammatical) methods, and rule-based classifiers.

   It is natural and intuitive to classify a pattern by asking a series of questions, in which the next question depends on the answer to the previous question. This approach is particularly useful for nonmetric (or categorical) data, because the questions can be posed to elicit "yes/no" or "true/false" answers, although it can also be used with quantitative data. The sequence of questions can be displayed as a *decision tree* in the form of a tree structure (Fig. 2.11), which has *decision nodes* that ask a question and have *branches* for each possible answer (outcome). These are connected until we reach the terminal or *leaf node* which indicates the classification.

   In the case of complex patterns, a pattern can be viewed as a hierarchical composite of simple sub-patterns which themselves are built from yet simpler

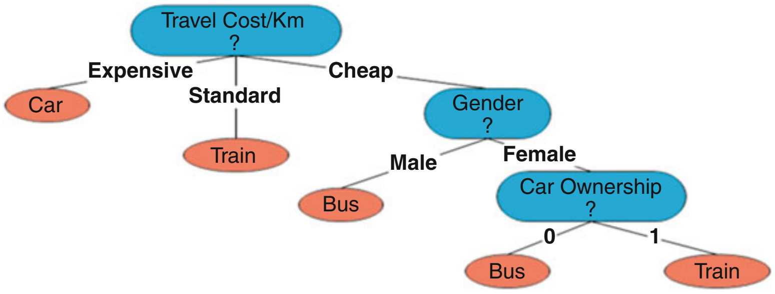

Fig. 2.11 A decision tree (the decision nodes are *colored blue*, and the leaf nodes *orange*)

sub-patterns (Fu 1982). The simplest sub-patterns are called *primitives*, and the complex pattern is represented in terms of relationships between these primitives in a way similar to the syntax of a language. The primitives are viewed as a language, and the patterns are sentences generated according to a certain grammar (i.e., set of rules) that is inferred from the available training samples. This approach is appealing in situations where patterns have a definite structure which can be coded by a set of rules (e.g., ECG waveforms, texture in images). However, difficulties in segmentation of noisy images to detect the primitives and the inference of the grammar from training data often impede their implementation. The syntactic approach may yield a combinatorial explosion of possibilities to be investigated, requiring large training sets and huge computational efforts (Perlovsky 1998).

3. Cognitive approaches, which include neural networks and support vector machines (SVMs).

   Neural networks are based on the organization of the human brain, where nerve cells (neurons) are linked together by strands of fiber (axons). Neural networks are massively parallel computing systems consisting of a huge number of simple processors with many interconnections. They are able to learn complex non-linear input–output relationships and use sequential training procedures. However, in spite of the seemingly different underlying principles, most of the neural network models are implicitly similar to statistical pattern recognition methods (Anderson et al. 1990; Ripley 1993). It has been pointed out (Anderson et al. 1990) that "neural networks are statistics for amateurs . . . Most NNs conceal the statistics from the user".

   Support Vector Machines, SVMs (Cristianini and Shawe-Taylor 2000), represent the training examples as points in p-dimensional space, mapped so that the examples of the data classes are separated by a $(p - 1)$-dimensional hyperplane, which is chosen to maximize the "margins" on either side of the hyperplane (Fig. 2.12).

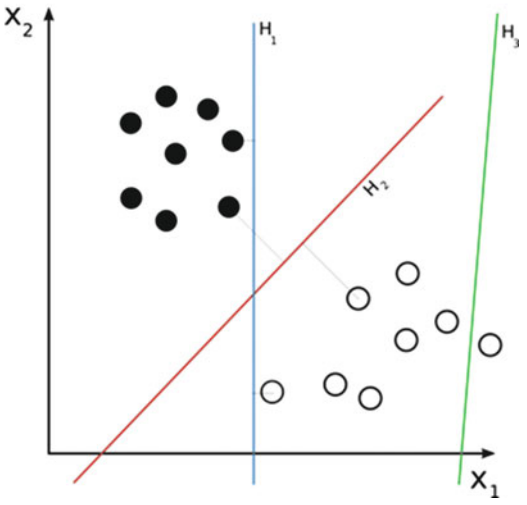

Fig. 2.12 A linear SVM in 2D feature space. H1 separates the two classes with a small margin, but H2 separates them with the maximum margin (H3 doesn't separate the two classes at all)

2.6 Examples

2.6.1 Classification by Shape

Figure 2.13a is an image containing both bolts and nuts, some of which lie on their sides. We should be able to distinguish (and therefore classify) the objects on the basis of their shape. The bolts are long, with an end piece, and the nuts either have a hole in them (the "face-on" nuts) or are short and linear (the "end-on" nuts). In this case, pre-processing was not required and automatic segmentation (using Otsu thresholding) produces a simplified, binary image (Fig. 2.13b).

The skeleton of this image shows the essential shape differences between the bolts and the two types of nut (Fig. 2.13c). A skeleton comprises pixels which can be distinguished on the basis of their connectivity to other pixels on the skeleton: end pixels (which have only one neighboring pixel on the skeleton), link pixels (which have two neighbors), and branch pixels (which have three neighbors). Because of their characteristic shape, only the skeletons of the bolts will have branch pixels. If they are used as a seed image, and *conditionally dilated* under the condition that the seed image is constrained to remain within the bounds of a mask image (the original binary image, Fig. 2.13b), then an image of the bolts alone results (Fig. 2.13d). The nuts can now be obtained (Fig. 2.13e) by logically combining this figure with the original binary figure (using (Fig. 2.13b AND (NOT Fig. 2.13d)). The nuts and bolts can then be joined in a color-coded image (Fig. 2.13f), which presents the nuts and bolts in different pseudocolors.

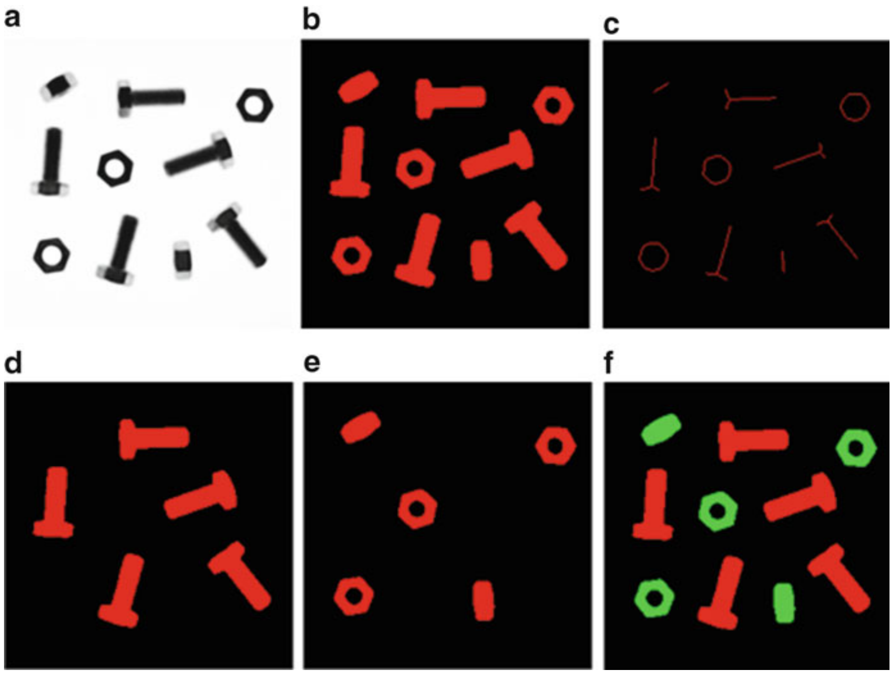

Fig. 2.13 (**a**) Original image, (**b**) after Otsu thresholding, (**c**) after subsequent skeletonization, (**d**) after conditionally dilating the branch pixels from (**c**), (**e**) after logically combining (**b**) and (**d**), (**f**) *color coding* the nuts and bolts

2.6.2 *Classification by Size*

An alternative approach to separating the nuts and bolts involves measuring different feature properties, such as the area, perimeter, or length. If we measure the area of the labeled objects in the segmented image (Fig. 2.14a) by counting the pixels belonging to each label and plot these values in one dimension (Fig. 2.14b), then we can see that the nuts and bolts are well discriminated on the basis of area with the bolts having larger areas. There are three *clusters*, comprising the bolts with the highest areas, followed by the face-on nuts with intermediate areas, and the edge-on nuts with the lowest areas. If the objects are then re-labeled with their area values (Fig. 2.14c), that image (or the "area" feature) can be thresholded to show just the bolts (Fig. 2.14d): in this particular case, a threshold of 800 (viz., an area of 800 pixels) would work well, although auto-thresholding, using either the *isodata* (Dubes and Jain 1976) or *Otsu* (Otsu 1979) algorithm, for example, is preferable since that will preserve generality. The nuts can then be found by logically combining this image with the segmented nuts-and-bolts image as before. Only one feature (area) is used to discriminate the two classes, that is, the feature space (Fig. 2.14b) is one-dimensional.

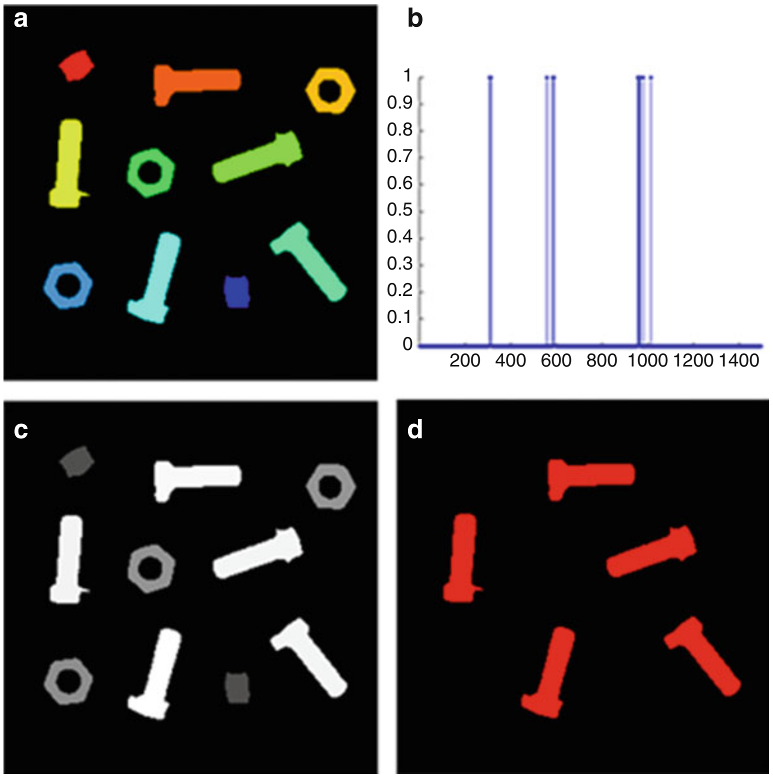

Fig. 2.14 (**a**) Segmented, labeled image (using Fig. 2.13a), (**b**) one-dimensional feature space showing the areas of the features, (**c**) the features "painted" with *grayscales* representing their measured areas, and (**d**) after thresholding image (**c**) at a value of 800

The two alternative measures, shape and size, could be tested for robustness on other images of nuts and bolts to see which performs better.

2.6.3 More Examples

Figure 2.15a is an image containing a number of electronic components, of different shapes and sizes (the transistors are three-legged, the thyristors are three-legged with a hole in them, the electrolytic capacitors have a round body with two legs, and the ceramic capacitors are larger than the resistors). A combination of the shape and size methods can be used to separate the objects into their different classes (Fig. 2.15b).

Similar techniques have been used to classify the fruit in Fig. 2.16 into three different classes. Think about the features that would be most discriminating in this case.

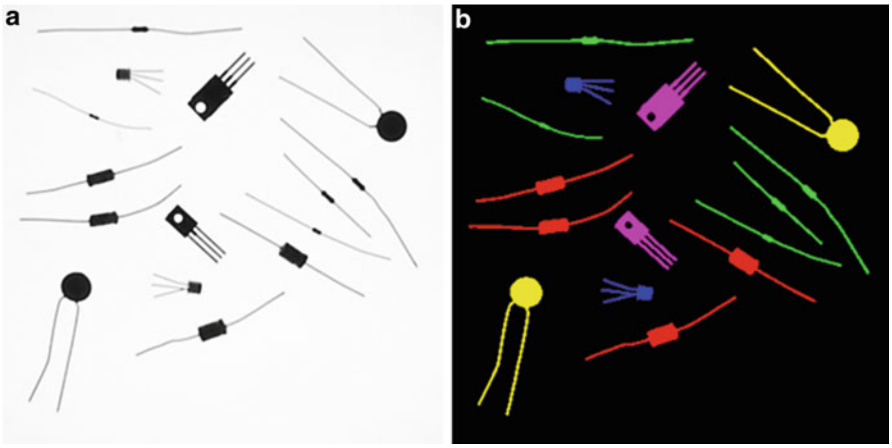

Fig. 2.15 (**a**) Electronic components (**b**) classified according to type, using shape and size

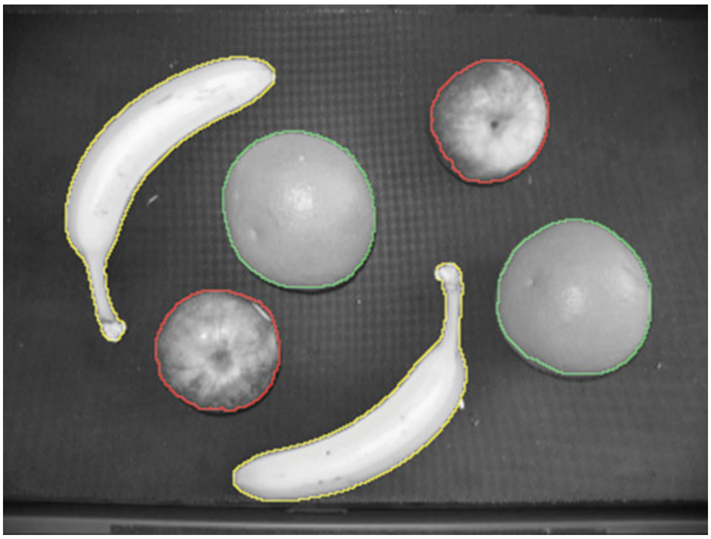

Fig. 2.16 Objects have been classified into three classes of fruit, and outlines superimposed on the original image

Circularity can distinguish the bananas from the other two fruit: size (or, perhaps texture, but not color in this grayscale image) could be used to distinguish the apples from the grapefruit. The single-pixel outlines of the fruit can be obtained from subtracting the segmented image from a dilated version of itself, and colored outlines have then been overlaid on the original image.

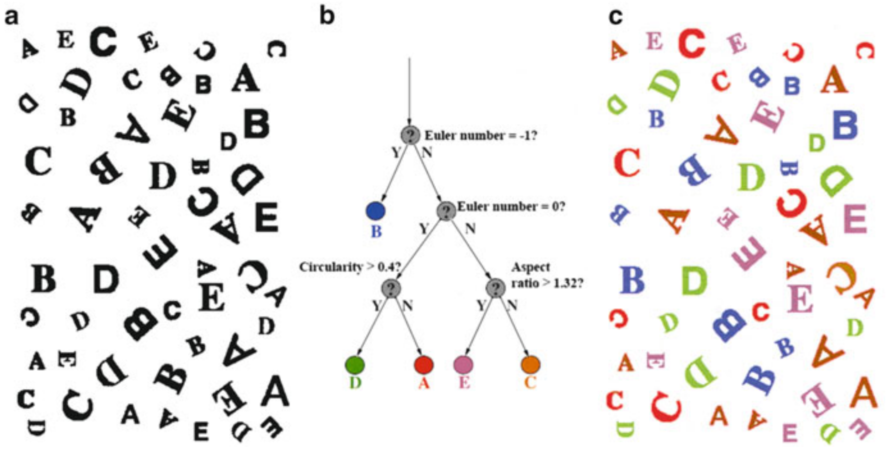

Fig. 2.17 (**a**) Letters A through E (**b**) shape factors used to classify them and (**c**) the resulting *color-coded image*

2.6.4 Classification of Letters

In Fig. 2.17a the letters A through E appear in different fonts, orientations and sizes, but are distinguished by shape factors (Euler number, aspect ratio, and circularity) which are invariant to size, position, and orientation. These can be used to classify the letters and color code them (Fig. 2.17b). This is an example of a decision tree (Fig. 2.17c), with three levels. It is important to design the system so that the most easily measured features are used first, to minimize the time for the overall identification (see Chap. 3). The decision values of the features for each letter were determined experimentally, by measuring several examples of each letter.

One of the disadvantages to such systems is that the addition of another class (e.g., the letter F) does not simply add another step to the process, but may completely reshuffle the order in which the rules are applied, or even replace some of the rules with others.

2.7 Exercises

1. Discuss the invariance of shape features to translation, rotation, scaling, noise, and illumination. Illustrate your answer with specific examples of features.
2. Explain the following terms (1) a pattern, (2) a class, (3) a classifier, (4) feature space, (5) a decision rule, and (6) a decision boundary.
3. What is a training set? How is it chosen? What influences its desired size?
4. There are two cookie jars: jar 1 contains two chocolate chip cookies and three plain cookies, and jar 2 contains one chocolate chip cookie and one plain cookie. Blindfolded Fred chooses a jar at random and then a cookie at random from that jar. What is the probability of him getting a chocolate chip cookie? (Hint: use a decision tree).

References

Aha, D.: Feature weighting for lazy learning algorithms. In: Liu, H., Motoda, H. (eds.) Feature Extraction, Construction and Selection: A Data Mining Perspective, pp. 13–32. Kluwer, Norwell, MA (1998)

Anderson, J., Pellionisz, A., Rosenfeld, E.: Neurocomputing 2: Directions for Research. MIT, Cambridge, MA (1990)

Barto, A.G., Sutton, R.S.: Reinforcement learning in artificial intelligence. In: Donahue, J.W., Packard Dorsal, V. (eds.) Neural Network Models of Cognition, pp. 358–386. Elsevier, Amsterdam (1997)

Batista, G., Monard, M.: An analysis of four missing data treatment methods for supervised learning. Appl. Artif. Intell. **17**, 519–533 (2003)

Cristianini, N., Shawe-Taylor, J.: An Introduction to Support Vector Machines. Cambridge University Press, Cambridge (2000)

Csiszar, I.: Maxent, mathematics, and information theory. In: Hanson, K.M., Silver, R.N. (eds.) Maximum Entropy and Bayesian Methods, pp. 35–50. Kluwer, Norwell, MA (1996)

De Mantaras, R.L., Armengol, E.: Machine learning from examples: inductive and lazy methods. Data Knowl. Eng. **25**, 99–123 (1998)

Dubes, R.C., Jain, A.K.: Clustering techniques: the user's dilemma. Pattern Recognit. **8**, 247–290 (1976)

Fu, K.S.: Syntactic Pattern Recognition and Applications. Prentice-Hall, Englewood Cliffs (1982)

Hodge, V.J., Austin, J.: A survey of outlier detection methodologies. Artif. Intell. Rev. **22**, 85–126 (2004)

Jain, A.K., Duin, R.P.W., Mao, J.: Statistical pattern recognition: a review. IEEE Trans. Pattern Anal. Mach. Intell. **33**, 1475–1485 (2000)

Jensen, F.V.: An Introduction to Bayesian Networks. UCL Press, London (1996)

Markovitch, S., Rosenstein, D.: Feature generation using general constructor functions. Mach. Learn. **49**, 59–98 (2002)

Mitchell, T.: Machine Learning. McGraw Hill, New York (1997)

Otsu, N.: A threshold selection method from gray-level histograms. IEEE Trans. Syst. Man Cybern. **SMC-9**, 62–66 (1979)

Perlovsky, L.I.: Conundrum of combinatorial complexity. IEEE Trans. Pattern Anal. Mach. Intell. **20**, 666–670 (1998)

Ripley, B.: Statistical aspects of neural networks. In: Bornndorff-Nielsen, U., Jensen, J., Kendal, W. (eds.) Networks and Chaos - Statistical and Probabilistic Aspects, pp. 40–123. Chapman and Hall, London (1993)

Yu, L., Liu, H.: Efficient feature selection via analysis of relevance and redundancy. J. Mach. Learn. Res. **5**, 1205–1224 (2004)

Chapter 3
Nonmetric Methods

3.1 Introduction

With nonmetric (i.e., categorical) data, we have lists of attributes as features rather than real numbers. For example, a fruit may be described as {(color=) red, (texture=), shiny, (taste=) sweet, (size=) large} or a segment of DNA as a sequence of base pairs, such as "GACTTAGATTCCA." These are discrete data, and they are conveniently addressed by decision trees, rule-based classifiers, and syntactic (grammar-based) methods.

3.2 Decision Tree Classifier

A decision tree is a simple classifier in the form of a hierarchical tree structure, which performs supervised classification using a *divide-and-conquer* strategy. It comprises a directed branching structure with a series of questions (Fig. 3.1), like the *Twenty Questions* game. The questions are placed at *decision nodes*; each tests the value of a particular attribute (feature) of the pattern (object) and provides a binary or multi-way split. The starting node is known as the *root node*, which is considered the parent of every other node. The branches correspond to the possible answers. Successive decision nodes are visited until a terminal or *leaf node* is reached, where the class (category) is read (assigned). (The decision tree is an upside-down tree, with the root at the top and the leaves at the bottom!). Classification is performed by routing from the root node until arriving at a leaf node. The tree structure is not fixed a priori but the tree grows and branches during learning depending on the complexity of the problem.

Figure 3.2 is an example of a three-level decision tree, used to decide what to do on a Saturday morning. Suppose, for example, that our parents haven't turned up and the sun is shining; the decision tree tells us to go off and play tennis. Note that the decision tree covers all eventualities: there are no values that the weather, our

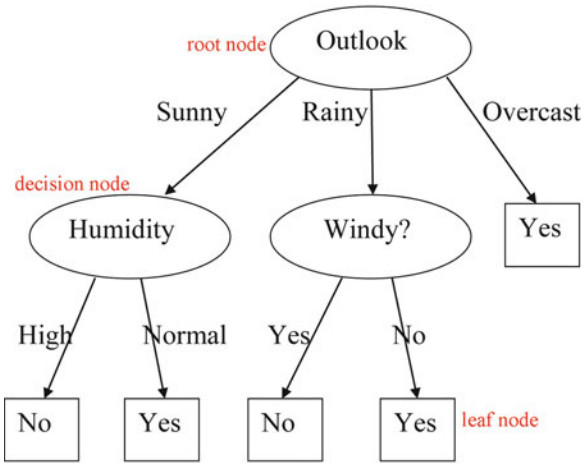

Fig. 3.1 A (two-level) decision tree for determining whether to play tennis. We have used *elliptical shapes* for the decision nodes (including the root node) and *rectangular shapes* for the leaf nodes

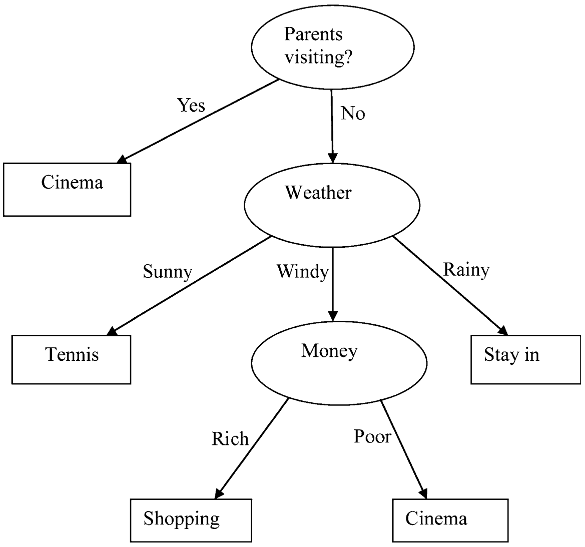

Fig. 3.2 A three-level decision tree for determining what to do on a Saturday morning

parents turning up or not, and our financial situation can take which aren't catered for in the decision tree.

Decision trees are more general than representations of decision-making processes. By rephrasing the questions, they can be applied to classification problems. An advantage of the decision tree classifier is that it can be used with nonmetric/categorical data, including nominal data with no natural ordering (although it can also be adapted to use quantitative data). Another benefit is its clear interpretability, providing a natural way to incorporate prior knowledge (and it is straightforward to convert the tests into logical expressions). Decision trees, once constructed, are very fast since they require very little computation.

The decision tree is easy to use; the more interesting question is how to construct the tree from training data (records), after having chosen a set of discriminating features. In principle, there are exponentially many decision trees that can be constructed from a given set of features. While some of the trees will be more accurate than others, finding the optimal tree is not computationally feasible. Nevertheless, a number of efficient algorithms have been developed to create or "grow" a reasonably accurate, albeit suboptimal, decision tree in a reasonable amount of time. These algorithms usually employ a *greedy* strategy that grows the tree using the *most informative* attribute (feature) at each step and does not allow backtracking. The most informative attribute will be the one which splits the set arriving at the node into the most homogeneous subsets.

3.2.1 Information, Entropy, and Impurity

Information can be thought of as the reduction of uncertainty, and informative attributes will be the ones that result in the largest reduction of uncertainty. The information content of a single message state in units of information is given by:

$$I(E) = \log \frac{1}{P(E)} = -\log P(E) \tag{3.1}$$

where $P(E)$ is the prior probability of occurrence of the message. Intuitively, the amount of information carried by a message is inversely related to the probability of its occurrence. Messages with a high probability of occurring carry little information, and conversely, messages that are least expected carry most information. If only two events are possible (0 and 1), the base of the logarithm in (3.1) is 2, and the resulting unit of information is the *bit*. If the two events are equally likely [$P_1(E) = P_2(E) = ½$] then $I(E_1) = I(E_2) = -\log_2(½) = 1$ bit, i.e., 1 bit of information is conveyed when one of the two possible equally likely events occurs. However, if the two possible events are not equally likely [for example, $P_1(E) = ¼$ and $P_2(E) = ¾$], then the information conveyed by the less common event [$I(E_1) = -\log_2(¼) = 2$] is greater than that conveyed by the more common event [$I(E_2) = -\log_2(¾) = 0.415$]. (Taking logs to the base 2 is less familiar to us, but remember that $\log_2 N = \log_{10} N / \log_{10} 2$).

Entropy is a measure of the disorder or unpredictability in a system. (It is used for discrete variables, whereas variance would be the metric for continuous variables). Given a binary (two-class) classification, C, and a set of examples, S, the class distribution at any node can be written as (p_0, p_1), where $p_1 = 1 - p_0$, and the entropy, H, of S is the sum of the information:

$$H(S) = -p_0 \log_2 p_0 - p_1 \log_2 p_1 \tag{3.2}$$

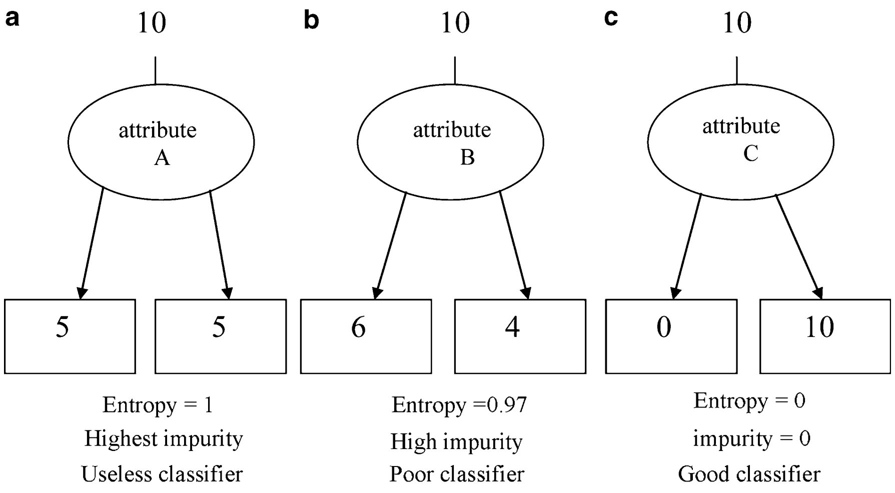

Fig. 3.3 Comparison of three decision nodes based on different attributes

If the attribute results in a classification that separates the examples into (0.5, 0.5) (as in Fig. 3.3a), the entropy (uncertainty) of that feature is at a maximum (equal to 1.0). This is *not* a useful attribute. If another attribute splits the examples into (0.6, 0.4), the entropy relative to this new classification is $-0.6 \log_2 0.6 - 0.4 \log_2 0.4 = 0.97$ (Fig. 3.3b). If all the test examples of a third attribute are of the same class [i.e., the split is (0, 1) or (1, 0) as in Fig. 3.3c], then the entropy (uncertainty) of that feature is zero and it provides good classification.

Entropy can be thought of as describing the amount of *impurity* in a set of features at a node. The smaller the degree of impurity, the more skewed the class distribution (and the more useful is the node). For example, a node with class distribution (0, 1) has zero impurity (and zero entropy) and is a good classifier; whereas a node with uniform class distribution (0.5, 0.5) has the highest impurity (and entropy = 1) and is a useless classifier.

In the general case, the target attribute can take on c different values (viz., a multi-way split) and the entropy of S relative to this c-wise classification is given by

$$H(p) = -\sum_{i=1}^{c} p_i \log_2 p_i \tag{3.3}$$

where p_i is the proportion of S belonging to class i. Note that the base of the logarithm is still 2, since we are continuing to measure the entropy in bits; and note that the maximum possible entropy relative to this attribute is $\log_2 c$.

Other impurity measures, which can be used to determine the best way to split a series of records include the *Gini impurity* and the *classification error*:

$$\text{Gini}(p) = 1 - \sum_i {p_i}^2 \tag{3.4}$$

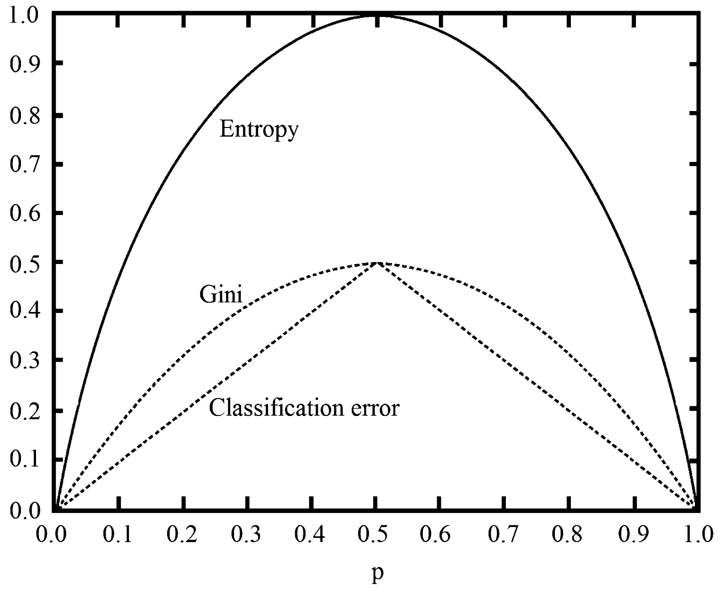

Fig. 3.4 Impurity measures for binary classification

$$\text{classification error}(p) = 1 - \max(p_i) \tag{3.5}$$

(the Gini impurity is actually the expected error rate if the class label is selected randomly from the class distribution present).

The values of these impurity measures for binary classification are shown in Fig. 3.4. All three measures attain a maximum value for a uniform distribution ($p = 0.5$), and a minimum when all the examples belong to the same class ($p = 0$ or 1). A disadvantage of the classification error is that it has a discontinuous derivative, which may be a problem when searching for an optimal decision over a continuous parameter space.

3.2.2 *Information Gain*

We now return to the problem of trying to determine the best attribute to choose for each decision node of the tree. The decision mode will receive a mixed bag of instances, and the best attribute will be the one that best separates them into homogeneous subsets (Fig. 3.5). The measure we will use is the *gain*, which is the expected reduction in impurity caused by partitioning the examples according to this attribute. More precisely, the gain, Gain(S, A), of an attribute A, relative to a collection of samples S, is defined as:

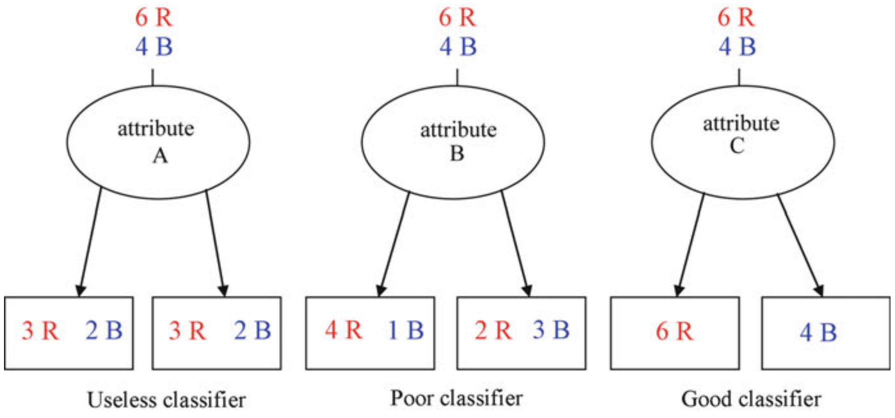

Fig. 3.5 Different attributes splitting a mixture of instances. Attribute C provides the purest split and is the best attribute to use for classification

$$\text{Gain}(S, A) = \text{Impurity}(S) - \sum_{i=1}^{k} \frac{|S_{vi}|}{|S|} \text{Impurity}(S_{vi}) \tag{3.6}$$

where the attribute A has a set of values $\{v_1, v_2, v_3 \ldots v_k\}$, and the number of examples within S with the value v_i is $|S_{vi}|$. The first term is just the impurity of the original collection S and the second term is the expected value of the impurity after S is partitioned using attribute A. The second term is simply the sum of the impurities of each subset S_{vi}, weighted by the fraction of examples that belong to S_{vi}. If entropy is used as the measure of impurity, then the gain is known as the *information gain*.

Example 3.1 Using the Gini index to find the gain

With reference to Fig. 3.6, there are two attributes, A and B, which can be used to split the data (comprising 12 instances) into smaller subsets. Before splitting (i.e., the parent node), the Gini index is 0.5 since there is an equal number of cases from both classes.

If attribute A is chosen to split the data, the Gini index for node N_1 is 0.4898 (i.e., $1 - [(4/7)^2 + (3/7)^2] = 24/49$) and for node N_2 it is 0.480 (i.e., $1 - [(2/5)^2 + (3/5)^2] = 12/25$). The weighted average for the two descendant nodes is $(7/12) \times 0.4898 + (5/12) \times 0.480 = 0.486$.

Similarly, if we use attribute B, the weighted average of the Gini index for attribute B is 0.375.

Since the subsets for attribute B have a smaller Gini index (i.e., smaller impurity), it is preferred to attribute A. [Or the gain in using attribute B is larger ($0.5 - 0.375 = 0.125$) than the gain in using attribute A ($0.5 - 0.486 = 0.014$).]

(continued)

(continued)

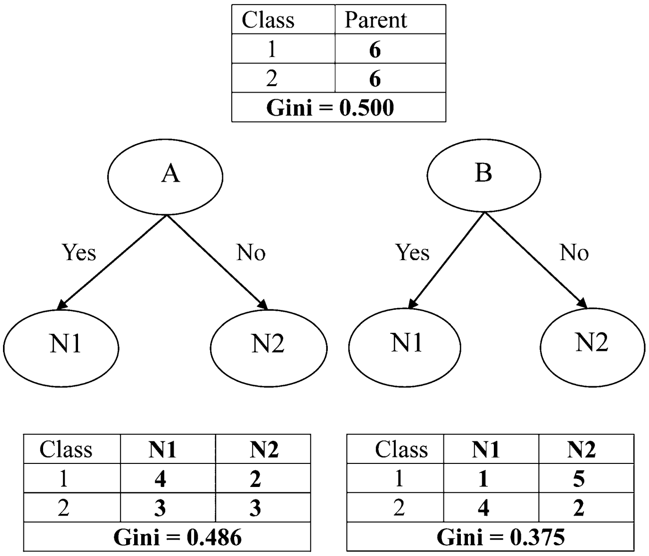

Fig. 3.6 Splitting binary attributes

This basic algorithm, the ID3 algorithm (Quinlan 1986), employs a top-down, greedy search through the space of possible decision trees. (The name ID3 was given because it was the third in a series of "interactive dichotomizer" procedures.)

Example 3.2 Using the ID3 algorithm to build a decision tree.

Suppose we want to train a decision tree using the examples (instances) in Table 3.1.

Table 3.1 Examples of decisions made over the past ten weekends

Examples	Weather	Parents visiting?	Money	Decision (category)
1	Sunny	Yes	Rich	Cinema
2	Sunny	No	Rich	Tennis
3	Windy	Yes	Rich	Cinema
4	Rainy	Yes	Poor	Cinema
5	Rainy	No	Rich	Stay in
6	Rainy	Yes	Poor	Cinema
7	Windy	No	Poor	Cinema
8	Windy	No	Rich	Shopping
9	Windy	Yes	Rich	Cinema
10	Sunny	No	Rich	Tennis

(continued)

(continued)

The first thing is to find the attribute for the root node. To do this, we need to calculate the entropy, $H(S)$, before any splitting. Using (3.3), this comes to $S = 1.571$ [viz., $-0.6 \log_2 0.6 - 0.2 \log_2 0.2 - 2 \times (0.1 \log_2 0.1)$].

Then we need to determine the values of Gain(S, parents), Gain(S, weather), and Gain(S, money), using (3.6):

$$\begin{aligned}\text{Gain}(S, \text{parents}) &= 1.571 - (|S_{\text{yes}}|/10) \times \text{Entropy}(S_{\text{yes}}) - (|S_{\text{no}}|/10) \\ &\quad \times \text{Entropy}(S_{\text{no}}) = 1.571 - (0.5) \times 0 - (0.5) \times (1.922) = 0.61\end{aligned}$$

If "parents coming?" is the node, then five instances will go down the "Yes" branch (and then will all be class "cinema," with an entropy of zero: this would be a terminal node) and five will go down the "No" branch [and they will comprise two "tennis," one "stay-in," one "cinema," and one "shopping": the entropy of this node is $-0.4 \log_2 0.4 - 3 \times (0.2 \log_2 0.2)$, which is 1.922].

$$\begin{aligned}\text{Gain}(S, \text{weather}) &= 1.571 - (|S_{\text{sun}}|/10) \times \text{Entropy}(S_{\text{sun}}) - (|S_{\text{wind}}|/10) \\ &\quad \times \text{Entropy}(S_{\text{wind}}) - (|S_{\text{rain}}|/10) \times \text{Entropy}(S_{\text{rain}}) \\ &= 1.571 - (0.3) \times (0.918) - (0.4) \times (0.8113) - (0.3) \\ &\quad \times (0.918) = 0.70\end{aligned}$$

$$\begin{aligned}\text{Gain}(S, \text{money}) &= 1.571 - (|S_{\text{rich}}|/10) \times \text{Entropy}(S_{\text{rich}}) \\ &\quad - (|S_{\text{poor}}|/10) \times \text{Entropy}(S_{\text{poor}}) \\ &= 1.571 - (0.7) \times (1.842) - (0.3) \times 0 = 0.2816\end{aligned}$$

This means that the weather attribute, with its three branches, should be the first (root) node (Fig. 3.7a).

Now we look at the branches. For the sunny branch, $S_{\text{sunny}} = \{1, 2, 10\}$. Since the classes (cinema, tennis, and tennis respectively) are not the same, we will need another decision node here (Fig. 3.7b). The same situation occurs for the other two branches (where $S_{\text{windy}} = \{3, 7, 8, 9\}$, and $S_{\text{rainy}} = \{4, 5, 6\}$).

Returning to the sunny branch, we are only interested in the three examples $\{1, 2, 10\}$ and we set S to be S_{sunny}, from which $H(S)$ turns out to be 0.918 (viz., $-0.1 \log_2 0.1 - 0.2 \log_2 0.2$), since two examples end up together (as "tennis") and one ends up on its own (as "cinema"). We now need to calculate Gain (S_{sunny}, parents) and Gain(S_{sunny}, money):

$$\begin{aligned}\text{Gain}(S_{\text{sunny}}, \text{parents}) &= 0.918 - (|S_{\text{yes}}|/|S|) \times \text{Entropy}(S_{\text{yes}}) - (|S_{\text{no}}|/|S|) \\ &\quad \times \text{Entropy}(S_{\text{no}}) \\ &= 0.918 - (1/3) \times 0 - (2/3) \times 0 = 0.918\end{aligned}$$

(continued)

(continued)

$$\begin{aligned}\text{Gain }(S_{\text{sunny}}, \text{money}) &= 0.918 - (|S_{\text{rich}}|/|S|) \times \text{Entropy}(S_{\text{rich}}) \\ &\quad - (|S_{\text{poor}}|/|S|) \times \text{Entropy}(S_{\text{poor}}) \\ &= 0.918 - (3/3) \times 0.918 - (0/3) \times 0 = 0\end{aligned}$$

Note that Entropy(S_{yes}) and Entropy(S_{no}) are both zero, because both S_{yes} and S_{no} contain examples which are all in the same category (cinema and tennis, respectively). Hence, the parents attribute should be chosen next. It has two branches for "Yes" and "No": the "Yes" branch contains a single example {1}, and the "No" branch contains two examples, {2, 10} which are in the same class. Hence both these branches end at leaf nodes (Fig. 3.7c).

The rest of the tree is left as an exercise for the reader!

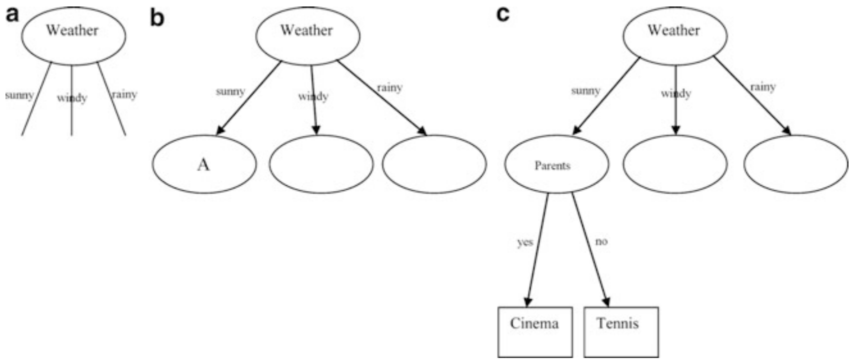

Fig. 3.7 Stages in building a decision tree

3.2.3 Decision Tree Issues

There are a number of issues arising with decision trees

- Decision trees partition feature space into disjoint regions, with decision boundaries that are rectilinear and parallel to the feature axes (Fig. 3.8).
  Oblique decision trees can be used to overcome this limitation by using test conditions such as $w_{11}x_1 + w_{12}x_2 + w_{10} > 0$, where x_1 and x_2 are the features, w_{11} and w_{12} are weights, and w_{10} is a *bias* or threshold value (Fig. 3.9). The decision tree is now a *linear*, *multivariate* tree. If these test conditions occur near the top of the tree, and the training set is large, then training can be slow.
- When should we stop splitting during training? If we continue splitting too far, the data will be *overfit*. In the extreme, each terminal (or leaf) node will correspond to a single training point and the full tree is merely a look-up table, which cannot be expected to generalize well to (noisy) test data. Conversely, if splitting is stopped too early, then the error on the training data is not sufficiently low and performance with test data will suffer.

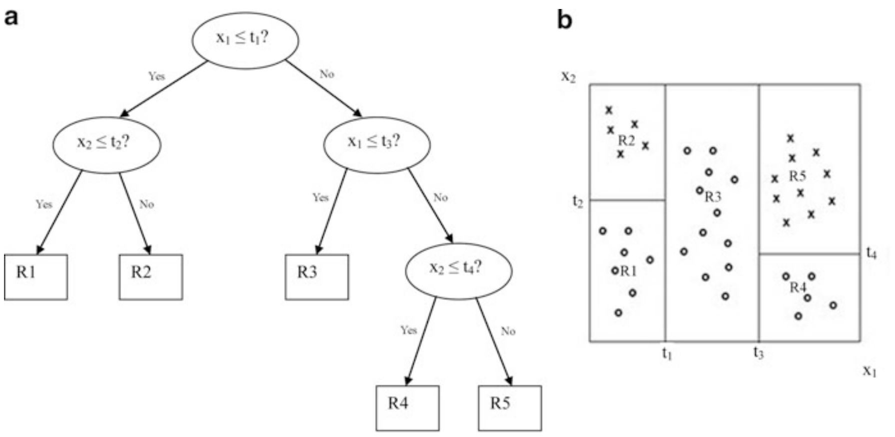

Fig. 3.8 (**a**) A decision tree and (**b**) the resulting decision boundaries in feature space

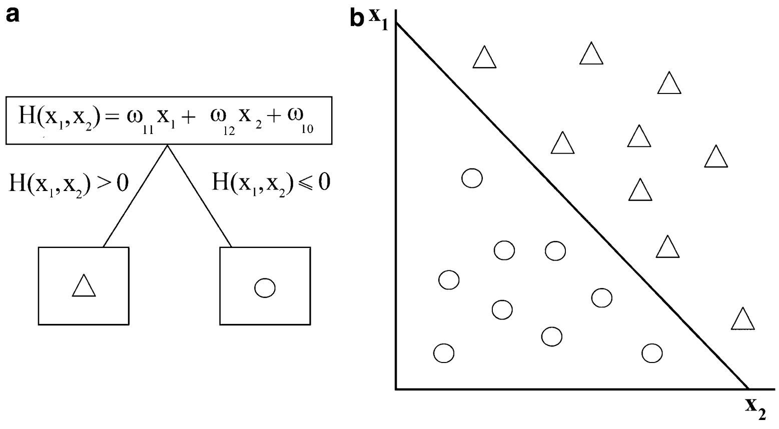
a
$H(x_1,x_2) = \omega_{11}x_1 + \omega_{12}x_2 + \omega_{10}$
$H(x_1,x_2) > 0$
$H(x_1,x_2) \leq 0$
b
x_1
x_2

Fig. 3.9 (**a**) An oblique decision tree and (**b**) the resulting decision boundary in feature space

The training and test error rates are large when the tree is very small. This situation is known as *underfitting*: the model has yet to learn the true structure of the data. As the number of nodes in the tree increases, it will have fewer training and test errors (Fig. 3.10). However, once the tree becomes large, its test error rate begins to increase even though its training error rate continues to fall. This is known as *overfitting*, where the tree contains some nodes that accidentally fit noisy points in the training data but do not generalize to the test data.

One way to decide when to stop splitting is by using *validation* or *cross-validation*. In validation, the tree is trained using a subset of the data (e.g., 90%) with the remaining (10%) kept as a validation set. We continue splitting until the error in the validation set is minimized. (In cross-validation several independently chosen subsets are used.)

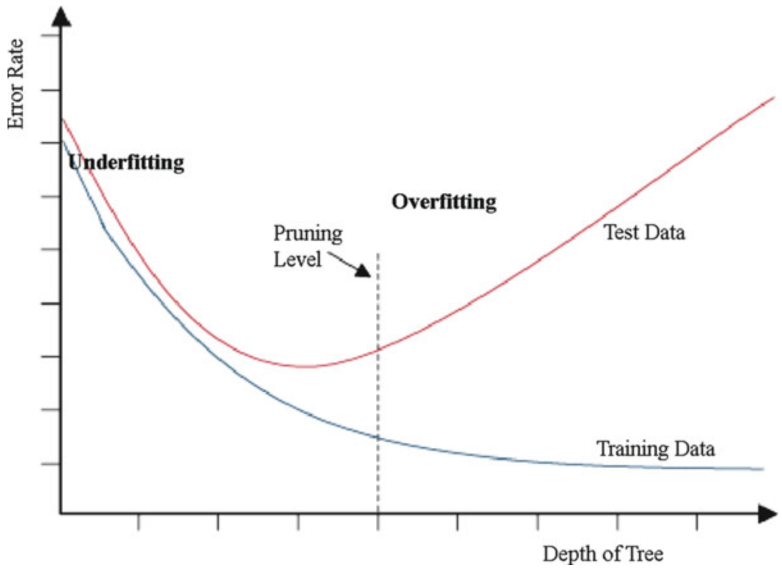

Fig. 3.10 Training and test error rates: a typical example. To avoid overfitting, the tree can be post-pruned; an appropriate pruning level is indicated

Another method is to stop splitting when the reduction in impurity falls below a certain threshold, or when a node represents less than a certain number of points (e.g., 5% of the total training set).

If the tree is grown too large, it can be *pruned* by trimming in a bottom-up fashion (Fig. 3.10). All pairs of neighboring leaf nodes (i.e., ones linked to a common parent) are considered for elimination. Any pair whose elimination results in a satisfactory (small) increase in impurity is eliminated, and the common parent node becomes a leaf node. (This node could then itself be pruned.) Pruning is incorporated in a successor to the ID3 algorithm known as C4.5 (Quinlan 1993), and in a modification of that, the J48 algorithm (Witten and Frank 2005).

- In certain cases, the available data may be missing values for some attributes. In such cases, it is common to estimate the missing attribute value based on other examples for which this attribute has a known value.

  Consider the situation in which the gain is to be calculated at a node in the decision tree to evaluate whether the attribute A is the best attribute to test at this decision node, and that the value $A(x)$ is unknown for one of the training samples. One strategy would be to assign it the value that is most common among training examples at this node. Alternatively, we might assign it the most common value among examples at this node that have the same classification.

  A second, more complex, procedure is to assign a probability to each of the possible values of A rather than simply assigning the most common value to $A(x)$.

These probabilities can be estimated again based on the observed frequencies of the various values for A among the examples at the particular node. For example, given a Boolean attribute A, if the node contains six known examples with $A = 1$ and four with $A = 0$, then we would say the probability that $A(x) = 1$ is 0.6, and the probability that $A(x) = 0$ is 0.4. A fractional 0.6 of instance x is now distributed down the branch for $A = 1$ and a fractional 0.4 of x down the other tree branch. These fractional examples are used for the purpose of computing the gain and can be further subdivided at subsequent branches of the tree if a second missing attribute value must be tested. This same fractioning of examples can also be applied after learning to classify new instances whose attribute values are unknown. In this case, the classification of the new instance is simply the most probable classification, computed by summing the weights of the instance fragments classified in different ways at the leaf nodes of the tree. This method for handling missing attribute values is incorporated in the C4.5 (Quinlan 1993) and J48 (Witten and Frank 2005) algorithms.

- When comparing binary splits with multi-way splits, the multi-way split is inherently favored. To avoid this, the gains should be normalized by dividing by $-\Sigma\, p_i \log_2 p_i$ (summed over the number of splits, k): if each attribute has the same number of cases, then $p_i = 1/k$ and the normalizing factor is $\log_2 k$. With multi-way splits, it is important to ensure that there are sufficient numbers of cases associated with each choice in order to make reliable predictions.
- With binary splits of continuous data, we have to decide the best value of the threshold at which the split is to occur, i.e., the threshold value that produces the greatest information gain. This could be achieved by histogramming the data (in which case a bin width has to be chosen), computing the Gini index for all the possible splits, and choosing the split that produces the smallest Gini index.

3.2.4 Strengths and Weaknesses

Decision trees are easy to understand, do not require much computation when performing classification, and provide a clear indication of which attributes (fields) are most important. They are most useful for categorical data but can be adapted to handle continuous data.

On the other hand, they are prone to errors when there are many classes and a relatively small number of training examples. They can be computationally expensive to train, and pruning is also computationally expensive. They tend to give rectangular decision regions, unless more computationally expensive strategies are used.

3.3 Rule-Based Classifier

In problems where classes can be characterized by general relationships, rather than just by examples (instances), it becomes attractive to build classifiers based on rules. Humans generally like explanations for most decisions, and sometimes there are legal and ethical requirements for this (e.g., rejection of a credit card application, medical diagnosis).

It is possible to extract rules from a decision tree. Each path from root to a leaf can be written down as a series of IF. . .THEN rules. For example, the left-most path in Fig. 3.1 would lead to the rule **IF** (outlook = sunny) **AND** (humidity = high) **THEN** do not play tennis. When more than one leaf is labeled with the same class, then the paths can be combined with a logical OR. It may be possible to prune the resulting rules, although they may not be able to be written back as a tree after that.

Another way is to learn the rules directly from the data. Such *rule induction* is similar to decision tree induction except that rule induction does a depth-first search and generates one rule (path) at a time, whereas tree induction goes breadth-first and generates all paths simultaneously.

Rules are learned one at a time. Each rule is a combination of conditions, which are added one at a time to minimize some criterion (such as entropy). Once a rule is grown and pruned, it is added to the *rule base* and all the training examples covered by that rule are removed from the training set: and the process continues until enough rules are generated. There is an outer loop of adding one rule at a time to the rule base and an inner loop of adding one condition at a time to the current rule. Both steps are greedy, and do not guarantee optimality; and both loops incorporate pruning for better generalization. An example of a rule-induction algorithm is *Ripper* (Cohen 1995), which is based on an earlier algorithm *Irep* (Furnkranz and Widmer 1994). It is well suited for handling datasets with imbalanced class distributions.

Rule-based classifiers give comparable performance to the decision tree classifier. They create rectilinear partitions similar to those created by (non-oblique) decision trees. Nevertheless, if the rule-based classifier allows multiple rules to be triggered for a given example, then a more complex decision boundary can be constructed.

3.4 Other Methods

Ordered sequences or strings of discrete items, as in a sequence of letters in an English word or a DNA sequence, such as “AGCTTGGCATC” (where A, G, C, and T stand for the nucleic acids adenine, guanine, cytosine, and thymine, respectively), are nominal elements. The strings can be of different lengths and there is no obvious distance metric. *String matching* involves finding whether a sub-string appears in a string for a particular *shift* of characters. An *edit distance*, based on the nearest neighbor distance (Chap. 5), can be invoked to measure the similarity or difference between two strings. Such an edit distance describes how many fundamental operations (substitution, insertion, or deletion of a character) are required to transform one string into another.

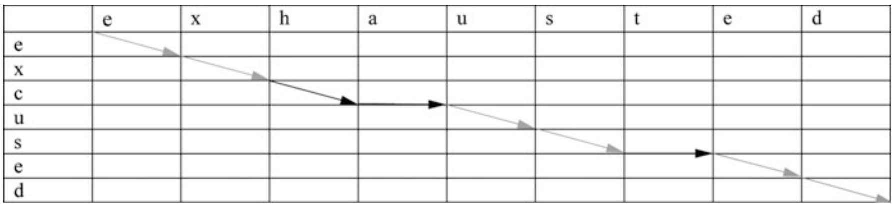

Fig. 3.11 The edit distance calculation for strings x and y can be illustrated in a table. (A *gray arrow* indicates no change. A *black diagonal arrow* indicates substitution, and a *black horizontal arrow* an insertion)

For example, the string $\mathbf{x}$ = "excused" can be transformed into the string $\mathbf{y}$ = " exhausted" using one substitution and two insertions (Fig. 3.11). If these operations are equally costly, then the edit distance is 3.

The sequence of characters may be generated according to particular structural rules, viz., grammar. An example would be valid telephone numbers, with international, national, and local codes. Often this structure is hierarchical, with "noun" and "verb" phrases. Grammatical methods can be used to provide constraints and improve accuracy. For example, an optical character recognition (OCR) system that recognizes and interprets mathematical equations based on a scanned pixel image can have particular "slots" which can be filled by only a limited set of symbols.

The string generated by a set of rules is referred to as a *sentence*; and the rules are specified by a *grammar*. In pattern recognition, we are given a sentence and a grammar and seek to determine whether the sentence was generated by the grammar. The general process is known as *parsing*. Many parsing methods depend on the model underlying the grammar. One popular such model is *finite-state machines*.

3.5 Exercises

1. Suppose that the probability of five events are $P(1) = 0.5$, and $P(2) = P(3) = P(4) = P(5) = 0.125$. Calculate the entropy. Explain in words what this means.
2. Three binary nodes, N_1, N_2, and N_3, split examples into (0, 6), (1,5), and (3,3), respectively. For each node, calculate its entropy, Gini impurity, and classification error.
3. Build a decision tree that computes the logical AND function.
4. Imagine that there are four things that you like to do in the evening: going to a pub, watching TV, going to a party, or studying (!). The choice is sometimes made for you—if you have an assignment due the next day, you need to study, if you're feeling lazy then the pub isn't for you, and if there isn't a party then you can't go to it. You are looking for a decision tree which will help you decide what to do each evening. Here is a list of everything you've done in the past 10 days.

Deadline?	Is there a party?	Lazy?	Activity
Urgent	Yes	Yes	Party
Urgent	No	Yes	Study
Near	Yes	Yes	Party
None	Yes	No	Party
None	No	Yes	Pub
None	Yes	No	Party
Near	No	No	Study
Near	No	Yes	TV
Near	Yes	Yes	Party
Urgent	No	No	Study

(The first thing to do is to work out which feature to use as the starting (root) node. For this you need to compute the entropy, and then find out which feature has the maximal information gain).

5. Write out the steps in the ID3 algorithm in pseudo code.
6. Consider the training data from the alphabet $A = \{a, b, c\}$:

$\omega 1$	$\omega 2$	$\omega 3$
aabbc	Bccba	caaaa
ababcc	Bbbca	cbcaab
babbcc	cbbaaaa	baaca

Use the edit distance to classify each of the following strings [if there are ambiguities in the classification, state which two (or all three) categories are candidates]: "abacc," "abca," "ccbba," "bbaaac"

References

Cohen, W.: Fast effective rule induction. In: Prieditis, A., Russell, S.J. (eds.) Twelfth International Conference on Machine Learning, pp. 115–123. Morgan Kaufmann, San Mateo, CA (1995)

Furnkranz, J., Widmer, G.: Incremental reduced error pruning. In: Cohen, W., Hirsch, H. (eds.) Eleventh International Conference on Machine Learning, pp. 70–77. Morgan Kaufmann, San Mateo, CA (1994)

Quinlan, J.R.: Induction of decision trees. Mach. Learn. **1**, 81–106 (1986)

Quinlan, J.R.: C4.5: Programs for Machine Learning. Morgan Kaufmann, San Mateo, CA (1993)

Witten, I.H., Frank, E.: Data Mining: Practical Machine Learning Tools and Techniques. Morgan Kaufmann, San Mateo, CA (2005)

Chapter 4
Statistical Pattern Recognition

4.1 Measured Data and Measurement Errors

It is unrealistic to expect that data will be perfect. There may be problems related to human error (e.g., transcription errors), limitations of the measuring sensors (e.g., limited resolution), or flaws in the data collection process (e.g., missing values).

Measured data comes with a margin of error or uncertainty. The term *measurement error* refers to any problem resulting from the measurement process. In statistics and experimental sciences, this error is measured by *precision* (repeatability or random error—the closeness of repeated measurements of the same feature to one another) and *accuracy* (systematic error—a fixed bias in all the measurements), as shown in Fig. 4.1. Data may be subject to various amounts of one or both of these types of errors, as illustrated by darts around a bull's eye (Fig. 4.2).

Probability theory helps us to model random error and is therefore a solid basis for classifier design [Systematic error requires that the actual (true) values are known by some external means].

4.2 Probability Theory

4.2.1 Simple Probability Theory

If A, B, C, ... are events, the probability of these events can be denoted by a real number between 0 and 1, viz., $P(A)$, $P(B)$, $P(C)$, ... (The probability is linked to the relative frequency of that event happening, i.e., an experiment is observed a large number of times (N), and if event A occurs M times then $P(A) = M/N$).

A Venn diagram can be used to illustrate these events, where the whole area represents the *sample space*, S (the set of all possible outcomes). If A and B are

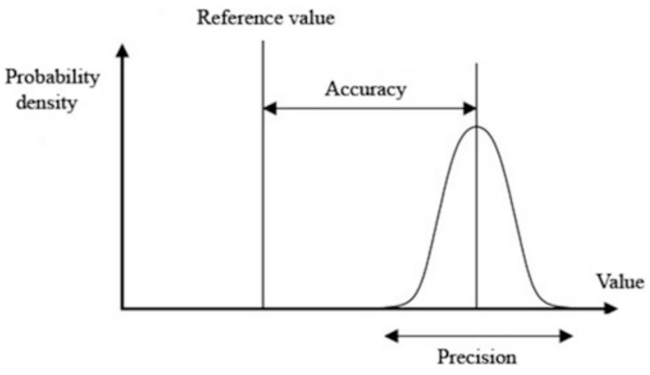

Fig. 4.1 Diagram illustrating precision and accuracy

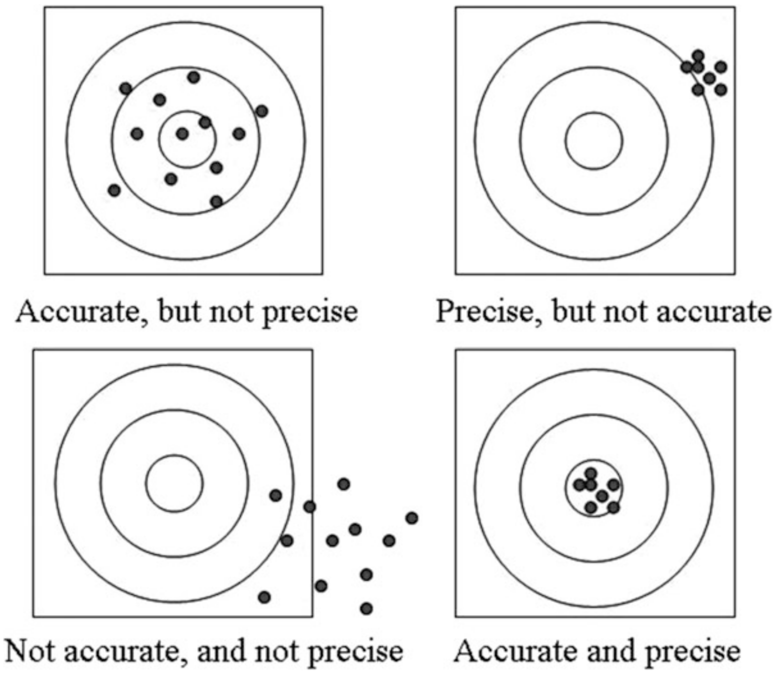
Accurate, but not precise
Precise, but not accurate
Not accurate, and not precise
Accurate and precise

Fig. 4.2 Showing data with large (and small) errors in precision and accuracy

mutually exclusive (i.e., they cannot occur simultaneously) they are shown as in Fig. 4.3a. The probability that either A or B occur is denoted by $P(A \text{ or } B)$ (or $P(A \cup B)$), which is given by

$$P(A \text{ or } B) = P(A) + P(B) \tag{4.1}$$

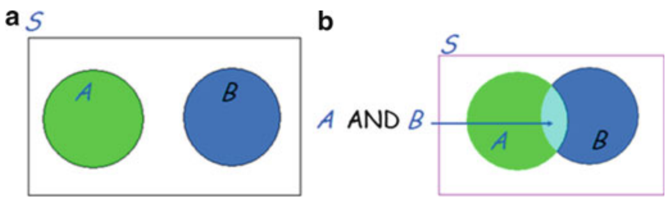

Fig. 4.3 Venn diagrams if events A and B are (**a**) mutually exclusive (nonoverlapping) and (**b**) not mutually exclusive (overlapping)

If events A and B can occur simultaneously, then a more general relationship holds

$$P(A \text{ or } B) = P(A) + P(B) - P(A \text{ and } B) \tag{4.2}$$

where $P(A \text{ and } B)$ (or $P(A \cap B)$) is the overlapping area (Fig. 4.3b). This is sometimes called the General Addition Rule.

Also note that the sum of the probabilities of all possible events is 1 (i.e., certainty).

If an event A is certain, then $P(A) = 1$; if it is impossible, $P(A) = 0$. The complement of an event is everything that is not part of A, and its probability (P(not A)) or $P(\bar{A})$ is given by

$$P(\bar{A}) = 1 - P(A) \tag{4.3}$$

Example 4.1

If two independent dice are thrown, the sample space (i.e., all possible outcomes) is shown in Fig. 4.4. The probability of event A (the first dice showing a "1") is $P(A) = 6/36 = 1/6$. And the probability of event B (the second dice showing a "1") is $P(B) = 6/36 = 1/6$.

The probability of either dice showing a "1" (i.e., P(A or B)) is

$$P(A \text{ or } B) = P(A) + P(B) - P(A \text{ and } B) = 6/36 + 6/36 - 1/36 = 11/36$$

using (4.2) or by inspection of the sample space.

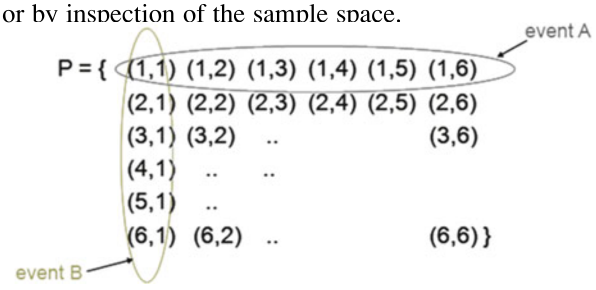

Fig. 4.4 The sample space for rolling two dice, with events A (the first dice showing a "6") and B (the second dice showing a "6") marked

Table 4.1 A contingency table

	Age (years)			
Sex	<30	30–45	>45	Total
Male (M)	60	20	40	120
Female (F)	40	30	10	80
Total	100	50	50	200

Events, A and B, are *independent* if

$$P(A \text{ and } B) = P(A) \cdot P(B) \tag{4.4}$$

This would be true, for example, in the throwing of two dice; the score on the second is independent of the throw on the first.

A contingency table (Table 4.1) is used to display the (multivariate) frequency distribution of two or more variables, most commonly categorical variables, i.e., variables which are classifying labels, such as sex, race, birthplace, etc. The numbers in the right-hand column and the bottom row are called marginal totals and the figure in the bottom right-hand corner is the grand total.

Provided the entries in the table represent a random sample from the population, probabilities of various events can be read from it or calculated, e.g., the probability of selecting a male, $P(M)$, is 120/200, i.e., 0.6; and the probability of selecting a person under 30 years old, $P(U)$, is 100/200, i.e., 0.5. The probability of selecting a person who is female *and* under 30 years old, $P(F$ and $U)$, is 40/200, i.e., 0.2. This is often called the *joint probability*. (Note that the events F and U are independent of each other, so that the joint probability is equal to the product of the individual probabilities, 0.4×0.5.) The probability of selecting a person who is male *or* under 30 years old, $P(M$ or $U)$, is 160/200, i.e., 0.8.

4.2.2 Conditional Probability and Bayes' Rule

Conditional probability is the probability of some event A, given the occurrence of some other event B. Conditional probability is written $P(A|B)$, and is read "the probability of A, given that B is true". Conditional probability can be explained using the Venn diagram shown in Fig. 4.3b. The probability that B is true is $P(B)$, and the area within B where A is true is $P(A$ and $B)$, so that the conditional probability of A given that B is true is

$$P(A|B) = P(A \text{ and } B)/P(B) \tag{4.5a}$$

Note that the conditional probability of event B, given that A is true, is

$$P(B|A) = P(A \text{ and } B)/P(A) \tag{4.5b}$$

(If the events A and B are statistically independent, (4.4) would reduce to

$$P(A|B) = P(A) \tag{4.6a}$$

and

$$P(B|A) = P(B) \tag{4.6b}$$

which can be used as an alternative to (4.4) as a test for independence).

The general conditional probability definitions, (4.5a) and (4.5b), can be cross-multiplied to give the so-called multiplicative rule

$$\begin{aligned} P(A \text{ and } B) &= P(A|B) \cdot P(B) \\ &= P(B|A) \cdot P(A) \end{aligned} \tag{4.7}$$

Manipulating this further, by equating the equivalent two terms on the right, and re-arranging gives Bayes' Rule:

$$P(A|B) = \frac{P(B|A) \cdot P(A)}{P(B)} \tag{4.8}$$

where $P(A|B)$ is known as the *posterior probability*. Bayes' rule is one of the most useful relations in probability and statistical theory. It can be paraphrased as:

$$\text{Posterior(probability)} = \frac{\text{likelihood} \times \text{prior(probability)}}{\text{evidence}} \tag{4.9}$$

If $\{A_1, A_2, A_3, \ldots A_n\}$ are a set of mutually exclusive outcomes that together form the sample space, S, $P(B)$ is constant for each of them so that it can be regarded as a normalizing constant which ensures that the probabilities sum to unity. In this general case

$$P(A|B) = \frac{P(B|A) \cdot P(A)}{\Sigma P(B|A_i) \cdot P(A_i)} \tag{4.10}$$

In the case of a binary partition, where S is comprised of $\{A, \bar{A}\}$

$$P(A|B) = \frac{P(B|A) \cdot P(A)}{P(B|A) \cdot P(A) + P(B|\bar{A}) \cdot P(\bar{A})} \tag{4.11}$$

Example 4.2 Let's Make a Deal

In a game show (Monty Hall's *Let's Make a Deal*) there are three closed doors. Behind one of these doors is a car, and behind the other two are goats. The contestant picks a door, and Monty opens one of the remaining doors to reveal a goat. The contestant is then given the option to switch doors. Is it to their advantage to do so? Think about it for a while. (This problem has attracted a lot of coverage, and it has been said that no other statistical problem comes so close to fooling all of the people all of the time!)

One way to explain this is as follows. Suppose the doors are labeled 1, 2 and 3. Let's say the contestant picks door 1: the probability that the car is behind door 1 is 1/3. The probability that it is either behind doors 2 or 3 is the remaining 2/3. Now, Monty Hall knows which door the car is behind, and always opens a door to reveal a goat. Once the goat is revealed (behind door 2 or 3), then the probability that the car is there drops to zero, and the probability that the car is behind the other door is the full 2/3. So it is better to switch to the other (unopened) door than to remain with door 1. The chance of winning rises from 1/3 to 2/3! Note that Monty Hall does not open his door randomly (which would not affect the outcome of sticking or switching): he knows where the car is. The additional information that he gives the contestant changes the (prior) probability (1/3) into a (posterior) probability, which is 2/3 if the contestant decides to switch.

In a statistical formulation, let $C =$ the door number hiding the car and $H =$ the number of the door opened by the host. As the initial choice of the player is independent of the placing of the car, the solution may be given on the condition of the player having initially chosen door 1. Then:

$P(C = 1) = P(C = 2) = P(C = 3) = 1/3$ (the car is placed randomly)
The strategy of the host is reflected by:
$P(H = 1|C = 1) = 0$ (the host never opens the chosen door)
$P(H = 2|C = 1) = P(H = 3|C = 1) = 1/2$ (the host acts randomly if needed)
$P(H = 2|C = 3) = 1$ (the host has no other option)
$P(H = 3|C = 2) = 1$ (the host has no other option)

The player now may calculate the probability of finding the car behind door No. 2, after the host has opened door No. 3, using Bayes' rule:

$$P(C = 2|H = 3) = \frac{P(H = 3|C = 2)P(C = 2)}{P(H = 3|C = 2)P(C = 2) + P(H = 3|C = 1)P(C = 1)}$$

$$= \frac{1 \cdot \frac{1}{3}}{1 \cdot \frac{1}{3} + \frac{1}{2} \cdot \frac{1}{3}} = \frac{2}{3}$$

Diagnostic testing of a person for a disease typically delivers a score, e.g., a red blood cell count, which is compared with the range of scores that random samples

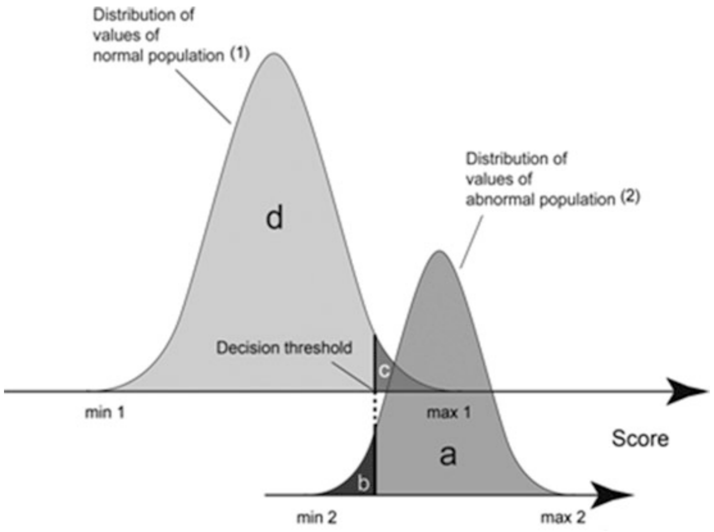
Distribution of values of normal population (1)
Distribution of values of abnormal population (2)
d
Decision threshold
c
a
b
min 1
max 1
min 2
max 2
Score

Fig. 4.5 Diagnostic test score distributions for normal (1) and abnormal (2) population samples

Table 4.2 Contingency table for the diagnostic test illustrated in Fig. 4.5 (Actual rows by predicted columns)

	B	$\bar{B}$
A	a (TP)	b (FN)
$\bar{A}$	c (FP)	d (TN)

from normal and abnormal (diseased) populations obtain on the test. The situation is shown in Fig. 4.5, where the ranges of scores for the normal and abnormal population samples are shown as Gaussian distributions. We would like to have a decision threshold, below which a person tested would be diagnosed disease-free and above which the person would be diagnosed as having the disease. The complication is that the two ranges of scores overlap and the degree of overlap will affect the goodness of our diagnosis of the tested patient, viz., the more the overlap, the less likely that our diagnosis will be definitive.

The decision threshold should be in the region of overlap, i.e., between min 2 and max 1. It distinguishes between those who will receive a negative diagnosis (test negative) from those who will receive a positive diagnosis (test positive). The distribution of the scores from the normal population (1) is split into two regions, "*d*" (below the threshold) and "*c*" (above the threshold), and the distribution of the scores from the abnormal or diseased population (2) is split into "*b*" (below the threshold) and "*a*" (above the threshold).

The sample space thus can be arranged in a contingency table (Table 4.2), to show the relationship between the two events—event A (actually having the disease) and event B (having a positive result that indicates having the disease).

Table 4.3 Contingency table with marginal probabilities (Actual rows by predicted columns)

Actual	Predicted			
		B	$\bar{B}$	Sum
	A	$P(A \text{ and } B)$	$P(A \text{ and } \bar{B})$	$P(A)$
	$\bar{A}$	$P(\bar{A} \text{ and } B)$	$P(\bar{A} \text{ and } \bar{B})$	$P(\bar{A})$
		$P(B)$	$P(\bar{B})$	1

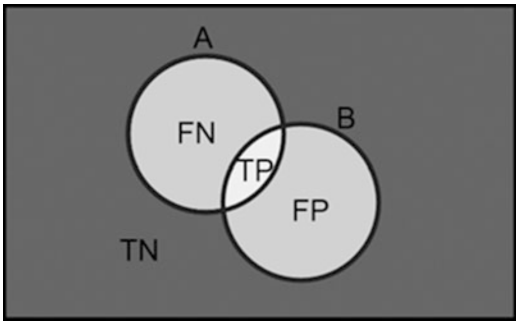

Fig. 4.6 Venn diagram for diagnostic testing

Events A and B are not identical since the test will not be ideal. Thus a person may or may not have the disease and the test may or may not indicate that he/she has the disease. There are four mutually exclusive events. A person from region "a" tests positive and actually has the disease and is known as a true positive (TP). A person from region "b" tests negative although he/she actually has the disease and is known as a false negative (FN). A person from region "c" tests positive but does not have the disease and is known as a false positive (FP). And a person from region "d" tests negative and does not have the disease, and is known as a true negative (TN). A good test would have a large TP and TN, and a small FP and FN, i.e., little overlap of the two distributions.

This table can be written in terms of probabilities (Table 4.3), where the marginals are shown around the periphery.

The corresponding Venn diagram is shown in Fig. 4.6, in which the areas are not drawn to scale.

The traditional measures of the diagnostic value of a test are its sensitivity [the (conditional) probability of the test identifying those with the disease given that they have the disease] and its specificity [the (conditional) probability of the test identifying those free of the disease given that they do not have the disease]. With reference to Figs. 4.5 and 4.6

$$\text{sensitivity}, P(B|A) = \text{TP}/(\text{TP} + \text{FN}) = a/(a + b) \tag{4.12}$$

$$\text{specificity}, P(\bar{B}|\bar{A}) = \text{TN}/(\text{TN} + \text{FP}) = d/(d + c) \tag{4.13}$$

where a, b, c, and d are the areas of the labeled regions in Fig. 4.4. However, sensitivity and specificity do not answer the more clinically relevant questions.

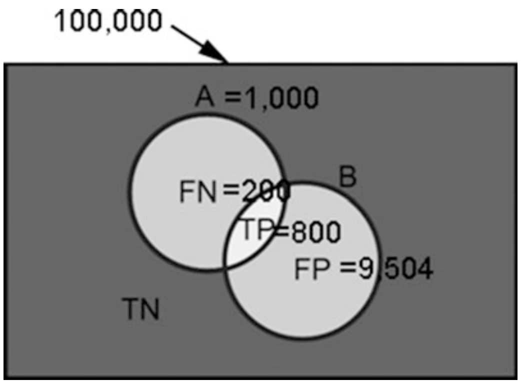

Fig. 4.7 Venn diagram for mammographic testing example

If the test is positive, how likely is it that an individual has the disease? Or, if the test is negative, how likely is it that an individual does not have the disease? The answers to these questions require the posterior probabilities from Bayes' rule [(4.8)].

For example, the posterior probability of having the disease (after having tested positive), the conditional probability $P(A|B)$, is obtained from the probability of testing positive, given that you have the disease, i.e., the sensitivity, $P(B|A)$; the occurrence of the disease in the population, i.e., the prior probability, $P(A)$; and the probability of testing positive, i.e., the evidence, $P(B)$. This is also known as the *predictive value* of a positive test; from Figs. 4.5 and 4.6 it is equal to TP/((TP + FP) = $a/(a + c)$). (The predictive value of a negative test, $P(\bar{A}|\bar{B})$, is equal to TN/(TN + FN) = $d/(d + b)$).

Example 4.3 Breast Screening

About 1% of women who participate in routine breast screening have breast cancer.

About 80% of those with breast cancer get a positive test result and 9.6% without breast cancer also get a positive result. A woman gets a positive test result. What is the probability that she has breast cancer?

The women who have a positive mammography results *and* actually have breast cancer amount to 80% of 1%, or 0.8%, of all the women who were tested. The women who do *not* have breast cancer, but still show a (false) positive mammography results, amount to 9.6% of 99%, or 9.504%, of all the women who were tested. Therefore, total positive mammography results amount to 0.8% + 9.504%, or 10.304%, of all the women who were tested. Of this percentage, the women who actually have cancer (0.8%) are in the distinct *minority*. The probability of a woman who has a positive test result actually having cancer, $P(A|B)$, is 0.8/10.304 = 0.0776 or **7.76%**.

We can see this by using a Venn diagram and taking a population of 100,000 (Fig. 4.7). About 1% of these have breast cancer, i.e., A = 1,000. Now 80% of

(continued)

(continued)

these test positive (TP = 800, and the remaining 200 are FN). Now 9.6% of those without breast cancer (FP + TN = 99,000) get a positive result (FP): therefore FP is 9,504. The probability of a woman who has a positive test result actually having cancer is TP/(TP + FP) = 7.76%.

This is not as bad as you may have thought given the large values of sensitivity (80%) and specificity of the test (100 − 9.6% = 90.4%). Since the probability of having the disease after having tested positive is low, 7.76% in this example, this is sometimes known as the *False Positive Paradox*. The reason for this low probability is because the disease is comparatively rare (1%). Although the probability of having the disease is small despite having tested positive, the test has been useful. By testing positive, the probability of having the disease has increased from the prior probability of 1% to the posterior probability of 7.76%. And the posterior probability, $P(A|B)$ (or positive predictive value) is seen to be a more useful parameter than the sensitivity of the test, $P(B|A)$.

Alternatively, we could approach the problem like this:

A = have breast cancer

B = test positive

$P(A) = 0.01$

Sensitivity $P(B|A) = 0.8P(B|\bar{A}) = 0.096$

Therefore,

Specificity $P(\bar{B}|\bar{A}) = 1 - 0.096 = 0.904$ and $P(\bar{A}) = 1 - 0.01 = 0.99$

Using $P(A \text{ and } B) = P(A|B) \cdot P(B)$;

$P(B \text{ and } A) = P(B|A) \times P(A) = 0.8 \times 0.01 = 0.008$

$P(B \text{ and } \bar{A}) = P(B|\bar{A}) \times P(\bar{A}) = 0.096 \times 0.99 = 0.09504$

Filling in these values into the contingency table (Table 4.3) gives:

Actual	Predicted			
		B	$\bar{B}$	
	A	0.00800	0.00200	0.01000
	$\bar{A}$	0.09504	0.89496	0.99000
		0.10304	0.89696	1.00000

$$\begin{aligned}\text{The posterior probability of having breast cancer} = P(A|B) &= P(A \text{ and } B)/P(B) \\ &= 0.008/0.10304 \\ &= 0.07764 \\ &= \mathbf{7.76\ \%}\end{aligned}$$

The Excel file, CondProb.xls (which can be downloaded from http://extras.springer.com) finds the posterior (or predictive) probability of a positive test, $P(A|B)$, and the posterior (or predictive) probability of a negative test (NPV), $P(\bar{A}|\bar{B})$, given the sensitivity and specificity of the test and the prior probability of the disease (Formulation I) or the contingency table (Formulation II). Try solving Example 4.3 using this file, paying special attention to the formulae in the cells.

4.2.3 Naïve Bayes Classifier

A *naïve Bayes classifier* is a simple probabilistic classifier based on applying Bayes' rule, but assuming that the features ($f_1, f_2, f_3, \ldots, f_n$) are independent.

Bayes' rule [(4.8)] for a classifier can be written as:

$$P(C|f_1,f_2,f_3,\ldots,f_n) = \frac{P(C)P(f_1,f_2,f_3,\ldots,f_n|C)}{P(f_1,f_2,f_3,\ldots,f_n)} \tag{4.14}$$

where the class, C, is dependent on several features ($f_1, f_2, f_3, \ldots, f_n$).The denominator is a constant designed to normalize the probabilities so that they add to 1: it does not depend on C, and can effectively be ignored in the classification.

If the features are all independent (viz., the assumption for the naïve Bayes classifier), then the term $P(f_1, f_2, f_3, \ldots, f_n|C)$ can be re-written as a product of the component probabilities [as in (4.4)], and the posterior probability becomes

$$\begin{aligned} P(C|f_1,f_2,f_3,\ldots,f_n) &\propto P(C)P(f_1|C)P(f_2|C)P(f_3|C)\ldots P(f_n|C) \\ &\propto P(C)\prod_{i=1}^{n} P(f_i|C) \end{aligned} \tag{4.15}$$

Using this formulation, the naïve Bayes classifier assigns a test sample to the class with the maximum a posterior (MAP) probability.

Despite the fact that the far-reaching independence assumptions are often inaccurate, the naïve Bayes classifier works well in many real-world situations. The decoupling of the class conditional feature distributions means that each distribution can be independently estimated as a one-dimensional distribution. This in turn helps to alleviate problems stemming from the curse of dimensionality. [In the language of the next section, we need only determine the variances of the features in each class and not the covariances (because the features are considered to be independent.)] Like all probabilistic classifiers under the MAP decision rule, it arrives at the correct classification as long as the correct class is more probable than any other class; hence, class probabilities do not have to be estimated very well. In other words, the overall classifier is robust enough to ignore serious deficiencies in its underlying naïve probability model.

Bayesian spam filtering of e-mails uses a (naïve) Bayes classifier to identify spam. Bayesian spam filtering can tailor itself to the e-mail needs of individual users and gives low false-positive spam detection rates that are generally acceptable to users. Particular words have particular probabilities of occurring in spam e-mail and in legitimate e-mail (e.g., the word "Viagra"). The classifier does not know these probabilities in advance, and must first be trained so it can build them up. To train the classifier, the user must manually indicate whether a new e-mail is spam or not. For all words in each training e-mail, the classifier will adjust the probabilities that each word will appear in spam or legitimate e-mail in its database. After training, the word probabilities are used to compute the probability that an e-mail with a particular set of words in it belongs to either category. Using Bayes' rule

$$P(S|W) = \frac{P(W|S) \cdot P(S)}{P(W|S) \cdot P(S) + P(W|\bar{S}) \cdot P(\bar{S})} \tag{4.16}$$

where $P(S|W)$ is the probability that a message is spam, given that a particular word is in it, and the other terms have their usual meaning. Recent statistics show that the probability of any message being spam is $\geq 80\%$, but most Bayesian spam detection considers spam and no spam to have equal probabilities of 50%. Such a classifier is said to be *unbiased*. Each word in the message contributes to the e-mail's spam probability, so that the (posterior) probability is computed over all words in the e-mail. The classifier makes the naïve assumption that the words present in the message are independent [see (4.4)]: so that

$$P = \frac{P_1 P_2 \ldots P_N}{P_1 P_2 \ldots P_N + (1 - P_1)(1 - P_2) \ldots (1 - P_N)} \tag{4.17}$$

Under this assumption it is a *naïve Bayes classifier*. If the total spam probability exceeds a certain threshold (say 95%), the classifier marks the e-mail as spam.

4.3 Continuous Random Variables

Since a measurement has some uncertainty, it can be likened to an experiment (like rolling a dice) whose outcome is not known in advance. The variable that associates a number with the outcome of a random experiment is referred to as a *random variable*. Owing to its random nature, we may assign probabilities to the possible values (events) of the variable. If a random value can assume any value, not just certain discrete values, it is called a *continuous random variable*, X.

If X is a continuous random variable, then the *probability density function* (PDF) of X is a function $f(x)$ such the probability of X taking on a value between $x = x_1$ and $x = x_2$ is

$$P(x_1 \leq X \leq x_2) = \int_a^b f(x)\mathrm{d}x \tag{4.18}$$

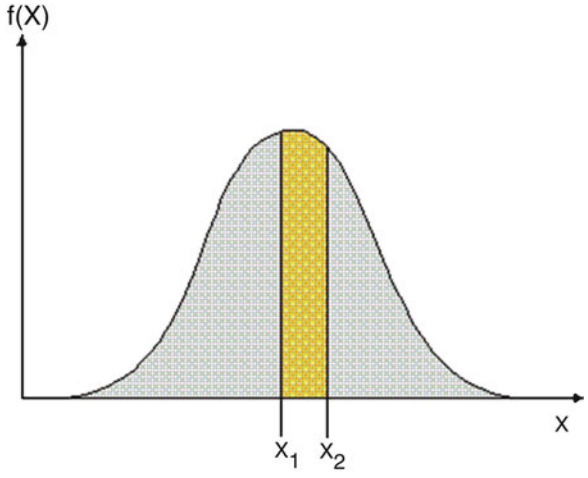

Fig. 4.8 The probability function, $f(x)$

i.e., the area under the PDF from x_1 to x_2 (Fig. 4.8). The total area under the curve equals unity (i.e., certainty).

The *cumulative distribution function* (CDF) is a function $F(x)$, of a random variable X, that is defined for a number x by

$$F(x) = P(X \leq x) = \int_0^x f(u)\mathrm{d}u \tag{4.19}$$

i.e., for a number x, $F(x)$ is the probability that the observed value will be at most x.

The mathematical relationship between the PDF and the CDF is given by

$$F(x) = \int_0^x f(s)\mathrm{d}s \tag{4.20}$$

where s is a dummy variable.

Conversely:

$$f(x) = -\frac{\mathrm{d}(F(x))}{\mathrm{d}x} \tag{4.21}$$

i.e., the CDF is the integral of the PDF and, conversely, the PDF is the differential of the CDF (Fig. 4.9).

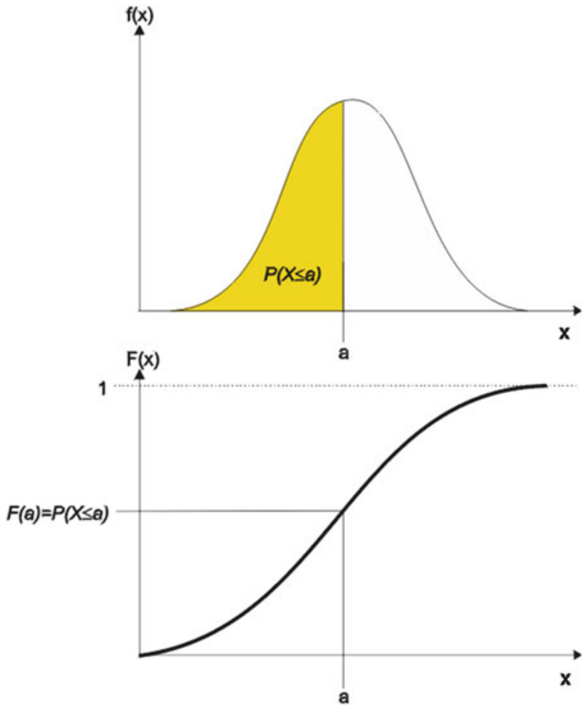

Fig. 4.9 Graphical representations of the PDF (*top*) and CDF (*bottom*)

An example of a PDF is the well-known normal (or Gaussian) distribution (Fig. 4.9), for which the PDF is given by:

$$f(x) = \frac{1}{\sqrt{2\pi\sigma^2}} e^{-\frac{(x-\mu)^2}{2\sigma^2}} \tag{4.22}$$

where μ is the mean, or expected, value of X, denoted as $E[X]$. [The normal distribution is often referred to as $N(\mu, \sigma^2)$]. For a random variable it is the weighted average of all possible values that this random variable can take. The weights used in computing this average correspond to the probabilities (p_i) in the case of a discrete random variable, or the probability densities (pdf's) in the case of a continuous random variable, i.e.,

$$\mu(= E[X]) = \sum_{i=1}^{N} x_i p_i \tag{4.23a}$$

or

$$\mu(= E[X]) = \int_{-\infty}^{\infty} x f(x) \mathrm{d}x \tag{4.23b}$$

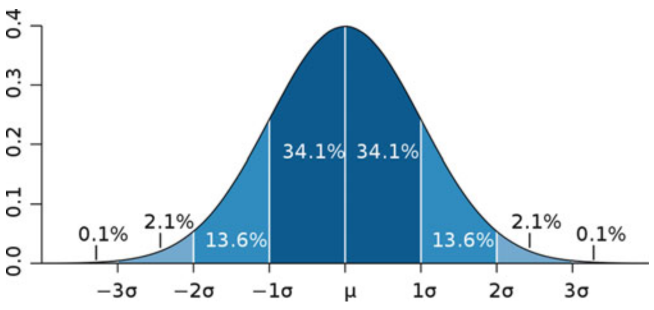

Fig. 4.10 The normal (or Gaussian) distribution function

and σ^2 (or Var[X]) is the variance of X, a measure of the spread of the distribution, given by

$$\sigma^2 (= E[(X - \mu)^2]) = \sum_{i=1}^{N} (x_i - \mu)^2 p_i \tag{4.24a}$$

or

$$\sigma^2 (= E[(X - \mu)^2]) = \int_{-\infty}^{\infty} (x_i - \mu)^2 f(x) \mathrm{d}x \tag{4.24b}$$

for discrete and continuous random variables, respectively.

The standard deviation, σ (or SD[X]), is the square root of the variance. For a normal (Gaussian) distribution, about 68% of the data values are within one standard deviation of the mean, and about 95% are within two standard deviations (Fig. 4.10).

The normal/Gaussian distribution is very convenient, since the parameters μ and σ are sufficient to uniquely characterize it. The normal distribution is the most widespread probability distribution used to describe measurements. It arises as the outcome of the Central Limit Theorem, which states that under mild conditions the sum of a large number of random variables will distribute approximately normally (e.g., the distribution of the sum (or average) of the rolled numbers from a large number of identical dice will be well approximated by a normal distribution). It can be shown that the Gaussian distribution has the maximum entropy (randomness) of all distributions having a given mean and variance.

4.3.1 The Multivariate Gaussian

The multivariate normal/Gaussian is a generalization of the one-dimensional (univariate) normal/Gaussian distribution to a higher number of dimensions, n.

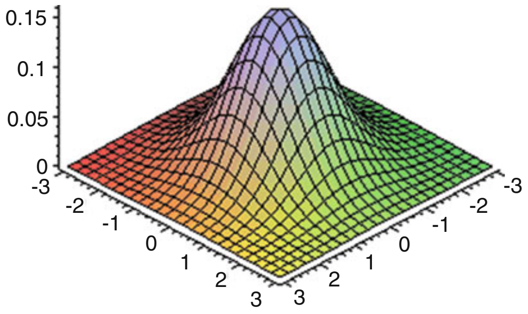

Fig. 4.11 A bivariate normal/Gaussian distribution

(A random variable is multivariate normally distributed if every linear combination of its components has a univariate normal distribution.) The multivariate normal distribution is often used to describe, at least approximately, any set of (possibly) correlated real-valued random variables each of which clusters around a mean value.

Compared to (4.22), **X**, $\boldsymbol{\mu}$ are now vectors of dimension n, and the variance (σ^2) has been replaced by the *covariance matrix*, $\boldsymbol{\Sigma}$. Note the use of $\boldsymbol{\Sigma}$ as the symbol for the covariance matrix; not to be confused with its use as a summation symbol! (T indicates the transpose, viz., columns changed to rows). Figure 4.11 shows the multivariate distribution for a 2D variable.

The formula for the multivariate Gaussian is a generalization of the formula for the one-dimensional Gaussian [(4.22)—note the similarity in form, and how the covariance matrix, $\boldsymbol{\Sigma}$, takes the place of the variance, σ^2]:

$$f(\mathbf{X}) = \frac{1}{((2\pi)^{n/2}|\Sigma|^{1/2})}\exp(-\tfrac{1}{2}(\mathbf{X}-\mu)^{\mathrm{T}}\Sigma^{-1}(\mathbf{X}-\mu)) \tag{4.25}$$

where $^{\mathrm{T}}$ indicates the transpose operator. [We may also use the alternative notation of it as $N(x;\, \boldsymbol{\mu},\, \boldsymbol{\Sigma})$].

Example 4.4 Factorization of a 2D Gaussian

For a 2D normal/Gaussian distribution, where the variables (features) are uncorrelated (which means that the covariance terms are zero), show that the distribution can be factorized into two 1D Gaussians.

$$\mathbf{X} = \begin{bmatrix} x_1 \\ x_2 \end{bmatrix} \mu = \begin{bmatrix} \mu_1 \\ \mu_2 \end{bmatrix} \Sigma = \begin{bmatrix} \sigma_1^2 & 0 \\ 0 & \sigma_2^2 \end{bmatrix}$$

(continued)

(continued)

$$p(x:\mu,\Sigma)=\frac{1}{2\pi\begin{vmatrix}\sigma_1^2 & 0\\ 0 & \sigma_2^2\end{vmatrix}^{\frac{1}{2}}}\exp\left(-\frac{1}{2}\begin{bmatrix}x_1-\mu_1\\x_2-\mu_2\end{bmatrix}^{\mathrm{T}}\begin{bmatrix}\sigma_1^2 & 0\\ 0 & \sigma_2^2\end{bmatrix}^{-1}\begin{bmatrix}x_1-\mu_1\\x_2-\mu_2\end{bmatrix}\right)$$

$$=\frac{1}{2\pi(\sigma_1^2\times\sigma_2^2-0\times 0)^{\frac{1}{2}}}\exp\left(-\frac{1}{2}\begin{bmatrix}x_1-\mu_1\\x_2-\mu_2\end{bmatrix}^{T}\begin{bmatrix}\frac{1}{\sigma_1^2} & 0\\ 0 & \frac{1}{\sigma_2^2}\end{bmatrix}\begin{bmatrix}x_1-\mu_1\\x_2-\mu_2\end{bmatrix}\right)$$

$$=\frac{1}{2\pi\sigma_1^2\sigma_2^2}\exp\left(-\frac{1}{2}\begin{bmatrix}x_1-\mu_1\\x_2-\mu_2\end{bmatrix}^{\mathrm{T}}\begin{bmatrix}\frac{1}{\sigma_1^2}(x_1-\mu_1)\\ \frac{1}{\sigma_2^2}(x_2-\mu_2)\end{bmatrix}\right)$$

$$=\frac{1}{2\pi\sigma_1^2\sigma_2^2}\exp\left(-\frac{1}{2\sigma_1^2}(x_1-\mu_1)^2-\frac{1}{2\sigma_2^2}(x_2-\mu_2)^2\right)$$

$$=\frac{1}{\sqrt{2\pi}\sigma_1}\exp\left(-\frac{1}{2\sigma_1^2}(x_1-\mu_1)^2\right)\times\frac{1}{\sqrt{2\pi}\sigma_2}\exp\left(-\frac{1}{2\sigma_2^2}(x_2-\mu_2)^2\right)$$

This shows that for uncorrelated variables, the 2D Gaussian can be factorized into two 1D Gaussians. (This holds true for higher numbers of variables too!)

4.3.2 The Covariance Matrix

The variance is a measure of the amount that a distribution varies about its mean. The covariance, on the other hand, is a measure of the similarity between two random variables (say, X_1 and X_2), i.e., how they vary with respect to each other. If there is no similarity, they are independent. The similarity could be so strong that knowing one determines the other without any uncertainty. Or the similarity could be somewhere in between, where knowing one of the variables reduces the uncertainty about the value the other will take. For a pair of random variables, X_1 and X_2, their covariance is defined as

$$\sigma_{12}^2=\mathrm{Cov}(X_1,X_2)=E[(X_1-\mu_1)\cdot(X_2-\mu_2)] \tag{4.26}$$

where μ_1, μ_2 are the respective means (or expected values, $E[X_1]$, $E[X_2]$).

In the case of $X_1 = X_2$ the covariance reduces to the variance

$$\sigma_1^2=\mathrm{Cov}(X_1,X_1)=E[(X_1-\mu_1)\cdot(X_1-\mu_2)] \tag{4.27}$$

When working with multiple variables, *the covariance matrix* provides a succinct way to summarize the covariances of all pairs of variables. In particular, the covariance matrix, $\boldsymbol{\Sigma}$, is the $n \times n$ matrix whose (i, j)th entry is $\mathrm{Cov}(X_i, X_j)$; by definition, it is square and symmetric.

For the case of three random variables (i.e., features), the covariance matrix is

$$\Sigma = \begin{bmatrix} \mathrm{Cov}(X_1, X_1) & \mathrm{Cov}(X_1, X_2) & \mathrm{Cov}(X_1, X_3) \\ \mathrm{Cov}(X_2, X_1) & \mathrm{Cov}(X_2, X_2) & \mathrm{Cov}(X_2, X_3) \\ \mathrm{Cov}(X_3, X_1) & \mathrm{Cov}(X_3, X_2) & \mathrm{Cov}(X_3, X_3) \end{bmatrix} \tag{4.28}$$

where the terms on the leading diagonal are the variances, σ_1^2, σ_2^2, and σ_3^2, and the off-diagonal terms are the covariances between pairs of variables (features), σ_{ij}^2, i.e.,

$$\Sigma = \begin{bmatrix} \sigma_1^2 & \sigma_{1,2}^2 & \sigma_{1,3}^2 \\ \sigma_{2,1}^2 & \sigma_2^2 & \sigma_{2,3}^2 \\ \sigma_{3,1}^2 & \sigma_{3,2}^2 & \sigma_3^2 \end{bmatrix} \tag{4.29}$$

Example 4.5

Five measurements (observations) each are taken of three features, X_1, X_2, and X_3, so that the feature vector is

	X_1	X_2	X_3
X	4.0	2.0	0.6
	4.2	2.1	0.59
	3.9	2.0	0.58
	4.3	2.1	0.62
	4.1	2.2	0.63

The mean values are given by $\boldsymbol{\mu} = |4.10\ 2.08\ 0.604|$
And the covariance matrix by

$$\Sigma = \begin{bmatrix} 0.025 & 0.0075 & 0.00175 \\ 0.0075 & 0.0070 & 0.00135 \\ 0.00175 & 0.00135 & 0.0043 \end{bmatrix}$$

where 0.025 is the variance of X_1, 0.0075 is the covariance between X_1 and X_2, 0.00175 is the covariance between X_1 and X_3, etc.

(The calculation of the individual terms in the covariance matrix introduces a subtle point. The variance is calculated from (4.24a). It is the mean of the squares of the deviations. However we do not know the mean of the population, so that we will have to use the sample values to calculate $\bar{x}$, and then reuse the sample values to calculate the variance. This gives the result a bias, which can be removed by using "$n - 1$" rather than "n" in the division to get the mean of the squares of the deviations ("$n - 1$" is known in statistics as the number of

(continued)

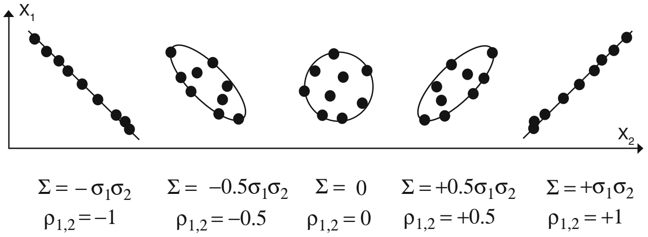

Fig. 4.12 The values of covariance and correlation coefficient for various data sets

(continued)

degrees of freedom). In practice, it is not going to make much difference if we divide by n or $n - 1$, as long as n is reasonably large (i.e., we have a reasonable amount of data, say $n > 10$). However, in this example, n is only 5 and it will make a difference: you need to divide by 4 (i.e., $n - 1$) to get the values of variance (and covariance) shown above).

The covariance matrix can be factorized as

$$\Sigma = \Gamma \mathbf{R} \Gamma = \begin{bmatrix} \sigma_1 & 0 & \dots & 0 \\ 0 & \sigma_2 & \dots & 0 \\ \dots & \dots & \dots & \\ 0 & \dots & \dots & \sigma_n \end{bmatrix} \begin{bmatrix} 1 & \rho_{12} & \dots & \rho_{1n} \\ \rho_{21} & 1 & \dots & \rho_{2n} \\ \dots & \dots & \dots & \dots \\ \rho_{n1} & \dots & \dots & 1 \end{bmatrix} \begin{bmatrix} \sigma_1 & 0 & \dots & 0 & \\ 0 & \sigma_2 & \dots & 0 & \\ \dots & \dots & \dots & \dots & \dots \\ 0 & \dots & \dots & \sigma_n & \end{bmatrix} \tag{4.30}$$

This is convenient since the diagonal matrix $\mathbf{\Gamma}$ contains the scales of the features, and $\mathbf{R}$ retains the essential information of the relationship between the features. $\mathbf{R}$ is called the *correlation matrix*. The individual terms of the correlation matrix are the (Pearson) correlation coefficients between pairs of variables/features and are equal to the corresponding covariances scaled by the standard deviations, i.e.,

$$\rho_{ij} = \mathrm{Cov}(X_i, X_j)/\sigma_i \cdot \sigma_j (\text{or}\, \sigma_{ij}/\sigma_i \cdot \sigma_j) \tag{4.31}$$

Thus the correlation between two random variables is simply the covariance of the corresponding standardized random variables ($Z = (X - E[X])/\mathrm{SD}[X]$ or $(X - \mu)/\sigma$).

Both the covariance and the correlation (coefficient) describe the degree of similarity between two random variables (and assume a linear link). The correlation coefficient is dimensionless due to the scaling and assumes a value between −1 and +1 (Fig. 4.12). The more dispersed the data points, the lower the value of the correlation coefficient. (Note that although best-fitted straight lines have been included in the figure, the correlation does *not* depend on their gradient.)

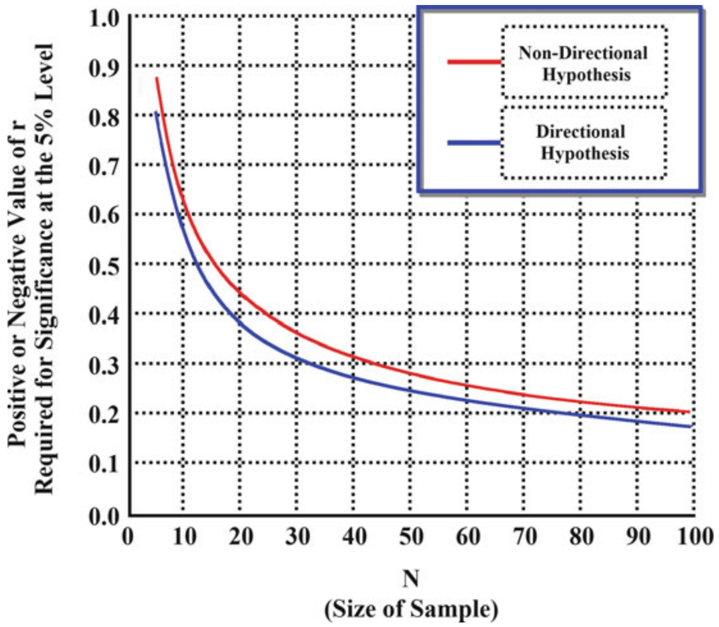

Fig. 4.13 Values of r required for statistical significance at the 5 % level, for samples of size $N = 5$ through $N = 100$

In passing we should note that the square of the correlation coefficient, r^2, known as *r-squared* or the *coefficient of determination*, gives the proportion of the variance (fluctuation) of one variable that is predictable from the other variable. For example, if the correlation between height and weight measurements is $r = 0.70$, then the coefficient of determination is 0.49. Thus, 49% of the weight is directly accounted for by the height and vice versa.

We have made a distinction between **r**, the correlation coefficient measured from a limited sample of X_i, Y_i pairs, and $\boldsymbol{\rho}$, the correlation that exists in the larger population, between X and Y, in general. It is possible, by chance, to obtain rather impressive-looking values of **r** within a sample, even when the correlation between X and Y, in general, is zero. This is especially true when the size of the sample is small. We need to address the question of the statistical significance of a given value or r (for a particular sample size, N), viz., what confidence can we have that a particular observed correlation value is not just a result of chance/coincidence in the sampling. Statistical significance is conventionally set at the 5% level. That is, an observed result is regarded as statistically significant—as something more than a mere fluke—only if it had a 5% or smaller likelihood of occurring by mere chance. Otherwise, it is regarded as statistically nonsignificant. Figure 4.13 plots the values of r that are required for statistical significance (at the 5% level) for various sample sizes. (In a directional hypothesis the relationship is expected

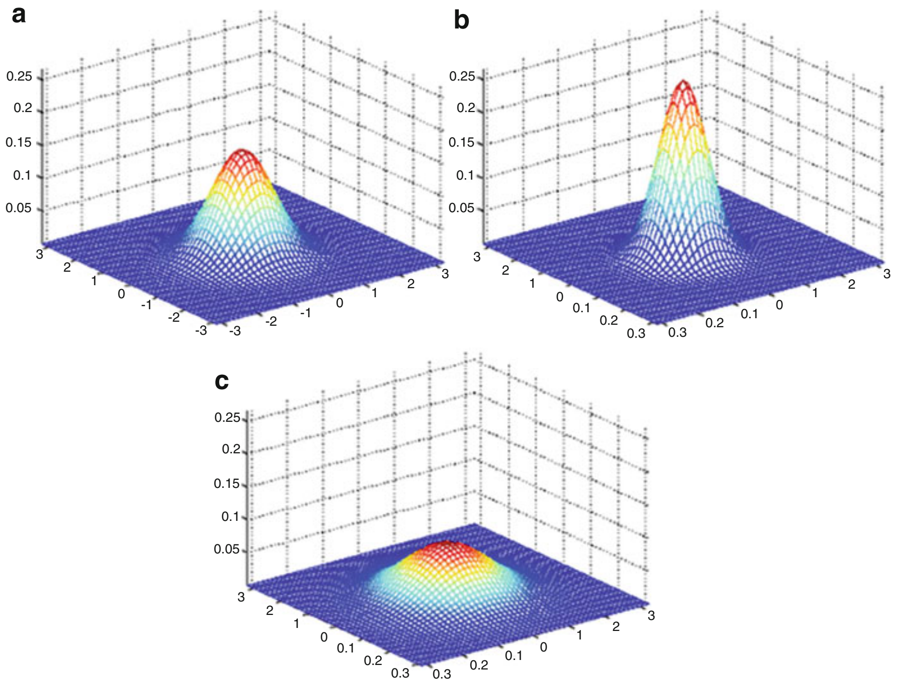

Fig. 4.14 2D Gaussians with (**a**) $\mathbf{\Sigma} = \mathbf{I}$ (the identity matrix, $\begin{vmatrix} 1 & 0 \\ 0 & 1 \end{vmatrix}$), (**b**) $\mathbf{\Sigma} = 0.6\ \mathbf{I}$, and (**c**) $\mathbf{\Sigma} = 2\ \mathbf{I}$

to show either a positive *or* negative correlation; in a nondirectional hypothesis either type of correlation is acceptable.)

Returning to the 2D Gaussian, we should appreciate that if $\mathbf{\Sigma}$ is diagonal the variables are uncorrelated. If $\mathbf{\Sigma}$ is a multiple of the identity matrix, then the isocontours of the Gaussian [slices through the Gaussian at varying heights/probabilities, centered on the mean values (μ_1, μ_2)] are circular. Changing the values on the diagonal of the covariance matrix simultaneously gives a narrower or broader Gaussian (Fig. 4.14).

If the values along the diagonal of the covariance matrix are not equal, then the isocontours of the Gaussian are elliptical, elongated along the feature axis with the larger variance (Fig. 4.15).

If there are off-diagonal elements in the covariance matrix, then the features are correlated (i.e., not independent). Increasingly large off-diagonal elements within $\mathbf{\Sigma}$ reflect increasing correlation between the variables (features) (Fig. 4.16). The isocontours of the Gaussian are elliptical, but are not aligned with the feature axes. (In *Principal Component Analysis*, the covariance matrix is diagonalized to remove the off-diagonal, correlated elements.)

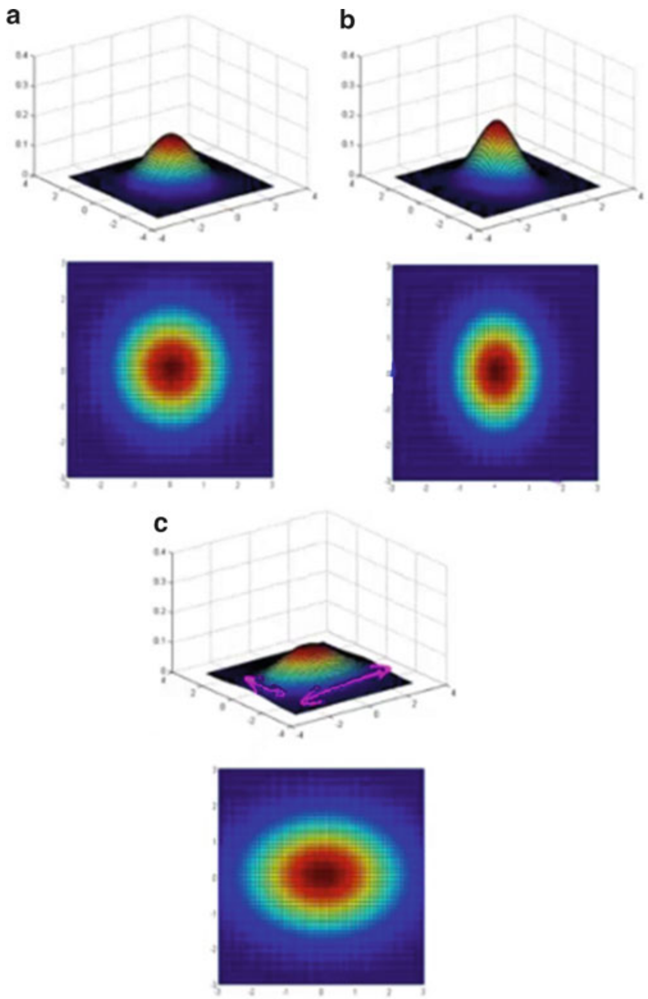

Fig. 4.15 2D Gaussians with (**a**) $\Sigma = \begin{vmatrix} 1 & 0 \\ 0 & 1 \end{vmatrix}$, (**b**) $\begin{vmatrix} 0.6 & 0 \\ 0 & 1 \end{vmatrix}$, (**c**) $\begin{vmatrix} 2 & 0 \\ 0 & 1 \end{vmatrix}$

Consider the case of a zero mean random vector with a diagonal covariance matrix. The isocontours are obtained by computing the curves of constant values for the exponent, that is,

$$\mathbf{x}^{\mathrm{T}}\boldsymbol{\Sigma}^{-1}\mathbf{x} = [x_1, x_2]\begin{vmatrix} 1/\sigma_1^2 & 0 \\ 0 & 1/\sigma_2^2 \end{vmatrix}\begin{vmatrix} x_1 \\ x_2 \end{vmatrix} = C \tag{4.32}$$

$$\text{or} \quad \frac{x_1^2}{\sigma_1^2} + \frac{x_2^2}{\sigma_2^2} = C \tag{4.33}$$

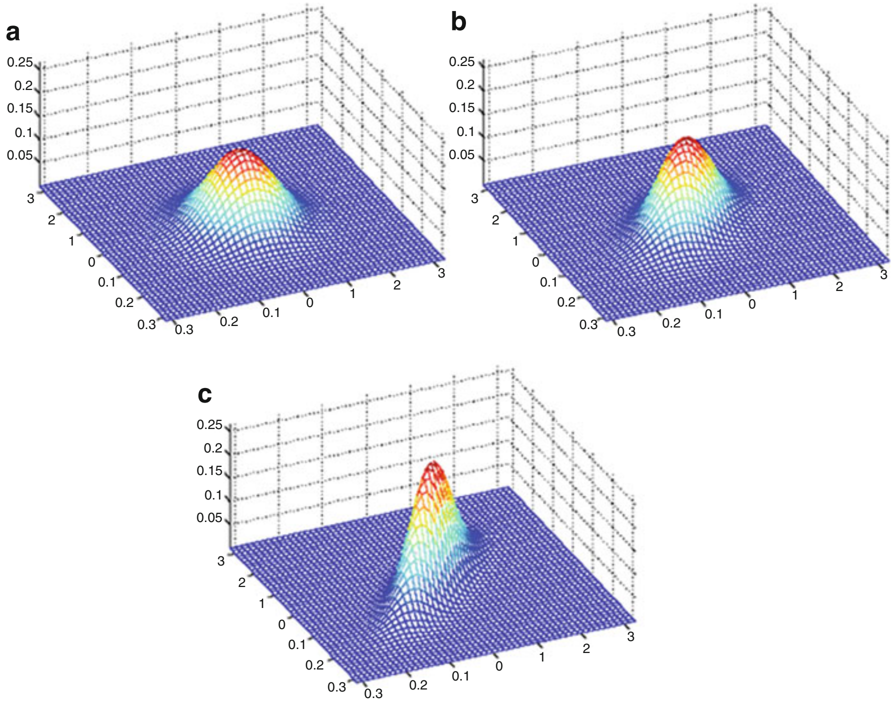

Fig. 4.16 2D Gaussians with (**a**) $\Sigma = \begin{vmatrix} 1 & 0 \\ 0 & 1 \end{vmatrix}$, (**b**) $\Sigma = \begin{vmatrix} 1 & 0.5 \\ 0.5 & 1 \end{vmatrix}$, (**c**) $\Sigma = \begin{vmatrix} 1 & 0.8 \\ 0.8 & 1 \end{vmatrix}$

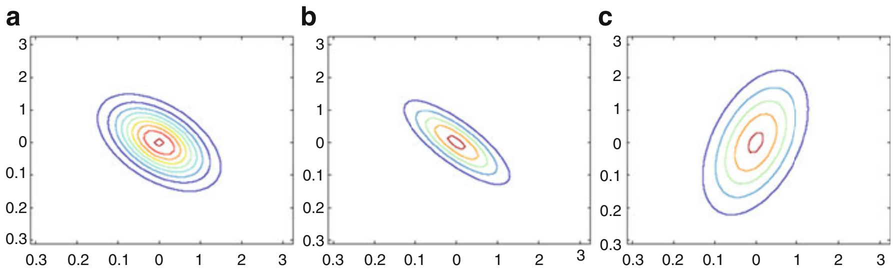

Fig. 4.17 Isocontours for 2D Gaussians with (**a**) $\Sigma = \begin{vmatrix} 1 & -0.5 \\ -0.5 & 1 \end{vmatrix}$, (**b**) $\Sigma = \begin{vmatrix} 1 & -0.8 \\ -0.8 & 1 \end{vmatrix}$, (**c**) $\Sigma = \begin{vmatrix} 3 & 0.8 \\ 0.8 & 1 \end{vmatrix}$

for some constant. This is the equation of an *ellipse* whose axes are determined by the variances of the respective features.

If there are nonzero off-diagonal elements in the covariance matrix (e.g., Figs. 4.16b, c, and 4.17) the ellipses are rotated relative to the feature axes, and the angle of rotation depends on the eigenvectors/eigenvalues of the covariance matrix.

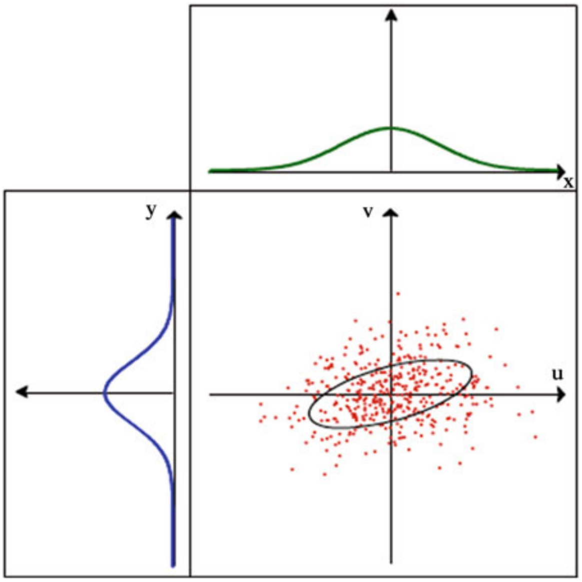

Fig. 4.18 Bivariate Gaussian comprising a univariate Gaussian (*green*) whose variance is 1.6 times the variance of the other (*blue*) univariate Gaussian. The correlation coefficient between the two variables is 0.3

The covariance matrix describes the shape and orientation of sample points using their variances and covariances. If the distribution of samples is known to be *multinormal* (i.e., multivariate Gaussian), then the covariance matrix completely specifies the distribution (except for the position of its mean) and its isocontours are ellipses centered on the centroid of the distribution. Figure 4.18 shows an isocontour of a bivariate Gaussian distribution of samples corresponding to a value of one standard deviation from the mean (in any direction). The long axis of the ellipse (x') is the direction such that the projection of the sample data on x' has the largest possible variance. In intuitive terms, the sample stretches out more in this direction than in any other direction. (In Principal Components Analysis (PCA), x' is known as the *First Principal Component* of the sample.) The small axis of the ellipse y' (the *Second Principal Component* of the sample) is defined as being orthogonal to x'. It is the direction such that the projected sample has the smallest possible variance.

Diagonalization of the covariance matrix rotates the isocontours into line with axes corresponding to new features (x', y'), which are linear combinations of the original features (Fig. 4.19). The diagonal elements are the variances of the projections of the sample points on the x' and y' axes. The first value is the largest possible variance of the projection of the sample points on any axis (Notice that it is larger than either variance in the original covariance matrix). In the language of PCA, this value is the first *eigenvalue* of the (original) covariance matrix. The half-length of the long axis of the ellipse is the square

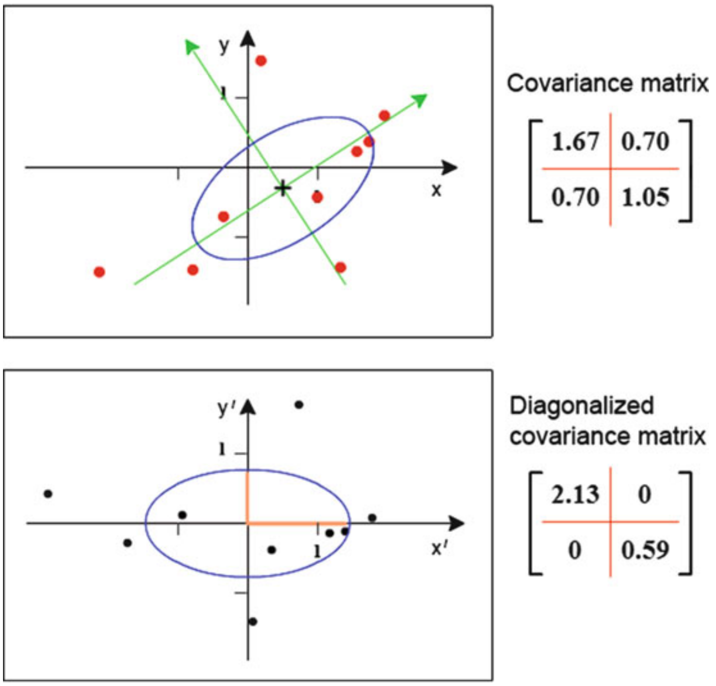

Fig. 4.19 Showing the covariance matrix and a corresponding isocontour of a bivariate Gaussian distribution, before (*top*) and after (*bottom*) diagonalization. [The *blue ellipses* represent one standard deviation from the mean. The *orange segments* (the half-lengths of the rotated ellipse) are the square root of the eigenvalues of the covariance matrix]

root of the first eigenvalue. The second value (second eigenvalue) is the smallest possible variance of the projection of a sample on any axis, and its square root gives the half-length of the short axis of the ellipse. The sum of the two variances in the (original) covariance matrix is equal to the sum of the variances in the diagonalized covariance matrix, viz., the *trace* of a square matrix is invariant under a change of unitary orthogonal frame. Both off-diagonal elements are zero, of course, indicating that the new variables x' and y' have zero covariance and are therefore uncorrelated, i.e., the projections of $\boldsymbol{x}$ on the eigenvectors of the covariance matrix are uncorrelated random variables.

Diagonalization has rotated and shifted the elliptical isocontours, so that they are now centered on the centroid of the data points.

The variance of a probability distribution is analogous to the moment of inertia in classical mechanics of a corresponding mass distribution along a line, with respect to rotation about its center of mass.

Example 4.6 Eigenvalues and eigenvectors

Find the eigenvalues and corresponding eigenvectors of the matrix, $A = \begin{vmatrix} 5 & 3 \\ 3 & 5 \end{vmatrix}$

(Note that this is a real, *symmetric* matrix, i.e., $A = A^{\mathrm{T}}$, typical of the covariance matrix).

In the equation $A\mathbf{x} = \lambda\mathbf{x}$, x is an eigenvector of A and λ its corresponding eigenvalue. We can re-write this as $A\mathbf{x} = \lambda I\mathbf{x}$, where I is the identity matrix, or as $(\lambda I - A)\mathbf{x} = 0$

For λ to be an eigenvalue, there must be a nonzero solution of this equation: and this occurs when $\det(\lambda I - A) = 0$ (called the *characteristic equation* of A).

$$\det(\lambda I - A) = \begin{vmatrix} \lambda - 5 & -3 \\ -3 & \lambda - 5 \end{vmatrix} = 0$$

$$\lambda^2 - 10\lambda + 16 = 0$$
$$(\lambda - 2)(\lambda - 8) = 0$$

So the eigenvalues of A are $\lambda_1 = 2$ and $\lambda_2 = 8$.
Substituting $\lambda_1 = -2$ into $A\mathbf{x} = \lambda\mathbf{x}$

$$\begin{vmatrix} 5 & 3 \\ 3 & 5 \end{vmatrix}\begin{vmatrix} x_1 \\ x_2 \end{vmatrix} = 2\begin{vmatrix} 0 \\ 0 \end{vmatrix}$$

which gives $3x_1 + 3x_2 = 0$
from which we deduce that the corresponding eigenvector, $\mathbf{e}_1 = \begin{vmatrix} 1 \\ -1 \end{vmatrix}$

In a similar manner, for the eigenvalue $\lambda_2 = 8$, we get $-3x_1 + 3x_2 = 0$; from which $\mathbf{e}_2 = \begin{vmatrix} 1 \\ 1 \end{vmatrix}$

The eigenvectors are orthogonal (which only happens for a real, symmetric matrix) and, in this case, are rotated $\pi/4$ rad from the original axes. In the coordinate system of these new (principal) directions the isocontours will be ellipses and the ellipse corresponding to one standard deviation will be

$$\frac{u^2}{8^2} + \frac{v^2}{2^2} = 1$$

It is sometimes convenient to transform an arbitrary multivariate distribution (i.e., with ellipsoidal isocontours) into a distribution with spherical isocontours. Such a transform is known as a *whitening* transform. This achieves the same result as standardizing or normalizing the data (to zero mean and unit variance) during pre-processing.

4.3.3 The Mahalanobis Distance

The Mahalanobis distance is a generalization of Euclidean distance. It is an appropriate measure when variables have different scales and are correlated, but still are approximately Gaussian distributed. The Mahalanobis distance between two objects, D, in feature space is given by

$$D_{\mathrm{m}}(\mathbf{x}, \mathbf{y}) = \mathrm{sqrt}((\mathbf{x} - \mathbf{y})\Sigma^{-1}(\mathbf{x} - \mathbf{y})^{\mathrm{T}}) \tag{4.34}$$

where $\boldsymbol{\Sigma}^{-1}$ is the inverse of the covariance matrix of the data. It is common to work with the square of the Mahalanobis distance, and this is what appears within the exponential in the multivariate Gaussian [(4.23)]. Thus, the isocontours of the multivariate Gaussian are ellipsoids of constant Mahalanobis distance.

Consider the problem of estimating the probability that a test data point in N-dimensional feature space belongs to a (labeled) class. The first step would be to find the average or center of mass of the sample points, $\boldsymbol{\mu}$. Intuitively, the closer the point in question is to this center of mass, the more likely it is to belong to the class. However, we also need to know if the class is spread out over a large range or a small range, so that we can decide whether a given distance from the center is significant or not. The simplistic approach would be to estimate the width of the class distribution (viz., the standard deviation of the distances of the sample points from the center of mass). If the distance between the test point and the center of mass is less than one standard deviation, then we might conclude that it is highly probable that the test point belongs to the class. The further away it is, the more likely that the test point should not be classified as belonging to the class.

This intuitive approach can be made scale-independent by using normalized distances, i.e., $(x - \mu)/\sigma$. However, this assumes that the sample points are distributed about the center of mass in a spherical manner. This is not the case for a multivariate Gaussian distribution: the isocontours are elliptical (in 2D) or ellipsoidal (in 3D) and the probability of the test point belonging to the class will depend not only on the distance from the center of mass, but also on the direction. In those directions where the ellipsoid has a short axis, the test point must be closer, while in those where the axis is long the test point can be further away from the center. The isocontours can be estimated by building the covariance matrix of the samples. The Mahalanobis distance is then the distance of the test point from the center of mass, normalized (i.e., divided) by the width of the ellipsoid in the direction of the test point. Figure 4.20 shows two points in feature space which are at the same Mahalanobis distance from the center of a distribution. The square of their Mahalanobis distance is given by

$$D_{\mathrm{m}}^2 = (\mathbf{x} - \mu) \quad \Sigma^{-1}(\mathbf{x} - \mu)^{\mathrm{T}} \tag{4.35}$$

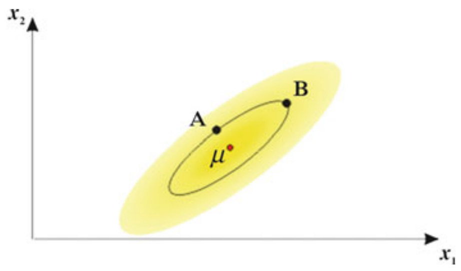

Fig. 4.20 Two points, *A* and *B*, at the same Mahalanobis distance from the centroid, μ

If the covariance matrix is diagonal, the Mahalanobis distance reduces to the *normalized Euclidean distance*; and if the covariance matrix is the identity matrix, the Mahalanobis distance reduces to the (standard) Euclidean distance.

The Mahalanobis distance is widely used in supervised classification techniques (e.g., Fisher's Linear Discriminant Analysis (LDA), see Sect. 7.3.2) and in cluster analysis (see Chap. 7). A test point is classified as belonging to that class for which the Mahalanobis distance is minimal.

Example 4.7

In a two-class, two-feature classification task, the feature vectors are described by two normal distributions sharing the same covariance, $\Sigma = \begin{vmatrix} 1.1 & 0.3 \\ 0.3 & 1.9 \end{vmatrix}$ and the mean vectors are $\boldsymbol{\mu_1} = [0, 0]^T$, $\boldsymbol{\mu_2} = [3, 3]^T$, respectively.

1. Classify the vector $[1.0, 2.2]^T$.
   Compute the Mahalanobis distances from the two means

$$D_m^2(\mu_1, \mathbf{x}) = (\mathbf{x} - \mu_1)^T \Sigma^{-1} (\mathbf{x} - \mu_1) = [1.0, 2.2] \begin{vmatrix} 0.95 & -0.15 \\ -0.15 & 0.55 \end{vmatrix} \begin{vmatrix} 1.0 \\ 2.2 \end{vmatrix}$$
$$= 2.952$$

$$D_m^2(\mu_2, \mathbf{x}) = (\mathbf{x} - \mu_2)^T \Sigma^{-1} (\mathbf{x} - \mu_2) = [-2.0, -0.8] \begin{vmatrix} 0.95 & -0.15 \\ -0.15 & 0.55 \end{vmatrix} \begin{vmatrix} -2.0 \\ -0.8 \end{vmatrix}$$
$$= 3.672$$

   The vector is assigned to class 1, since it is closer to $\boldsymbol{\mu_1}$. (Note that it is closer to $\boldsymbol{\mu_2}$ if Euclidean distances are taken.)
2. Compute the principal axes of the ellipse centered at $[0, 0]^T$ that corresponds to a constant Mahalanobis distance $D_m = \sqrt{2.952}$ from the center.
   Calculating the eigenvalues of $\boldsymbol{\Sigma}$

$$\det \begin{vmatrix} 1.1 - \lambda & 0.3 \\ 0.3 & 1.9 - \lambda \end{vmatrix} = \lambda^2 - 3\lambda + 2 = 0$$

(continued)

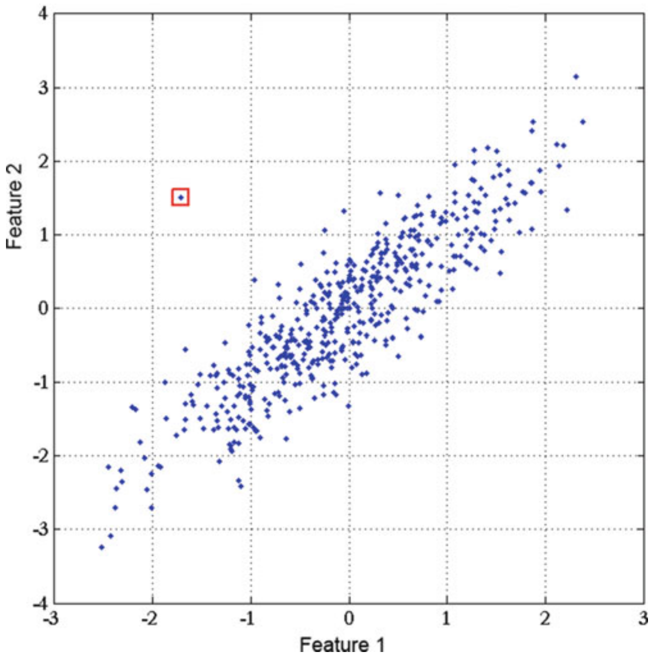

Fig. 4.21 Example of a multivariate outlier

(continued)

gives $\lambda_1 = 1$ and $\lambda_2 = 2$. Substituting these values back into the characteristic equation gives the unit norm eigenvectors $\begin{vmatrix} 3/\sqrt{10} \\ -1/\sqrt{10} \end{vmatrix}$ and $\begin{vmatrix} 1/\sqrt{10} \\ 3/\sqrt{10} \end{vmatrix}$.

The eigenvectors give the axes of the isocontours (note that they are mutually orthogonal), and the half-lengths of the axes are proportional to the square roots of the corresponding eigenvalues.

The principal axes have lengths 3.436 (i.e., $2 \times \sqrt{2.952}$) and 4.860 (i.e., $\sqrt{2} \times$ minor axis), respectively.

The Mahalanobis distance can also be used to detect outliers, as samples that have a significantly greater Mahalanobis distance from the mean than the rest of the samples.

In Fig. 4.21 the sample point enclosed by the red square clearly does not belong to the distribution exhibited by the rest of the sample points. Simple univariate tests for outliers would fail to detect it as an outlier. Although there are quite a few sample points with more extreme values of both feature 1 and feature 2, the Mahalanobis distance of this sample point would be larger than for any other point.

The Mahalanobis distance could be used to measure the separation between two classes (i.e., their *dissimilarity*), by measuring the distance between their respective centers. Each class may have different numbers of samples. For two classes with identical covariance matrices, the Mahalanobis distance is $D_{\mathrm{m}}(1, 2) = (\mu_1 - \mu_2)^{\mathrm{T}} \boldsymbol{\Sigma}^{-1} (\mu_1 - \mu_2)$. A Mahalanobis distance greater than 3 (i.e., the two centers differ by more than three standard deviations) would indicate that the overlap between the two classes is small.

4.4 Exercises

1. Three coins are tossed simultaneously. What is the probability of them showing two heads?
2. (a) What is the probability of getting at least one "6" if three dice are rolled? (b) What is the probability of getting at least one "6" in four rolls of a single die? (c) What is the probability of getting at least one double-6 in 24 throws of a pair of dice?
3. Consider a family with two children. Given that one of the children is a boy, what is the probability that both children are boys?
4. There are two cookie jars. Jar 1 contains two chocolate chip cookies and a plain cookie, and jar 2 contains one chocolate chip cookie and one plain cookie. If Fred is blind-folded and chooses a jar at random, and then a cookie at random from that jar, what is the probability that he will choose a chocolate chip cookie? What is the probability that it came from jar 1?
5. Suppose that a rare disease affects 1 out of every 1,000 people in a population, i.e., the prior probability is 1/1,000. And suppose that there is a good, but not perfect, test for the disease. For a person who has the disease, the test comes back positive 99% of the time (sensitivity = 0.99) and if for a person who does not have the disease the test is negative 98% of the time (specificity = 0.98). You have just tested positive; what are your chances of having the disease? (Try by calculation, and then check using CondProb.xls).
6. Consider the situation discussed in Example 4.3 in the text. The woman in question tested positive and her posterior probability of having breast cancer was calculated to be 7.76%. If she decides to go for another test and she tests positive a second time, what is the probability of her having breast cancer? (And what if a third, fourth, fifth test was positive, what would the corresponding probabilities be? Of course, this is an unlikely scenario since each test exposes her to X-rays and a consequent risk of actually causing cancer.) (Try by calculation, and then check using CondProb.xls.)

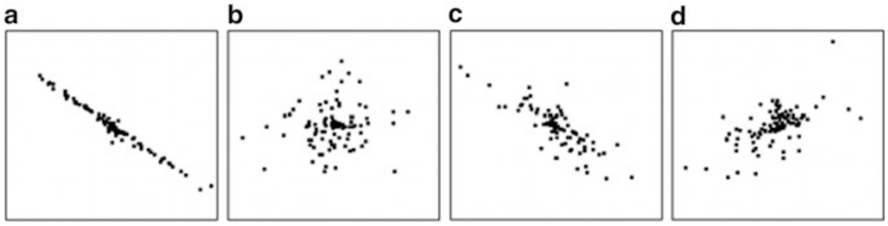

Fig. 4.22 Scatter plots

7. Consider the following feature vector:

$$x = \begin{bmatrix} 7 & 4 & 3 \\ 4 & 1 & 8 \\ 6 & 3 & 5 \\ 8 & 6 & 1 \\ 8 & 5 & 7 \\ 7 & 2 & 9 \\ 8 & 2 & 2 \\ 7 & 4 & 5 \\ 9 & 5 & 8 \\ 5 & 3 & 3 \end{bmatrix}$$

representing a set of ten observations of three features of an object. Calculate the covariance matrix (and check it using MatLab (with the command `cov`(A))).

8. We want to classify a given person as male or female based on height, weight, and foot size. The data from an example training set (assumed Gaussian) is:

Sex	Height (feet)	Weight (lbs)	Foot size (inches)
M	6	180	12
M	5.92 (5′11″)	190	11
M	5.58 (5′7″)	170	12
M	5.92 (5′11″)	165	10
F	5	100	6
F	5.5 (5′6″)	150	8
F	5.42 (5′6″)	130	7
F	5.75 (5′9″)	150	9

How would you classify a sample with height $= 6'$, weight $= 130$ lbs., and foot size $= 8''$? Use (1) the naïve Bayes' classifier (i.e., assuming no covariance between thefeatures) (2) the covariance matrices and the Mahalanobis distances (Hint: use MatLab).

9. Match the scatter plot (a–d) in Fig. 4.22 to the correct correlation coefficient (1) 0.14, (2) −0.99, (3) 0.43, and (4) −0.77.

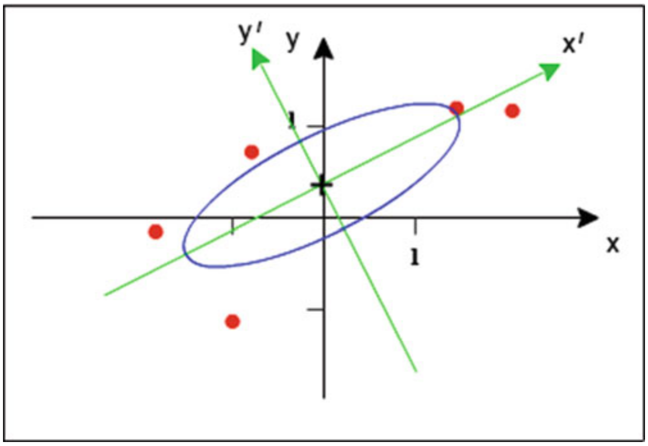

Fig. 4.23 Data points in feature space (assumed bivariate Gaussian) and a corresponding isocontour

10. Tabulate the data shown in Fig. 4.23 (download it from the http://extras.springer.com) and obtain the coordinates [in (x, y)] using an imaging program (ImageJ or Photoshop, or similar). Construct the covariance matrix (in the (x, y) coordinate system) from the data shown. Diagonalize the matrix (to get the coordinates in (x', y')) (Use $[V, D] =$ `eig`(A) in MatLab: the eigenvalues of A are obtained in D, and the columns of V are the eigenvectors of A).
11. Find the eigenvalues and eigenvectors of the matrix $\begin{vmatrix} 1 & 3 \\ 4 & 2 \end{vmatrix}$ (using MatLab's `eig`(A)).

References

Fisher, R.A.: The use of multiple measurements in taxonomic problems. Ann. Eugen. **7**, 179–188 (1936)

Gonick, L., Smith, W.: The Cartoon Guide to Statistics. Harper Collins, New York (1993)

Zhang, H.: The optimality of Naïve Bayes. Proceedings of 17th International FLAIRS (Florida Artificial Intelligence Research Society) Conference. AAAI Press (2004)

Chapter 5
Supervised Learning

5.1 Parametric and Non-parametric Learning

Parametric methods of statistical classification require probability distributions and estimate parameters derived from them such as the mean and standard deviation to provide a compact representation of the classes. Examples include *Bayes' decision rule*, based explicitly on probability distributions, and *discriminant analysis*, a parametric method based on functions which separate the classes. Parametric methods tend to be slow at training, but once trained they are fast at classifying test data. If the probability distributions are not known, then we must use *non-parametric* methods. In this case, we either estimate the density functions (e.g., the *Parzen window* approach) or bypass the probabilities and directly construct decision boundaries based on the training data (e.g., the *k-nearest neighbor* rule). (In fact, the multilayer perceptron can also be viewed as a supervised non-parametric method which constructs a decision boundary).

5.2 Parametric Learning

5.2.1 Bayesian Decision Theory

5.2.1.1 Single Feature (1D)

In statistical pattern recognition approaches, we develop classifiers which use all the available information, such as measurements and an a priori (or simply prior) probability. Combining this information leads to a measurement-conditioned or a posteriori (or posterior) probability. We can formulate a decision rule based on the posterior probabilities.

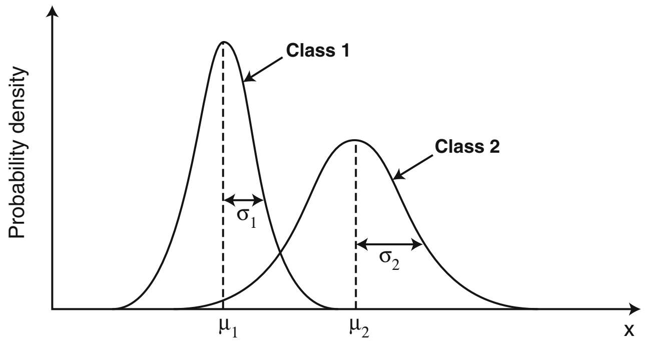

Fig. 5.1 Probability density functions for two classes, 1 and 2; often they will be Gaussian in shape

Let us consider that there are just two classes [class 1 (ω_1) and class 2 (ω_2)] and that the (prior) probabilities are known [for example, $P(\omega_1) = 0.7$ and $P(\omega_2) = 0.3$ (which sum to unity)]. Faced with a new sample and **no** additional information, the decision rule would be to classify this sample as belonging to ω_1, since $P(\omega_1) > P(\omega_2)$. The probability of classification error, in general, is

$$P(\text{error}) = P(\text{choose } \omega_2|\omega_1) \cdot P(\omega_1) + P(\text{choose } \omega_1|\omega_2) \cdot P(\omega_2) \tag{5.1}$$

In this case, since we always choose ω_1, $P(\text{error}) = P(\text{choose } \omega_1|\omega_2)$. $P(\omega_2) = 1.0 \times 0.3 = 0.3$.

Now consider that we have a single feature, x (e.g., a length or brightness). We have a training set, which includes representative examples from both classes; so that we can measure the feature for both classes and construct probability distributions for each (Fig. 5.1). These are formally known as the probability density functions or *class-conditional probabilities*, $p(x|\omega_1)$ and $p(x|\omega_2)$, i.e., the probabilities of measuring the value x, given that the feature is in class 1 or class 2, respectively. If we have a large number of examples in each class, then the probability density functions will be Gaussian in shape (the Central Limit Theorem).

The classification problem is: given a new object with a particular value of this feature, to which class does this object belong? If the two probability density functions overlap, then this cannot be answered definitively, only statistically.

If the probability density functions and the prior probabilities are known, then the posterior probability, $P(\omega_i|x)$ (i.e., the probability that given a feature value of x, the feature belongs to class ω_i) can be calculated using Bayes' rule (from Chap. 4)

$$P(A|B) = \frac{P(B|A) \cdot P(A)}{P(B)}$$

which will help in the decision. We would evaluate the posterior probability of each class and choose the class with the largest posterior probability [i.e., this is a *maximum a posteriori* (MAP) classifier]. Using Bayes' rule, the posterior probability for each class ($i = 1, 2$) of measuring a particular feature, x, is

$$P(\omega_i|x) = \frac{p(x|\omega_i) \cdot P(\omega_i)}{p(x)} \tag{5.2}$$

and our decision rule becomes

$$\begin{aligned} &\text{If} \quad \frac{p(x|\omega_1) \cdot P(\omega_1)}{p(x)} > \frac{p(x|\omega_2) \cdot P(\omega_2)}{p(x)} \quad \text{choose } \omega_1 \\ &\qquad\qquad\qquad\qquad\qquad\qquad \text{else} \quad \text{choose } \omega_2 \end{aligned}$$

(where we are using upper-case P for probability and lower-case p for probability density). The term $p(x)$ can be considered a scale factor that states how frequently we will actually measure an object with value x: it guarantees that the posterior probabilities sum to unity, but is unimportant in making a decision.

Dividing through by $p(x)$ and re-arranging, the decision rule can be written in a different (but equivalent) form

$$\begin{aligned} &\frac{p(x|\omega_1)}{p(x|\omega_2)} > \frac{P(\omega_2)}{P(\omega_1)} \quad \text{choose } \omega_1 \\ &\qquad\qquad\qquad \text{else} \quad \text{choose } \omega_2 \end{aligned}$$

The quantity on the left-hand side of this equation (the ratio of the class-conditional density functions) is called the *likelihood ratio*, and the decision rule is called the *likelihood ratio test*.

Example 5.1

Let us suppose that a single measurement has Gaussian class-conditional densities of equal variance ($\sigma^2 = 1$) but different means ($\mu_1 = 4$ and $\mu_2 = 10$) and that the prior probabilities are equally likely [$P(\omega_1) = P(\omega_2) = 0.5$]. The corresponding class-conditional probability density functions and posterior probabilities are shown in Fig. 5.2.

Using (1D) Gaussians [(4.22)] as the class-conditional probability functions, and the given values for the means, the variances and the prior probabilities, the likelihood ratio test [(5.4)] becomes

$$\begin{aligned} &\frac{\exp(-\frac{1}{2}(x-4)^2)}{\exp(-\frac{1}{2}(x-10)^2)} > \frac{0.5}{0.5} > 1 \quad \text{choose } \omega_1 \\ &\qquad\qquad\qquad\qquad\qquad \text{else} \quad \text{choose } \omega_2 \end{aligned}$$

(continued)

(continued)

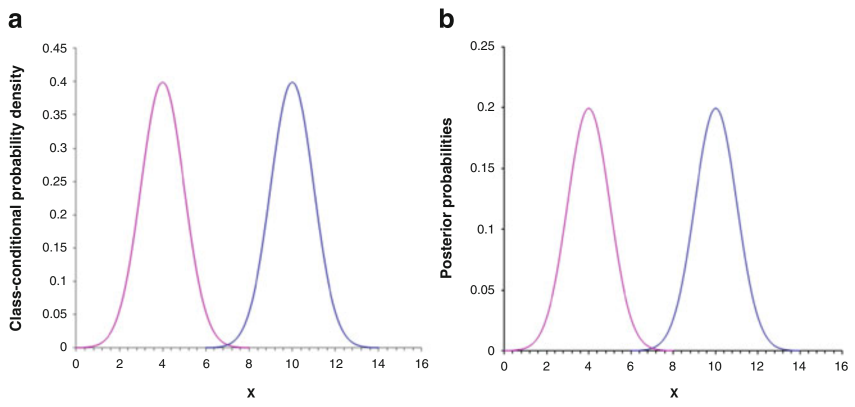

Fig. 5.2 For Gaussians with means of $\mu_1 = 4$ and $\mu_2 = 10$ and equal variances $(\sigma_1^2 = \sigma_2^2 = 1)$ (**a**) the class-conditional probabilities and (**b**) the posterior probabilities of measuring a feature, x

Cross-multiplying, taking the natural logs and simplifying gives

$$(x-4)^2 - (x-10)^2 < 0$$

or

$$\begin{array}{ll} x<7 & \text{choose } \omega_1 \\ \text{else} & \text{choose } \omega_2 \end{array}$$

As intuitively expected for this case, the decision threshold is mid-way between the two means. The decision threshold is the value at which the two posterior probabilities are equal, given by the intersection of the posterior probabilities in Fig. 5.2b. (In the case of equal prior probabilities, this corresponds to the intersection of class-conditional probability densities). Note that the area under each class-conditional probability function equals unity, whereas it is the sum of the areas under the posterior probabilities which sums to unity.

Example 5.2

If the prior probabilities are equal $[P(\omega_1) = P(\omega_2) = 0.5]$, the means remain the same as before ($\mu_1 = 4$ and $\mu_2 = 10$), but the class-conditional densities have different variances, $\sigma_1^2 = 4$ and $\sigma_2^2 = 1$ (Fig. 5.3), the decision rule becomes

$$\frac{\frac{1}{2}\cdot\exp(-1/(2\times 4)(x-4)^2)}{\exp(-\frac{1}{2}(x-10)^2)} > 1 \quad \text{choose } \omega_1 \text{else} \quad \text{choose } \omega_2$$

(continued)

(continued)

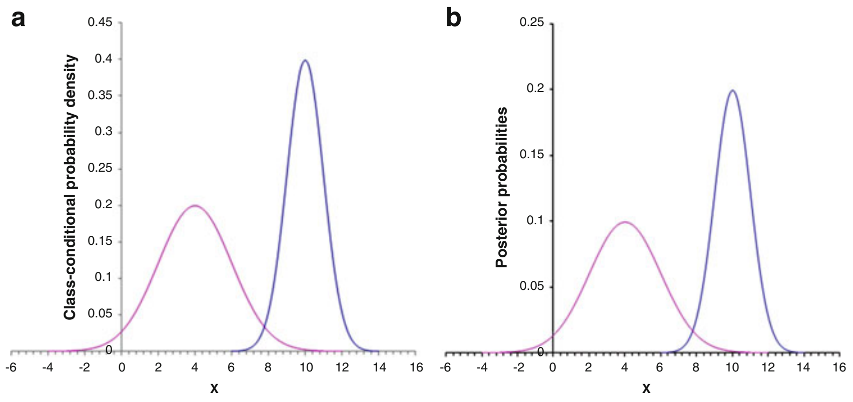

Fig. 5.3 For Gaussians with means of $\mu_1 = 4$ (in *red*) and $\mu_2 = 10$ (in *blue*), and variances of $\sigma_1^2 = 4$ and $\sigma_2^2 = 1$ (**a**) the class-conditional probabilities and (**b**) the posterior probabilities of measuring a feature, x

Cross-multiplying, taking the natural logs and simplifying gives

$$8\ln\frac{1}{2} - (x-4)^2 > -4(x-10)^2 \quad \text{choose } \omega_1$$
$$3x^2 - 72x + (384 + 8\ln\frac{1}{2}) > 0$$

Solving this quadratic gives two different roots, and therefore two different decision thresholds, at

$$x = (72 \pm 25.3)/6$$
$$= 7.78 \text{ and } 16.22$$

The class-conditional probability densities and posterior probabilities are shown in Fig. 5.3. (Since the prior probabilities, $P(\omega_i)$, are equal, the class-conditional and posterior probability functions are just scaled version of each other). The lower decision threshold (corresponding to the smaller root, $x = 7.78$) is easily seen, but the upper decision threshold (corresponding to the larger root, $x = 16.22$) is not so obvious in Fig. 5.3b. However, if we note that the posterior probability for class ω_1 does not decay as fast as that for class ω_2 at higher values of x, we can understand that a second intersection will occur (and this is at $x = 16.22$). With reference to Fig. 5.3b, we can see that the decision rule is

(continued)

(continued)

$$x<7.78 \text{ or } x>16.22 \quad \text{choose } \omega_1$$
$$7.78<x<16.22 \quad \text{choose } \omega_2$$

(Note that it is much easier to get the "greater than" and "less than" signs correct if there is a diagram with which to visualize the situation).

Example 5.3

If the prior probabilities are not equal [say $P(\omega_1) = 2/3$ and $P(\omega_2) = 1/3$], but the variances are equal $(\sigma_1^2 = \sigma_2^2 = 1)$ the likelihood test becomes

$$\frac{\exp(-\frac{1}{2}(x-4)^2)\cdot 2/3}{\exp(-\frac{1}{2}(x-10)^2)\cdot 1/3} > 1 \quad \text{choose } \omega_1$$
$$\text{else} \quad \text{choose } \omega_2$$

Solving this gives a single decision boundary at $x = 7.12$ (Fig. 5.4), because the roots of the resulting quadratic are equal. The decision threshold(s) is/are given by the intersection(s) of the posterior probabilities. (Note that in the case of unequal priors, this does not correspond to the intersection of the class-conditional probabilities). In the case of several features, the *decision boundaries* will be lines or planes.

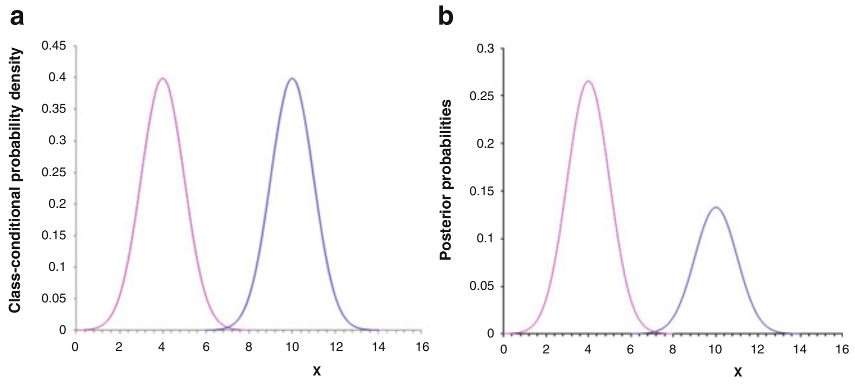

Fig. 5.4 For Gaussians with means of $\mu_1 = 4$ and $\mu_2 = 10$, equal variances $(\sigma_1^2 = \sigma_2^2 = 1)$ and prior probabilities $P(\omega_1) = 2/3$ and $P(\omega_2) = 1/3$ (**a**) the class-conditional probabilities and (**b**) the posterior probabilities of measuring a feature, x

In the case of two Gaussian distributions with equal priors (Fig. 5.5a), the decision threshold (D_1) will be at the intersection of the probability distribution functions, and there will be misclassification errors (shown by the striped areas in the figure): both false positives (or type I errors) and false negatives (or type II

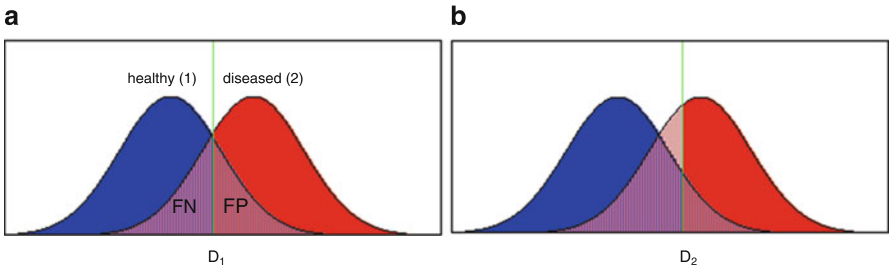

Fig. 5.5 Intersecting distributions with a decision threshold (**a**) at the intersection point and (**b**) higher than the intersection point

errors). Moving the decision threshold changes the classification. For example, moving the decision threshold higher (to D_2 in Fig. 5.5b) reduces the number of false positives but unfortunately it also increases the number of false negatives. (Moving the decision threshold lower will increase the number of false positives and reduce the number of false negatives). From Fig. 5.5b, we see that the false negatives will be reduced somewhat, but the false positives will be increased by an even larger amount; so that the total number of errors in classification (FP + FN) will actually increase (by the area shown in light brown in Fig. 5.5b). (This is also the case if the decision threshold is lowered from D_1). Thus taking the decision threshold at the intersection of the distributions minimizes the total errors (FPF + FNF). This general geometric argument also holds if the Gaussians have different variances or if they are scaled by different priors. Indeed, the posterior probabilities do not even have to be Gaussian; they just need to be monotonic in the region around their intersection point(s). Thus Bayes' rule, whereby we choose the class according to the maximum (posterior) probability, corresponds to minimizing the (total) probability of error (the *error rate*) and therefore our decision rule is an *optimal* decision rule.

Let us consider the problem of classifying two types of fish: sea bass (class ω_1) and salmon (class ω_2) as they travel down a conveyor belt in a canning factory. Let us say that the lightness of the fish are measured for samples of the two types of fish, and the resulting class-conditional probability density functions, $p(x|\omega_1)$ and $p(x|\omega_2)$, are shown in Fig. 5.6.

The season and the locale (and many other variables) determine directly the probability of the two different types of fish being caught, but suppose that for this particular catch, twice as many sea bass as salmon were caught, so that $P(\omega_1) = 2/3$ and $P(\omega_2) = 1/3$. We can determine the posterior probabilities using (5.2), by scaling the class-conditional probabilities by the priors, and dividing by the evidence term to ensure that the probabilities sum to 1 (Fig. 5.7). Check on this figure that any feature measurement for a test sample (e.g., lightness = 13) results in posterior probabilities that sum to 1 (in the case of lightness = 13, the posterior probabilities are 0.79 and 0.21 for class 1 and 2, respectively): note that the two curves are mirror images of each other about the (horizontal) $P(\omega_i|x) = 0.5$ line.

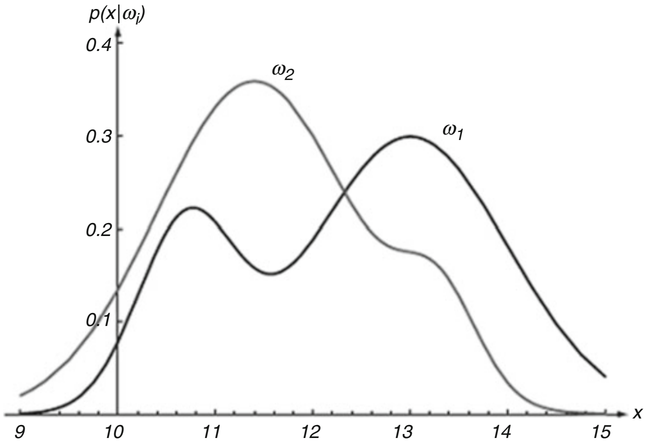

Fig. 5.6 Class-conditional probability functions of measuring the lightness, x, of fish that are in classes ω_1 (sea bass) and ω_2 (salmon). (Note that the area under each density function is unity) (after Duda et al. 2001)

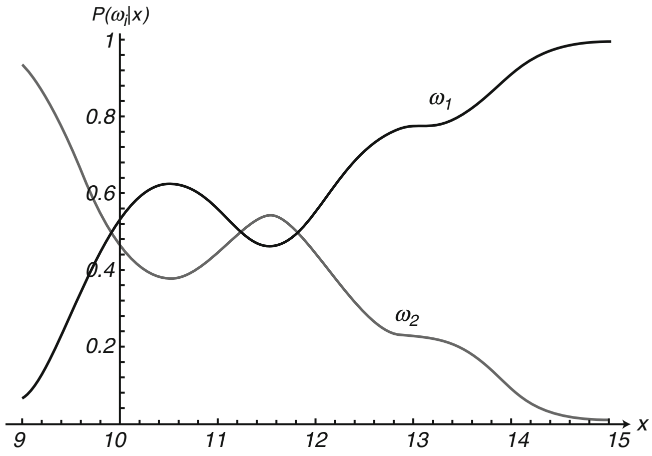

Fig. 5.7 Posterior probabilities corresponding to the class-conditional probabilities of Fig. 5.4, with $P(\omega_1) = 2/3$ and $P(\omega_2) = 1/3$. Note that the posterior probabilities sum to unity, at every value of x

The lightness of each new fish coming along the conveyor belt is measured, and we will classify it as sea bass or salmon according to the posterior probabilities. Specifically, we will choose the class with the larger posterior probability of having that value of lightness. From Fig. 5.7, we will classify the fish as sea bass (ω_1) if its lightness, x, is $9.9 < x < 11.2$ or $x > 11.8$, otherwise we will classify it as salmon (ω_2).

We have assumed that the two types of classification errors (misclassifying sea bass as salmon, and misclassifying salmon as sea bass) are of equal importance. However, this may not always be true. For example, our customers may not mind some of the more expensive salmon turning up in their cans of sea bass, but they may have more objections to misclassified sea bass turning up in their salmon cans. [Or, in our medical example, it may be less serious to misdiagnose a benign tumor as a malignant cancer (a false positive), than to misdiagnose a malignant cancer as a benign one (a false negative): the false positive will result in unnecessary treatment, but the false negative may result in no treatment being given resulting in the death of the patient.] For these cases, we can introduce a penalty term, λ_{ij}, known as the *loss*, associated with a wrong decision (viz., a misclassification). λ_{ij}, is the loss associated with deciding ω_i when the correct state is ω_j. (The expected loss by deciding ω_i when the correct state is ω_j, is called a *risk*, R, in this case the conditional risk). The complete *loss matrix* for a two-class problem would be

$$\lambda = \begin{vmatrix} \lambda_{11} & \lambda_{12} \\ \lambda_{21} & \lambda_{22} \end{vmatrix} \tag{5.5}$$

where the diagonal terms are usually set to zero (i.e., no cost for making the correct decision). In the case where ω_1 represents the healthy distribution and ω_2 the diseased distribution, then λ_{12} (the loss associated with a false negative) $> \lambda_{21}$ (the loss associated with a false positive). If action α_1 corresponds to deciding that the true state of nature is ω_1, and action α_2 corresponds to deciding that the true state of nature is ω_2, then λ_{ij} is shorthand for $\lambda(\alpha_i|\omega_j)$. The conditional risks involved in choosing either way are

$$R(\alpha_1|x) = \lambda_{11}P(\omega_1|x) + \lambda_{12}P(\omega_2|x) \tag{5.6a}$$

$$R(\alpha_2|x) = \lambda_{21}P(\omega_1|x) + \lambda_{22}P(\omega_2|x) \tag{5.6b}$$

Generalizing (5.4), to include the loss terms, the decision rule (in terms of the likelihood ratio) can be written

$$\frac{p(x|\omega_1)}{p(x|\omega_2)} > \frac{(\lambda_{12} - \lambda_{22}) \cdot P(\omega_2)}{(\lambda_{21} - \lambda_{11}) \cdot P(\omega_1)} \quad \text{choose } \omega_1$$
$$\text{else} \quad \text{choose } \omega_2$$

The effect of introducing loss terms such that $\lambda_{12} > \lambda_{21}$ is to shift the decision threshold in Fig. 5.5a to the left, reducing the number of false negatives. [In the case where the diagonal terms are zero and the errors are equally costly ($\lambda_{12} = \lambda_{21}$), then λ is the so-called symmetrical or *zero-one* loss function, and (5.7) reduces to (5.4)].

Example 5.4

Select the optimal decision where $p(x|\omega_1) = N(2, 0.25), p(x|\omega_2) = N(1.5, 0.04)$; $P(\omega_1) = 2/3$, $P(\omega_2) = 1/3$; and $\lambda = \begin{pmatrix} 0 & 1 \\ 2 & 0 \end{pmatrix}$.
Since $\lambda_{21} > \lambda_{11}$, decide ω_1, if

$$\frac{p(x|\omega_1)}{p(x|\omega_2)} > \frac{\lambda_{12} - \lambda_{22} \cdot P(\omega_2)}{\lambda_{21} - \lambda_{11} \cdot P(\omega_1)}$$

$$p(x|\omega_1) = \frac{2}{\sqrt{2\pi}} \mathrm{e}^{-2(x-2)^2} \quad \text{and} \quad p(x|\omega_2) = \frac{5}{\sqrt{2\pi}} \mathrm{e}^{-\frac{25}{2}\left(x-\frac{3}{2}\right)^2}$$

The likelihood ratio for the two normal distributions is

$$\frac{p(x|\omega_1)}{p(x|\omega_2)} = \frac{2}{5} e^{-2(x-2)^2 + \frac{25}{2}(x-1.5)^2} > \frac{1-0}{2-0} \cdot \frac{1/3}{2/3} = \frac{1}{4}$$

$$\mathrm{e}^{-2(x-2)^2 + \frac{25}{2}(x-1.5)^2} > \frac{5}{8}$$

taking (natural) logs $\Rightarrow -2(x - 2)^2 + 25(x - 1.5)^2/2 > -0.47$

- $x^2 - 2.8095x + 1.9614 > 0$
- $x = 1.514$ or $x = 1.296$

Therefore, $x > 1.514$ or $x < 1.296$ to decide ω_1;
and if $1.296 < x < 1.514$, decide ω_2.

In the general univariate case, the decision rule of (5.7) could be re-written as

$$\text{If} \quad \frac{p(x|\omega_1)}{p(x|\omega_2)} > k \quad \text{choose } \omega_1 : \text{else choose } \omega_2 \tag{5.8}$$

$$\text{where } k = \frac{(\lambda_{12} - \lambda_{22}) \cdot P(\omega_2)}{(\lambda_{21} - \lambda_{11}) \cdot P(\omega_1)}$$

If the class-conditional probabilities are Gaussian distributions, $N(\mu_1, \sigma_1^2)$ and $N(\mu_2, \sigma_2^2)$, substituting them into (5.8), taking (natural) logs and simplifying gives:

$$((x - \mu_2)/\sigma_2)^2 - ((x - \mu_1)/\sigma_1)^2 > 2 \ln \frac{(\sigma_1 \cdot k)}{(\sigma_2)} \tag{5.9}$$

which is a quadratic in x. The terms can be collected into the form $ax^2 + bx + c$, and solved to give solutions ("roots") for x, which are the decision thresholds. There are two roots, $x+$ and $x-$, which are equal when $(b^2 - 4ac)^{½} = 0$.

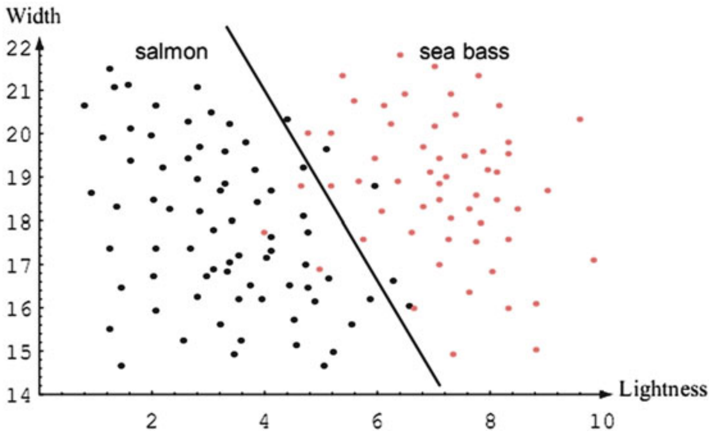

Fig. 5.8 2D feature space for training samples of lightness and width in sea bass and salmon, and a putative linear decision boundary (after Duda et al. 2001)

The Excel file,CondProb.xls (downloadable from http://extras.springer.com), solves for the roots in "Formulation III". It also displays derived quantities, such as sensitivity and specificity, the joint and marginal probabilities and the conditional probabilities.

5.2.1.2 Multiple features

Since a single feature cannot achieve error-free classification if there is an overlap of the pdfs, we should consider measuring an additional independent, i.e., uncorrelated, feature (even if it is also not perfect). In our example of classifying the fish, we might consider measuring their width as well as their lightness. As sea bass are typically wider than salmon, we now have two features to help classify the fish: lightness and width. Using two features, our training data is plotted in two-dimensional *feature space* (Fig. 5.8), and our problem becomes one of partitioning the feature space into two regions, one for each class of fish. The decision threshold(s) (in 1D feature space) become *decision boundaries*, separating regions which may or may not be simply connected. The simplest case would be a linear decision boundary. When is this justified? And how would we find the best linear boundary? (By finding the centroids of the two classes, and constructing a line perpendicular to it?)

We could choose a more complex decision boundary, even to the point where it could separate the training data perfectly (Fig. 5.9). However, this is tuned too tightly to the specific training samples and is unlikely to perform as well with new test samples. It seems unlikely that such a complex boundary actually corresponds to a true model of nature for all sea bass and salmon.

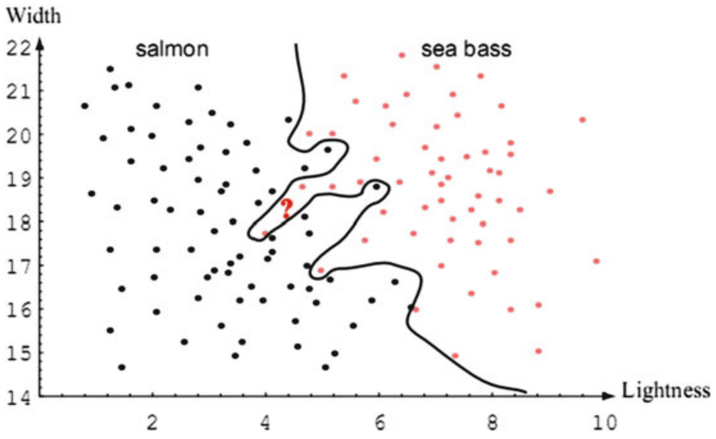

Fig. 5.9 Overly complex decision boundary. The new test data, marked with a *question mark*, is more likely a salmon, but this decision boundary classifies it as a sea bass (after Duda et al. 2001)

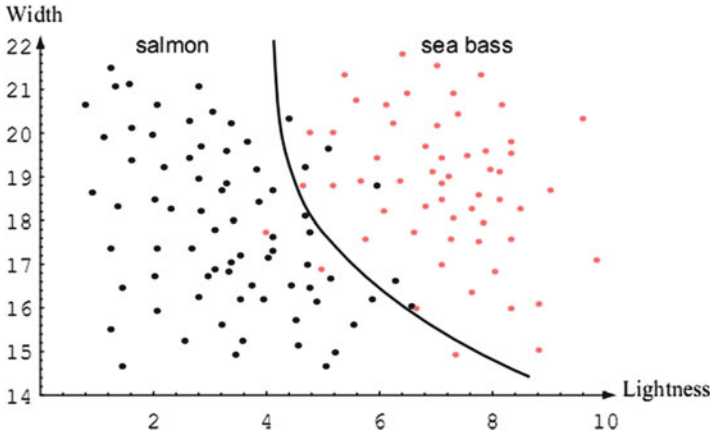

Fig. 5.10 A decision boundary that might represent the optimal tradeoff between performance on the training set and simplicity of classifier, giving the highest accuracy on new data (after Duda, Hart and Stork 2001)

We might decide to trade off performance on the training set for increased generalization, and settle for a decision boundary based on a quadratic (Fig. 5.10). As we might imagine, the shape of the optimal decision boundary in a particular situation cannot be chosen arbitrarily, but is determined by the actual distributions of the training samples for the classes (see Sect. 5.2.2).

5.2.2 *Discriminant Functions and Decision Boundaries*

There are many different ways to represent pattern classifiers. One of the most useful is to obtain *decision boundaries* by considering a set of *discriminant functions*, $g_i(\mathbf{x})$ for each class, $i = 1, 2, 3 \ldots, M$, where $\mathbf{x}$ is the feature vector: classification is based on finding the largest discriminant function. For the Bayes' classifier (minimum-error-rate classification), the discriminant functions are the posterior probabilities, $P(\omega_i|x)$. Using Bayes' rule gives

$$g_i(\mathbf{x}) = P(\omega_i|\mathbf{x}) = \frac{p(\mathbf{x}|\omega_i) \cdot P(\omega_i)}{p(\mathbf{x})} \tag{5.10}$$

The discriminant function is not unique. It can be multiplied by a constant or shifted by adding a constant, without affecting the classification. Indeed, any monotonically increasing function of $g_i(\mathbf{x})$ is also a valid discriminant function. For Bayes' classification, it is convenient to use the natural log of the numerator of (5.8), viz.,

$$g_i(\mathbf{x}) = \ln p(\mathbf{x}|\omega_i) + \ln P(\omega_i) \tag{5.11}$$

Using these discriminant functions, the decision rules will divide the feature space into *decision regions*, separated by decision boundaries or surfaces.

The multivariate Gaussian is the most frequently used (class-conditional) probability density function because of its tractability and its relationship to the Central Limit Theorem. The n-dimensional Gaussian is given by

$$f_{\mathbf{X}}(\mathbf{x})(\text{or } N(\mu, \Sigma) = \frac{1}{((2\pi)^{n/2}|\Sigma|^{1/2})} \exp(-\tfrac{1}{2}(\mathbf{x}-\mu)^{\mathrm{T}}\Sigma^{-1}(\mathbf{x}-\mu)) \tag{5.12}$$

where $\boldsymbol{\mu}$ is the mean value of $\mathbf{x}$, and $\boldsymbol{\Sigma}$ is the $(n \times n)$ covariance matrix.

In this case, the discriminant functions are

$$g_i(\mathbf{x}) = -\tfrac{1}{2}(\mathbf{x}-\mu_i)^{\mathrm{T}}\Sigma_i^{-1}(\mathbf{x}-\mu_i) - n/2 \cdot \ln 2\pi - \tfrac{1}{2}\ln|\Sigma_i| + \ln P(\omega_i) \tag{5.13}$$

Let us examine several special cases:

Case 1: Independent features, each with the same variance ($\boldsymbol{\sigma}^2$).

Let us consider the case where all features are represented by circular contours. Circular (or spherical, in 3D) isocontours result from a covariance matrix which is diagonal and equal to $\sigma^2\mathbf{I}$. It follows that $|\boldsymbol{\Sigma}_i| = \sigma^{2n}$ and $\Sigma_i^{-1} = (1/\sigma^2)\mathbf{I}$. The second and third terms in (5.11) are class-independent constant biases and can be eliminated, giving

$$g_i(\mathbf{x}) = -\tfrac{1}{2}(\mathbf{x}-\mu_i)^{\mathrm{T}}\Sigma_i^{-1}(\mathbf{x}-\mu_i) + \ln P(\omega_i) \tag{5.14}$$

In this case, this simplifies to

$$g_i(\mathbf{x}) = -\frac{\|\mathbf{x} - \mu_i\|^2}{2\sigma^2} + \ln P(\omega_i) \tag{5.15}$$

Where ||●|| denotes the Euclidean norm, i.e.,

$$\|\mathbf{x} - \mu_i\|^2 = (\mathbf{x} - \mu_i)^{\mathrm{T}}(\mathbf{x} - \mu_i) \tag{5.16}$$

Expansion of the squared term in (5.15) gives

$$g_i(\mathbf{x}) = -\frac{1}{2\sigma^2}[\mathbf{x}^{\mathrm{T}}\mathbf{x} - 2\mu_i^{\mathrm{T}}\mathbf{x} + \mu_i^{\mathrm{T}}\mu_i] + \ln P(\omega_i) \tag{5.17}$$

The term $\mathbf{x}^{\mathrm{T}}\mathbf{x}$ is constant for all i, and can be ignored. Thus

$$g_i(\mathbf{x}) = \mathbf{w}_i^{\mathrm{T}}\mathbf{x} + w_{i0} \tag{5.18}$$

where

$$\mathbf{w}_i = \frac{1}{\sigma^2}\mu_i \tag{5.19}$$

and

$$w_{i0} = -\frac{1}{2\sigma^2}\mu_i^{\mathrm{T}}\mu_i + \ln P(\omega_i) \tag{5.20}$$

(w_{i0} is known as the *threshold* or *bias* for the ith class).

Equation (5.18) defines a *linear discriminant function*; the associated Bayesian classifier is linear in nature, and the approach to classification is known as *linear discriminant analysis* (LDA).

The decision surfaces are defined by the linear equations $g_i(\mathbf{x}) = g_j(\mathbf{x})$ for the two classes with the highest posterior probabilities. For this case

$$\mathbf{w}^{\mathrm{T}}(\mathbf{x} - \mathbf{x}_0) = 0 \tag{5.21}$$

where

$$\mathbf{w} = \mu_i - \mu_j \tag{5.22}$$

and

$$\mathbf{x}_0 = \frac{1}{2}(\mu_i + \mu_j) - \frac{\sigma^2}{\|\mu_i - \mu_j\|^2} \cdot \ln P(\omega_i) \cdot (\mu_i - \mu_j) \tag{5.23}$$

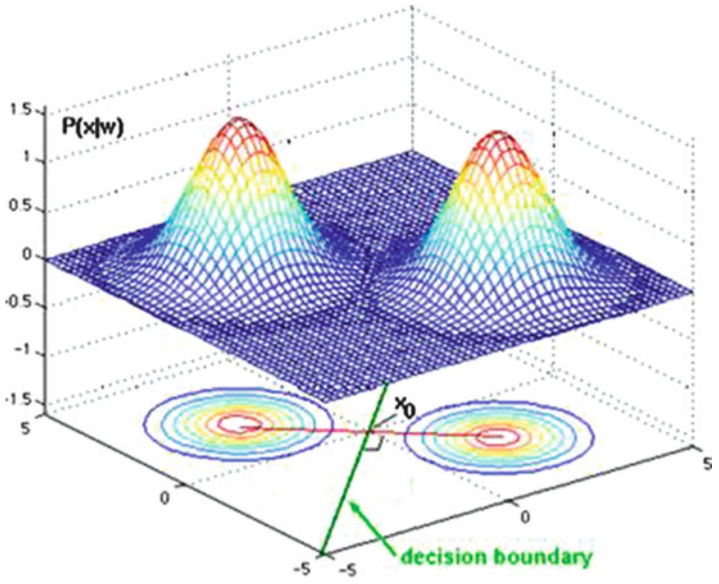

Fig. 5.11 Two bivariate normal distributions, whose priors are equal. Therefore, the decision boundary is exactly at the midpoint between the two means. The decision boundary is the perpendicular bisector of the line between the centroids

This defines a hyperplane through the point $\mathbf{x}_0$, orthogonal to $\mathbf{w}$. Since $\mathbf{w} = \boldsymbol{\mu}_i - \boldsymbol{\mu}_j$, the hyperplane is orthogonal to the line that links their means. (A classifier that uses linear discriminant functions is called a *linear machine*).

If $P(\omega_i) = P(\omega_j)$, then $\mathbf{x}_0$ is midway between the means, and the decision hyperplane is the perpendicular bisector of the line between the means (i.e., centroids), as in Fig. 5.11. [If $P(\omega_i) \neq P(\omega_j)$ then $\mathbf{x}_0$ shifts away from the mean with the higher (prior) probability. However, if the variance σ^2 is small relative to the squared distance $\|\boldsymbol{\mu}_i - \boldsymbol{\mu}_j\|^2$, then the position boundary if fairly insensitive to the values of the prior probabilities.]

If the prior probabilities, $P(\omega_i)$, are the same for all classes, the $P(\omega_i)$ in (5.23) disappears and the optimum decision rule becomes: measure the Euclidean distance of a feature vector to the centroids of each class, $\|\mathbf{x} - \boldsymbol{\mu}_i\|$, and assign $\mathbf{x}$ to the class corresponding to the shortest distance. The classifier is therefore a *minimum-distance classifier*.

Note that the condition that the posterior probabilities are equal on the decision boundary means that the log of the ratio of posterior probabilities must be zero. If the data in each class is Gaussian with equal variance, then the boundary between any two classes is a straight line. For three classes, there will be three lines (Fig. 5.12).

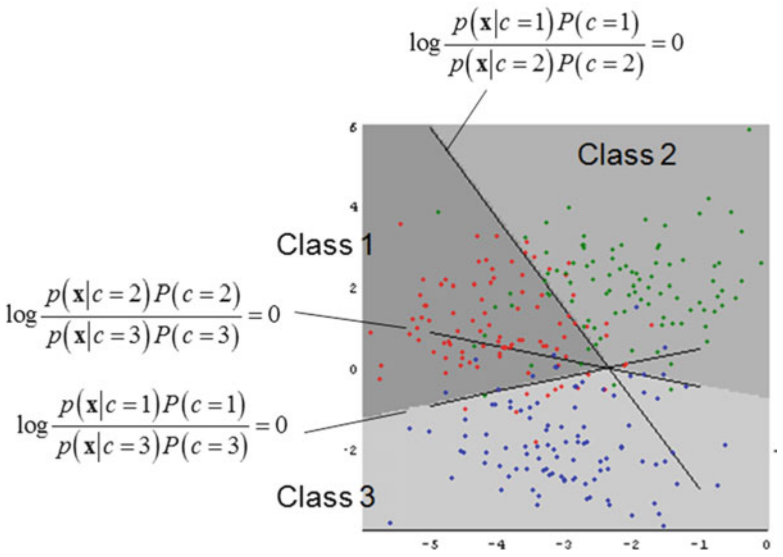

Fig. 5.12 Showing the decision lines between three classes of equal variance. A new data point is assigned to the class that gives the largest numerator in the posterior probability ratio

Case 2: When the covariance matrices for all the classes are equal, but otherwise arbitrary (so that the isocontours are ellipses (in 2D) of similar size and orientation).

Geometrically, this corresponds to having samples in (hyper)ellipsoidal clusters of equal size and shape: the elliptical contours are parallel to each other. Since both (n/2) and $|\boldsymbol{\Sigma}_i|$ in (5.13) are independent of i, they can be ignored as superfluous additive constants. (It is left as an exercise to work through the math and find the decision boundary).

Again, the decision boundary is a linear surface (or line for 2D feature space), although it is not orthogonal to the line joining the means. If the priors are equal it intersects mid-way between the means (Fig. 5.13). (If the priors are not equal, then the decision boundary shifts away from the mean with the higher (prior) probability).

Case 3: General case, with different covariance matrices for each class.

In the general case, only the constant term, (n/2) ln2π, drops out of (5.13) and the resulting discriminant functions are inherently quadratic, giving rise to decision curves which are *hyperquadrics* for the two-class case. For two features, they will be ellipses, circles, parabolas, hyperbolas, lines or pairs of lines. In such cases, the Bayesian classifier is a *quadratic classifier*, and the approach is known as *quadratic discriminant analysis* (QDA).

When one class has circular contours, a parabolic decision boundary is the result (Fig. 5.14).

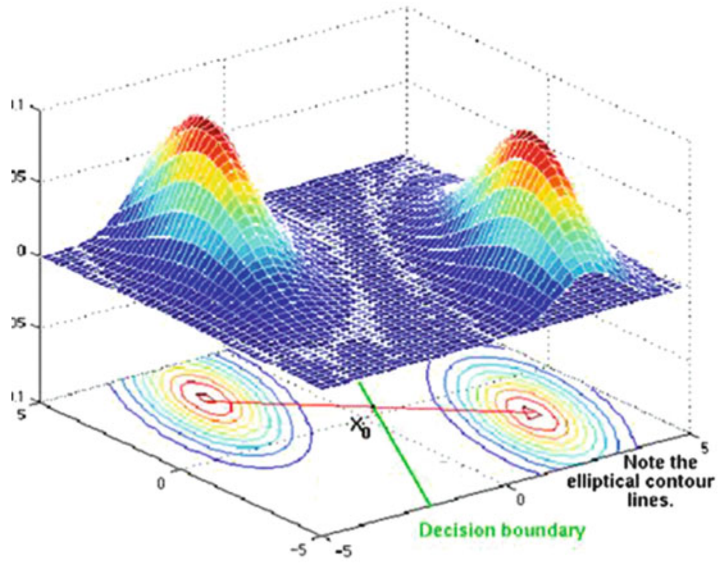

Fig. 5.13 Two classes with equal covariance matrices, showing the line between the centroids and the linear discriminant function which intersect it mid-way (but *not* at right-angles)

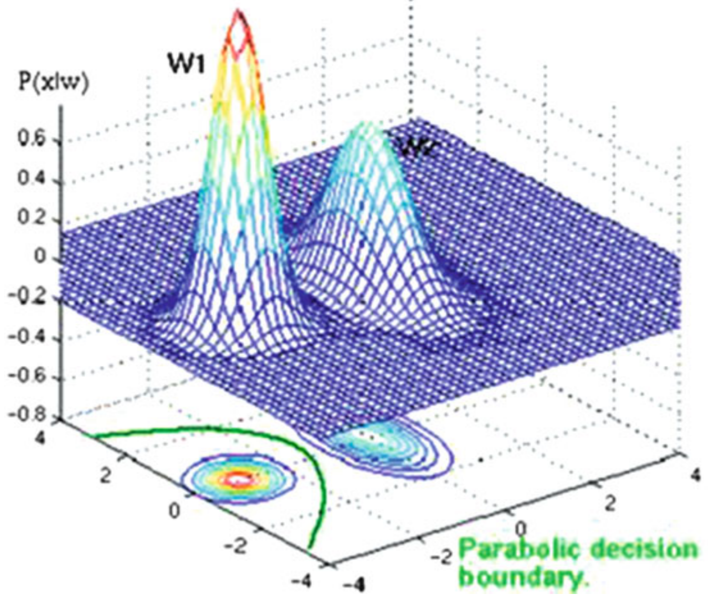

Fig. 5.14 Parabolic decision boundary when one distribution has circular isocontours

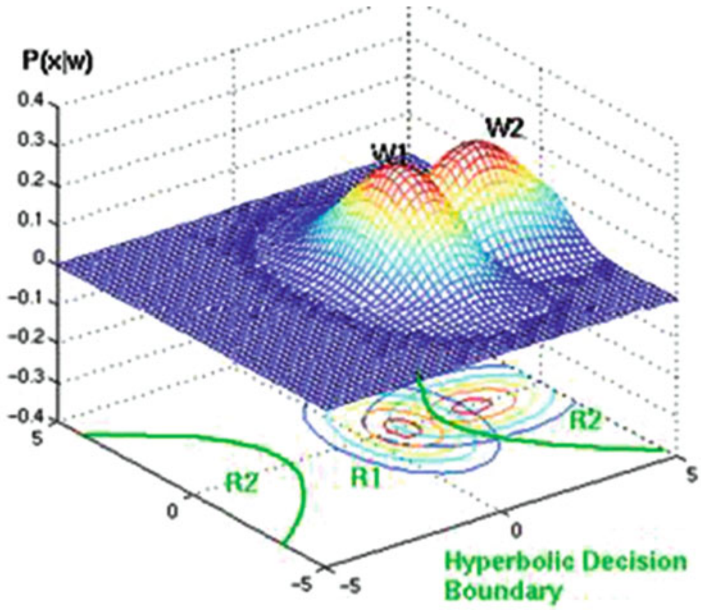

Fig. 5.15 Hyperbolic decision boundaries from two (equiprobable) sets of orthogonal elliptical isocontours

In the case of (equiprobable) distributions with elliptical contours, oriented orthogonally to each other, the decision boundary will be hyperbolic (Fig. 5.15).

It is left to the reader to determine the conditions under which the decision boundaries will be ellipses, and when they degenerate into lines (Fig. 5.16).

To clarify these ideas, let us consider two examples. In both cases the priors are equal. In the first example, the means are $\boldsymbol{\mu}_1 = [0, 0]$ and $\boldsymbol{\mu}_2 = [4, 0]$, and the covariance matrices are

$$\Sigma_1 = \begin{vmatrix} 0.3 & 0.0 \\ 0.0 & 0.35 \end{vmatrix} \quad \Sigma_2 = \begin{vmatrix} 1.2 & 0.0 \\ 0.0 & 1.85 \end{vmatrix}$$

There are no covariance terms, but the variances are different in each covariance matrix and the covariance matrices are not equal. The resulting isocontours are ellipses (of different sizes) oriented parallel to the feature axes. Figure 5.17 shows the two pdfs, where the red color (class ω_1) indicates the points where the posterior probability is greater for class ω_1. The decision curve is an ellipse.

For the second example, $\boldsymbol{\mu}_1 = [0, 0]$ and $\boldsymbol{\mu}_2 = [3.2, 0]$ and

$$\Sigma_1 = \begin{vmatrix} 0.1 & 0.0 \\ 0.0 & 0.75 \end{vmatrix} \quad \Sigma_2 = \begin{vmatrix} 0.75 & 0.0 \\ 0.0 & 0.1 \end{vmatrix}$$

Again, these are ellipses, with axes parallel to the feature axes but inspection of the variances shows that their isocontours are orthogonal to each other. This results in a hyperbolic decision boundary (Fig. 5.18).

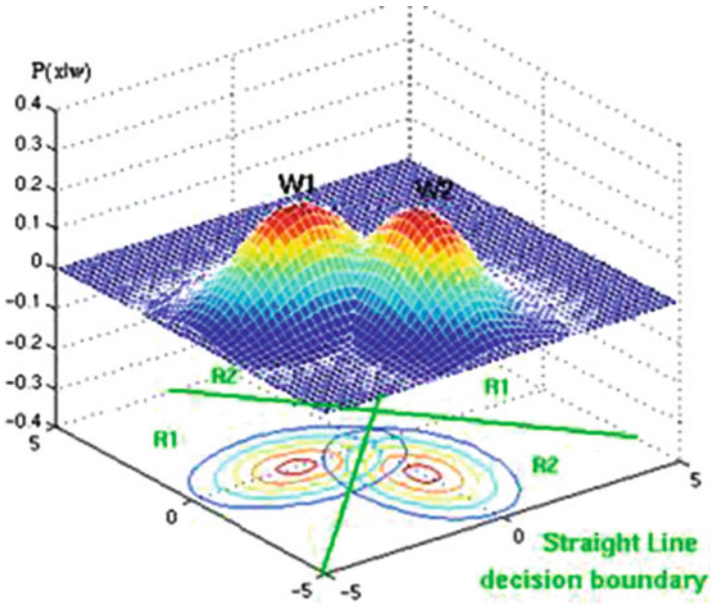

Fig. 5.16 A linear decision boundary

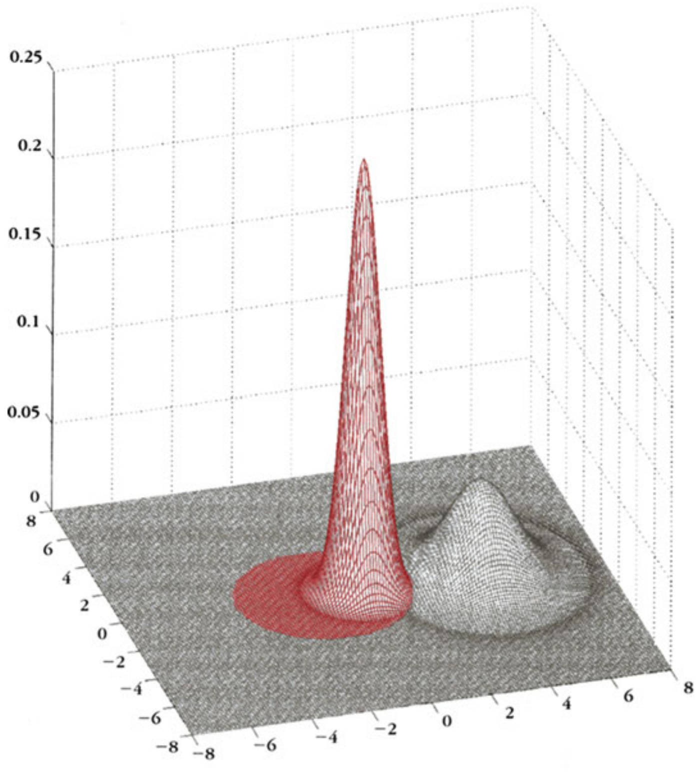

Fig. 5.17 The pdfs of two equiprobable normally distributed classes with different covariance matrices (after Theodoridis and Koutroumbas 2009)

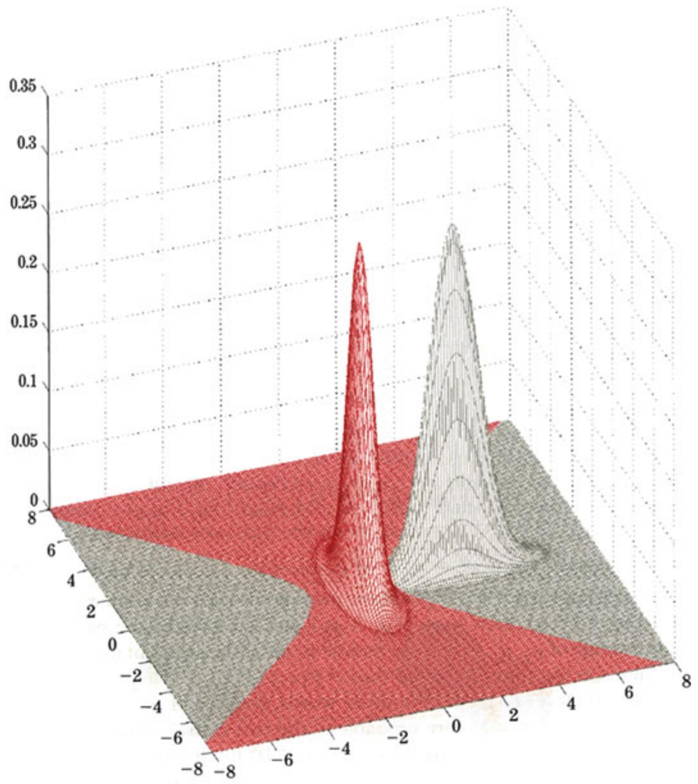

Fig. 5.18 The pdfs of two equiprobable normally distributed classes with different covariance matrices (after Theodoridis and Koutroumbas 2009)

Figure 5.19 shows the decision curves for an example with three classes (and two features, viz., 2D feature space).

We should also note that even in 1D feature space, the case of two unequal variances can result in a parabolic decision curve, which results in two decision thresholds, and a disconnected decision region (Fig. 5.20). We have seen this earlier in the chapter (Example 5.2).

5.2.3 MAP (Maximum A Posteriori) Estimator

With the MAP variant of the classifier, the new object is assigned to the class with the largest posterior probability. For multivariate data (viz., several features), the multivariate Gaussian is used. Figure 5.21 illustrates the case where there are two features (y_1 and y_2) and three classes (A, B, and C), each with its own mean (μ_A, μ_B, and μ_C). The covariance matrix is

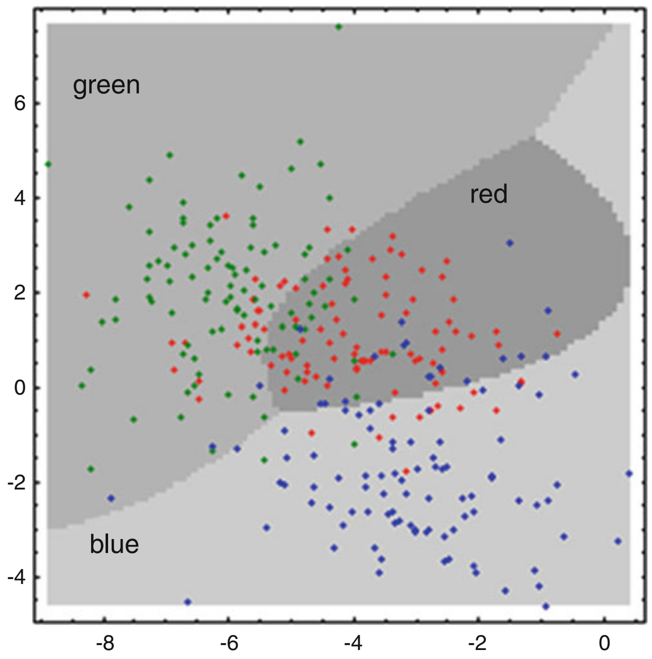

Fig. 5.19 The decision curves between any two of the three classes (*red*, *green*, and *blue*) are quadrics

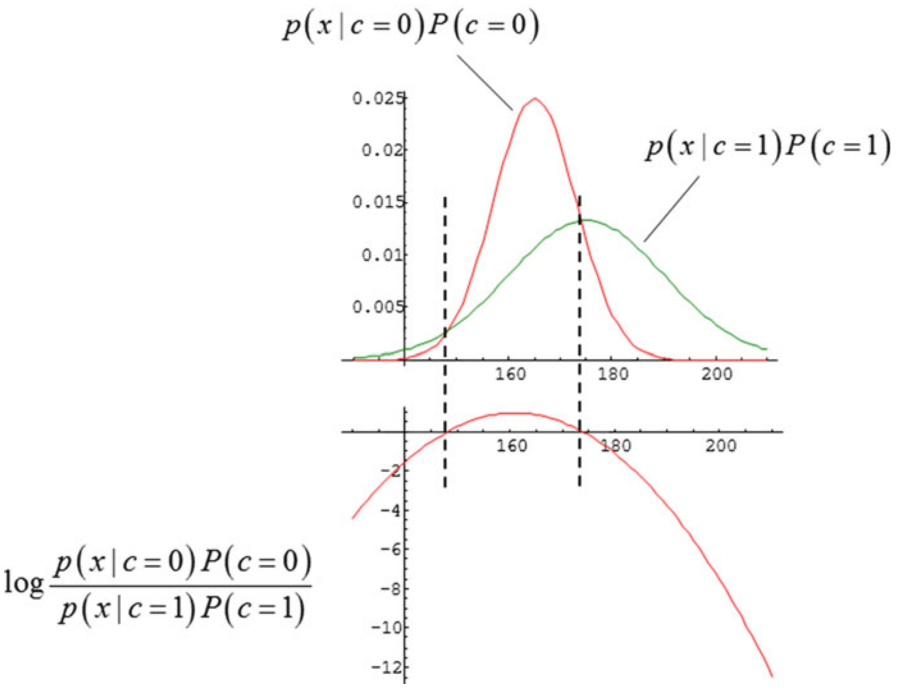

Fig. 5.20 The decision curve in 1D feature space for normal distributions with unequal variance

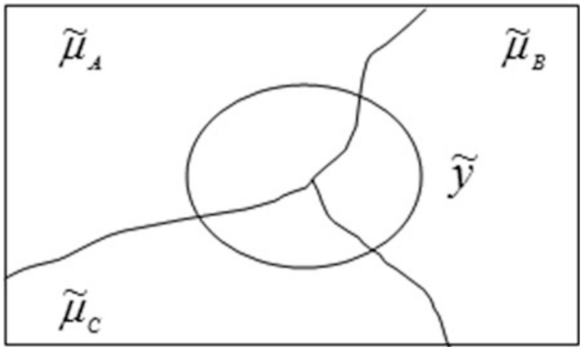

Fig. 5.21 Three-class problem

$$\Sigma = \begin{bmatrix} \sigma_{11} & \sigma_{12} \\ \sigma_{12} & \sigma_{22} \end{bmatrix}$$

Then the posterior probabilities are calculated using

$$\begin{aligned}
P(\tilde{\mu}_j|\tilde{y}) &= \frac{P(\tilde{\mu}_j \cap \tilde{y})}{P(\tilde{y})} \\
&= \frac{P(\tilde{\mu}_j)P(\tilde{y}|\tilde{\mu}_j)}{P(\tilde{\mu}_\mathrm{A} \cap \tilde{y}) + P(\tilde{\mu}_\mathrm{B} \cap \tilde{y}) + P(\tilde{\mu}_\mathrm{C} \cap \tilde{y})} \\
&= \frac{P(\tilde{\mu}_j)P(\tilde{y}|\tilde{\mu}_j)}{P(\tilde{\mu}_\mathrm{A})P(\tilde{y}|\tilde{\mu}_\mathrm{A}) + P(\tilde{\mu}_\mathrm{B})P(\tilde{y}|\tilde{\mu}_\mathrm{B}) + P(\tilde{\mu}_\mathrm{C})P(\tilde{y}|\tilde{\mu}_\mathrm{C})} \\
&= \frac{P(\tilde{\mu}_j)\left[\dfrac{\mathrm{e}^{-\frac{1}{2}(\tilde{y}-\tilde{\mu}_j)'\Sigma_j^{-1}(\tilde{y}-\tilde{\mu}_j)}}{|\Sigma_j|^{\frac{1}{2}}}\right]}{P(\tilde{\mu}_\mathrm{A})\left[\dfrac{\mathrm{e}^{-\frac{1}{2}(\mathrm{SqDist}_\mathrm{A})}}{|\Sigma_\mathrm{A}|^{\frac{1}{2}}}\right] + P(\tilde{\mu}_\mathrm{B})\left[\dfrac{\mathrm{e}^{-\frac{1}{2}(\mathrm{SqDist}_\mathrm{B})}}{|\Sigma_\mathrm{B}|^{\frac{1}{2}}}\right] + P(\tilde{\mu}_\mathrm{C})\left[\dfrac{\mathrm{e}^{-\frac{1}{2}(\mathrm{SqDist}_\mathrm{C})}}{|\Sigma_\mathrm{C}|^{\frac{1}{2}}}\right]}
\end{aligned} \tag{5.24}$$

and an object is classified into one of the classes (A, B, or C) based on its highest posterior probability.

5.3 Exercises

1. Suppose that the class-conditional probability functions for ω_1 and ω_2 are Gaussians with (μ_i, σ_i) of (4, 2) and (10, 1), and that they have equal prior probabilities ($P_1 = P_2 = ½$). What is the optimal decision threshold?
(Try by calculation, and then check using CondProb.xls).
2. What are the decision thresholds for two class-conditional probabilities which are Gaussian in shape, with means $\mu_1 = 4$ and $\mu_2 = 10$, variances $\sigma_1^2 = 4$ and $\sigma_2^2 = 1$, and prior probabilities $P(\omega_1) = 2/3$ and $P(\omega_2) = 1/3$?
(Try by calculation, and then check using CondProb.xls).

3. Select the optimal decision where the class-conditional probabilities are Gaussians (i.e., $N(\mu, \sigma^2)$), given by $N(2, 0.5)$ and $N(1.5, 0.2)$ and the corresponding priors are 2/3 and 1/3.
   (Try by calculation, and then check using CondProb.xls).
4. For the fish canning problem discussed in this chapter, customers may not mind some of the more expensive salmon turning up in their cans of sea bass, but may have more objections to misclassified sea bass turning up in their salmon cans. We can factor this into the analysis with the loss function: which term should we set to be the larger . . . λ_{12} [the loss associated with misclassifying a sea bass (ω_1) as salmon (ω_2)] or λ_{21} [the loss associated with misclassifying a salmon (ω_2) as a sea bass (ω_1)]?
5. In a two-class problem with a single feature, x, the pdfs are Gaussians (i.e., $N(\mu, \sigma^2)$) given by $N1(0, ½)$ and $N2(1, ½)$. If $P(\omega_1) = P(\omega_2) = ½$, find the decision thresholds for (1) minimum error probability and (2) minimum risk if the loss matrix is $\lambda = \begin{vmatrix} 0 & 0.5 \\ 1.0 & 0 \end{vmatrix}$
   (Use CondProb.xls).
6. In a two-class, two-feature classification task, the feature vectors described by Gaussian distributions with the same covariance matrix

$$\Sigma = \begin{vmatrix} 1.1 & 0.3 \\ 0.3 & 1.9 \end{vmatrix}$$

   And the means are $\boldsymbol{\mu}_1$ [0, 0] and $\boldsymbol{\mu}_2 = [3, 3]$.
   Classify the vector [1.0, 2.2] according to the Bayesian classifier. (Hint: use the Mahalanobis distances to the two means).
7. Given the following labeled samples:

Class ω_1	Class ω_2	Class ω_3
(2.491, 2.176)	(4.218, −2.075)	(−2.520, 0.483)
(1.053, 0.677)	(−1.156, −2.992)	(−1.163, 3.161)
(5.792, 3.425)	(−4.435, 1.408)	(−13.438, 2.414)
(2.054, −1.467)	(−1.794, −2.838)	(−4.467, 2.298)
(0.550, 4.020)	(−2.137, −2.473)	(−3.711, 4.364)

   Classify each of the following vectors
   (2.543, 0.046)
   (4.812, 2.316)
   (−2.799, 0.746)
   (−3.787, −1.400)
   (−7.429, 2.329)
   by using
   (1) the 1-NN rule.
   (2) the 3-NN rule.

References

Duda, R.O., Hart, P.E., Stork, D.G.: Pattern Classification. Wiley, New York, NY (2001)
Theodoridis, S., Koutroumbas, K.: Pattern Recognition, 4th edn. Academic, Amsterdam (2009)

Chapter 6
Nonparametric Learning

6.1 Histogram Estimator and Parzen Windows

For the one-dimensional case, if we have N independent samples $(x_1, x_2, x_3, \ldots x_N)$ of a random variable x (our chosen feature). The density function (pdf) can be approximated by a histogram formed from the samples with bins that are Δx $(=2h)$ wide (Fig. 6.1). If there are a large number of samples and k is the number of samples in a bin, of mid-point x_i, then the probability that a sample is in that bin $(x_i \pm h)$ can be estimated by the relative frequency, k/N, and the density at x_i, $p(x_i)$, estimated by $k/(2hN)$. In constructing the histogram, we have to choose both an origin and a bin width. The estimate of the pdf is affected by the choice of origin, but mostly by the bin width: with small bins the estimate is spiky, and with large bins it is smoother.

To get a smoother estimate, without smoothing out the details, we use a smooth weighting function, called a *kernel* function or *Parzen window*. The most popular is the Gaussian kernel (Fig. 6.2). The estimate of the pdf is then the sum of the kernels placed at each data point.

The width of the kernel (just as the histogram bin width) has to be chosen with care. A large width will over-smooth the density and mask the structure in the data, while a small width will yield a density estimate that is spiky and very hard to interpret (Fig. 6.3). The density estimate will inherit all the continuity and differentiability properties of the kernel, so that for a Gaussian kernel, it will be smooth and have all the derivatives.

We would like to find a value of the smoothing parameter, the kernel width, which minimizes the error between the estimated density and the true density. A natural measure is the mean square error at the estimation point x. This expression is an example of the bias–variance tradeoff; the bias can be reduced at the expense of the variance, and vice versa. (The bias of an estimate is the systematic error incurred in the estimation; the variance of an estimate is the random error incurred in the estimation). The bias–variance dilemma applied to window width selection simply means that a large window width will reduce the differences among the estimates of

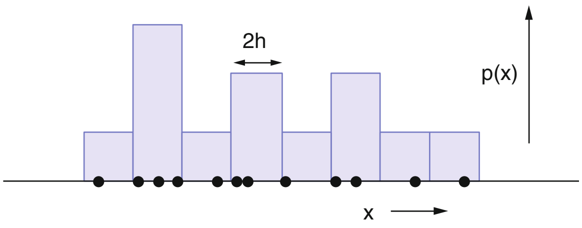

Fig. 6.1 Estimation of the probability distribution function by a histogram

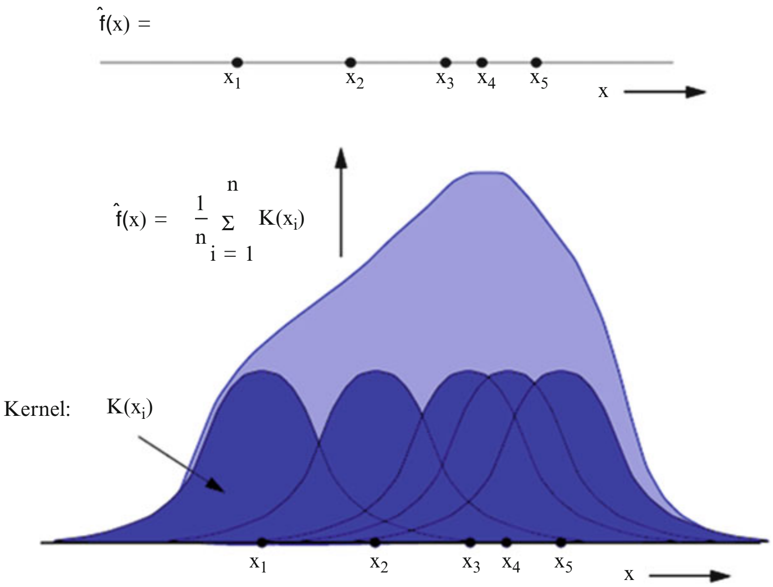
$\hat{f}(x) =$
x_1 x_2 x_3 x_4 x_5
x
$\hat{f}(x) = \frac{1}{n}\sum_{i=1}^{n} K(x_i)$
Kernel: $K(x_i)$
x_1 x_2 x_3 x_4 x_5
x

Fig. 6.2 Using a Gaussian kernel to weight each sample in the training set

density function for different data sets (the variance). A small window width will reduce the bias of density function, at the expense of a larger variance in the estimates of density function (Fig. 6.4).

6.2 *k*-Nearest Neighbor (*k*-NN) Classification

Since the kernel in the Parzen density estimate is fixed in size, it may be difficult to obtain a satisfactory estimate of the density everywhere when the samples are not evenly distributed. One way is to fix the number of samples, *k*, and let the width change so that each region contains exactly *k* samples. This is the *k-nearest neighbor* classification approach. The classifier exemplifies the following saying

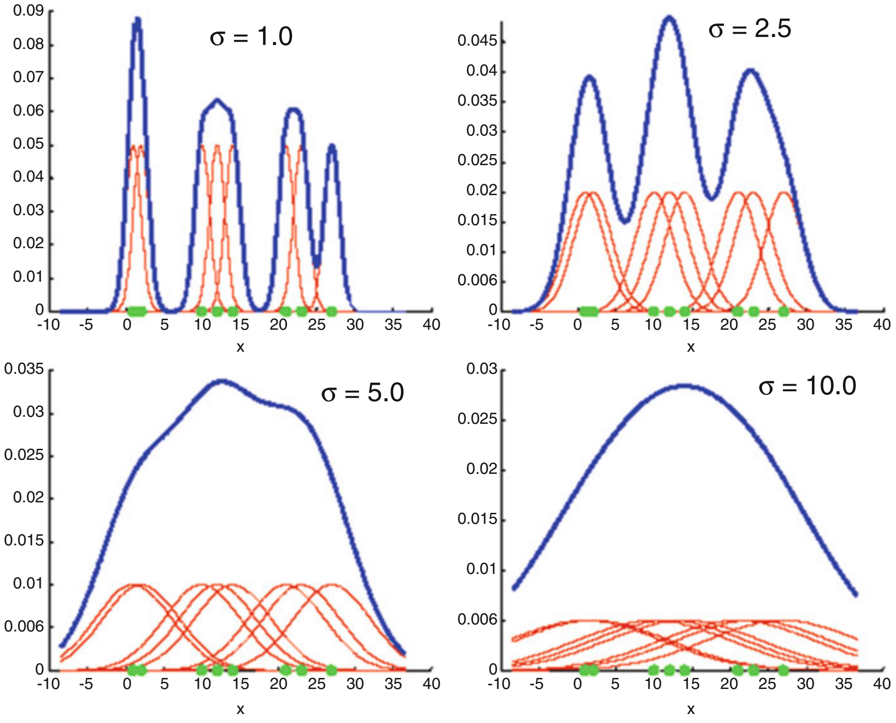

Fig. 6.3 Choosing the kernel width

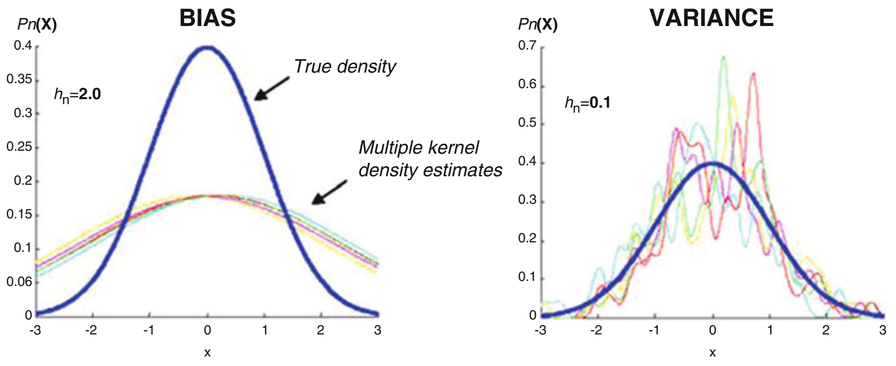

Fig. 6.4 The bias–variance tradeoff

"If it walks like a duck, quacks like a duck, and looks like a duck, then it probably is a duck": i.e., the class of a test instance is determined by the class of its nearest neighbors.

The *k*-NN process starts at the test point and grows a region until it encloses *k* training samples and it labels the test point **x** by a majority vote of these samples (Fig. 6.5).

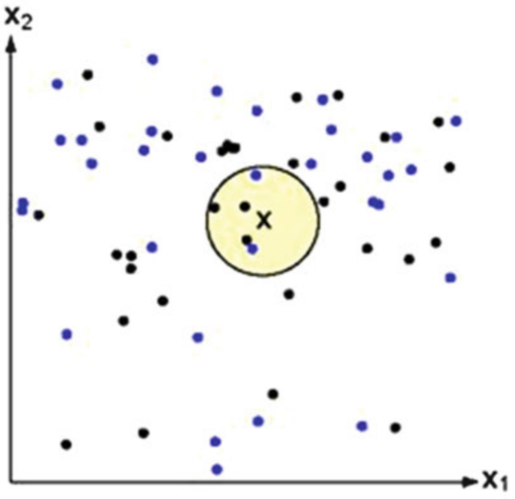

Fig. 6.5 In this case, with $k = 5$, the test point would be labeled in the class of *black points*

For two classes, the value of k should be odd to avoid a tie. For more than two classes, k being odd is insufficient to avoid a tie [e.g., with three classes, we may choose $k = 5$, and still end up with a tie (2, 2, 1) in some cases]: larger values of k are more likely to resolve ties. The region will be circular (or spherical in 3D) if the data have been normalized.

In general, the estimates that can be obtained with the k-NN method are not very satisfactory. The estimates are prone to local noise. The method produces estimates with very heavy tails, and the density estimate will have discontinuities since it is not differentiable (see Figs. 6.6 and 6.7).

The larger the value of k, the smoother the classification boundary; and the smaller the value of k, the more convoluted the boundary (Fig. 6.8).

There is essentially no training involved in the k-NN method; it is considered a *lazy* learning algorithm. It defers data processing until it receives a request to classify an unlabeled (test) example, it classifies it, and then discards any intermediate results. (This is the opposite strategy to decision trees and rule-based classifiers, which are known as *eager* learning classifiers: they learn a model that maps the input attributes to the classes as soon as the training data become available). Its advantages are that it is intuitive, analytically tractable and simple to implement, and it lends itself easily to parallel implementation. Because it uses local information, it can be used adaptively (by, for example, stretching the region in the dimension of lowest variance). It is, however, highly susceptible to the *curse of dimensionality* [viz., you need increasing amounts of training data as the dimensionality (number of features) increases: a rule of thumb is to use at least ten times as many training samples per class as the number of features].

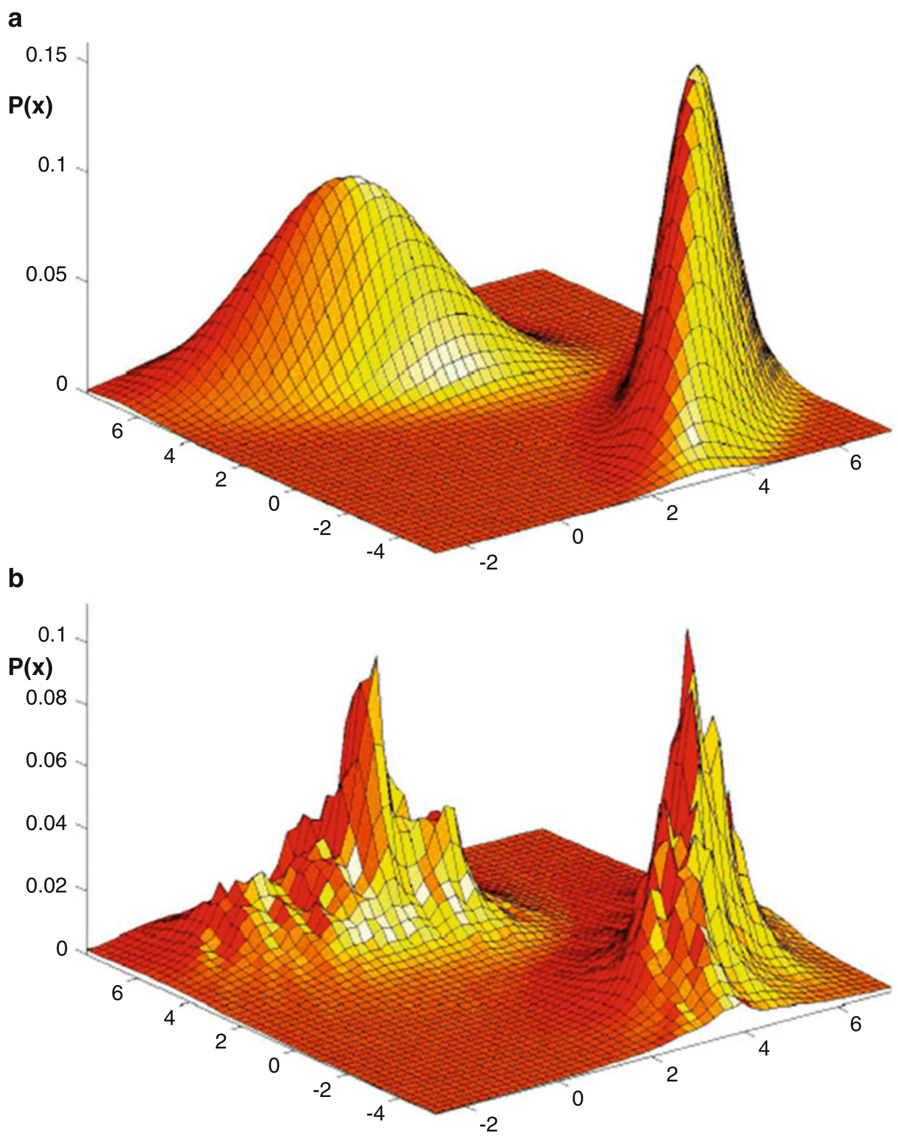

Fig. 6.6 An illustration of the performance of the k-NN method. (**a**) The true density, which is a mixture of two bivariate Gaussians and (**b**) the density estimate for $k = 10$ and $N = 200$ examples

When distinguishing normal and abnormal classes in, for example, tumor detection, it is more useful to modify the criterion to assign a new vector to a particular class if at least l of the k nearest neighbors is in that particular class. This is useful when (1) the penalty for misclassifying one class (e.g., abnormal as normal—*false negatives*) is much greater than the penalty for misclassifying the other class (e.g., normal as abnormal—*false positives*) and (2) when there is an unbalanced training set, with many more samples in one class than the other.

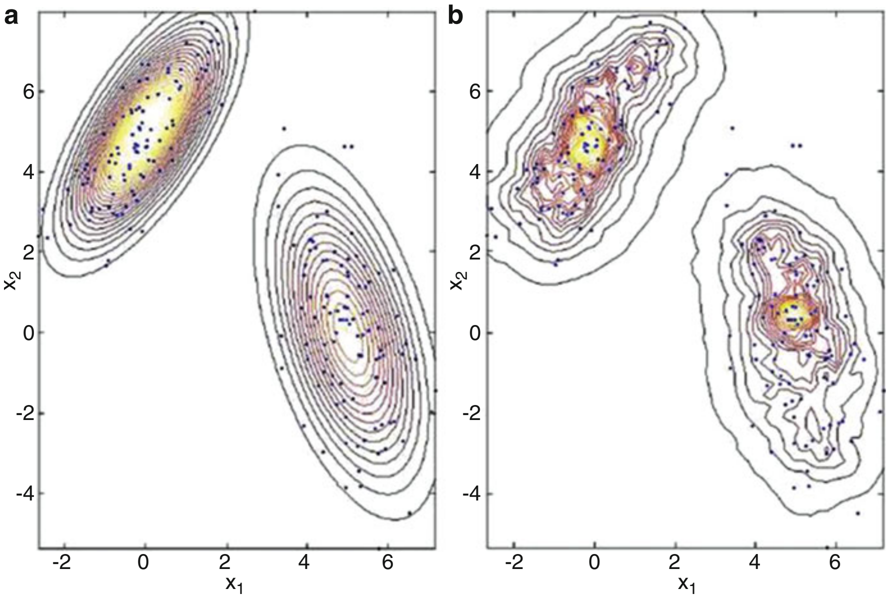

Fig. 6.7 Isocontours of Fig. 6.6. (**a**) The true density and (**b**) the *k*-NN estimate

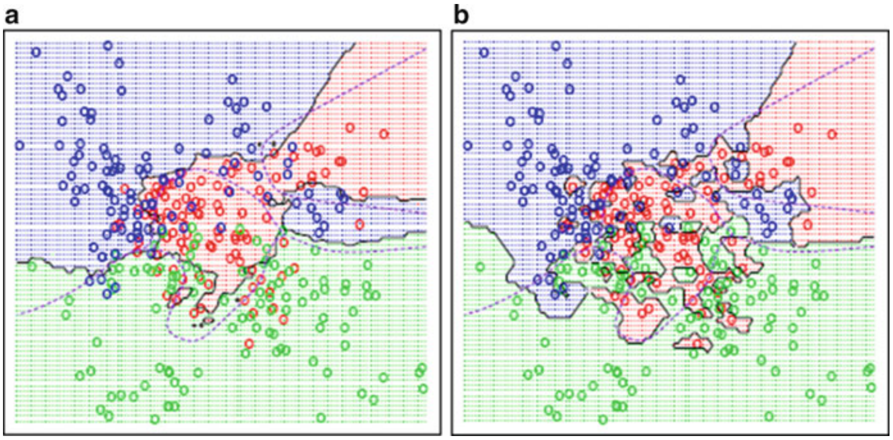

Fig. 6.8 *k*-NN classifiers (**a**) $k = 15$, (**b**) $k = 1$ (the *broken curve* is the Bayes decision boundary)

6.3 Artificial Neural Networks

Artificial neural network (ANN) models take their motivation from the human nervous system. Signals from sensors in the body convey information for sight, hearing, taste, smell, touch, balance, temperature, pain, etc. The nerve cells

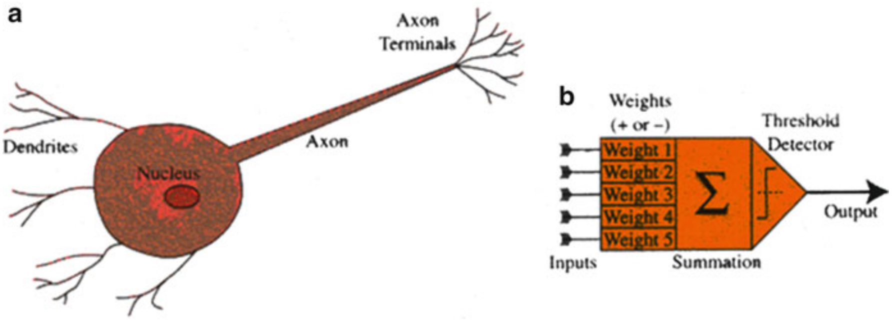

Fig. 6.9 Structure of (**a**) a neuron, (**b**) an artificial neuron

(or *neurons*) are autonomous cells specialized in transmitting, processing and storing this information, which is essential for us to respond properly to external and internal stimuli. The neuron transmits spikes of electrical activity along a long, thin strand known as an *axon*, which splits into thousands of branches or terminals, where they can fire across a gap (*synapse*) to the dendrites of other neurons depending on the size of the signal (Fig. 6.9a). The brain is composed of a very large number ($\sim 2 \times 10^{10}$) of neurons acting in parallel. It is believed that in the brain both the processing (by the neurons) and the memory (in the synapses) are distributed together over the network. Information is processed and stored according to the threshold levels for firing, and the weights assigned by each neuron to each of its inputs.

A mathematical model of the neuron [called the perceptron (Fig. 6.9b)] has been used to try and mimic our understanding of the functioning of the brain, in particular its parallel processing characteristics, in order to emulate some of its pattern recognition capabilities. An artificial neural network is a *parallel* system, which is capable of resolving paradigms that linear computing cannot resolve. Like its biological predecessor, an ANN is an *adaptive* system, i.e., parameters can be changed during operation (training) to suit the problem. They can be used in a wide variety of classification tasks, e.g., character recognition, speech recognition, fraud detection, medical diagnosis. The wide applicability of neural networks once led aviation scientist John Denker (AT&T Bell laboratories) to remark that "neural networks are the second best way of doing just about anything."

The artificial neuron is a threshold logic unit that accepts multiple inputs, which are weighted and summed; if the sum exceeds a certain threshold, the perceptron fires and an output value (a probability) is transmitted to the next unit.

The artificial neuron or perceptron (McCulloch and Pitts 1943) has n inputs x_1, x_2, … x_n that model the signals coming from dendrites (Fig. 6.10). Each input is connected by a weighted link to an output. The inputs are labeled with the corresponding, generally real, weights w_1, w_2, … w_n. According to the neurophysiological motivation, some of these synaptic weights may be negative to express their inhibitory character. w_0 is the *bias*, an intercept value to make the model more general that comes from an extra bias unit x_0, which is always +1. If the sum

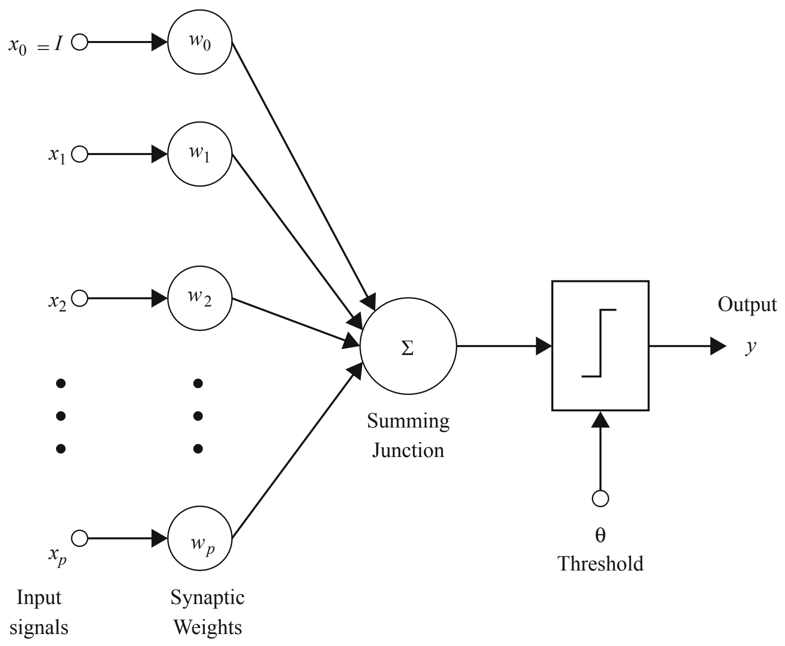

Fig. 6.10 The McCullough and Pitts (MCP) neuron

of the weighted inputs is greater than a threshold value, θ, then the neuron fires, producing an output of +1: otherwise it does not fire, and the output is 0. (Note that the threshold, θ, can be set to zero without loss of generality; in this case the actual threshold is modeled by the bias term w_0x_0).

Consider the implementation of the logical AND function. The inputs are binary and the output is 1 if the function is true (i.e., if input x_1 and input x_2 are both 1's) and 0 otherwise (Fig. 6.11a). Therefore, it can be seen as a two-class classification problem. A possible discriminant function for the AND function is

$$g = x_1 + x_2 - 1.5 \tag{6.1}$$

It takes the value zero on the decision boundary line, and positive and negative values to the right and left of the line respectively (Fig. 6.11b).

This could be implemented by a single neuron whose output is

$$y = \text{step}(1x_1 + 1x_2 + (-1.5)x_0) \tag{6.2}$$

The inputs (including the bias) are summed and passed to the threshold function (which has a threshold of 0, in this case). For ([0,0]) it receives an input of -1.5, for ([0,1]) it receives -0.5, and for ([1,0]) it receives -0.5, all below the threshold, producing outputs of "0" in each case: for ([1,1]) it receives 0.5, above the threshold, producing an output of "1."

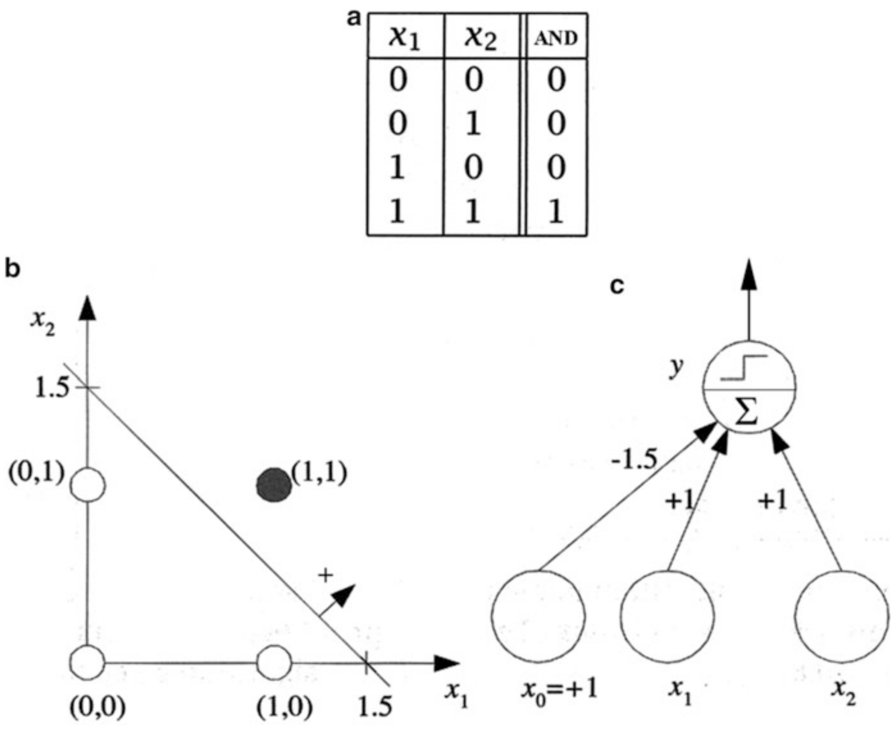

x_1	x_2	AND
0	0	0
0	1	0
1	0	0
1	1	1

Fig. 6.11 (**a**) Truth table for the logical AND function, (**b**) the required discriminant function in feature space [where the *filled circle* indicates an output of 1 (“true”), and *hollow circles* indicate outputs of 0 (“false”)], and (**c**) the perceptron which implements it

Similarly, the discriminant function

$$g = x_1 + x_2 - 0.5 \tag{6.3}$$

would implement the logical OR function.

The perceptron models a *linear discriminant function*, which partitions feature space using a decision boundary that is a straight line in two dimensions, a plane in three dimensions or a hyperplane in higher dimensions. The bias term (w_0) alters the position, but not the orientation, of the decision boundary; and the weights (w_1, w_2, … w_n) determine the gradient.

The outputs of the logical XOR (exclusive OR) function are shown in Fig. 6.12a; it produces an output of “1” if either input, but not both, is a “1.” Feature space (Fig. 6.12b) shows that there is no single line that separates the two classes (“0” and “1,” i.e., “true” and “false”). The XOR function is said to be not *linearly separable*. The situation is more complicated than with the AND or OR logical functions, and generally we would use a *multilayer neural network* to model the XOR function (see later in this section). Indeed, when it was first realized that the perceptron could only learn (i.e., model) linearly separable functions (Minsky and Papert 1969),

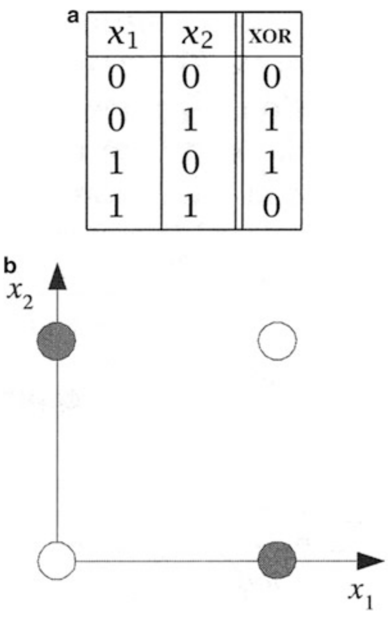

x_1	x_2	XOR
0	0	0
0	1	1
1	0	1
1	1	0

Fig. 6.12 (**a**) Truth table for the XOR function and (**b**) the required outputs in feature space

research into neural networks declined. However, it was revived in the 1980s when it was shown that multilayer networks could learn nonlinearly separable functions (Parker 1985; Le Cun 1986).

For a single perceptron with two binary inputs and one binary output, there are four possible input patterns each of which can produce a "0" or a "1." Of the 16 possible logic functions, only 14 (those that are linearly separable) can be realized. The two that cannot be learned are the exclusive OR (XOR) and the exclusive NOR functions.

However, there is a trick to implementing the XOR function using a linear function. It involves using a third (dummy) input, which transforms the problem into three dimensions (Fig. 6.13). The dummy input does not change the data when looked at in the (x_1, x_2) plane (which is the floor of the cube in Fig. 6.13), but moves the point [(1,1)] along a third dimension (x_3). This allows a plane to separate the two classes.

x_1	x_2	x_3	Output
0	0	0	0
0	1	0	1
1	0	0	1
1	1	1	0

The third input, x_3, is obtained from the first two inputs (by ANDing them); so that we have effectively introduced another layer into the network. (We will return to multilayer networks shortly).

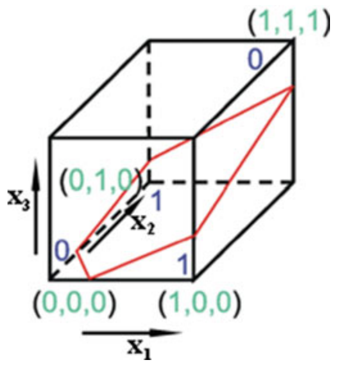

Fig. 6.13 The decision plane (in three dimensions) for the XOR problem, using an additional (dummy) input, x_3

Returning to the general case of a single neuron, the output, y, in general is

$$y = \sum_{j=1}^{n} w_j x_j + w_0 = \mathbf{w}^{\mathrm{T}}\mathbf{x} + w_0 \tag{6.4}$$

where **w** is the *weight vector* and w_0 is the *bias*, an intercept value to make the model more general that comes from an extra bias unit x_0, which is always +1 ($\mathbf{w}^{\mathrm{T}}$ is the transpose of **w**, used to make it into a column vector). We can write the output as a dot product (sometimes referred to as a scalar product, or inner product).

$$y = \mathbf{w}^{\mathrm{T}} \cdot \mathbf{x} \tag{6.5}$$

where **w** and **x** are *augmented* vectors that include the bias weight (and the threshold, $\theta = 0$). (Remember that the dot product of two vectors, **a** and **b**, $\mathbf{a}\cdot\mathbf{b} = \|\mathbf{a}\|\cdot\|\mathbf{b}\| \cos\theta$, where $\|\mathbf{a}\|$ is the length of the vector **a**, and θ is the angle between the two vectors).

Neural networks learn using an algorithm called *backpropagation*. The input data are repeatedly presented to the network. With each presentation, the output of the network is compared to the desired output and an error is computed. This error is then fed back (backpropagated) to the neural network and used to adjust the weights such that the error decreases with each iteration and the neural model gets closer and closer to producing the desired output. This process is known as *training*.

During *training*, the weights are adjusted until the outputs of the perceptron become consistent with the true outputs of the training examples, y_i. The weights are initially assigned to small random values and the training examples are used one after another to tweak the weights in the network: all the examples are used, and then the whole process is iterated until all examples are correctly classified by the output. This constitutes *learning*. Mathematically, after the initial random weights are chosen, the predicted outputs $\hat{y}_i^{(k)}$ are computed; and then each weight w_j is updated according to

$$w_j^{(k+1)} = w_j^{(k)} + \eta\left(y_i - \hat{y}_i^{(k)}\right)x_{ij} \tag{6.6}$$

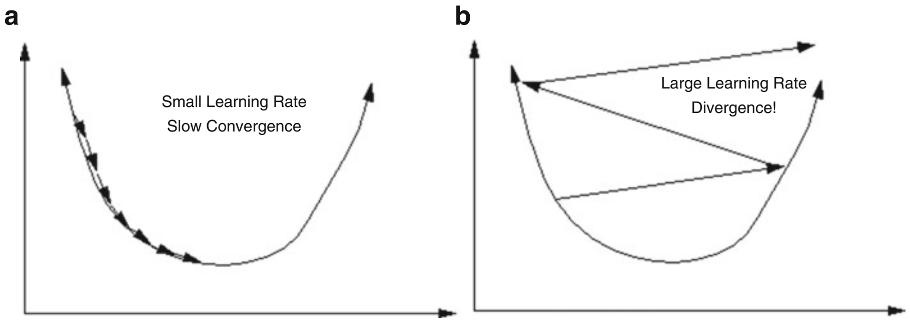

Fig. 6.14 (**a**) A small value of η results in slow convergence, while (**b**) a large value of η can result in divergence!

where $w^{(k)}$ is the weight associated with the *i*th input link after the *k*th iteration, η is known as the *learning rate*, and w_{ij} is the value of the *j*th attribute of the training parameter $\mathbf{x}_i$. In the weight update formula, links that contribute most to the error term are the ones that require the largest adjustment. However, the weights should not be changed too drastically because the error term is computed only for the current training example: otherwise, the adjustments made in earlier iterations will be undone. The learning rate (between 0 and 1, but typically set to $0.1 < \eta < 0.4$) is used to control the amount of adjustments made in each iteration. If $\eta \sim 0$, then the new weight is mostly influenced by the old weight; if $\eta \sim 1$, then the new weight is sensitive to the adjustment in the current iteration. Learning continues until either the iteration error, $y_i - \hat{y}_i^{(k)}$, is less than a user-specified threshold or a predetermined number of iterations has been completed.

The weight learning problem can be seen as finding the global minimum error, calculated as the proportion of misclassified training examples, over a space where all the input values can vary. Therefore, it is possible to move too far in a direction and improve one particular weight to the detriment of the overall sum. While the sum may work for the training example being looked at, it may no longer be a good value for classifying all the examples correctly. For this reason, η restricts the amount of movement possible. If a large movement is actually required for a weight, then this will happen over a series of iterations through the example set. If η is too small, the weights change very little at each step, and the algorithm takes a long time to converge (Fig. 6.14a). Conversely, if η is too large we may bounce around the error surface with the algorithm diverging (Fig. 6.14b): this usually ends up with an overflow error in the computer's floating-point arithmetic.

Sometimes, η is set to decay as the number of such iterations through the whole set of training examples increases, so that it can move more slowly toward the global minimum in order not to overshoot in one direction. (This is the kind of *gradient descent* used in the learning algorithm for *multilayered networks*).

Example 6.1 Learning

For a neuron with two inputs, we can easily decide what weights to use to give us the correct output, but with more complex functions (more inputs or more layers) it will not be so easy to decide. We would like our perceptron to "learn" so that it can come up with its own weights. Let us consider the AND function again (Fig. 6.11). We want to be able to assign random weights, and to train the perceptron to give the correct output (which we will present as the training value required) by adjusting these weights as it is presented with the entire training set (this presentation being known as an *epoch*) a number of times. This adjusting of the weights will proceed according to (6.6).

Look at the spreadsheet, `perceptron.xls` (downloadable from http://extras.springer.com), which allows us to learn simple functions such as AND.

If we start with weights of $w_0 = w_1 = w_2 = 0.5$, and present the network with the first training pair ([0,0]), from the first epoch, the network produces an output of 1, when it should produce a 0: the error is -1 and so the weights will change. Using (6.6) and a learning rate, $\eta = 0.1$,

$$\begin{aligned} w_0 &= 0.5 + (0.1 \times 1 \times -1) = 0.4 \\ w_1 &= 0.5 + (0.1 \times 0 \times -1) = 0.5 \\ w_2 &= 0.5 + (0.1 \times 0 \times -1) = 0.5 \end{aligned}$$

These values become the new weights. The next training pair ([0,1]) also produces a 1, when it should produce a 0, and so again the weights need to be re-computed. The following training pair ([1,0]) also produces an output of 1, when the required output is 0, and the weights have to be adjusted again. Finally, we apply the input ([1,1]) to the network. This produces an output of 1, which is the required output: no error has occurred here, so the weights remain the same. As this presentation of the epoch produced three errors, we need to continue the training and present the network with another epoch. Training continues until an epoch is presented that does not produce an error (i.e., until the outputs have converged on the required outputs); at this stage, after the fourth epoch, the weights have become -0.3, 0.2, and 0.2 respectively. These are different values for the weights to those in Fig. 6.11c, but the weights are in the same ratio so that the resulting decision boundary turns out to be the same. (But note that the decision boundary could be moved around a little and still implement the AND function: it just needs to be able to distinguish the two classes).

We could keep track of the decision boundary after each epoch, and plot them, confirming that only after the fourth epoch is the decision boundary able to discriminate the two classes of output.

What is the effect of changing the starting weights?

What happens if the learning rate, η, is changed?

What happens if you try to get the perceptron to learn the OR, NAND, and XOR functions?

The perceptron learning algorithm does not terminate if the learning set is not linearly separable. In many real-world cases, however, we may want to find the “best” linear separation even when the learning sets are not ideal. The *pocket algorithm* (Gallant 1990) is a modification of the perceptron rule. It solves the stability problem by storing the best weight vector so far in its “pocket” while continuing to learn. The weights are actually modified only if a better weight vector is found. In another variant, ADALINE (Adaptive Linear Element or Adaptive Linear Neuron), a correction is applied to the weights (using approximate gradient descent) before the thresholding step (Widrow and Hoff 1960).

We could make our perceptron even more useful by arranging to use an *activation function* at the output other than the threshold function. Examples of other activation functions which are in common use include the linear function, the sigmoid (logistic) function

$$y = \mathrm{sigmoid}(o) = 1/(1 + \exp(-\mathbf{w}^{\mathrm{T}}\mathbf{x}) \tag{6.7}$$

which would give a smooth transition between the low and high input of the neuron, and the hyperbolic tangent (tan*h*) function (Fig. 6.15).

In a *neural network*, large numbers of simple elements (neurons) are connected together in a variable topology. The objective is to develop a topology during training so that patterns are correctly classified. The network is dynamic since the weights and activation functions can change over time. In a *multilayer network* [or *multilayer perceptron* (*MLP*)], the neurons are arranged in a layered configuration containing an input layer, one or two “hidden” layers, and an output layer. Figure 6.16 shows a two-layer network (the input neurons are not normally form a layer since they are just a means of getting the data into the network: the hidden layer is the first layer, and the output layer is the second layer) with four inputs, five hidden nodes, and one output. In a *feed-forward* network, the nodes in one layer are connected only to the nodes in the next layer. (In a *recurrent* network, the nodes can connect to others in the same or previous layers).

Training optimizes all of the weights and threshold values (or other activation function parameters) using some fraction of the available data. Optimization routines can be used to determine the ideal topology and the nature of the activation functions.

The *universal approximation theorem* (Cybenko 1989; Hornik 1991) for ANNs states that every continuous function that maps intervals of real numbers to some output interval of real numbers can be approximated arbitrarily closely by a multilayer perceptron with just one hidden layer. Having two hidden layers rarely improves the situation, and may introduce a greater risk of converging to a local minimum. (Note that two hidden layers are required for data with discontinuities).

One of the most important questions is how many neurons to use in the hidden layer. If an inadequate number of neurons is used, the network will be unable to model complex data and the resulting fit will be poor. If too many neurons are used, the training time may become excessively long, and, worse, the network may *overfit*

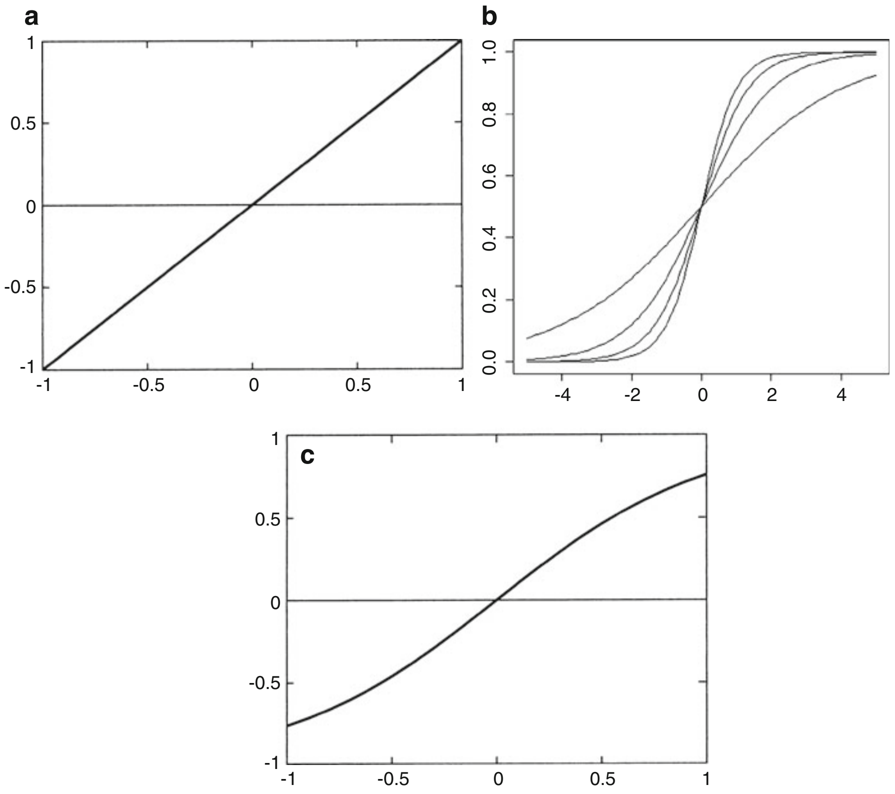

Fig. 6.15 Activation functions (**a**) linear, (**b**) sigmoid, where changing the weight, **w**, alters the steepness of the function (**c**) tan*h*

Fig. 6.16 A simple two-layer (feed-forward) ANN

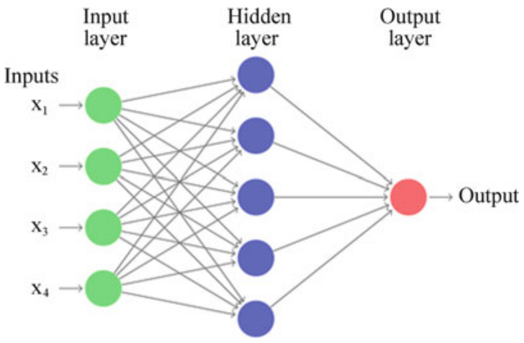

the data. When overfitting occurs, the network will begin to model random noise in the data. The result is that the model fits the training data extremely well, but it generalizes poorly to new, test data. Validation must be used to check for this.

Example 6.2 Implementation of the logical XOR function

x_1	x_2	y
0	0	0
0	1	1
1	0	1
1	1	0

Let us return to the XOR function, which we saw could not be solved using a decision boundary that is a single line (Fig. 6.12). However, two discriminant lines could be used to separate "true" from "false" (Fig. 6.17a); the discriminant functions could be

$$y_1 = x_2 - x_1 - 0.5$$
$$y_2 = x_2 - x_1 + 0.5$$

which would require a two-layer network (Fig. 6.17b), with $w_{11} = w_{12} = -1$; $w_{21} = w_{22} = 1$; $b_1 = -0.5$; and $b_2 = 0.5$. We could also make $w_1 = -1$, $w_2 = 1$ and $b_0 = 0$. (What are the three required thresholds?)

Alternatively, we could have $w_{11} = w_{12} = w_{21} = w_{22} = 1$: $w_1 = 1$, $w_2 = -1$: $b_0 = b_1 = b_2 = -0.5$. For an input of (1,0), the input to the top neuron in the hidden layer is 0.5, which is above the threshold (0), so that this neuron fires giving an output of 1. The input to the bottom neuron in the hidden layer is 0, so it does not fire and the output is 0. The signal reaching the output neuron is then 0.5, so this neuron fires to give an output of 1. You should check the outputs for all the other possible inputs. You should be able to see that the neuron in the output layer fires (giving 1), when the inputs x_1 and x_2 are different to each other, but does not fire when they are the same: this is exactly the XOR function.

To learn the weights of an artificial neural network model, we need an efficient algorithm that converges to the correct solution when a sufficient number of training samples are provided. The goal is to determine a set of weights **w** that minimizes the total sum of squared errors:

$$y_1 = x_2 - x_1 - 0.5$$
$$y_2 = x_2 - x_1 + 0.5$$

Note that the sum of the squared errors depends on **w** because the predicted class $\hat{y}$ is a function of the weights assigned to the hidden and output nodes. If we replace $\hat{y}$ by $\mathbf{w}^T\mathbf{x}$ then the error function is a quadratic surface.

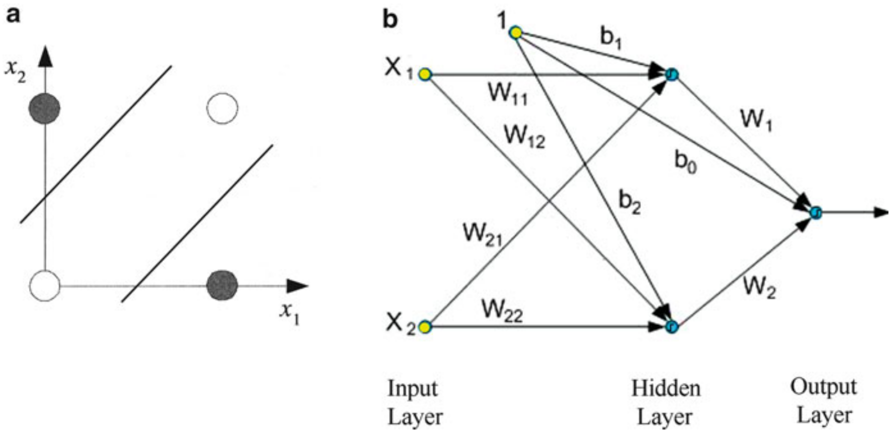

Fig. 6.17 (**a**) The required discriminant functions in feature space [where the *dark circle* indicates the "true" output ("1"), and *white circles* indicates the "false" outputs ("0")], and (**b**) the corresponding neural network to implement it

Optimization methods such as *steepest (*or *gradient) descent* and *conjugate gradient* are highly susceptible to finding local minima if they begin the search in a valley near a local minimum. They have no ability to see the big picture and find the global minimum. Several methods have been tried to avoid local minima. The simplest is just to try a number of random starting points and use the one with the best value. A more sophisticated technique called *simulated annealing* improves on this by trying widely separated random values and then gradually reducing ("cooling") the random jumps in the hope that the location is getting closer to the global minimum.

The computation of the weights for the hidden nodes is not trivial because it is difficult to assess their error term without knowing what their output values should be. *Backpropagation* (more specifically, the backpropagation of errors) has been developed to address this issue for multilayered networks. With backpropagation, the input data are repeatedly presented to the neural network. With each presentation, the output of the neural network is compared to the desired output and an error is computed (Fig. 6.18). This error is then fed back (backpropagated) to the neural network and used to adjust the weights such that the error decreases with each iteration and the neural model gets closer and closer to producing the desired output. This sequence of events is repeated until an acceptable error has been reached or until the network no longer appears to be learning. This process is known as *training*.

Training an ANN is a time-consuming process, especially when the number of hidden nodes is large. The training set (i.e., the patterns whose class labels are known) are presented to the network, and the weights are adjusted to make the output similar to the target values. In *stochastic training* patterns are chosen randomly from the training set, and the network weights are updated for each pattern presentation.

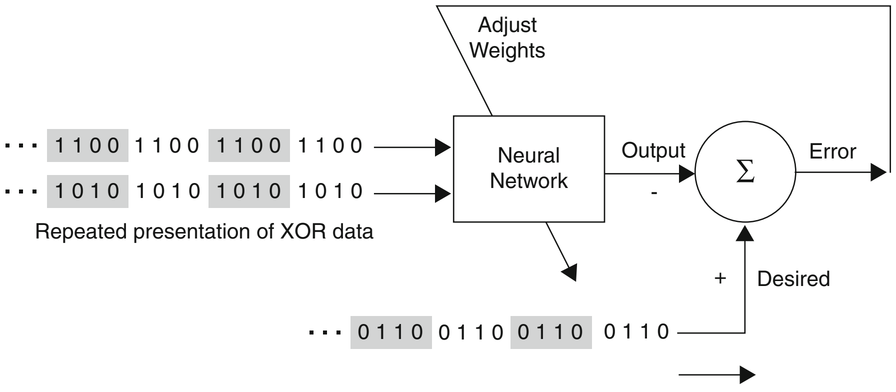

Fig. 6.18 Multilayer neural network learning to model the XOR function

In stochastic training, a weight update may reduce the error on the single pattern being presented, yet increase the error on the full training set. However, given a large number of such individual updates the total error decreases. In *batch training*, all patterns are presented to the network before learning takes place. In virtually every case, we must make several passes through the training data. In the batch training protocol, all the training patterns are presented first and their corresponding weight updates summed; only then are the actual weights in the network updated. This process is iterated until some stopping criterion is met. In *on-line training*, each pattern is presented once and only once; there is no use of memory for storing the patterns.

Before training has begun, the error on the training set is typically high; through learning, the error becomes lower, as shown in a learning curve (Fig. 6.19). The average error (per pattern) on an independent test set is always higher than on the training set, and while it generally decreases, it can increase or oscillate. A *validation set* (comprising new representative test patterns) is used to decide when to stop training: we stop training at the minimum of the average error on this set. The curve for the validation set in Fig. 6.19 indicates that training should stop at about the fifth epoch. (We will consider validation, or more generally cross-validation, in some detail in Chap. 8). The *test set* is used to measure the performance of the network.

Table 6.1 summarizes the advantages and disadvantage of a neural network.

In separable problems, perceptrons can find different solutions. It would be interesting to find the hyperplane that assures the maximal safety tolerance training, i.e., the largest separating margin between the classes (Fig. 6.20). The margins of that hyperplane touch a limited number of special points (called the *support vectors*), which define the hyperplane. Only the support vectors are required to obtain this hyperplane, the other training samples can be ignored.

This so-called *optimal perceptron* (i.e., having optimal stability) can be determined by means of iterative training and optimization schemes [such as the Min-Over algorithm (Krauth and Mezard 1987) or the AdaTron (Anlauf and Biehl 1989)]. The perceptron of optimal stability is, together with the *kernel trick*, one of the conceptual foundations of the *support vector machine*.

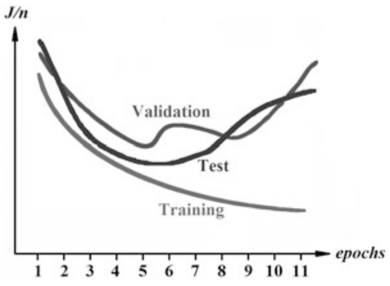

Fig. 6.19 A typical learning curve. The average error per pattern is plotted as a function of the number of epochs

Table 6.1 The advantages and disadvantages of neural networks

Advantages	Disadvantages
It can perform tasks which a linear classifier cannot	It needs training to operate
If a neuron fails, the network can continue because of its parallel nature	It uses a different architecture from most microprocessors (needs emulation mode)
It learns and does not need to be reprogrammed	Large networks require high processing time
It can be implemented easily for any application	

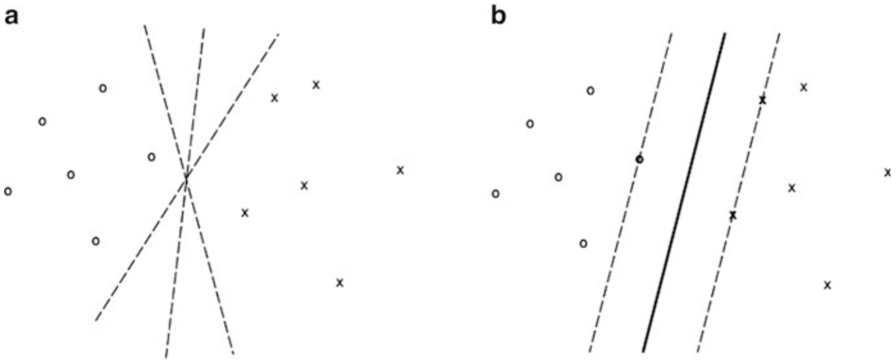

Fig. 6.20 (**a**) A perceptron can find different solutions to a linearly separable problem. (**b**) This solution assures the maximal safety tolerance

6.4 Kernel Machines

The *support vector machine*, SVM (Cortes and Vapnick 1995), later generalized under the name *kernel machine*, became popular when it was applied to a handwriting recognition task, given pixel maps as input, and produced very accurate results. For linearly separable problems, it finds the optimal separating hyperplane

Fig. 6.21 Support vectors and classification margin

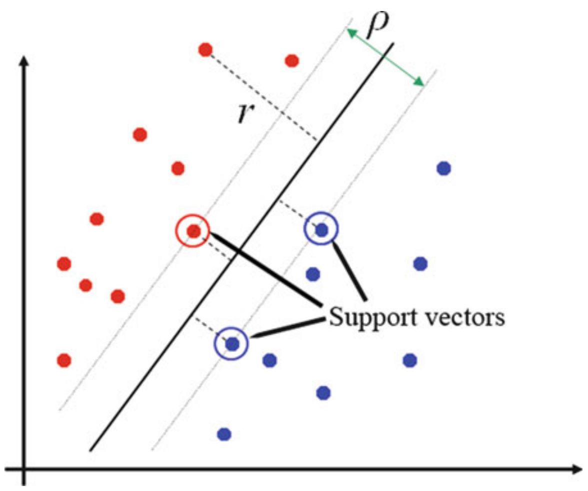

by maximizing the margin, the perpendicular distance across the hyperplane to the closest instances (the support vectors) on either side of it. For nonlinearly separable problems, we can settle on the hyperplane that incurs the least error; or we can map the data by doing a nonlinear transformation using suitable chosen basis functions into a higher-dimensional space, where the problem may become linear. For example, we saw in Sect. 6.3 that the XOR problem is a nonlinearly separable problem. However, it is possible to solve it by transforming the inputs into a higher-dimensional space, where it is linearly separable (Fig. 6.13). This is the basic idea behind the *kernel trick* (and the origin of the name *kernel machine*).

Maximizing margins around the separating hyperplane seems a good idea both intuitively and according to PAC (Probably Approximately Correct) theory. Given that the equation of a separating hyperplane is

$$\mathbf{w}^{\mathrm{T}}\mathbf{x} + b = 0 \tag{6.9}$$

where $\mathbf{w}$ and b are parameters of the model, the distance from an example, $\mathbf{x}_i$, to the hyperplane is given by

$$r = (\mathbf{w}^{\mathrm{T}}\mathbf{x} + b)/\|\mathbf{w}\| \tag{6.10}$$

The examples closest to the hyperplane are called the *support vectors*, and the (classification) *margin* of the separator is the distance between support vectors from the different classes (Fig. 6.21). The problem is one of quadratic optimization subject to linear constraints. These are a well-known class of mathematical programming problems, albeit beyond the scope of this text.

SVMs are basically two-class classifiers. If the training set is not linearly separable, it may still be possible to find a solution by introducing *slack variables*

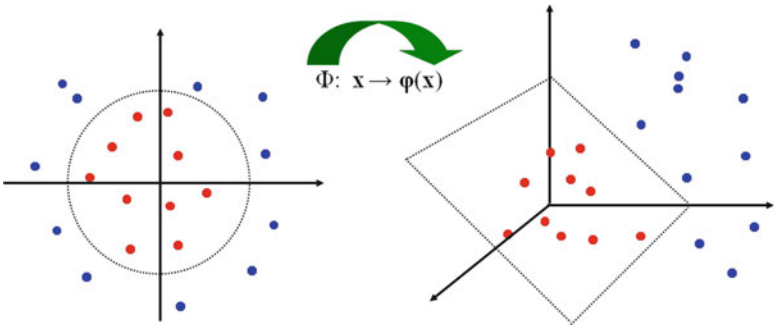

Fig. 6.22 Transform nonlinear SVM into a higher-dimensional feature space

to allow misclassification of difficult or noisy examples, resulting in a so-called *soft* margin. If this does not work, the original feature space needs to be mapped to a higher-dimensional feature space where the training set is separable (Fig. 6.22). This involves the so-called *kernel trick*, and relies on computing the inner product between vectors, $\mathbf{x}_i^T\mathbf{x}_j$. Typical kernel functions are linear, polynomials, and Gaussians (radial basis functions).

Example 6.3 Using a polynomial kernel

Suppose we have five 1D data points, $x_1 = 1$, $x_2 = 2$, $x_3 = 4$, $x_4 = 5$ and $x_5 = 6$, with 1, 2 and 6 as class 1 and 4, 5 as class 2 (Fig. 6.23a). This is clearly a nonlinear problem.

Introducing a second dimension, y, with $y_1 = 1$, $y_2 = 1$, $y_3 = -1$, $y_4 = -1$, $y_5 = 1$, and using a polynomial kernel of degree 2, $K(x, y) = (xy + 1)2$ gives a discriminant function, $f(y) = 0.6667x^2 - 5.333x + 9$ which successfully separates the two classes (Fig. 6.23b).

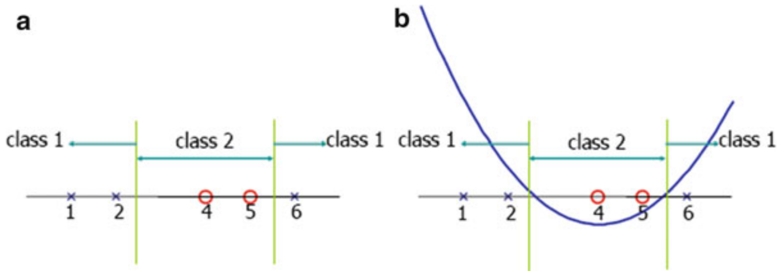

Fig. 6.23 (**a**) Original 1D data (**b**) transformed to 2D

6.5 Exercises

1. Show how a perceptron can be used to implement the logical OR function. Sketch the discriminant function.
2. Consider a neuron with two inputs, one output and a threshold activation function. If the two weights are $w_1 = w_2 = 1$, and the bias is -1.5, what is the output for an input of ([0,0])? What about inputs ([0,1]), ([1.0]) and ([1,1]). Draw the discriminant function, and write down its equation. What logic function does it represent?
3. An approach to solving the XOR function is to map the problem to three dimensions, by including a third input, x_3, which moves the point at $x_1 = 1$, $x_2 = 1$ along a third dimension but does not change the result when it is looked at using a projection into the x_1, x_2 plane. This allows a linear plane (the 2D analog of a straight line) to separate the points. (a) Construct a truth table for XOR with three inputs, (b) plot a decision plane in a 3D diagram and (c) show how this could be implemented with a neural network.
4. The following Fig. 6.24 shows a multilayer neural network involving a single hidden neuron and jumping connections from the inputs to the output directly. (a) Construct a truth table for all variables x_1, x_2, x_3, and x_4. Show that the network solves the XOR problem. (b) Plot the decision boundary of x_3 in the x_1–x_2 plane; (c) Plot the decision boundary of x_4 in the x_1–x_2 plane and explain how you derive it. (Note that your decision boundary should not be limited to the unit square only). Note that the number on top of each neuron is the threshold and it is subtracted from the net input. For instance, the equation for x_3 is $x_3 = \text{step}(x_1 + x_2 - 1.5)$.

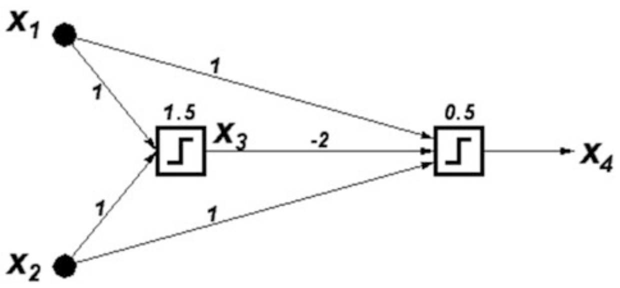

Fig. 6.24 XOR implementation

5. Example 6.2 in the text considers a two-layer network (Fig. 6.17b) to implement the XOR function, with $w_{11} = w_{12} = -1$; $w_{21} = w_{22} = 1$; $b_1 = -0.5$; and $b_2 = 0.5$. We could also make $w_1 = -1$, $w_2 = 1$ and $b_0 = 0$. Follow the signals through the network, and find the required values of the three thresholds. (See spreadsheet, Q6.5.xls, downloadable from http://extras.springer.com).

References

Anlauf, J.K., Biehl, M.: The AdaTron: an adaptive perceptron algorithm. Europhys. Lett. **10**, 687–692 (1989)

Cortes, C., Vapnick, V.N.: Support-vector networks. Mach. Learn. **20**, 273–297 (1995)

Cybenko, G.: Approximations by superpositions of sigmoidal functions. Math Control Signal Syst **2**, 303–314 (1989)

Gallant, S.I.: Perceptron-based learning algorithms. IEEE Trans. Neural Netw. **1**, 179–191 (1990)

Hornik, K.: Approximation capabilities of multilayer feedforward networks. Neural Netw. **4**, 251–257 (1991)

Krauth, W., Mezard, M.: Learning algorithms with optimal stability in neural networks. J. Phys. A **20**, 745–752 (1987)

Le Cun, Y.: Learning processes in an asymmetric threshold network. In: Bienenstock, E., Fogelman-Smith, F., Weisbuch, G. (eds.) Disordered Systems and Biological Organization, NATO ASI Series, F20. Springer-Verlag, Berlin (1986)

McCulloch, W., Pitts, W.: A logical calculus of the ideas immanent in nervous activity. Bull. Math. Biophys. **7**, 115–133 (1943)

Minsky, M.L., Papert, S.A.: Perceptrons. MIT Press, MA (1969)

Parker, D.: Learning Logic. Technical Report TR-87. MIT Center for Computational Research in Economics and Management Science, Cambridge, MA (1985)

Widrow, B., Hoff, M.E.: Adaptive switching circuits. In 1960 IRE WESCON Convention Record, part 4, pp. 96–104. IRE, New York (1960)

Chapter 7
Feature Extraction and Selection

7.1 Reducing Dimensionality

In most classification applications, the complexity depends on the number of features, d (which result in a d-dimensional feature space) and the number of (training) data samples, N. As the dimensionality (number of features) increases, increasing amounts of training data are required (this is called the *curse of dimensionality*). In order to reduce the computational complexity, the number of features should be reduced to a sufficient minimum. When we decide that a feature is unnecessary, we save the cost of extracting it. When data can be explained in terms of fewer features, the data can be analyzed visually more easily and we get a better idea about the underlying process. Humans have an extraordinary capacity to discern patterns and clusters in one, two or three dimensions, but these abilities degrade drastically for four or higher dimensions. If we keep features that have little discriminative power (because of a high correlation with another feature), the classifier will be more complex and is likely to perform poorly. Simple models will consequently require smaller datasets.

For a finite sample size, N, increasing the number of features (from 1) will initially improve the performance of a classifier, but after a critical value, further increase in the number of features (d) will reduce the performance resulting in *overfitting* the data (Fig. 7.1). This is known as the *peaking phenomenon*. In most cases, the additional information that is lost by discarding some features is (more than) compensated by a more accurate mapping in the lower-dimensional space.

There are two main methods for reducing dimensionality; *feature selection* and *feature extraction*. In feature selection, we want to select the k features (out of d) that provide the most information, discarding the other $(d - k)$ features. Methods to implement feature selection include using the inter/intraclass distance and *subset selection*. In feature extraction, we find a new set of k $(<d)$ features which are combinations of the original d features. These methods may be supervised or unsupervised. The most widely used feature extraction methods are *Principal Components Analysis (PCA)* and *Linear Discriminant Analysis (LDA)*, which are both linear projection methods, unsupervised and supervised respectively.

DOI 10.1007/978-1-4614-5323-9_7, © Springer Science+Business Media New York 2013

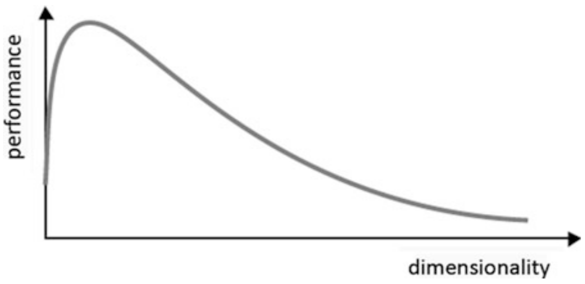

Fig. 7.1 The performance of a classifier in terms of the dimensionality of the feature space

7.1.1 Preprocessing

Prior to using the data we should remove outliers, scale the features to comparable dynamic ranges (viz., normalization), and treat incomplete data.

Outliers are data that lie far from the mean of the corresponding random variable. They can produce large errors during training, especially when they are a result of noise. For a normal distribution, we could remove data points which are more than three standard deviations from the mean (since they have less than a 1% chance of belonging to the distribution).

The features can be normalized to have zero mean and unit variance using the transform

$$x' = \frac{(x - \bar{x})}{\sigma} \tag{7.1}$$

where $\bar{x}$ and σ are the mean and standard deviation of the original feature values. If the original data are not evenly distributed around the mean, then a further transform (so-called *softmax* scaling) can be used:

$$x' = \frac{1}{1 + \exp(-x')} \tag{7.2}$$

One way of dealing with incomplete data is to generate missing values randomly from the distribution characterized by the known values.

7.2 Feature Selection

7.2.1 Inter/Intraclass Distance

Good features are discriminative. Intuitively, there should be a large intraclass distance and a small interclass distance. Figure 7.2 shows the case for a single feature, two equiprobable class situation.

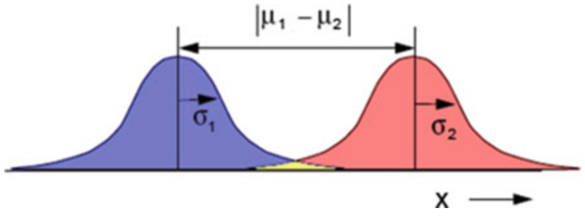

Fig. 7.2 Single feature, x, distinguishing two equiprobable classes

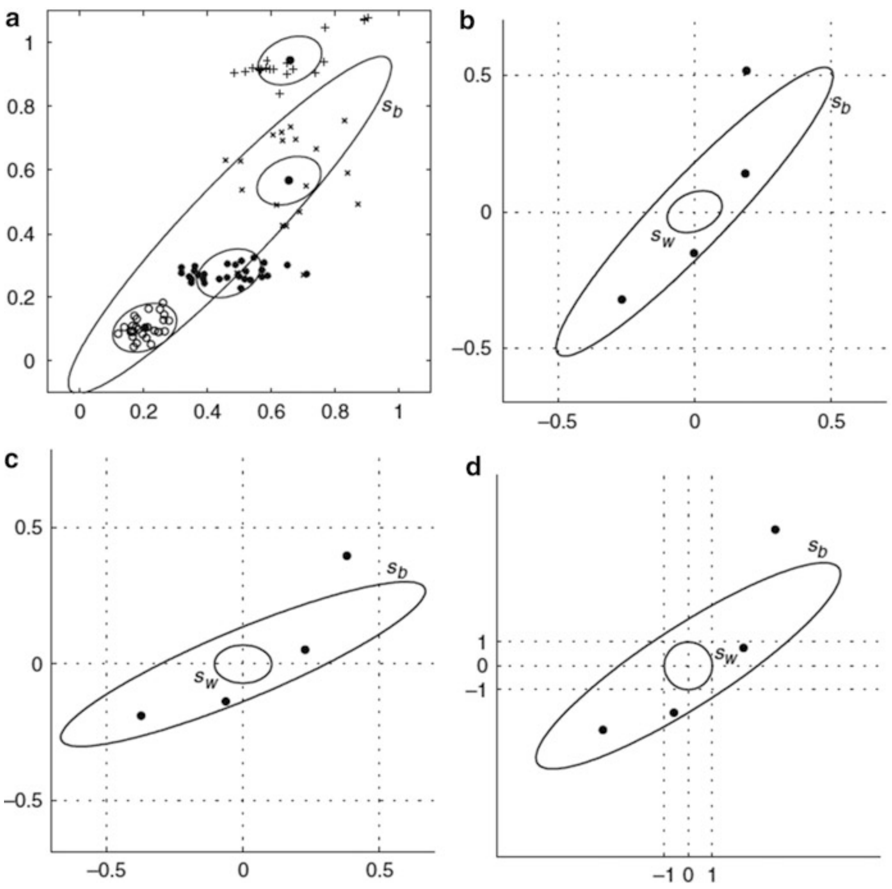

Fig. 7.3 Two-feature, four-class data: (**a**) scatter diagram, (**b**) after normalization, (**c**) after decorrelation, and (**d**) after whitening. (After Van der Heijden et al. 2004)

Figure 7.3 shows a more complicated case, a training set with two features and four classes. The scatter diagram shows the four classes, each of which has its own (within-scatter) matrix, S_w, describing the scattering within each class and resulting in characteristic elliptical isocontours around the class means, and one isocontour is shown for each class (Fig.7.3a). There is also a between-scatter matrix, S_b, which describes the scatter of the class means about the overall mean, and a resulting isocontour is shown. The separability of the classes is the ratio of the *intraclass distance*, J_{INTRA} [given by trace(S_b)] and the *interclass distance*, J_{INTER} [given by trace(S_w)], i.e., trace(S_b)/trace(S_w). This can be regarded as a signal-to-noise ratio. The data can then be normalized (to the range [−½, +½]) (Fig.7.3b), decorrelated (to remove cross-correlations) (Fig. 7.3c), and *whitened* so that $S_w = \mathbf{I}$ and its isocontour becomes a circle with unit radius (Fig. 7.3d). In this transformed space the area of the ellipse associated with the between-scatter, called the *inter/intra distance*, is a useable performance measure, and is given by

$$J = \text{trace}({S_w}^{-1} S_b) \tag{7.3}$$

This criterion takes a special form in the one-dimensional, two-class problem. For equiprobable classes, $|S_w|$ is proportional to ${\sigma_1}^2 + {\sigma_2}^2$, and $|S_b|$ is proportional to $({\mu_1}^2 - {\mu_2}^2)^2$. Combining them gives *Fisher's discriminant ratio* (FDR):

$$\text{FDR} = \frac{{\mu_1}^2 - {\mu_2}^2}{{\sigma_1}^2 + {\sigma_2}^2} \tag{7.4}$$

7.2.2 Subset Selection

The best subset contains the least number of features that contribute to accuracy. There are 2^d possible subsets of d features, but we cannot test for all of them unless d is small. There are two approaches: in *forward selection*, we start with no variables and add them one by one, at each step adding the one that decreases a suitable error metric the most, until any further addition does not decrease the error (or decreases it only slightly). In *backward selection*, we start with all the variables and remove them one by one, at each step removing the one that decreases the error the most (or increases it only slightly), until any further removal increases the error significantly. In either case, we need to check the error on a validation set distinct from the training set because we want to test the generalization accuracy.

Depending on the application, the error metric is either the mean square error or the misclassification error. In both forward and backward selection, the process is costly and does not guarantee finding the optimal subset.

Subset selection would not be useful in face recognition, for example, because individual pixels by themselves do not carry much discriminative information: it is a combination of several pixels that carries the information about the face identity.

7.3 Feature Extraction

In projection methods, we want to find a mapping from the original d-dimensional space to a new k ($<d$)-dimensional space, with minimum loss of information. An *optimal* mapping would be one that results in no increase in the minimum probability of error, i.e., a Bayes decision rule applied to the initial (d-dimensional) space and to the reduced (k-dimensional) space yields the same classification error. In general, optimal mapping will require a nonlinear function, but we will restrict ourselves to linear mapping. Within the realm of linear feature extraction, two techniques are in common use: Principal Component Analysis (PCA) and Linear Discriminant Analysis (LDA).

7.3.1 *Principal Component Analysis*

The goal of Principal Component Analysis [also known as the *Karhunen–Loève* (*KL*) transform] is to represent the data accurately in a lower-dimensional space. As much of the randomness (variance) in the higher-dimensional space as possible should be preserved. This is achieved by a transformation that centers the data and rotates the axes to line up with the direction of highest variance (Fig. 7.4).

Each principal component (PC_1, PC_2, ...) is a linear combination of the original variables, and there are as many principal components as original variables. The first principal component has as high a variance as possible (i.e., it accounts for as much of the variability in the data as possible), and each succeeding component in turn has the highest variance possible under the constraint that it is orthogonal to (i.e., uncorrelated with) the preceding components. Usually, the variance of the original data can be explained by the first few principal components and the rest can be ignored. In this case, using the principal components reduces the dimensionality of the data, making it more amenable to visual inspection, clustering, and pattern

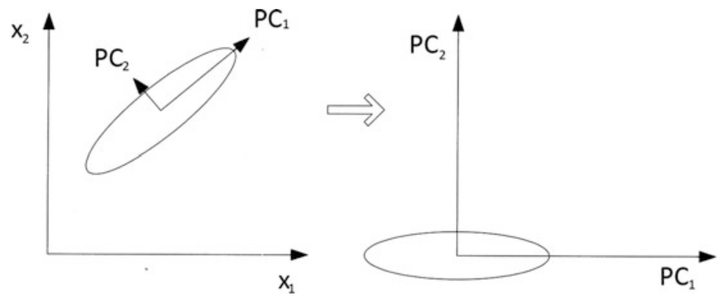

Fig. 7.4 Principal components analysis centers the data and then rotates the axes to line up with the directions of highest variance. If the variance on PCA2 is small, it can be ignored and the dimensionality reduces from two to one

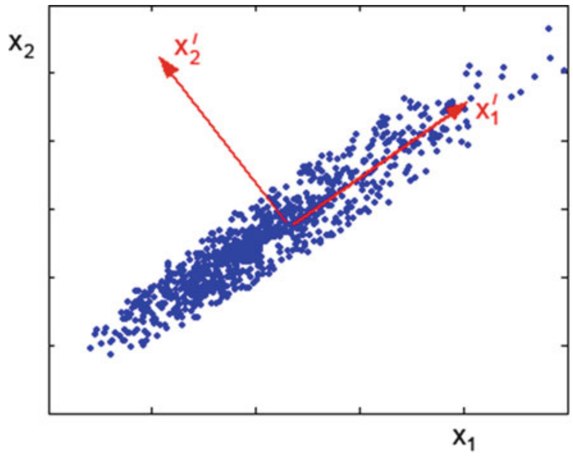

Fig. 7.5 PCA in 2D: rotation of axes to line up with direction of largest variance (x_1').

recognition efforts. In Fig. 7.5, most of the variance occurs in the x_1' direction, and x_2' can be ignored.

PCA can reveal the internal structure of the data in a way that best explains its variance, but it treats the total data and does not take into account class labels (i.e., it is unsupervised). There is no guarantee that the directions of maximum variance will make good features for discrimination.

The principal components are obtained by diagonalizing the covariance matrix of the original data (Fig. 7.6). Their directions and magnitudes are given by the *eigenvectors* and *eigenvalues*, respectively, of the original covariance matrix.

$$\Sigma\mathbf{x} = \lambda\mathbf{x}$$
$$(\Sigma - \lambda\mathbf{I})\mathbf{x} = 0$$

where the λ's are the eigenvalues of $\mathbf{\Sigma}$, and the $\mathbf{x}$'s are the corresponding eigenvectors.

If we order the eigenvalues in descending order, then the first eigenvector will be the directional cosines of the first principal component axis and the first eigenvalue will be the variance along this axis, and so on. Note that the total invariance is conserved, i.e., the sum of the variances of the principal components is equal to the sum of the variances [trace ($\mathbf{\Sigma}$)] of the original variables. Thus the contribution of any eigenvalue, λ_i, to the total variance is λ_i/trace ($\mathbf{\Sigma}$).

It is important to realize that principal components analysis only helps if the original variables are correlated. If they are highly correlated, there will be a small number of eigenvectors with large eigenvalues; a large reduction in dimensionality can be obtained by keeping only the k largest principal components.

(Note that if the data are extremely noisy, PCA may end up suggesting that the noisiest variables are the most significant: measuring the entropy of the variables would be a way to identify whether some variables are too noisy to be included in the analysis).

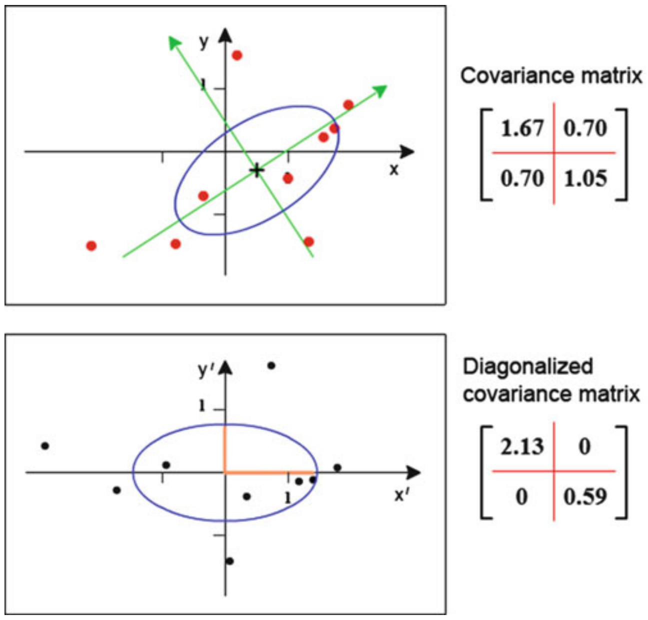

Fig. 7.6 The covariance matrix and a corresponding isocontour of a bivariate Gaussian distribution, before (*top*) and after (*bottom*) diagonalization

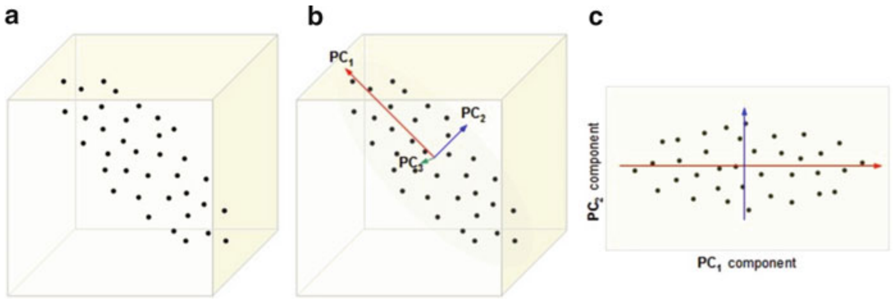

Fig. 7.7 (**a**) A dataset in 3D, (**b**) the principal component directions, (**c**) the two largest principal components

In 3D, there will be three principal components (Fig. 7.7), ranked from the most significant to the least.

A classic multivariate dataset is Fisher's iris data [Fisher 1936], comprising 50 samples from each of three species (*setosa*, *virginica*, and *versicolor*) of iris flowers (Fig. 7.8). Four features (the length and width of the sepal and the petal) were measured from each sample.

A *scatter plot matrix* of the features (in pairs) is useful to see whether any of the features are correlated, i.e., whether they are connected to some degree within the dataset (Fig. 7.9).

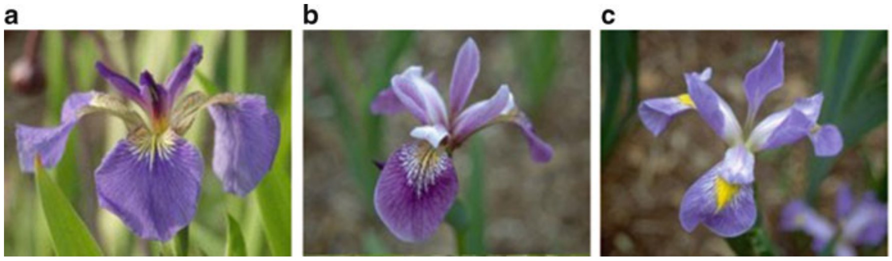

Fig. 7.8 Iris flowers (**a**) *Iris setosa*, (**b**) *Iris versicolor*, and (**c**) *Iris virginica*

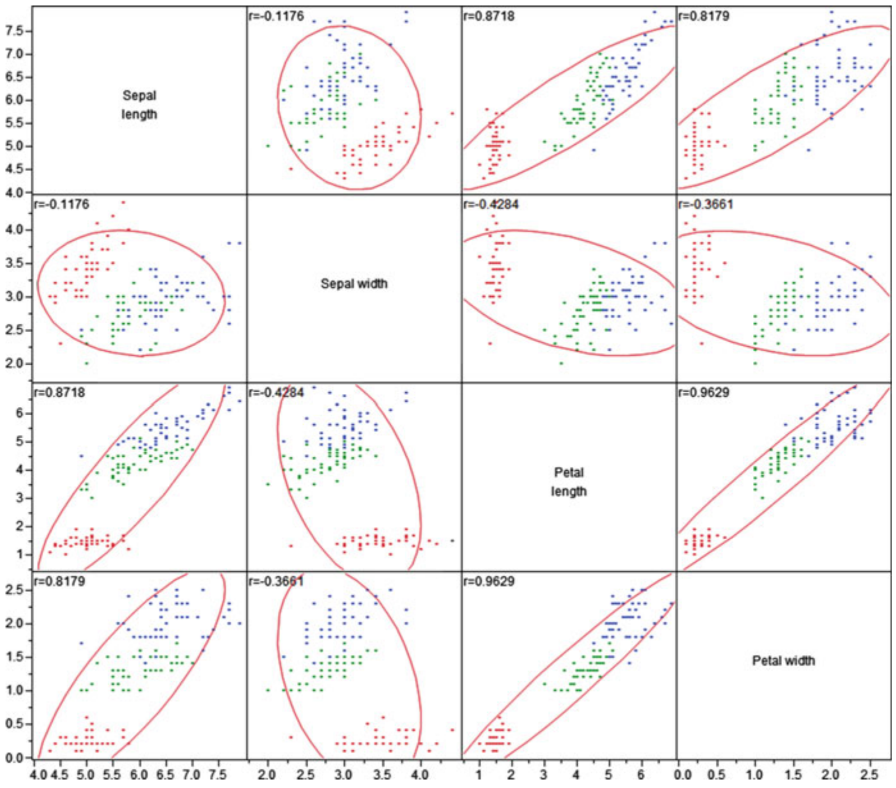

Fig. 7.9 Scatter plot matrix of Fisher's iris data. (The features from *Iris setosa* are plotted in *red*, those from *Iris versicolor* are plotted in *green*, and those from *Iris virginica* are plotted in *blue*; the elliptical contours enclose 95% of the features in each plot.)

The correlation coefficients from the scatter plot matrix form a correlation matrix (Table 7.1).

The petal length is highly correlated with the petal width, somewhat less correlated with the sepal length and the sepal width. Because of the high

Table 7.1 Correlation matrix showing the correlation coefficients corresponding to the scatter plot matrix of Fig. 7.9

	Sepal length	Sepal width	Petal length	Petal width
Sepal length	1	−0.118	0.872	0.818
Sepal width	−0.118	1	−0.428	−0.366
Petal length	0.872	−0.428	1	0.963
Petal width	0.818	−0.366	0.963	1

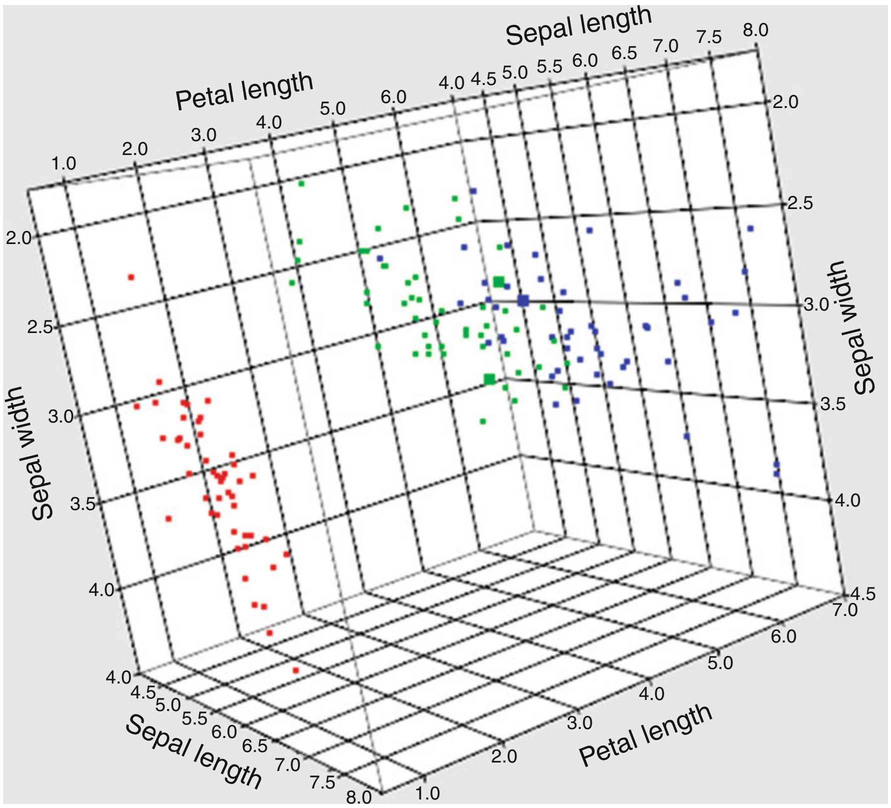

Fig. 7.10 3D scatterplot of Fisher's iris data showing sepal length, sepal width, and petal length

correlation, the petal width is not providing much information that is not already provided by the petal length.

We can produce a 3D scatterplot of any three of the features (e.g., Fig. 7.10), but cannot visualize all four together. The scatterplot can be rotated, and it is clear that it will be easy to distinguish *setosa* (red) from the other two species, but not so easy to distinguish *versicolor* (green) from *virginica* (blue).

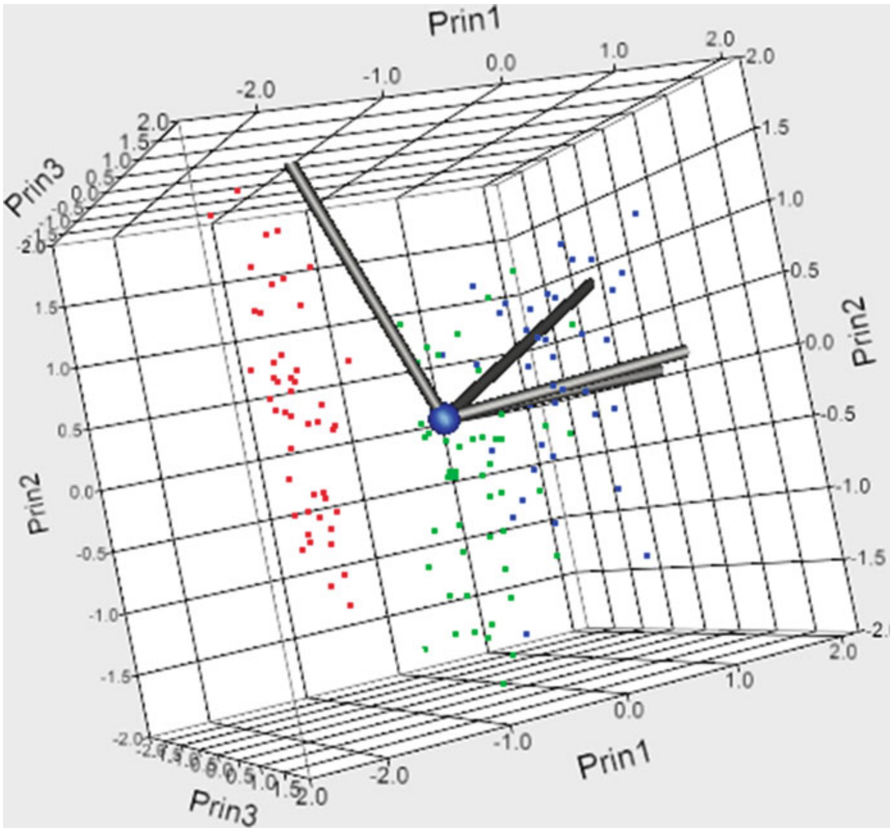

Fig. 7.11 3D scatterplot of the three largest principal components. The overlaid biplot shows the directions of the original four variables. It can be seen that two of them are highly correlated (i.e., in very similar directions)

PCA reveals the directions of greatest variance. For the iris data, the three largest principal components are shown in Fig. 7.11. The overlaid *biplot* shows the directions of the original four variables. It can be seen that two of them are highly correlated (i.e., in very similar directions).

The percentage of the total variance accounted for by each of the principal components is proportional to the value of the individual eigenvalues (Fig. 7.12a). The eigenvalues (or percentage contributions) plotted against the number of principal components is known as a *scree plot* and is useful for determining how many principal components need to be kept to capture most of the variability of the data. The first two principal components account for 95.8% of the variation, so that keeping only them will preserve most of the variability of the data and reduce the dimensionality from four to two. This is shown in the so-called *scree plot* of Fig. 7.12b. (Scree is a term for the rubble that accumulates at the bottom of steep cliffs, which this plot resembles).

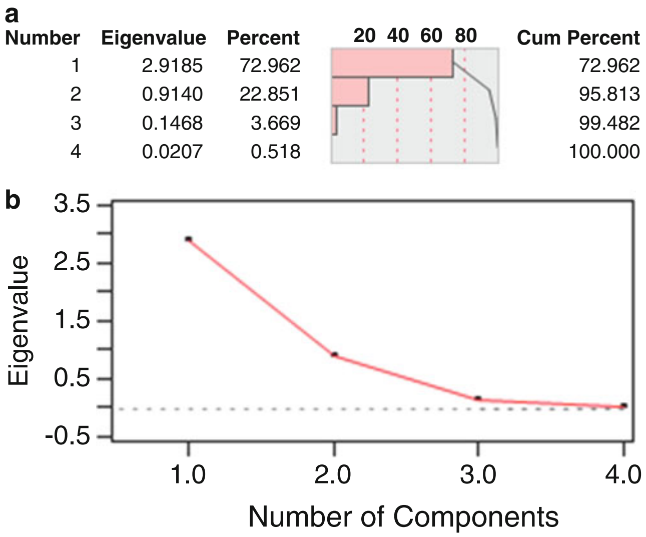

a

Number	Eigenvalue	Percent	20 40 60 80	Cum Percent
1	2.9185	72.962		72.962
2	0.9140	22.851		95.813
3	0.1468	3.669		99.482
4	0.0207	0.518		100.000

Fig. 7.12 (**a**) The eigenvalues and contributions of the principal components to the total variance, (**b**) the scree plot

The principal components are linear combinations of the original variables; for these data, the first two principal components, P_1 and P_2, are given by

$P_1 = (0.3683 \times \text{Sepal length}) + (-0.3617 \times \text{Sepal width}) + (0.1925 \times \text{Petal length}) + (0.4338 \times \text{Petal width}) + (-2.2899)$

$P_2 = (0.4767 \times \text{Sepal length}) + (2.2156 \times \text{Sepal width}) + (0.0145 \times \text{Petal length}) + (0.0919 \times \text{Petal width}) + (-9.7245)$

(Note the constant term which comes from moving the original axis to the centroid if the dataset).

Figure 7.13 shows a scatterplot of the iris data based on the first two principal components. PCA is sensitive to outliers (which should be discarded on the basis of their Mahalanobis distances to the centroids) and noise (see earlier comments on entropy).

We must remember that PCA is a one-class procedure (even though we have colored our iris data according to class) and therefore cannot help in separating classes. [The *Karhunen–Loève expansion* allows the use of class information; instead of using the covariance matrix of the whole sample, it estimates separate class covariance matrices, take their average (weighted by the priors), and use its eigenvectors.]

PCA is limited to finding *linear* combinations of the original features, which is sufficient in many applications but may result in the loss of too much information. To retain such information, a nonlinear mapping method [such as *multi-dimensional scaling* (*MDS*) (Kruskal and Wish 1977)] is needed.

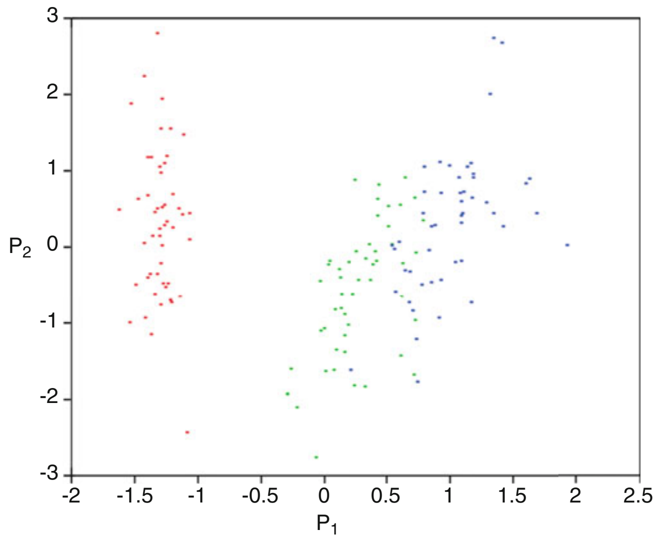

Fig. 7.13 Scatterplot of the first two principal components of the iris data

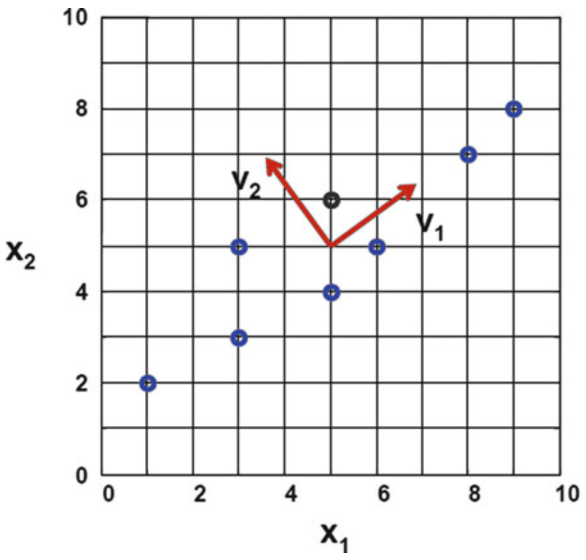

Fig. 7.14 Dataset, **x**, and the eigenvectors (principal component axes)—not drawn to scale

Example 7.1

Find the principle components of the following dataset (Fig. 7.14):

$\mathbf{x} = (x_1, x_2) = \{(1, 2), (3, 3), (3, 5), (5, 4), (5, 6), (6, 5), (8, 7), (9, 8)\}$

The covariance matrix, $\sum = \begin{vmatrix} 6.254.25 \\ 4.253.50 \end{vmatrix}$

The eigenvalues are the zeros of the characteristic equation

$$\sum v = \lambda v \Rightarrow |\Sigma - \lambda I| = 0 \Rightarrow \begin{vmatrix} 6.25 - \lambda 4.25 \\ 4.253.5 - \lambda \end{vmatrix} = 0 \Rightarrow \lambda_1 = 9.34;\ \lambda_2 = 0.41$$

And the eigenvectors are the solutions of the system

$$\begin{bmatrix} 6.254.25 \\ 4.253.5 \end{bmatrix} \begin{bmatrix} v_{11} \\ v_{12} \end{bmatrix} = \begin{bmatrix} \lambda_1 v_{11} \\ \lambda_1 v_{12} \end{bmatrix} \Rightarrow \begin{bmatrix} v_{11} \\ v_{12} \end{bmatrix} = \begin{bmatrix} 0.81 \\ 0.59 \end{bmatrix}$$

$$\begin{bmatrix} 6.254.25 \\ 4.253.5 \end{bmatrix} \begin{bmatrix} v_{21} \\ v_{22} \end{bmatrix} = \begin{bmatrix} \lambda_2 v_{21} \\ \lambda_2 v_{22} \end{bmatrix} \Rightarrow \begin{bmatrix} v_{21} \\ v_{22} \end{bmatrix} = \begin{bmatrix} -0.59 \\ 0.81 \end{bmatrix}$$

7.3.2 Linear Discriminant Analysis

Discriminant analysis is a supervised method (i.e., it recognizes that the data comprise several, labeled classes) which is useful for dimensionality reduction. It explicitly attempts to optimize class separability [while PCA finds directions that are efficient for representation of the total (pooled) dataset]. It is appropriate for the task of classifying iris flowers into three classes, corresponding to the three different species, on the basis of these features.

The basis vectors of this transformation, known as canonicals (which are linear combinations of the original features), are found by maximizing the Fisher discriminant ratio, FDR (or, in general, **J**), which for two-class problems is given by (7.4). That is, the mean classifier outputs for the two classes should be as well separated as possible and their variances should be as small as possible.

For the two-dimensional (i.e., two features), two-class problem we want to find the direction, such that when the data are projected onto this direction, the examples from the two classes are as well separated as possible. In Fig. 7.15 this would be the direction shown in Fig. 7.15b. In such a case, the dimensionality can be reduced from two to one, while preserving (most of) the discriminative information in the data.

The direction that produces the best discrimination is the one which maximizes the distance between the means of the projected data classes, normalized by a measure of the within-class scatter. It is the direction that maximizes the Fisher discriminant function (7.4).

Fisher's LDA generalizes very well to multi-class problems. For C classes, we look for the (C − 1) projections that best separate the classes. The canonical plot is

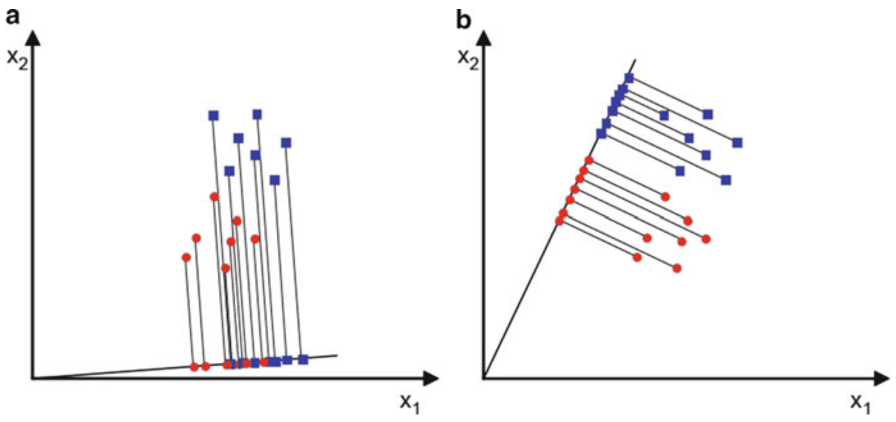

Fig. 7.15 Two-dimensional, two-class data and canonical direction **w**

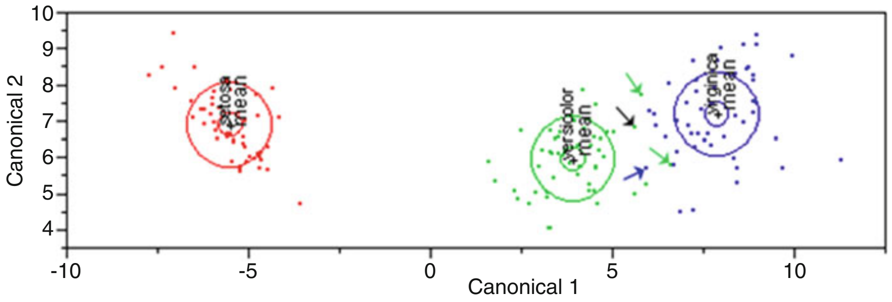

Fig. 7.16 Canonical plot for the iris data, using linear discriminant analysis. The three samples that are misclassified (see Table 7.1) using this classifier are marked with *colored arrows*; the *black arrow* shows an additional sample that is misclassified if *cross-validation* is used. (The *small colored circles* are 95% confidence limits for the positions of the means; and the *larger colored circles* contain 50% of the samples for that class.)

normally presented for only the two most significant canonicals, and shows the data in the directions that maximally separate the classes. This is what is required with the iris data. Figure 7.16 is the canonical plot for the iris data. Each multivariate mean is surrounded by confidence ellipses which are circular in canonical space if we use *linear discriminant analysis* [with a common (i.e., within) covariance matrix for all the classes], and the decision boundaries (not shown) are linear. The three species are optimally separated. Iris *setosa* is well-separated from the other two species, which are close enough that some misclassification occurs.

For these data, the eigenvalues of the canonicals, C_1 and C_2, are 32.192 and 0.285 respectively (the eigenvalues of C_3 and C_4 are 1.691×10^{-15} and 3.886×10^{-16} respectively!) so that the first canonical explains 99.1% of the variance in the data, and the second canonical the remaining 0.9%. The two canonicals, C_1 and C_2, are given by

Table 7.2 Confusion matrix showing the results of linear discriminant analysis used to distinguish three species of iris flower

	Predicted		
Actual	*setosa*	*versicolor*	*virginica*
Class 1 (*setosa*)	50	0	0
Class 2 (*versicolor*)	0	48	1
Class 3 (*virginica*)	0	2	49

Table 7.3 Confusion matrix showing the results of linear discriminant analysis if cross-validation is used with the iris data

	Predicted		
Actual	*setosa*	*versicolor*	*virginica*
Class 1 (*setosa*)	50	0	0
Class 2 (*versicolor*)	0	47	1
Class 3 (*virginica*)	0	3	49

$C_1 = (-0.8294 \times \text{Sepal length}) + (-1.5345 \times \text{Sepal width}) + (2.2012 \times \text{Petal length})$

$(2.8105 \times \text{Petal width})$

$C_2 = (0.0241 \times \text{Sepal length}) + (2.1645 \times \text{Sepal width}) + (-0.9319 \times \text{Petal length})$

$(2.8392 \times \text{Petal width})$

Samples are assigned to the class whose multivariate mean is closest. (Since different features have different scales, and likely have different dimensions, the appropriate distances to calculate are the Mahalanobis distances rather than Euclidean distances). For these data, the three samples marked in Fig. 7.16 are misclassified, i.e., assigned to the wrong classes. Two features from *versicolor* are misclassified as *virginica*, because they are closer to its mean; and one feature from *virginica* is misclassified as *versicolor*, because it is closer to that mean. The final classifications can be tallied in a *confusion matrix* (Table 7.2), which is a contingency table in which the actual (in the rows) and the predicted (in the columns) classes of the data (or vice versa in some implementations) are presented. Entries on the diagonal of the matrix are the correct classifications; and entries off the diagonal are the misclassifications. The confusion matrix shows the *performance* of the classifier. In this case, three features were misclassified and appear as off-diagonal entries, representing a total misclassification rate of 2% (i.e., 3 out of 150).

Cross-validation shows the prediction for a given observation if it is left out of the estimation sample [a re-sampling technique known as *jack-knifing* (or *leave-one-out*)]. In this case an additional sample is misclassified if cross-validation is used (Fig. 7.16). The confusion matrix if cross-validation is used is displayed below (Table 7.3).

If a separate covariance matrix is used for each class, which is preferable, the analysis is quadratic discriminant analysis; the isocontours (Fig. 7.17) are ellipses

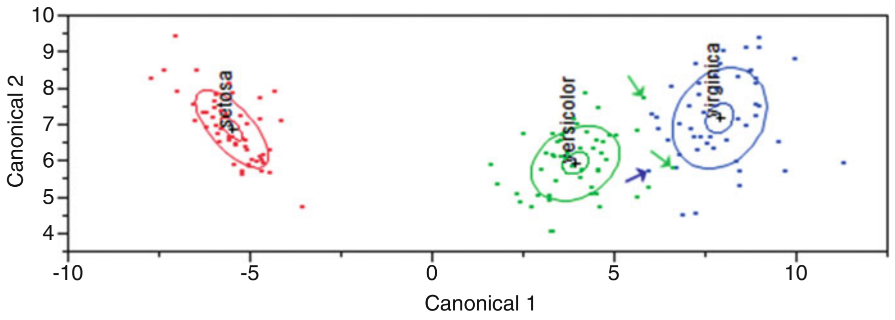

Fig. 7.17 Canonical plot for the iris data, using quadratic discriminant analysis. The three samples that are misclassified (see Table 7.4) using this classifier are marked with *colored arrows*. (The *small colored circles* are 95% confidence limits for the positions of the means; and the *larger colored circles* contain 50% of the samples for that class.)

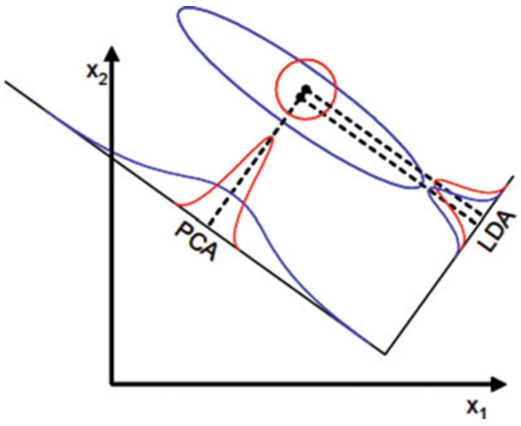

Fig. 7.18 LDA is not successful if the discriminatory information is in the variance

and the decision boundaries (not shown) are quadrics. For this particular dataset, the same three samples are misclassified but this will not generally be the case.

Quadratic discriminant analysis suffers in small datasets because it does not have enough data to make nicely invertible and stable covariance matrices.

Of course Fisher's discriminant analysis (whether linear or quadratic) works in higher dimensions and with multiple classes, always seeking to project the data onto a lesser-dimensional space and maximize the separability of the classes. It is a parametric method since it assumes unimodal Gaussian likelihoods, and will not work properly if the distributions are significantly non-Gaussian. It does depend on the prior probabilities; these can either be taken as proportional to the occurrence of the classes in the sample set, or, preferably, if these are known, to the occurrences in the whole population. Linear Discriminant Analysis will fail when the discriminatory information is not in the mean, but rather in the variance of the data (Fig. 7.18).

Example 7.2

For the small sample of business executives given below, is it possible to discriminate them into classes according to their education (viz., Associate, Bachelors or Masters degree) based on their current salary, age, and number of times that they have been promoted?

Number	Education	Gender	Annual salary (,000’s)	Age (years)	Number of promotions
1	Masters	M	94	63	5
2	Associate	F	54	38	2
3	Bachelors	M	89	54	4
4	Associate	F	68	42	3
5	Bachelors	F	71	47	3
6	Bachelors	F	48	41	2
7	Bachelors	F	65	51	3
8	Masters	M	85	58	4
9	Associate	F	50	35	2
10	Masters	M	103	60	5
11	Masters	F	75	48	4
12	Associate	M	73	53	3

The resulting canonical plot, using linear discriminant analysis (with separate covariances), is shown in Fig. 7.19. The canonical have eigenvalues of 4.241 and 0.1149, so that canonical1 accounts for 97.36% of the discriminative information. The formula for canonical1 is $-0.1935 \times$ Salary + $0.0433 \times$ Age + $4.4920 \times$ Promotions: it is not immediately clear which of the variables is the most important because they have not been standardized.

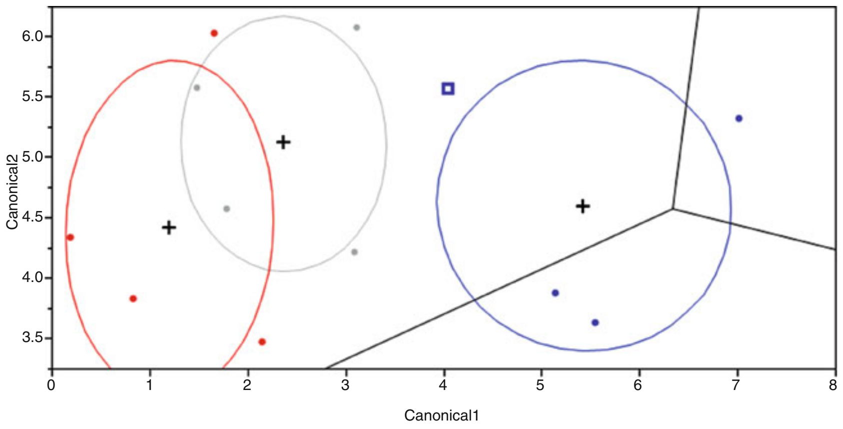

Fig. 7.19 Canonical plot showing contours around the three classes. The misclassified sample is shown as a *blue square*

(continued)

(continued)

The confusion matrix is given in Table 7.4. Only one of the executives (number 8) is misclassified; he actually has a Masters degree but is predicted as having a Bachelors degree.

Table 7.4 Confusion matrix showing the results of linear discriminant analysis used to distinguish three classes on the basis of their education (actual rows by predicted columns)

	Associate	Bachelors	Master
Associate	4	0	0
Bachelors	0	4	0
Masters	0	1	3

Example 7.3

The Excel file, `LDA with Priors and losses.xls`, downloadable from http://extras.springer.com contains the embedded equations to calculate the state-conditional density functions and the posterior probabilities, from which a prediction can be made on the basis of maximum a posteriori (MAP) probability. It also incorporates the prior probabilities, and allows easy entry of loss function terms, λ_{ij}, and inspection of the effect on the decision.

Using the same dataset of business executives as in Example 7.2, viz., can we predict their education based on their current salary, age, and number of times that they have been promoted. With equal losses, the predictions are correct except for executive number 8, who is predicted to have a Bachelors education, rather than a Masters.

The diagonal terms of the loss function matrix are zero (reflecting no penalty for a correct prediction), and non-zero off-diagonal terms (often taken as 1s). If we double the loss associated with predicting an actual Masters as a Bachelors (Table 7.5), we can follow through the calculations on the spreadsheet and find 100% accuracy in prediction.

Table 7.5 Loss function terms (actual rows by predicted columns)

	Losses		
	Associate	Bachelors	Master
Associate	0	1	1
Bachelors	1	0	1
Masters	1	2	0

7.4 Exercises

(These are most conveniently done with access to either MatLab or JMP (SAS, Inc.). Indeed Q.7.2 and 7.3 use datasets in the .JMP format (which can be downloaded from http://extras.springer.com).

1. Principal Components Analysis (PCA) and Linear Discriminant Analysis (LDA) have different purposes. The former operates on the total (unlabeled) dataset to find the directions that contain the maximum variance; the latter operates on labeled data to find the directions which are best at distinguishing the labeled classes. In general, the results (principal components and canonicals, respectively) will be quite different. However, for special examples of data the principal components and canonicals could be in the same directions. (1) Draw an example of two-class, two-dimensional data such that PCA and LDA find the same directions. (2) Draw an example of two-class, two-dimensional data such that PCA and LDA find totally different directions.
2. The data in `socioeconomic.jmp` consists of five socioeconomic variables/features for 12 census tracts in the LA Metropolitan area.
   (a) Use the Multivariate platform to produce a scatterplot matrix of all five features.
   (b) Conduct a principal component analysis (on the correlations) of all five features. Considering the eigenvectors, which are the most useful features? Considering the eigenvalues, how many principal components would you use in subsequent analysis?
3. The measurements in `adolescent.jmp` are of 58 high-school students. Using LDA (quadratic) explore how well the variables height, and length of arm, leg and hand are at distinguishing the ethnicity of the students. Use the occurrence of the classes in the sampled set as the prior probabilities. What happens if a fifth variable, the length of the foot, is included? What if weight and the size of the wrist and neck are included? How independent are the measured features? What additional factor is limiting the usefulness of the results?

References

Fisher, R.A.: The use of multiple measurements in taxonomic problems. Ann. Eugen. **7**, 179–188 (1936)

Kruskal, J.B., Wish, M.: Multidimensional Scaling. Sage, Beverly Hills, CA (1977)

Van der Heijden, F., Duin, R.P.W., de Ridder, D., Tax, D.M.J.: Classification, Parameter Estimation and State Estimation. Wiley, Chichester (2004)

Chapter 8
Unsupervised Learning

8.1 Clustering

With unsupervised learning, the class labels are unknown, and the data are plotted to see whether it clusters naturally. Cluster analysis divides the data into clusters (classes) that are hopefully meaningful and/or useful: the clusters may or may not correspond with the human perception of similarity.

Cluster analysis has been used in a wide variety of fields, e.g.,

- In biology, to find groups of genes that have similar functions
- In climatology, to find clusters of atmospheric pressure that have an impact on climate
- In medicine, to identify different variants of a disease
- In business, to cluster customers for marketing activities
- In information retrieval, to group search results into clusters and subclusters in a hierarchical structure
- In imaging, to segment an image (into several different regions): or to compress image and video data by replacing objects by the prototype of each cluster (known as *vector quantization*).

Clusters should comprise objects that are similar to each other and different from those in other clusters. This will require adoption of a (dis)similarity measure, which is often taken as a proximity measure (e.g., a power norm, such as the L_1 norm (the Manhattan or city-block distance), given by $|x_1 - y_1| + |x_2 - y_2|$; the L_2 norm (the Euclidean distance), given by $\sqrt{(x_1 - y_1)^2 + (x_2 - y_2)^2}$; or the L_∞ norm (the Chebyshev or chess-board distance), given by $\max\{x_1 - y_1, x_2 - y_2\}$). Once a (dis) similarity measure has been chosen, we need to define a criterion to be optimized. The most widely used criterion function for clustering is the sum of the squared error (SSE). We calculate the error of each data point (i.e., its distance to the closest centroid), and then compute the total sum of the squared errors. Clustering methods which use this criterion are known as *minimum variance* methods. Other criterion

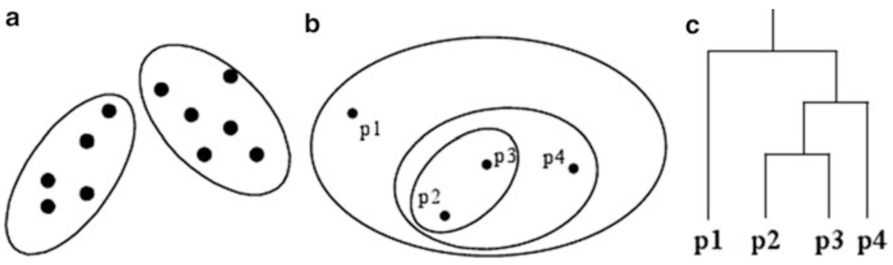

Fig. 8.1 (**a**) Partitional clustering (**b**) hierarchical clustering, represented as (**c**) a dendrogram

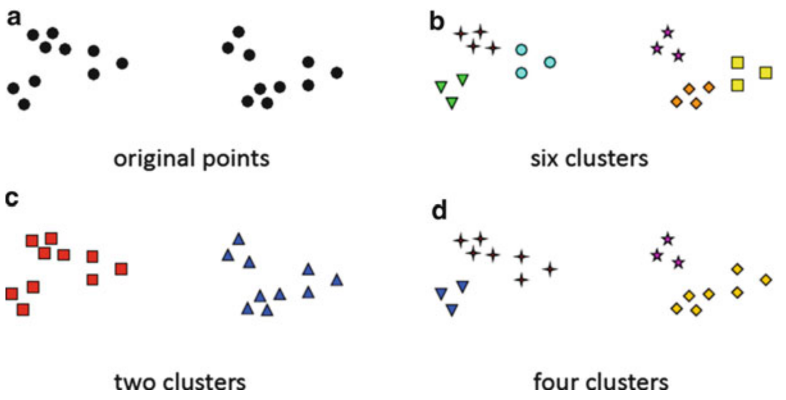

Fig. 8.2 Different ways of clustering the same set of points

functions exist, based on the scatter matrices used in linear discriminant analysis (LDA).

Clusters can be either *partitional* (or *flat*), in which the data are divided into nonoverlapping subsets (clusters) such that each data point is in exactly one subset (Fig. 8.1a), or they may be *hierarchical*, in which the clusters are nested (Fig. 8.1b). Nested clusters are often represented by a hierarchical tree or dendrogram (Fig. 8.1c).

The notion of a cluster is not well defined; they are often in the eye of the beholder. For example, in Fig. 8.2 it is unclear whether there are two, four, or six partitional clusters. It may even be that there are two partitional clusters, with nested (*hierarchical*) subclusters. Because clusters are not well defined, we can anticipate that it may be difficult to determine the extent to which clustering should continue in a clustering algorithm.

In non-exclusive clusters, data points may belong to multiple clusters. In addition, in fuzzy clustering, a data point belongs to every cluster with some weight (or probability) between 0 and 1.

We will consider one example of each clustering technique: *k*-means clustering, and its variants, as an example of partitional clustering, and agglomerative hierarchical clustering as an example of hierarchical clustering.

8.2 *k*-Means Clustering

k-Means clustering (MacQueen 1967) is one of the oldest and most widely used clustering algorithms. It is a partitional clustering approach. Each cluster is represented by one prototype object, and a new data sample is assigned to the nearest prototype and therefore to that cluster. The training consists of a very simple iterative scheme to adjust the placing of the prototypes:

(i) Randomly choose *k* objects from the training set, which become the prototypes
(ii) Assign all the other objects to the nearest prototype to form clusters; "nearness" is measured by Euclidean distance (or some other norm)
(iii) Update the new prototype of each cluster as the centroid of all the objects assigned to that cluster
(iv) Return to step (ii) until convergence (i.e., when no data point changes clusters, or equivalently, until the centroids remain the same. Because most of the convergence occurs in the early iterations, this condition is often replaced by a weaker condition, e.g., repeat until only 1% of the points change clusters).

Figure 8.3 shows the result of several iterations on a particular dataset.

The "assignment" step is also referred to as the *expectation* step, and the "update step" as the *maximization* step, making this algorithm a variant of the generalized *expectation–maximization* (EM) algorithm.

As it is a heuristic algorithm, there is no guarantee that *k*-means clustering will converge to the global optimum. The result is sensitive to the initial choice of objects as cluster centers, especially for small data sets. Larger data sets comprising approximately 200–100,000 observations are best. Since the algorithm is usually very fast, it is common to run it multiple times with different starting conditions to minimize this effect.

The algorithm can be viewed as a greedy algorithm for partitioning *n* samples into *k* clusters so as to minimize an *objective function*, which can be taken as the sum of the squared distances to the cluster centers, the sum of the squared error (SSE). We calculate the error of each data point (i.e., its distance to the closest centroid), and then compute the total sum of the squared errors.

$$\mathrm{SSE} = \sum_{i=1}^{K} \sum_{x \in C_i} \mathrm{dist}(c_i, x)^2 \tag{8.1}$$

where c_i is the center of the *i*th cluster, and dist is the Euclidean distance [in which case it is better to work with *standardized* features, and the clusters become circular

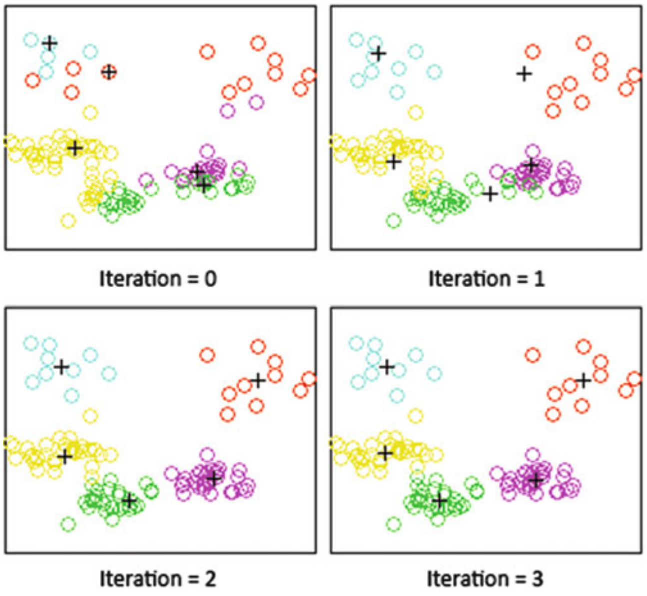

Fig. 8.3 Results of *k*-means clustering in various iterations (The prototypes in each iteration are marked with a "*plus*.")

(or spherical) in shape]. For two different runs of *k*-means, with the same value of *k* but different starting prototypes, we will choose the one with the smallest value of SSE. The complexity of the algorithm is $O(n \times k \times I \times d)$, where n is the number of data points, k the number of clusters, I the number of iterations, and d is the number of features.

Pre-processing and post-processing steps can be used to improve the final result. Pre-processing steps include standardizing (or normalizing) the data, and eliminating or reducing the effect of outliers. Outliers can pull the centroid away from its true position; to prevent this, the median can be used instead of the average in finding the new prototype during each iteration. Post-processing can include splitting "loose" clusters, i.e., clusters with relatively high SSEs, and merging "close" clusters, i.e., those with relatively low SSEs.

A variant of the *k*-means algorithm, called the *bisecting k-means algorithm*, can be used to minimize the dependence on the initial set of prototypes. The basic idea is to split the points into two clusters, then split each of these into two, and so on. There are a number of different ways to do this. You could compute the centroid of all the data points, select a point at random (cL), and construct a point (cR) which is symmetrically placed with regard to the centroid. Cluster the data around these two points, and then repeat the process within these two clusters. If you want k clusters, where k is a power of 2, say 2^m, you iterate m times. If you want k clusters with k not a power of 2 (say, 24), you take the closest inferior power of 2 (i.e., 16), take these 16 clusters, and then randomly choose 8 of them to subcluster.

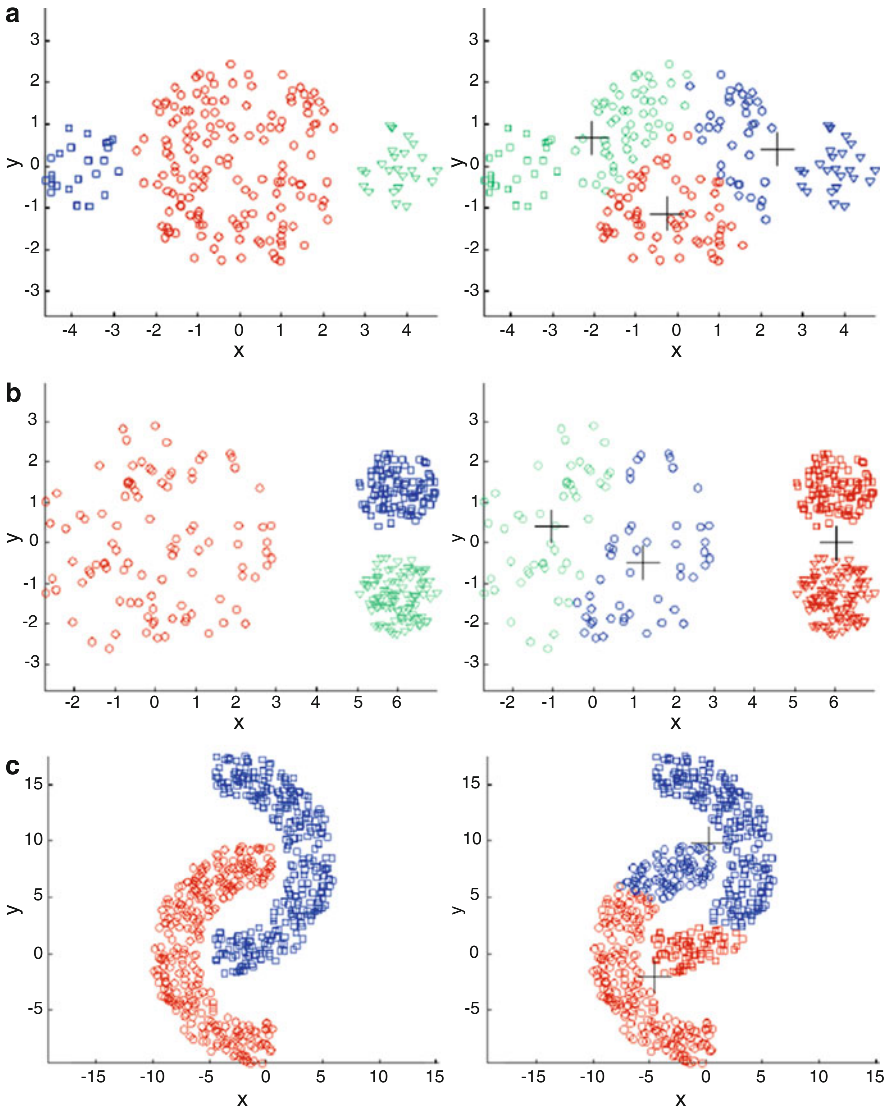

Fig. 8.4 Natural clusters and the results of *k*-means clustering when (**a**) the sizes are very different, (**b**) the densities are very different, and (**c**) the shapes are non-spherical

k-Means and its variants have a number of limitations for certain types of clusters. In particular, there are difficulties in detecting "natural" clusters when they have widely different sizes or densities, or when they have non-spherical shapes (Fig. 8.4). In Fig. 8.4a, the largest cluster is broken and pieces of it are assigned to the smaller clusters. In Fig. 8.4b, the two smaller clusters are much denser than the larger cluster and this confounds the algorithm. Finally, in Fig. 8.4c,

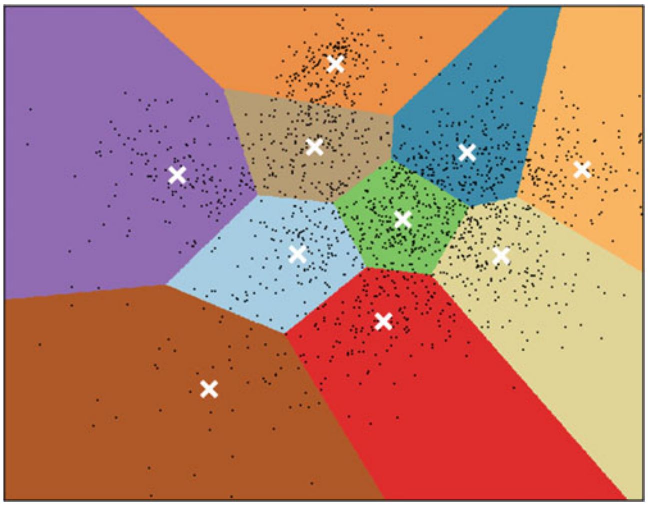

Fig. 8.5 The result of k-means clustering on handwritten digits data (The centroids of the clusters are marked with a white cross, and the Voronoi cells for each cluster are colorized)

k-means mixes the natural clusters because they are non-spherical in shape. These difficulties can be overcome to an extent if the user is willing to accept a larger number of clusters (say, six instead of two or three), and merge some of them later.

Unfortunately, there is no general theoretical solution to find the optimal number of clusters for any given dataset. A simple approach is to compare the results of multiple runs with different k classes and choose the best one, but we need to be careful because increasing k not only results in smaller error function values by definition but also an increasing risk of *overfitting*.

The result of k-means clustering can also be seen as the *Voronoi* cells (i.e., polygonal spheres of influence) of the cluster means (Fig. 8.5). Since data are split halfway between cluster means, this can lead to suboptimal splits. The Gaussian models used by the expectation–maximization (EM) algorithm (which can be seen as a generalization of k-means) are more flexible here by having both variances and covariances. The EM algorithm is thus able to accommodate clusters of variable sizes much better than k-means, as well as correlated clusters.

It has been shown (Zha et al. 2001; Ding and He 2004) that the "relaxed" solution of k-means clustering, specified by the cluster indicators, is given by the PCA principal components.

8.2.1 Fuzzy c-Means Clustering

k-Means clustering is an example of partitional clustering where the data are divided between nonoverlapping clusters, each represented by a prototype which is the centroid of the objects in a cluster. In such clustering, each data object belongs to just one cluster, whereas in *fuzzy clustering*, each object can belong to more than one cluster, and associated with each object is a set of membership weights, w_{ij}, representing the strength of the association between that $\mathbf{x}_i$ and a particular cluster C_j. Membership weights vary between 0 and 1, and all the weights for a particular object, $\mathbf{x}_i$, add up to 1. Fuzzy clustering is a process of assigning these membership weights.

One of the most widely used fuzzy clustering algorithms is the *fuzzy c-means* algorithm (Bezdek 1981), which is a direct generalization of the *k*-means clustering algorithm. With fuzzy *c*-means, the centroid of a cluster, c_j, is the weighted of all the points, weighted by their membership weight or degree of belonging to that particular cluster: The membership weight is inversely related to the distance of the object to the cluster center as calculated on the previous pass.

The training consists of a very simple iterative scheme to adjust the placing of the prototypes:

(i) Choose a number of clusters, k, and randomly assign weights, w_{ij}, to each of the m objects for being in the clusters
(ii) Compute the centroid for each cluster, c_j, as the weighted mean of each object

$$c_j = \frac{\sum_{i=1}^{m} w_{ij}^{p} x_i}{\sum_{i=1}^{m} w_{ij}^{p}} \tag{8.2}$$

(iii) For each object, update its membership weights of being in the clusters by minimizing the (modified) SSE:

$$\mathrm{SSE}(C_1, C_2, \ldots, C_k) = \sum_{j=1}^{k} \sum_{i=1}^{m} w_{ij}^{p} \mathrm{dist}(x_i, c_j)^2 \tag{8.3}$$

subject to the constraint that the weights sum to 1, where p is an exponent, the *fuzzifier*, that has a value between 1 and ∞, and determines the influence of the weights and, therefore, the level of cluster fuzziness. A large value results in smaller values of the membership weights and, hence, fuzzier clusters. Commonly p is set to 2. If p is close to 1, then the membership weights, w_{ij}, converge to 0 or 1, and the algorithm behaves like k-means clustering.
(iv) Finally, return to step (ii) until convergence (i.e., when the change of the weights is no more than a given sensitivity threshold).

The algorithm minimizes intra-cluster variance and is less susceptible to outliers, but still suffers from the problem that the minimum is likely to be a local minimum rather than the global minimum and the results depend on the initial choice of weights.

8.3 (Agglomerative) Hierarchical Clustering

Hierarchical clustering produces a set of nested clusters organized as a hierarchical tree, which can be visualized as a dendrogram that records the sequences of merges or splits (Fig. 8.6).

In (*agglomerative*, as opposed to *divisive*) *hierarchical clustering*, each instance starts off as its own cluster, and is subsequently joined to the "nearest" instance to form a new cluster. It is a bottom-up technique. At each step of the clustering, larger clusters are obtained. The algorithm is to:

(i) Find the two features that are "closest" in multivariate space
(ii) Replace them with a single feature at their mean
(iii) Repeat with the next two closest features, and continue until all the features are subsumed into one cluster

The key operation is the computation of the proximity in step (i). There are several definitions of cluster proximity that could be used. We could use the Euclidean distance between instances, if we make sure that all the features have the same scale, i.e., use standardized features. At each iteration, we choose the two closest groups to merge. In *single-link clustering*, this distance is defined as the smallest distance between all possible pairs of elements of the two groups, d_{min} (Fig. 8.7). The single-link method corresponds to constructing the *minimal spanning tree* (MST). In *complete-link clustering*, the distance between the groups is taken as the largest distance between all possible pairs, d_{max}. (Another option would be to use the distance between the centroids of the two groups). Complete-linkage clustering avoids the drawback of *chaining* that occurs with the single-linkage method, where clusters may be forced together due to single instances being close to each other even though many of the instances may be very distant to each other. Complete-linkage clustering tends to find compact clusters of approximately equal diameters. The resulting hierarchical tree is known as a *dendrogram*.

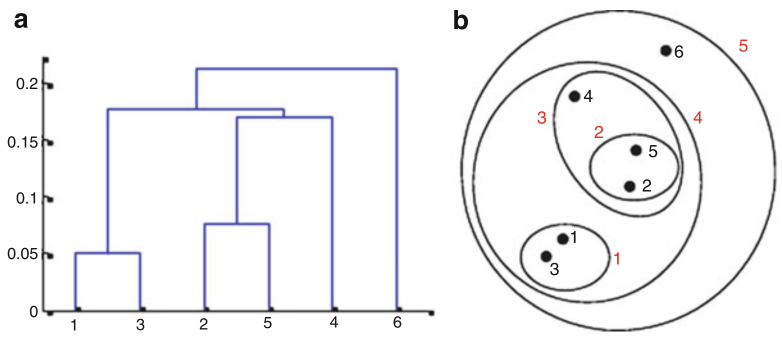

Fig. 8.6 (**a**) Dendrogram and (**b**) nested clusters

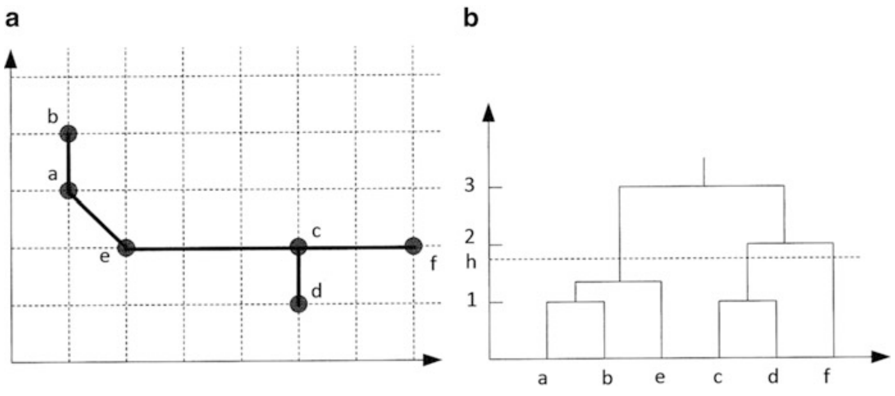

Fig. 8.7 (**a**) A 2D dataset and (**b**) the resulting dendrogram from single-link clustering (The dendrogram can be intersected at any value, *h*, to give the desired number of clusters)

In *Ward's* method (1963), the proximity between the two clusters is defined as the increase in the SSE (the sum of the squared distances to the cluster centers) that results from merging two clusters, i.e., it uses the same objective function as *k*-means clustering. When clusters are merged, we can either keep track of the number of data points in each cluster, or we can just treat all the merged clusters as equals. The first approach will result in a *weighted* averaging, the second to *unweighted* averaging when we come to compute the SSE increase in the next merging. In general, the unweighted approach is used.

The result of applying (agglomerative) hierarchical clustering to the Fisher iris data is the *dendrogram* shown in Fig. 8.8. Branches that merge on the left were joined earlier in the iterative algorithm. An advantage of the method is that you do not need to assume a particular number of clusters at the outset: any desired number can be obtained by cutting the dendrogram with a vertical line. Although there is no standard criterion for the optimal number of clusters, the *scree plot* (at the bottom of the figure) offers some guidance. It gets its name from the rubble that accumulates at the bottom of steep cliffs. The place where the scree plot changes from a sharp downward slope to a more level slope, not always obvious, is an indication of the optimal number of clusters.

With agglomerative hierarchical clustering, merging decisions are final: once a decision is made to merge two clusters, it cannot be undone at a later time. This approach prevents a local optimization criterion from becoming a global optimization criterion, and can prove troublesome with noisy, high-dimensional data such as document data. The algorithm is typically used when the underlying application requires a hierarchy, e.g., creation of a taxonomy. However, it is expensive in terms of computational and storage requirements.

Figure 8.9 shows how the classification changes as the number of clusters is changed. Three clusters (Fig. 8.9c) are satisfyingly simple classification, and correspond to the leveling off of the scree plot. [It is also desirable to have three classes, corresponding closely (one hopes!) to the three species of iris].

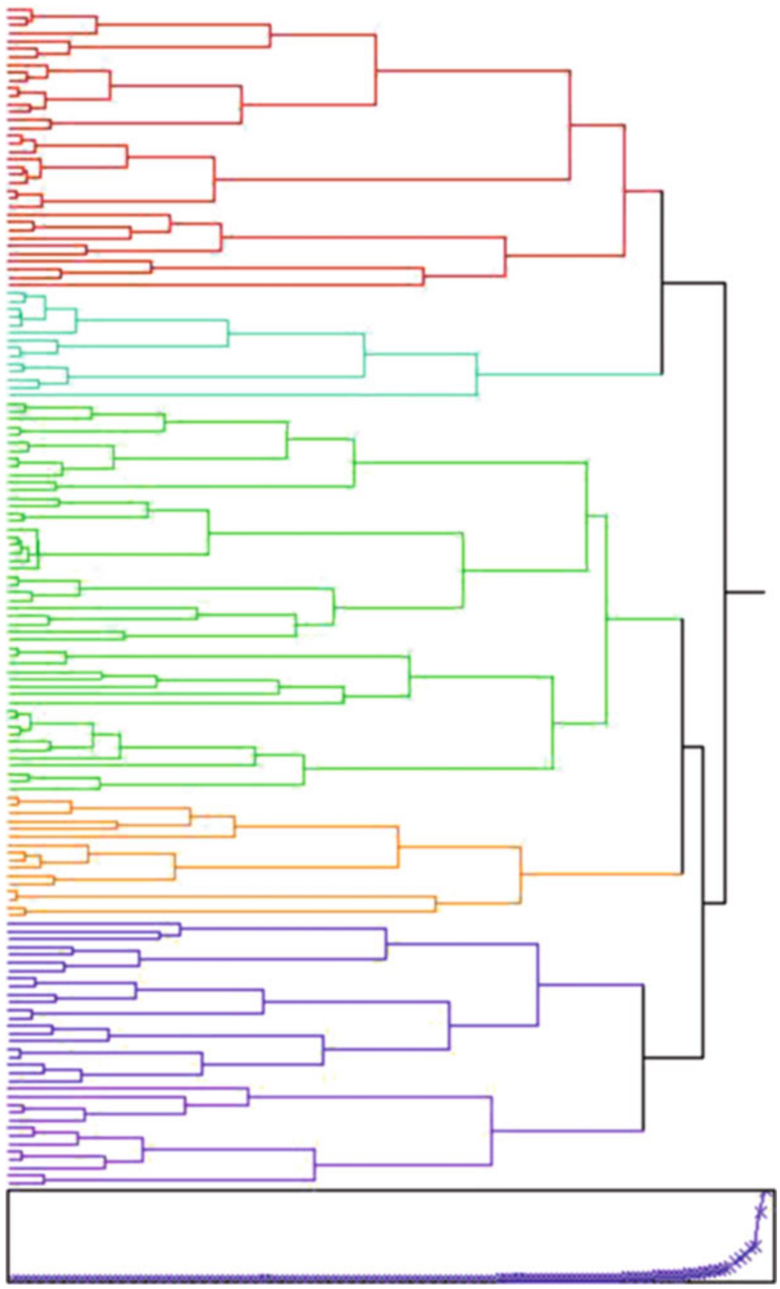

Fig. 8.8 Dendrogram and scree plot obtained by hierarchical clustering of the canonical data from the Fisher iris database, using Ward's method. The number of classes can be chosen by drawing a vertical line down the dendrogram at a particular position. The scree plot helps determine this position (Note: this dendrogram is oriented differently than the one in Fig. 8.7)

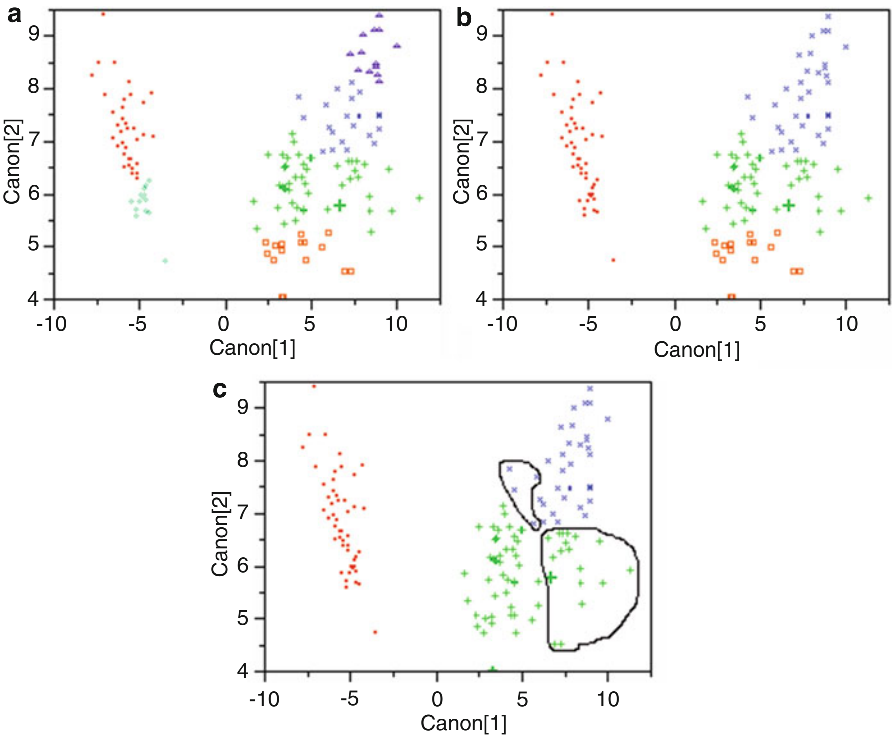

Fig. 8.9 Scatter plots of Fisher's canonicals with data colorized according to the number of clusters chosen in the dendrogram obtained by hierarchical clustering: (**a**) six clusters, (**b**) four clusters, and (**c**) three clusters. The data points within the *black lines* are misclassified

Table 8.1 Confusion matrix showing the results of hierarchical clustering used to distinguish three species of iris flower

	Predicted		
Actual	*setosa*	*versicolor*	*virginica*
Class 1 (*setosa*)	50	0	0
Class 2 (*versicolor*)	0	46	18
Class 3 (*virginica*)	0	4	32

There are a number of data points in the bottom right side of the plot which originate from *Iris virginica* and are mistakenly classified as *Iris versicolor*, and several other points which originate from *Iris versicolor* and are mistakenly classified as *Iris virginica*. These points are enclosed within the black lines overlaid on Fig. 8.9c. The resulting confusion matrix is given in Table 8.1. The misclassification rate of 14.7% [i.e., (4 + 18)/150] is significantly worse than the 2% achieved using discriminant analysis on the same data set.

Example 8.1
Perform agglomerative hierarchical clustering on the following dataset using nearest-neighbor (or single-linkage) clustering: {1, 3, 4, 9, 10, 13, 21, 23, 28, 29}.

Note that in the case of ties, you should merge the pair of clusters with the largest mean first (Fig. 8.10).

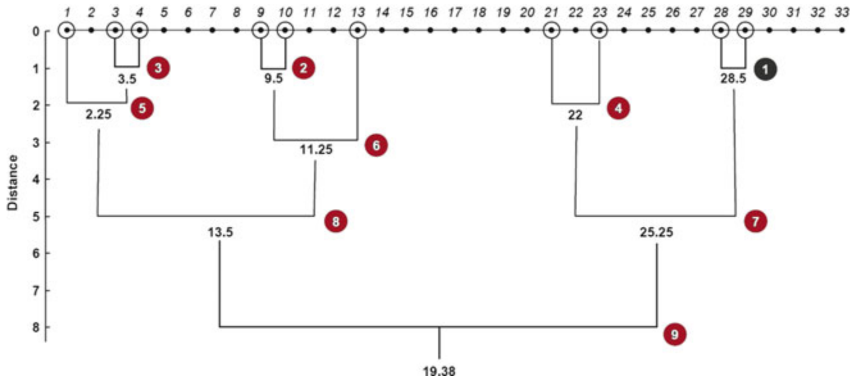

Fig. 8.10 Clustering, with the order in which the merging operations occur marked

Note that if the clustering is allowed to run until only one cluster remains, the result is the *minimum spanning tree (MST)*.

8.4 Exercises

1. The data set `Birth Death.jmp` contains mortality (i.e., birth and death) rates for several countries. Use cluster analysis to determine which countries share similar mortality characteristics. What do you notice that is similar among the countries that cluster together?
2. Consider the data in `teeth.jmp`, which contains data on the numbers of teeth of different types in a variety of mammals. Do hierarchical clustering to obtain the relevant dendrogram vary the number of clusters? With reference to the scree plot, and your own opinion of which animals should be clustered together, how many clusters do you think is optimal?
3. Consider the problem of clustering nine major cities in the United States. The distance between them (in miles) is given below:

	BOS	NYC	DC	MIA	CHI	SEA	SF	LA	DEN
BOS	0	206	429	1,504	963	2,976	3,095	2,979	1,949
NYC	206	0	233	1,308	802	2,815	2,934	2,786	1,771
DC	429	233	0	1,075	671	2,684	2,799	2,631	1,616
MIA	1,504	1,308	1,075	0	1,329	3,273	3,053	2,687	2,037
CHI	963	802	671	1,329	0	2,013	2,142	2,054	996

(continued)

(continued)

	BOS	NYC	DC	MIA	CHI	SEA	SF	LA	DEN
SEA	2,976	2,815	2,684	3,273	2,013	0	808	1,131	1,307
SF	3,095	2,934	2,799	3,053	2,142	808	0	379	1,235
LA	2,979	2,786	2,631	2,687	2,054	1,131	379	0	1,059
DEN	1,949	1,771	1,616	2,037	996	1,307	1,235	1,059	0

(i) Use single-linkage and (ii) complete-linkage.

References

Bezdek, J.C.: Pattern Recognition with Fuzzy Objective Function Algorithms. Plenum, New York (1981)

Ding, C., He, X.: K-means clustering via principal component analysis. In: Proceedings of the International Conference on Machine Learning, pp. 225–232 (2004)

MacQueen, J.B.: Some methods for classification and analysis of multivariate observations. In: Proceedings of the 5th Berkeley Symposium on Mathematical Statistics and Probability, pp. 281–297. University of California Press, Berkeley (1967)

Ward, J.H.: Hierarchical grouping to optimize an objective function. J. Am. Statist. Assoc. **48**, 236–244 (1963)

Zha, H., Ding, C., Gu, M., He, X., Simon, H.D.: Spectral relaxation for k-means clustering. Neural Information Processing Systems, vol. 14, pp. 1057–1064. Vancouver, Canada (2001)

Chapter 9
Estimating and Comparing Classifiers

9.1 Comparing Classifiers and the No Free Lunch Theorem

We can attempt to estimate the performance of a classifier, and use this metric to compare classifiers and choose between them, i.e., find a classifier of the right complexity that does not over-fit the data. However, we should bear in mind the so-called No Free Lunch Theorem, which says that *there is no one ideal solution to the classification problem*. That is, no one algorithm is guaranteed to perform best on every problem that is presented to it. It is the type of problem, the prior distribution and other information (such as the amount of training and the cost functions) that determine which classifier should provide the best performance. If one algorithm seems to outperform another in a particular situation, it is because it fits that particular task better, not because it is generally superior.

The error rate on the training set, by definition, is always smaller than the error rate on a test set containing data unseen during training. Similarly, training errors cannot be used to compare two algorithms since, over the training set, the more complex algorithm having more parameters will almost always give fewer errors than the simple one. This is why we need a validation set, and, even with a validation set, just one run may not be enough. There may be exceptional data, like noise and outliers, within the training and validation sets, and there may be random factors, such as starting weights, which may cause the algorithm to converge on a local minimum during training and validation. When we compare algorithms on a particular application, the comparison is only true for that application and that dataset.

If we want to select the classification model *and* estimate the errors simultaneously, the data should be divided into three disjoint sets. Given a particular dataset, we should leave a fraction of it aside as the test set (typically, one-third) and use the rest for training and validation. The remainder (typically, two-thirds) should be used for cross-validation to generate multiple training/validation set pairs, as explained shortly. The training set is used for learning, i.e., to optimize the parameters of the classifier, given a particular learning algorithm and model.

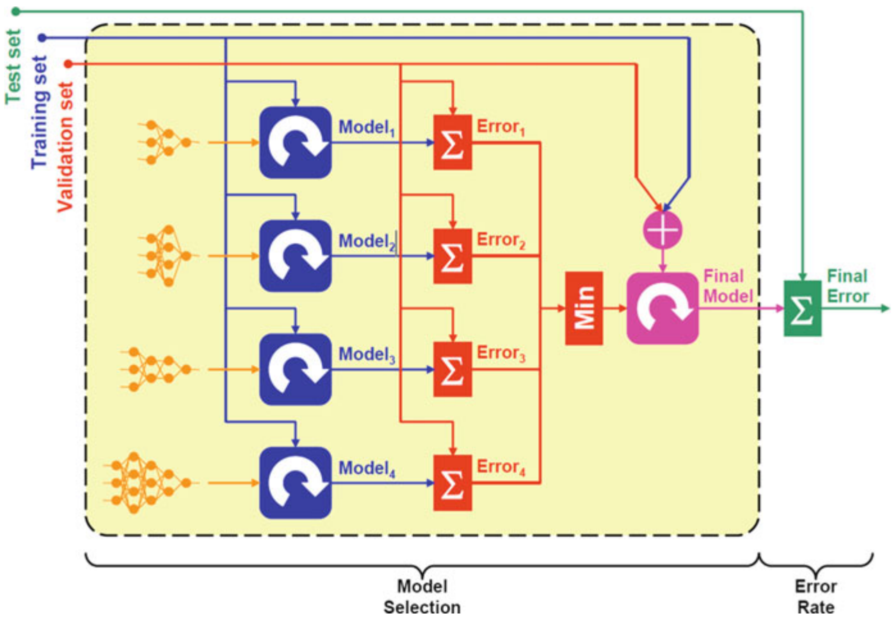

Fig. 9.1 Model selection and error estimation using three-way data split

The validation set is used to optimize the *hyperparameters* of the algorithm or model; and finally the test set is used, once both have been optimized. (For example, with neural networks, the training set is used to optimize the weights, and the validation set is used to decide on the number of hidden units, the length of training, and the training rate) Why separate the test and validation sets? Since the validation set is used to select the final model, it should not be used for estimating the true error rate as it will be biased. After assessing the final model on the test set, you should not tune the model any further.

The procedure, using a three-way data split (Fig. 9.1), is then

(i) Divide the available data into training, validation, and test data
(ii) Select the architecture and training parameters
(iii) Train the model using the training set
(iv) Evaluate the model using the validation set
(v) Repeat steps (ii)–(iv) using different architectures and training parameters
(vi) Select the best model and train it using data from the training and validation sets
(vii) Assess the model using the test set

(Note that Fig. 9.1 and the procedure describing it assume a holdout method. If cross-validation or bootstrap is used, steps (iii) and (iv) have to be repeated for each of the k folds)

The No Free Lunch Theorem throws into question our preference for avoiding over-fitting and choosing the simplest classifiers with fewer features and parameters. In the former case, there are indeed problems for which avoiding overfitting actually leads to worse performance. It is not overfitting per se that causes poor performance; it is rather the mis-match of the algorithm to the specific algorithm. Despite the qualifications here, we will keep an eye out for signs of overfitting. As for simple classifiers (in line with Occam's razor), our bias towards simple solutions may have an evolutionary basis, i.e., there is strong selection pressure for simple schemes which require fewer neurons and less computational time. The Scientific Method itself imposes a bias towards simplicity, where we accept solutions that are "good enough" to explain the data at hand. At the very least, it would be wise to adopt a balanced and flexible position between these competing philosophies.

In general we will compare algorithms by their error rates, but there are other criteria such as the training/testing time and space complexity, the complexity of the programming, and the ease of interpretability (viz., whether the results can be checked and validated by experts). The relative importance of these factors depends on the application.

9.1.1 Bias and Variance

The variance–bias tradeoff is most simply explained in terms of estimating a single parameter x with an estimator, $\bar{x}$. Then the mean-square error (MSE) of estimation for x provides an estimate of the accuracy of the estimator and is defined by

$$\mathrm{MSE}(x) = E\{(\bar{x} - x)^2\}$$

where E denotes mathematical expectation.

The bias is defined by $B(x) = E\{(\bar{x} - x)\}$ and the variance is $V(x) = E\{(\bar{x} - E(\bar{x}))^2\}$; hence

$$\mathrm{MSE}(x) = B^2(x) + V(x)$$

Thus there are two components to the error of estimation—one due to bias and the other due to variance.

We have previously encountered the tradeoff between bias and variance [Geman et al. 1992] (Sect. 6.1). In general terms, imagine that we have available several different, but equally good, training datasets. A learning algorithm is biased for a particular input **x** if, when trained on each of these datasets, it is systematically incorrect when predicting the correct output for **x**. A learning algorithm has high variance for a particular input **x** if it predicts different output values when trained on different training sets. The prediction error of a learned classifier is related to the

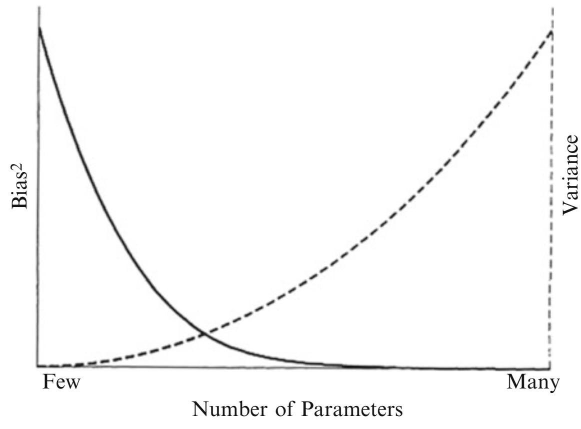

Fig. 9.2 Showing the bias–variance tradeoff

sum of the bias and the variance of the learning algorithm [James 2003]. Generally, there is a tradeoff between bias and variance (Fig. 9.2). A learning algorithm with low bias must be "flexible" so that it can fit the data well. But if the learning algorithm is too flexible, it will fit each training dataset differently, and hence have high variance. This paradigm is very general and includes all statistical modeling problems involving smoothing or parameter estimation. A key aspect of many supervised learning methods is that they are able to adjust this tradeoff between bias and variance (either automatically or by providing a bias/variance parameter that the user can adjust).

Models with too few parameters are inaccurate because of a large bias (not enough flexibility), while models with too many parameters are inaccurate because of a large variance (too much sensitivity to the sample). Identifying the best model requires trying to identify the best model complexity (viz., number of parameters).

9.2 Cross-Validation and Resampling Methods

Once we have chosen a classifier, how do we estimate its true error rate [i.e., the error (or misclassification) rate when tested on the entire population]? In real applications only a finite set of examples (or instances) is available, and that number is usually smaller than we would hope for! We may be tempted to use the entire data as the training set. However, that would result in a model that overfits the training data, and is unable to generalize to new data. The problem of overfitting is exacerbated with classifiers which have a large number of parameters. Moreover, the error rate estimate will be overly optimistic. Indeed, it is not uncommon to have 100% correct classification on training data. So we need to consider techniques which will allow us to make the best use of our (limited) data for training, model selection, and performance estimation.

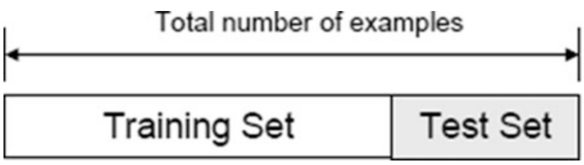

Fig. 9.3 The holdout method

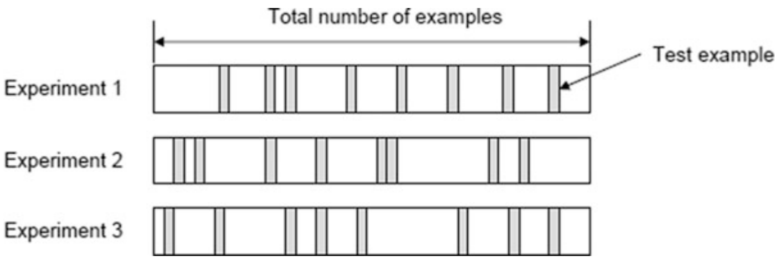

Fig. 9.4 Random subsampling

Cross-validation is a general method for evaluating a classifier, in which some of the data is removed before training. This "new" data is then used to test the performance of the learned model.

9.2.1 The Holdout Method

This is the simplest kind of cross-validation. The dataset is separated into two sets, called the training set and the test set (Fig. 9.3). The classifier learns (i.e., induces a model) on the training data, and its performance is measured on the test data. The proportion of the data used in the training set is typically either one-half or two-thirds.

The *holdout* method has certain well-known limitations. Not all the data is used for training; the smaller the training set, the larger the variance of the model. On the other hand, if the training set is too large, then the estimated accuracy (bias) computed from the smaller test set is poor. This is the essence of the bias–variance tradeoff. Furthermore, the training and test sets are not independent of each other; a class that is under-represented in one subset will be over-represented in the other.

In *random subsampling* the holdout method is repeated several times (Fig. 9.4), by randomly selecting a fixed number of examples. For each of these *k* data splits (or experiments) we retrain the classifier from scratch with the training examples, and estimate the error rate using the test examples. The estimate of the true error rate is obtained from the average of these separate estimates, which is significantly better than the holdout estimate. However, random subsampling still retains some of the problems associated with the holdout method.

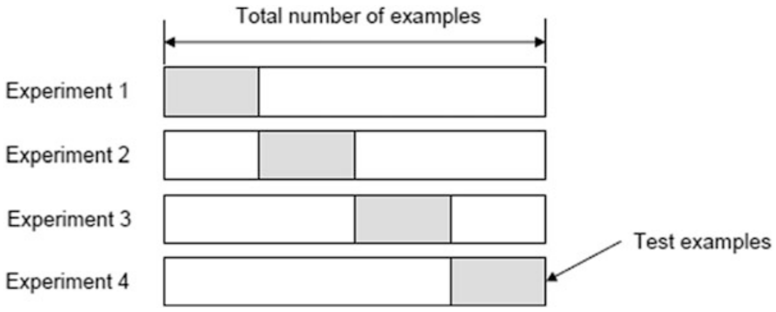

Fig. 9.5 k-Fold cross-validation, with $k = 4$

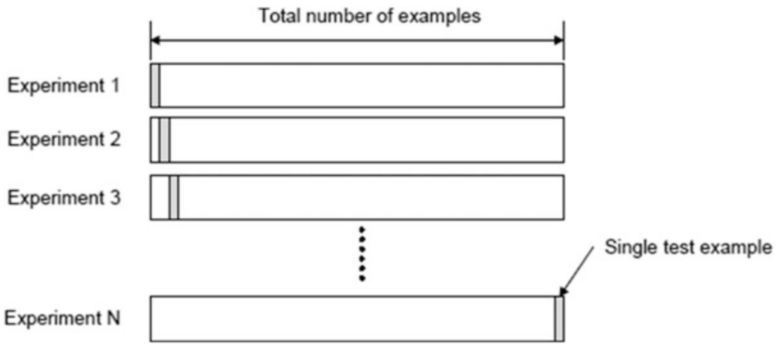

Fig. 9.6 Leave-one-out cross-validation

9.2.2 k-Fold Cross-Validation

In this approach, the dataset is divided into k equal-sized subsets (Fig. 9.5). One of the subsets is chosen for testing and the rest of them are used for training. This procedure is repeated k times, so that each subset is used for testing exactly once. The total error is obtained by averaging the errors for all the runs. The method is similar to random subsampling, except that all the examples in the dataset are eventually used for both training and testing.

A special case of the k-fold cross-validation method sets, $k = N$, the size of the dataset (Fig. 9.6). In this so-called *leave-one-out* approach, each test set contains only one sample. This uses as much data as possible for training. This is typically used in applications such as medical diagnosis, where labeled data is hard to find. The method can be computationally expensive, and the variance of the estimated performance metric tends to be high. *Jack-knifing* repeats the leave-one-out method N times, and takes the average of the estimates.

So how many folds should we use? With a large number of folds, the bias of the true error rate estimate will be small (i.e., it will be very accurate), but the variance of

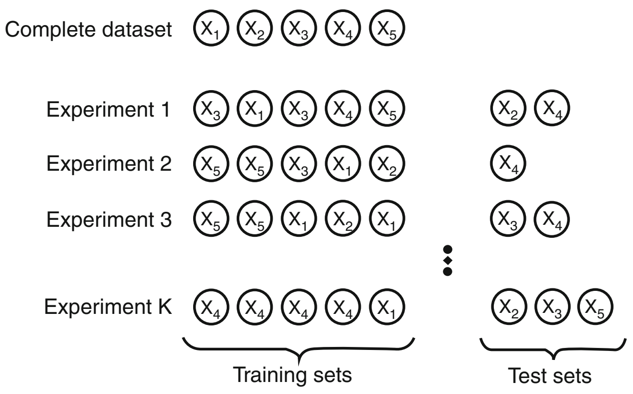

Fig. 9.7 The bootstrap method

the estimate will be large, as will the computation time. With a small number of folds, the variance and the computation time will be small, but the bias will be large. In practice, the choice of the number of folds depends on the size of the dataset. For large datasets, even threefold cross-validation will be quite accurate. For very sparse datasets, we may have to use the leave-one-out approach in order to train on as many examples as possible. For many cases, a value of $k = 10$ is a common choice.

9.2.3 Bootstrap

An alternative to the cross-validation techniques just described is the *bootstrap* method, in which the dataset is sampled with replacement (or resubstitution), i.e., a record already chosen for training is put back into the original pool and can be chosen again so that there can be duplicate objects in the training set (Fig. 9.7). This is considered the best way to do resampling for very small datasets. The remaining samples not selected for training are used for testing. The process is repeated for a specified number of folds, k. As before, the true error is estimated as the average error rate.

In the bootstrap, we sample N instances from a dataset of size N with replacement. The original dataset is used as the validation set. The probability that we pick an instance is $1/N$; and the probability that it is not picked is $1 - 1/N$. (Note that sampling with replacement preserves the a priori probabilities of the classes throughout the random selection process) The probability that we do not pick it after N draws is

$$(1 - 1/N)^N \approx \mathrm{e}^{-1} = 0.368$$

This means that the training data contains ~63.2% of the instances (but not the other 36.8%).

Compared to basic cross-validation, the bootstrap method increases the variance that can occur in each fold. This is a desirable property since it is a more realistic simulation of the real-life experiment from which our dataset was obtained.

9.3 Measuring Classifier Performance

There are a number of metrics for quantifying the performance of a classifier, especially for two-class problems. For the case of two overlapping probability density functions describing the distribution of a feature in two classes and equal prior probabilities, the posterior probabilities are just scaled versions of the probability density functions: and we can consider the pdf's (Fig. 9.8a). Misclassification errors are inevitable when a threshold (or decision point) is taken to discriminate the classes. We decide class ω_1 (the "negatives") for values to the left of the threshold, and class ω_2 (the "positives") for values to the right. For a positive example, if the prediction is also positive, this is a *true positive* (TP); if the prediction is negative, this is a *false negative* (FN). For a negative example, if the prediction is also negative, this is *a true negative* (TN); if the prediction is positive, this is a *false positive* (FP). The error probability of the false positive, known as a type I error, is denoted by α (in which case the probability of the true positive is $1 - \alpha$). The error probability of a false negative, known as a type II error, is denoted by β (and the probability of a true negative is $1 - \beta$).

A confusion matrix is a table that illustrates how well a classifier predicts (usually organized as actual rows versus predicted columns). Table 9.1 shows the corresponding confusion matrix for the two-class problem illustrated in Fig. 9.8. Both types of classification errors, type I and type II, are problematic. In medical diagnosis, a false positive causes unnecessary worry and unnecessary treatment, while a false negative gives the patient the dangerous illusion of good health and no treatment when treatment would be helpful. (In this situation we could adopt a larger loss factor for the false negatives).

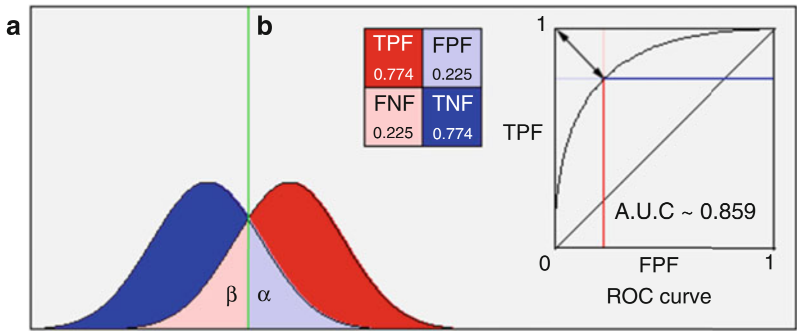

Fig. 9.8 (**a**) Overlapping pdf's of the same feature in two classes and (**b**) the resulting receiver operating characteristic (ROC) curve

Table 9.1 Confusion matrix for two classes

Predicted			
Actual	Positive	Negative	Total
Positive	TP	FN	p
Negative	FP	TN	n
Total	p'	n'	N

Table 9.2 Performance measures used in two-class problems

Name	Formula
(total) error	(FP + FN)/N (=$\alpha + \beta$)
Accuracy	(TP + TN)/N [=1 − (total) error]
FPF, false positive fraction (or FP rate)	FP/n (or α)
TPF, true positive fraction (or TP rate)	TP/p [or $(1 - \alpha)$]
Precision	TP/p'
Recall	TP/p (=TP fraction)
Sensitivity	TP/p (=TPF)
Specificity	TN/n (=TNF = 1 − FPF)

Different performance measures can be introduced in terms of these parameters (Table 9.2).

By moving the threshold point in Fig. 9.8a, we can obtain different values of α and β [and, therefore of $(\alpha + \beta)$]. We can move it from the minimum of class ω_1 to the maximum of class ω_2, but realistically the range is from the minimum of ω_2 to the maximum of ω_1. When the threshold is at the intersection of the two curves, the total error $(\alpha + \beta)$ is a minimum: choosing the threshold (i.e., decision point) at the intersection minimizes the (total) probability of error and is the optimal decision rule. On either side of the intersection, we can reduce α by increasing the threshold or we can reduce β by reducing the threshold, but the total error will be larger than at the intersection point.

The receiver operating characteristic (ROC) curve is a plot of the true positive fraction, TPF (or sensitivity), against the false positive fraction, FPF [or (1 − specificity)]. As the test threshold is swept from left to right, the corresponding point on the ROC curve moves from right to left (Fig. 9.8b). At a very low threshold there are almost no false negatives, and also very few true negatives; so that both TPF and FPF will be close to 1. As we increase the threshold, the number of true positives and false positives decreases. When we reach the intersection point, we will be at the point on the ROC plot which is closest to the left hand, top corner (where TPF = 1 and FPF = 0), which is the optimal condition. As the threshold is increased past this point, both TPF and FPF fall.

If the two distributions overlap a lot, the ROC line drops close to the diagonal and the area below it (the AUC, *a*rea *u*nder *c*urve, or A_z) drops towards 0.5 (Fig. 9.9): a value of exactly 0.5 indicates that there is complete overlap, and a classifier using this feature will be no better than random choice at discriminating the classes. If the two distributions are well separated, the ROC line rises and

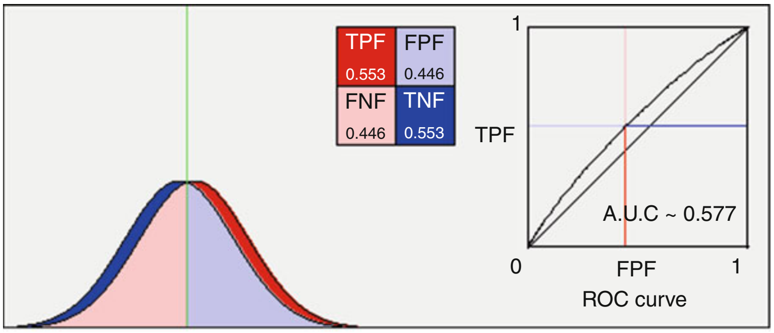

Fig. 9.9 Distributions with a lot of overlap result in a ROC plot, with an AUC close to 0.5

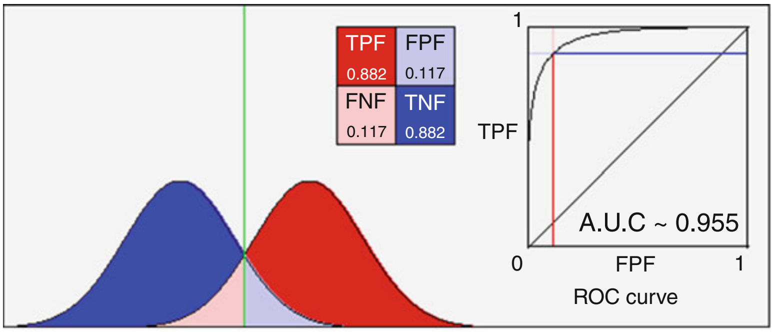

Fig. 9.10 Distributions that are well-separated result in a ROC plot, with an AUC close to 1

the AUC approaches 1 (Fig. 9.10). Thus, the AUC is a measure of the class discrimination ability of the specific feature used by a (single-feature) classifier. It is a measure of the probability that in randomly paired normal and abnormal images, the images will be correctly identified (Hanley and McNeil 1982). It does not require a quantitative scale of abnormality [in radiology, a five-category ranking (from definitely normal to definitely abnormal) is commonly used], nor does it require that the underlying distributions be Gaussian. Indeed, the AUC parameter (found by the trapezoidal rule) corresponds to the well-known Wilcoxon statistic.

In statistical test theory, the notion of statistical error is an integral part of hypothesis testing. The test requires an unambiguous statement of a null hypothesis, H_0, viz., that there is *no* statistically significant difference between two populations. For example, in a medical application, the null hypothesis is that a particular treatment has no effect. The extent to which the test supports the alternative hypothesis (i.e., that there is a statistically significant difference between the two populations) is called its *significance level*; and the higher the significance level, the less likely it is that there is no (statistically significant) difference between the two populations.

Table 9.3 Relation between truth/falseness of the null hypothesis and outcomes of a test

Decision		
Actual	Fail to reject null hypothesis	Reject null hypothesis
Null hypothesis (H_0) is true	Correct outcome	Type I error
Null hypothesis (H_0) is false	Type II error	Correct outcome

In medical diagnosis (with the null hypothesis of health), a false positive causes unnecessary worry and unnecessary treatment, while a false negative gives the patient the dangerous illusion of good health and no treatment when treatment would be helpful. (In this situation we could adopt a larger loss factor for the false negatives) A false positive in manufacturing quality control (with a null hypothesis of a product being well-made) discards a product, which is actually well-made, while a false negative passes a faulty product as well-made. A false positive (with null hypothesis of no effect) in scientific research suggests an effect, which is not actually there, while a false negative fails to detect an effect that is there.

A type I error is the wrong decision that is made when a test rejects a true null hypothesis (H_0). (It is usually identified as a false positive) The proportion of type I error (FPF) is denoted by α, and usually equals the significance level of a test. [If the null hypothesis is composite, α is the maximum (supremum) of the possible probabilities of a type I error.] Choosing the level of significance is a somewhat arbitrary task, but traditionally we allow a one in 20 chance that we have made a type I error; in other words, we set our criterion for a significant difference between two populations at the 5% level. A type II error is the wrong decision that is made when a test fails to reject a false null hypothesis, i.e., we accept our null hypothesis when, in fact, the two populations *do* differ, and the hypothesis should have been rejected (viz. a false negative). The probability associated with a type II error is denoted by β. Clearly, the smaller our sample size, the more likely is a type II error. It is common to be more tolerant with β—to accept, say, a one in ten chance that we have missed a significant difference between the two populations. Often, statisticians refer to the *power* of a test. The power is simply $(1 - \beta)$, so if β is 10%, then the power is 90%. (The power of a test is also known as its sensitivity) The relationship between truth/falseness of the null hypothesis and the outcomes of a test are shown in Table 9.3. (Note that what we actually call type I or type II error depends directly on the null hypothesis; negation of the null hypothesis causes type I and type II errors to switch roles)

Having obtained a parameter (AUC or A_z) which describes the performance of the test or classifier, it would be useful to estimate its standard error (SE). This estimate depends to some extent on the shapes of the underlying distributions, but is conservative so that even if the distributions are not normal, the estimates of the SE will tend to be a little too large, rather than too small. The standard error of A_z, SE, has been shown to be (Hanley and McNeil 1982)

$$\begin{aligned} \mathrm{SE} = \mathrm{sqrt}(\{\ & (A_z(1 - A_z) + (n_A - 1)(Q_1 - A_z{}^2) \\ & + (n_N - 1)(Q_2 - A_z{}^2)\}\ /\{n_A n_N\}) \end{aligned} \tag{9.1}$$

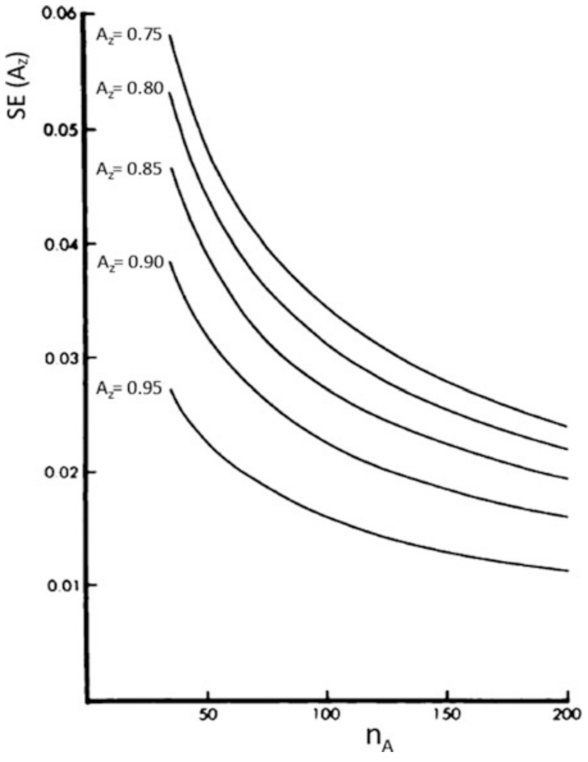

Fig. 9.11 Standard error (SE) for various values of A_Z in relation to sample size (n_A = number of abnormals = n_N) (after Hanley and McNeil 1982)

where n_A and n_N are the number of abnormal and normals (or class 1 and class 2), respectively, and

$$Q_1 = A_z/(2 - A_z) \tag{9.2}$$

$$Q_2 = 2{A_z}^2/(1 + A_z) \tag{9.3}$$

Now that we can calculate the standard error for a particular sample size, given a certain A_z, we can plan sample size for a study! Simply vary sample size until you achieve an appropriately small standard error. Note that, to do this, you *do* need an idea of the area under the ROC curve that is anticipated. Figure 9.11 plots standard error against n_A (assumed equal to n_N) for various values of A_z. As usual, standard errors vary with the square root of the number of samples, and (as you might expect) the numbers required will be smaller with larger values of A_z.

The probability that an observed positive result is a false positive may be calculated using Bayes rule. The key concept of Bayes rule is that the error rates (false positives and false negatives) are not a function of the accuracy of the test alone, but also the actual rate or frequency of occurrence within the test population; and, often, the more powerful issue is the actual rates of the condition within the sample being tested (or the rate in the whole population, i.e., the prior probability of the condition).

9.4 Comparing Classifiers

9.4.1 *ROC Curves*

ROC curves allow us to compare the performance of two different classifiers. Table 9.4 gives the numbers of normal and abnormal subjects required to provide a probability of 80, 90 or 95% of detecting differences between various ROC areas under the curve. For example, if we have one A_z of 0.775 and a second (A'_z) of 0.900, and we want a power of 90%, then we need 104 cases in each group (normals and abnormals). Note that generally, the greater the areas under both curves, the smaller the required *difference* between the areas in order to achieve significance. The tables are however not applicable where two tests are applied to the same set of cases. That requires more complex statistical tests (see Hanley and McNeil 1983).

Note that noise in the data will in general degrade test performance.

9.4.2 *McNemar's Test*

Given a training set and a validation set, we train two classifiers on the training set and test them on the validation set and compute their errors in the form of a contingency table such as Table 9.5.

Under the null hypothesis that the two classifiers have the same error rate, we expect $e_{01} = e_{10}$ and these to be equal to $(e_{01} + e_{10})/2$. We have the chi-squared statistic with one degree of freedom

$$\frac{(|e_{01} - -e_{10}| - 1)^2}{e_{01} + e_{10}} \sim \chi^2 \tag{9.4}$$

and McNemar's test rejects the hypothesis that the classifiers have the same error rate at significance level α if this value is greater than $\chi^2_{\alpha,1}$. For $\alpha = 0.05$, ${\chi_{0.05,1}}^2 = 3.84$.

9.4.3 *Other Statistical Tests*

There is a plethora of statistical tests that can be used to compare classifiers, but we will only mention some of them in passing. In the case of multiple classifiers, *analysis of variance* (ANOVA) can be used (e.g., Alpaydin 2010). This is based on binomial distributions being approximately normal. If we wish to compare two or more classifiers on several datasets, rather than just one, this is no longer applicable and we need to resort to non-parametric tests, such as the *Wilcoxon signed rank test*

Table 9.4 Number of normal and abnormals (or class I and class II) required to provide a probability of 80, 90 or 95% of detecting various differences between the AUCs, A_z and A'_z (using a one-sided test of significance with $p = 0.05$) (Top number = 80% probability; middle number = 90% probability; bottom number = 95% probability)

A'_z										
A_z	0.750	0.775	0.800	0.825	0.850	0.875	0.900	0.925	0.950	0.975
0.700	652	286	158	100	68	49	37	28	22	18
	897	392	216	135	92	66	49	38	29	23
	1,131	493	271	169	115	82	61	46	36	29
0.725		610	267	148	93	63	45	34	26	20
		839	366	201	126	85	61	45	34	27
		1,057	459	252	157	106	75	55	42	33
0.750			565	246	136	85	58	41	31	23
			776	337	185	115	77	55	41	31
			976	423	231	143	96	68	50	38
0.775				516	224	123	77	52	37	27
				707	306	167	104	69	49	36
				889	383	209	129	86	60	44
0.800					463	201	110	68	46	33
					634	273	149	92	61	43
					797	342	185	113	75	53
0.825						408	176	96	59	40
						557	239	129	79	52
						699	298	160	97	64
0.850							350	150	81	50
							477	203	108	66
							597	252	134	81
0.875								290	123	66
								393	165	87
								491	205	107
0.900								960	228	96
								1,314	308	127
								1,648	383	156
0.925									710	165
									966	220
									1,209	272
0.950										457
										615
										765

Table 9.5 Contingency table for McNemar's test

e_{00}: number of examples misclassified by both	e_{01}: number of examples misclassified by 1 but not by 2
e_{10}: number of examples misclassified by 2 but not by 1	e_{11}: number of examples correctly classified by both

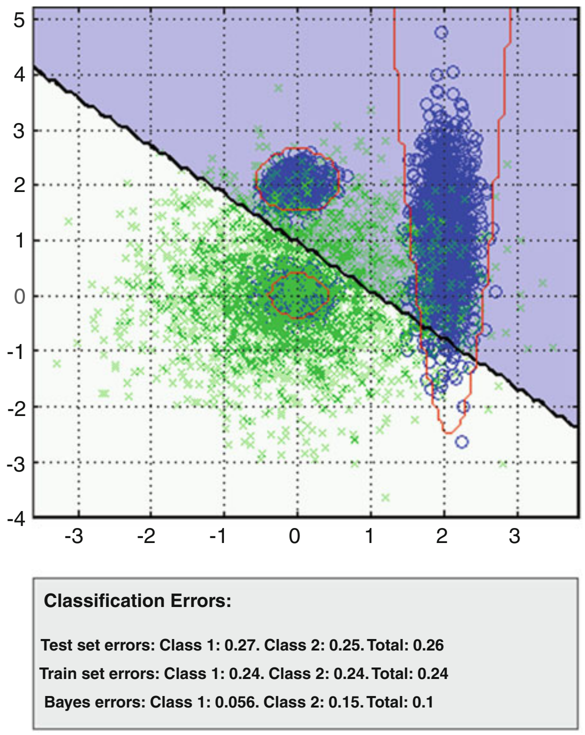

Classification Errors:

Test set errors: Class 1: 0.27. Class 2: 0.25. Total: 0.26

Train set errors: Class 1: 0.24. Class 2: 0.24. Total: 0.24

Bayes errors: Class 1: 0.056. Class 2: 0.15. Total: 0.1

Fig. 9.12 The least-squares (in *black*) and Bayes (in *red*) decision boundaries for a dataset comprising several Gaussian components (The data for class 0 is shown in *green*, for class 1 in *blue*.)

(for two classifiers) or the *Kruskal–Wallis test* and *Tukey's test* (for multiple classifiers). For details of these methods you should consult a text on statistics (e.g., Ross 1987; Daniel 1991).

9.4.4 The Classification Toolbox

The MATLAB classification toolbox (see Preface) is a comprehensive set of algorithms for classification, clustering, feature selection, and reduction. The algorithms are accessible through a simple graphic interface, which allows users to quickly compare classifiers across various datasets. The toolbox has three methods for estimating the error of the trained classifier: Holdout, Cross-Validation, and Resubstitution. If appropriate, the number of redraws specifies how many times a given dataset will be resampled for estimating the error.

Figure 9.12 compares the results of classification using a linear least-squares classifier (based on solving simultaneous linear equations, it minimizes the sum of the squares of the distances from training points to the decision boundary by linear regression, and is implemented by a perceptron) with a Bayes classifier. The underlying components of the dataset are Gaussian. In this example, it is trained on 20% of the data and tested on the remaining 80% using the holdout method.

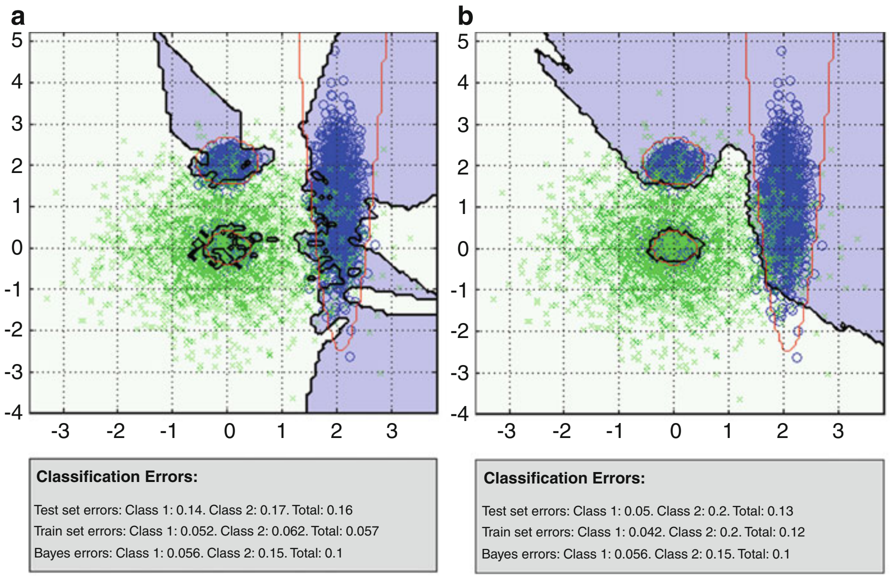

Classification Errors:

Test set errors: Class 1: 0.14. Class 2: 0.17. Total: 0.16
Train set errors: Class 1: 0.052. Class 2: 0.062. Total: 0.057
Bayes errors: Class 1: 0.056. Class 2: 0.15. Total: 0.1

Classification Errors:

Test set errors: Class 1: 0.05. Class 2: 0.2. Total: 0.13
Train set errors: Class 1: 0.042. Class 2: 0.2. Total: 0.12
Bayes errors: Class 1: 0.056. Class 2: 0.15. Total: 0.1

Fig. 9.13 The *k*-NN (in *black*) and Bayes (in *red*) decision boundaries for the same dataset used in Fig. 9.12 (20% training set). (**a**) $k = 1$ (**b**) 25

Clearly the least-squares classifier, which is constrained to producing a linear decision boundary, performs less well on this dataset. Both types of classification errors are shown both for the training set and the test set; they are around 25%. On the other hand, the Bayes' classifier uses non-linear decision boundary, and produces an average misclassification error of 105 with this dataset. The toolbox allows you to conveniently re-run the data, changing parameters such as the sampling method, the number of re-draws and the percentage of data points used for training. The data can also be preprocessed, e.g., using the *whitening transform* to translate and scale the axes so that each feature has zero mean and unit variance.

Figure 9.13 shows the results of using the *k*-NN classifier, for two different values of *k*. The decision boundary will change slightly from run to run as the classifier tries to learn the best way to classify the data, but a trend is clearly visible. Small values of *k* result in a very tortuous boundary, whereas larger values of *k* result in a smoother boundary. Using a small value of *k* results in few errors in the training set, but this will likely not be the case for the test set. Large values of *k* will not classify the training set particularly well, but the performance on the test set is likely to be similar.

The toolbox allows you to compare several classifiers on a particular dataset, using a chosen resampling method (Fig. 9.14).

There is a convenient method for manually entering distributions (specifying the number and relative weights of distributions within a class, their means, and covariances) and generating a sample dataset (of whatever size desired). Figure 9.15 shows an XOR distribution, and the decision boundaries obtained with a 5-NN classifier and a Bayes' classifier.

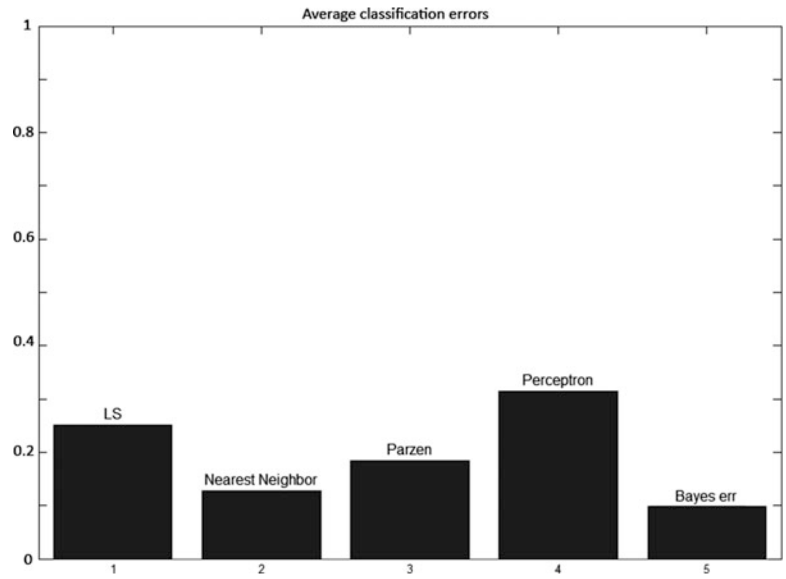

Fig. 9.14 Comparison of several classifiers on the dataset introduced in Fig. 9.12 (Cross-validation was used; and $k = 3$ was used in the k-NN classifier.)

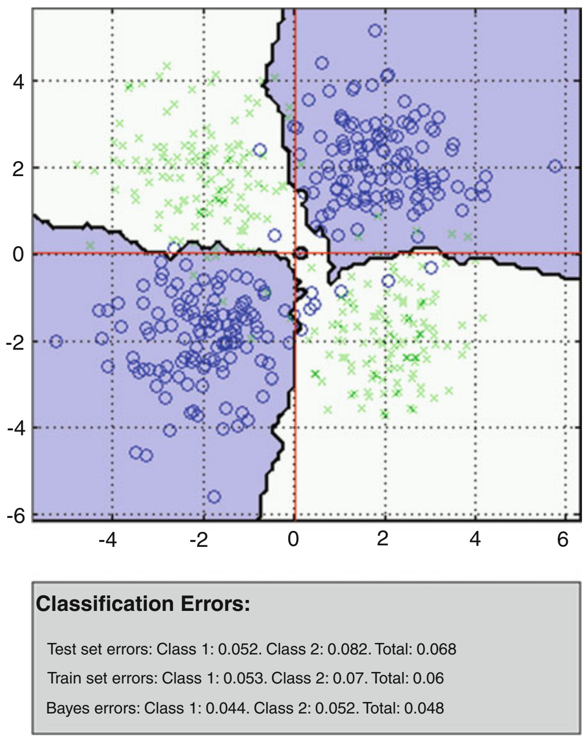

Classification Errors:

Test set errors: Class 1: 0.052. Class 2: 0.082. Total: 0.068

Train set errors: Class 1: 0.053. Class 2: 0.07. Total: 0.06

Bayes errors: Class 1: 0.044. Class 2: 0.052. Total: 0.048

Fig. 9.15 The decision boundaries obtained for an XOR distribution, using 5-NN and Bayes' classifiers

Any dataset can be imported (for example, from Excel or JMP) and used within the classification toolbox. The data must be read into MATLAB as a D-by-N matrix, `patterns`, where d is the number of dimensions of the data and N the number of examples. (If $D > 2$, a feature selection GUI will open and request the user preprocess the data to yield two-dimensional data to be compatible with the display) In addition, a 1-by-N vector, `targets`, is required to hold the category labels, 0 or 1. If the distribution is a mixture of Gaussians, and their parameters are known, these parameters can be stored in a structure, named `distribution_-parameters`, for computation of the Bayes error. (The fields of this structure are the means of the Gaussians in each class, the covariance matrices of the Gaussians, the relative weights of each of the Gaussians, and the prior probability of class 0)

9.5 Combining Classifiers

In any application, we can use a particular classifier, and try to optimize its performance. The No Free Lunch Theorem states that there is no single classifier that in any domain always induces the most accurate learner. The usual approach is to try several different classifiers and choose the one that performs the best on a separate validation set.

Each classifier comes with its own set of assumptions, which will lead to errors if the assumptions do not hold for the data. Learning itself is an ill-posed problem, and with finite data each classifier converges to a different solution. We can fine-tune the classifier to get the best possible accuracy on a validation set, but this is a complex task and there may be some data points which it may never handle well, and could be better handled by a completely different classifier. There is a saying that two heads are better than one, although extrapolation of the concept ends up with decision by committee, which is famously useless for human activities. Nevertheless, with appropriate safeguards, we might consider the idea of using several different classifiers, known as *base classifiers*, on a dataset—each learning in different ways—and combining their outputs in some way. This is known as *combining classifiers* or *ensemble learning*.

Example 9.1

Consider an ensemble of 25 binary classifiers, each of which has an error rate, ε, of 0.35. If they are independent and a majority vote is taken on their predictions, what will be the error rate of the ensemble classifier?

Of course, if the classifiers are identical, each will misclassify the same examples and the error rate of the ensemble will remain at 0.35. However, if they are independent (i.e., their errors are uncorrelated), then the ensemble makes a wrong prediction only if more than half of the base classifiers predict incorrectly. In this case, the error rate of the ensemble classifier will be

$$\varepsilon = \sum_{i=13}^{25} \binom{25}{i} \varepsilon^i (1-\varepsilon)^{25-i} = 0.06 \tag{9.5}$$

which is considerably lower than the error rate of the base classifiers.

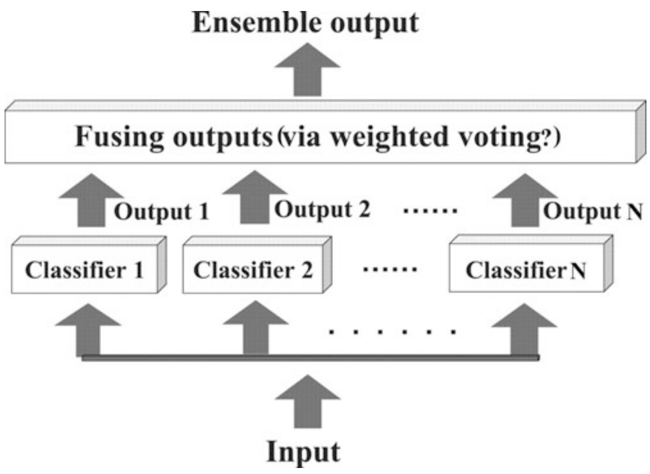

Fig. 9.16 An ensemble classifier, combining the outputs of *N* base classifiers

We want to choose a set of *diverse* classifiers: they should differ in their decisions but complement each other. And, in order to obtain an overall gain in performance, they should each be reasonably accurate, at least in their domain of expertise. [If we have lots of data, we might consider partitioning it and giving different sets of (overlapping or nonoverlapping?) data to different classifiers]. Ensemble methods work better with unstable classifiers, i.e., base classifiers that are sensitive to minor perturbations in the training set. Examples of unstable classifiers include decision trees, rule-based classifiers, and artificial neural networks. By combining or aggregating over a number of different base classifiers, we are likely to reduce variance and therefore error.

The simplest and most intuitive way to combine multiple classifiers is by *voting* (Fig. 9.16), which corresponds to taking a linear combination of the classifier outputs. In the simplest case, all the classifiers are given equal weight, but their outputs could be weighted by, say, the success rate of each base classifier acting alone or by respective posterior probabilities. There are other possibilities. Combining them via a median rule is more robust to outliers; a minimum or maximum rule is pessimistic or optimistic, respectively. Combining them as a product would give each classifier veto power.

Bagging, or *bootstrap aggregating*, is a voting method whereby classifiers are made different by training them over slightly different training sets, generated by the bootstrap method (resampling with replacement). Bagging is a *variance reducing algorithm*, although some might suspect it is just a case of throwing computer resources at a problem!

Whereas in bagging, generating complementary base classifiers is left to chance and to the instability of the classifier itself, in *boosting* we actively try to generate complementary classifiers by training the next classifier on the mistakes of the previous classifiers. The original boosting algorithm (Schapire 1990) combined three weak learners (each performing only just better than chance) to generate a strong learner (with a very small error probability). Given a large training set, it is randomly divided into three. A classifier was trained on the first third, and then tested on the second third. All of the data that was misclassified during that testing was used to form a new dataset, along with an equally sized random selection of the data that was correctly classified. A second classifier was trained on this new dataset, and then both of the classifiers were tested on the final third of the dataset. If they both produced the same output, then that datapoint was ignored, otherwise the datapoint was added to form yet another dataset, which formed the training set for the third classifier. The system reduced the final error rate, but was rather data hungry. Drucker et al. (1994) used a set of 118,000 instances in boosting multilayer perceptrons for optical handwritten digit recognition.

A variant, AdaBoost (adaptive boosting), gives weights to each datapoint according to how difficult previous classifiers have found to get it correct (Freund and Schapire 1996). These weights are given to the classifier as part of the input when it is trained. (They are initially all set to the same value, $1/N$, where N is the number of datapoints in the training set) AdaBoost can combine an arbitrary number of base classifiers, not just three. It uses classifiers that are simple and not particularly accurate, where the next classifier can focus on the incorrect choices. For example, with decision trees, it uses *decision stumps* (trees that are only grown to one or two levels). Clearly these are biased, but the decrease in variance is larger and the overall error decreases. A classifier such as linear discriminant analysis has low variance, and no gain can be achieved with it using AdaBoost.

References

Alpaydin, E.: Introduction to Machine Learning, 2nd edn. MIT, Cambridge, MA (2010). Chapter 19

Daniel, W.W.: Biostatistics: A Foundation for Analysis in the Health Sciences, 5th edn. Wiley, New York (1991)

Drucker, H., Cortes, C., Jackel, L.D., Le Cun, Y., Vapnik, V.: Boosting and other ensemble methods. Neural Comput. **6**, 1289–1301 (1994)

Freund, Y., Schapire, R.E.: Experiments with a new boosting algorithm. In: Saitta, L. (ed) Thirteenth International Conference on Machine Learning, pp. 148–156. Morgan Kaufmann, San Mateo, CA (1996)

Geman, S., Bienenstock, E., Doursat, R.: Neural networks and the bias/variance dilemma. Neural Comput. **4**, 1–58 (1992)

Hanley, J.A., McNeil, B.J.: The meaning and use of the area under a receiver operating characteristic (ROC) curve. Radiology **143**, 29–36 (1982)

Hanley, J.A., McNeil, B.J.: A method of comparing the areas under receiver operating characteristic curves derived from the same cases. Radiology **148**, 839–843 (1983)

James, G.: Variance and bias for general loss functions. Mach. Learn. **51**, 115–135 (2003)

Ross, S.M.: Introduction to Probability and Statistics for Engineers and Scientists. Wiley, New York (1987)

Schapire, R.E.: The strength of weak learnability. Mach. Learn. **5**, 197–227 (1990)

Chapter 10
Projects

10.1 Retinal Tortuosity as an Indicator of Disease

Retinal blood vessels can be viewed directly and noninvasively, offering a unique and accessible window to study the health of the human vasculature in vivo. Their appearance, as seen in retinal fundus images, is an important diagnostic indicator for much systemic pathology, including diabetes mellitus, hypertension and atherosclerosis (Fig. 10.1). Specifically, the blood vessels become dilated and tortuous in a number of disease conditions including high blood flow, angiogenesis, and blood vessel congestion. Tortuosity (i.e., integrated curvature) is a feature that may well be used to classify different retinal pathologies.

There are many different ways to define tortuosity, but useful metrics should be additive and scale invariant and largely independent of image noise and the resolution of the imaging system. One of these metrics, the mean tortuosity (M), is equivalent to the accumulating angle change along the length of a vessel considered to comprise straight-line segments between closely digitized points along its mid-line. There is an issue regarding the closeness of these digitized points. With small sampling intervals there are large digitization errors, which results in an artificially elevated tortuosity. Conversely, large sampling intervals miss high-frequency changes and underestimate the tortuosity of highly tortuous vessels. A compromise distance has to be struck to minimize digitization errors and accurately trace the vessels. An alternative metric is the normalized root-mean-square curvature (*K*) of the blood vessel (Johnson and Dougherty 2007). This incorporates approximate polynomial spline-fitting to "data balls" centered along the mid-line axis of the vessel, and avoids the arbitrary filtering of mid-line data needed with other methods to minimize digitization errors. Since tortuosity is additive, it is clear that it is the tortuosity per unit length, rather than tortuosity itself, that is the actual metric of interest.

Retinal images can be obtained from university departments of ophthalmology or from publicly available databases. The STARE (http://www.ces.clemson.edu/ahoover/stare) and DRIVE (http://www.isi.uu.nl/Research/Databases/DRIVE/)

DOI 10.1007/978-1-4614-5323-9_10, © Springer Science+Business Media New York 2013

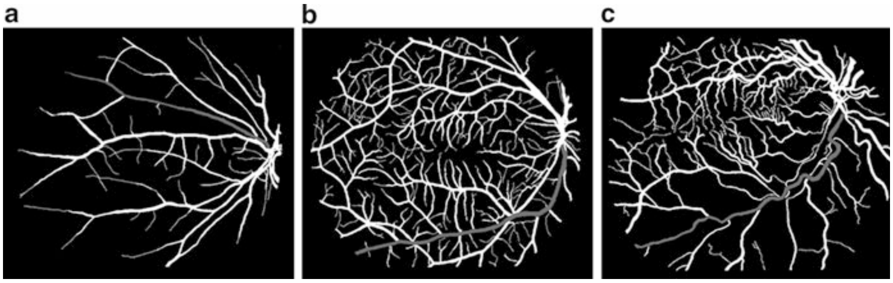

Fig. 10.1 Binarized retinal images: diagnosed as showing (**a**) vasculitis, (**b**) normal, and (**c**) retinitis pigmentosa. A typical vessel in each is shown in *gray*

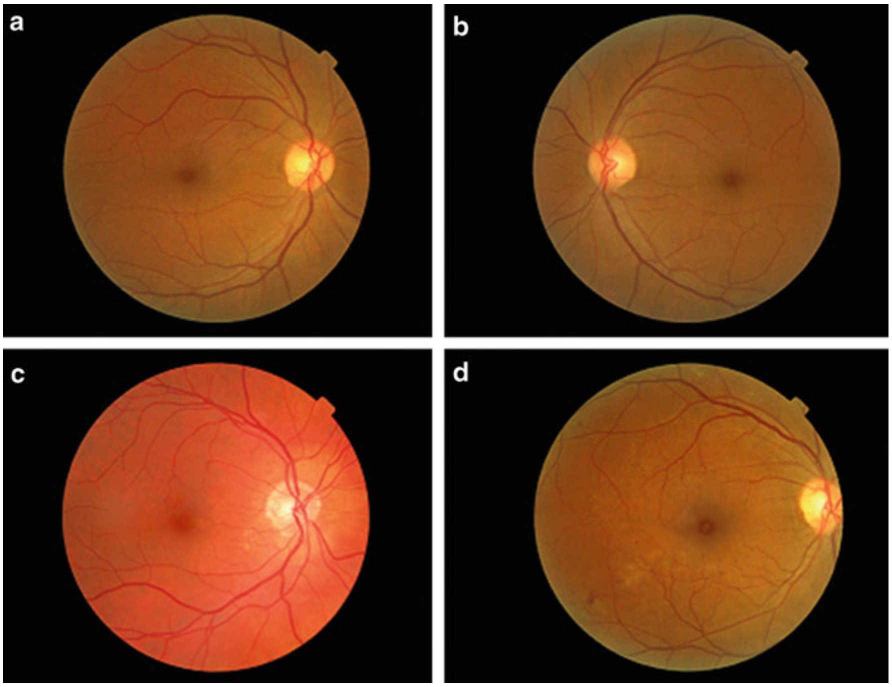

Fig. 10.2 Example images from the Messidor database showing various severities of diabetic retinopathy (**a**) grade 0, (**b**) grade 1, (**c**) grade 2, and (**d**) grade 3

databases of retinal images have been widely used to compare various vessel segmentation algorithms. The Messidor project database (Niemeijer et al. 2004) is the largest database of retinal images currently available on the internet. It was established to facilitate studies on computer-assisted diagnoses of diabetic retinopathy; each of the 1,200 images includes diagnoses by expert ophthalmologists (Fig. 10.2).

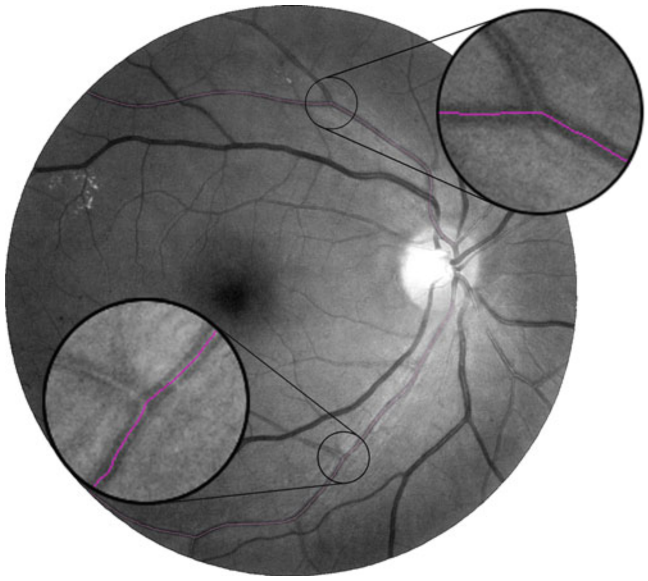

Fig. 10.3 Tracing of blood vessels using NeuronJ. The *magnified area* shows the choice of tracing (viz. the larger branch) at bifurcations

A common approach has been to segment retinal images, and skeletonize the resulting blood vessels to extract their centerlines prior to measuring the tortuosity. However, segmentation is a challenging process fraught with difficulties. It generally requires preprocessing to minimize noise and other artifacts, adaptive thresholding, and postprocessing for subsequent linking of broken vessels. Skeletonization is very sensitive to noise, and generally requires various filling and pruning strategies to rectify spurious gaps, branches, and crossings. An alternative approach, which circumvents the problems inherent in segmentation and skeletonization, is to obtain the centerlines directly from the gray-scale images by applying a Hessian (Fan et al. 2009) or Jacobian (Yuan et al. 2009)-based analysis of critical points, using matched or steerable filters (Sofka and Stewart 2006) or by nonmaximum suppression (Sun and Vallotton 2009). The Hessian is a generalization of the Laplacian operator; it is a square matrix comprising second-order partial derivatives of the image, and can therefore be used to locate the center of a ridge-like structure. Specifically, the local principal ridge directions at any point in an image are given by the eigenvectors of the second-derivative matrix computed from the intensity values around that point.

NeuronJ is a semi-automated tracing method which uses the Hessian to identify and trace vessels with minimal user intervention directly from a grayscale image (or the green plane of an RGB color image). It has been used successfully to trace the arterioles from retinal images (Fig. 10.3), producing digitized coordinates of the vessel centerlines that can be conveniently exported to an Excel file for the computation of mean tortuosity (Iorga and Dougherty 2011).

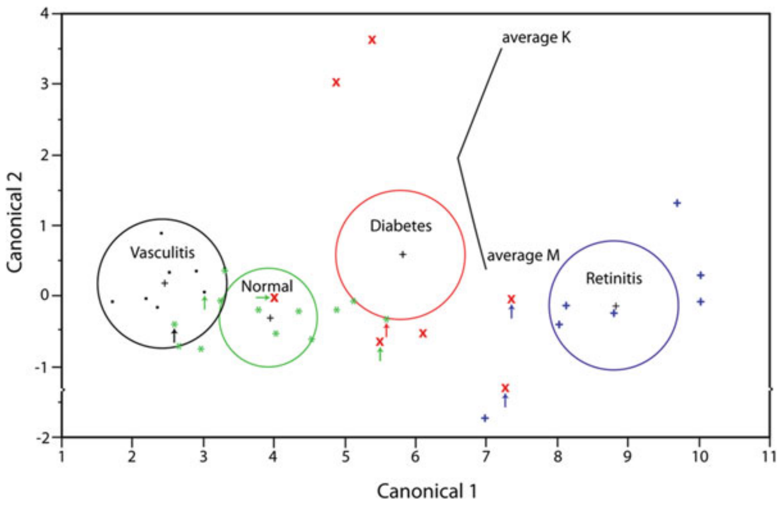

Fig. 10.4 Canonical plot. Data from the ground truth conditions are indicated by separate symbols (*black small square*, vasculitis; *asterisk*, normal; *multiplication sign*, diabetes; *plus*, retinitis), each indicating the mean of 10 measurements. The *directions of the features*, *M* and *K*, are shown in the canonical space by the labeled rays. The size of each *circle* corresponds to a 95% confidence limit for the mean (marked with *plus*) of that group. The *small arrows* indicate misclassified data points

Table 10.1 Contingency table using both *M* and *K* together, with the prevalences of the diseased conditions in the general population and in the samples (in parentheses)

Diagnosis					
		Diabetic retinopathy	Normal	Retinitis pigmentosa	Vasculitis
Actual condition	Diabetic retinopathy	20 (30)	50 (20)	0 (20)	0 (0)
	Normal	0 (10)	120 (100)	0 (0)	0 (10)
	Retinitis pigmentosa	20 (0)	10 (0)	40 (70)	0 (0)
	Vasculitis	0 (0)	70 (10)	0 (0)	0 (60)

In a preliminary study (Dougherty et al. 2010), using 120 images of normal retinal vessels and 70 images each of three retinopathies (diabetic retinopathy, retinitis pigmentosa, and retinal vasculitis), discriminant analysis was used to produce a canonical plot (Fig. 10.4) showing the linear combinations of the tortuosity features (*M* and *K*) in the two dimensions that best separate the groups. The conditions are fairly well separated, although the vessels showing diabetic retinopathy are often misclassified.

Classification depends on the prevalences of the conditions in the general population (the pretest probabilities). Taking these into account results in a contingency table (Table 10.1), in which the diagonal elements show correct diagnoses and the off-diagonal elements show mis-diagnoses. A total of 150 of the 330 images (45%) are misclassified. However, if we consider the images as a referred population with probabilities proportional to their occurrence, then the total number of misclassified images drops to 70 (i.e., 21%). Clearly tortuosity is a valuable feature in distinguishing these conditions. However, these high misclassification rates preclude the use of tortuosity for classifying all of these conditions *simultaneously*, even in a referred population. Other features need to be identified and measured to increase the accuracy of classification. A count of microaneurysms has been shown to be useful in identifying diabetic retinopathy (Iorga and Dougherty 2011). Further work needs to be done to identify other informative features, based on vessel morphology; and larger datasets should be explored.

An as yet unexplored application of retinal vasculature is biometric identification.

10.2 Segmentation by Texture

Texture is an intuitively obvious phenomenon, but it is very difficult to define precisely. It represents a variety in fine detail, and is distinct from pattern which measures regularity. Roughness or smoothness is an important component of texture, and is related to the decay of the Fourier transform (Dougherty and Henebry 2001). The radial Fourier power spectrum of rough (2D) images tend to decay as $1/\omega^2$, showing a gradient of -2 on a log–log plot; while smooth (2D) images decay as $1/\omega^4$ with a gradient of -4. By invoking fractional Brownian motion, we can use fractals as a model for texture. It can be shown that the fractal dimension, D, of an image (with Euclidean dimension $= 2$) is given by

$$D = 4 - \beta \tag{10.1}$$

where β is the magnitude of the slope of the radial power spectrum. This constrains D, averaged over all directions, to be between 2 (smooth) and 3 (rough) and up to 4 (for white noise).

So, while there is a multiplicity of possible definitions of texture (including statistical moments, edgeness, entropy, and terms related to the correlation and co-occurrence matrices), the use of fractal dimension as a compact descriptor and its estimation using the Fourier power spectrum has been widely used. Exact fractals have attractive properties, such as invariance to scale and projection. However, for real structures, fractality is present only in a statistical sense and only over a limited range of scales; hence the notion of a fractal signature.

There are a number of texture databases which can be used as a training set to investigate classification. Brodatz textures are a well-known benchmark for evaluating texture recognition algorithms, and digitized images of them, 512×512 and histogram-equalized, can be conveniently downloaded (http://sipi.usc.edu/database/database.php?volume=textures). A two-dimensional Fourier power spectrum (of intensity against spatial frequencies, u and v) can be conveniently obtained from most image analysis programs (e.g., ImageJ, MatLab). The spectrum can be radially averaged (Fig. 10.5a) for an image (Fig. 10.5b) to provide the radial

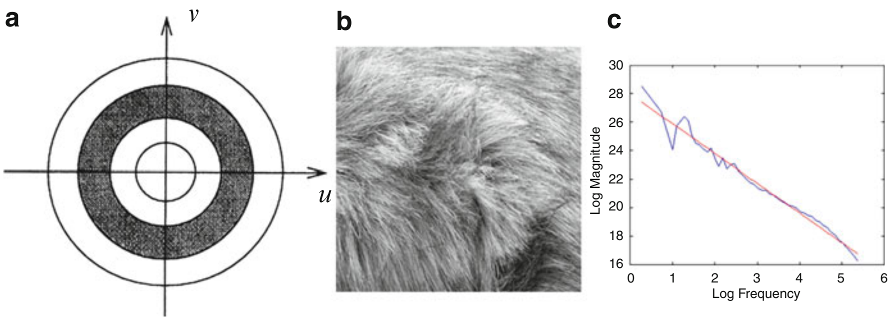

Fig. 10.5 (**a**) Radial averaging the spectrum involves averaging the spectrum over annuli corresponding to different frequencies, (**b**) an image of fur, and (**c**) its radial power spectrum plot (log–log)

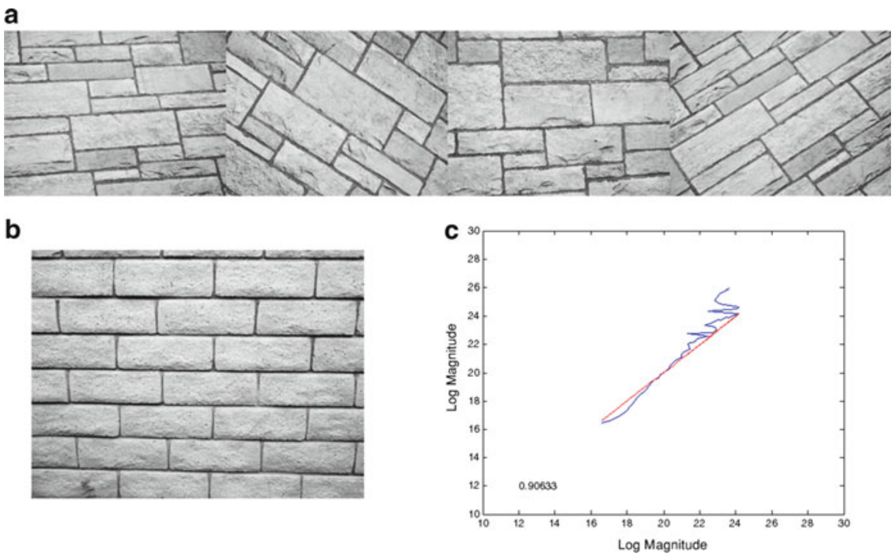

Fig. 10.6 (**a**) Four examples of wall images, (**b**) a test wall image, and (**c**) a log–log plot of the radial power magnitudes for image (**b**) against the average for the four images in (**a**)

power spectrum (Fig. 10.5c) which can then be fitted to a straight line to give an average fractal dimension for the image.

Different images of the same texture produce slightly different radial power spectra, but an average can be taken as the fractal signature. It should then be possible to classify an unknown texture by comparing its signature with the average signatures of a number of standard signatures, rather than attempting to extract a single fractal dimension from each plot. One way of doing this would be to plot the test signature against the standard signatures (over the whole range of spatial frequencies), and use the goodness-of-fit as a parameter to choose the best classification. Figure 10.6 shows this for a test image and four images of walls: the resulting

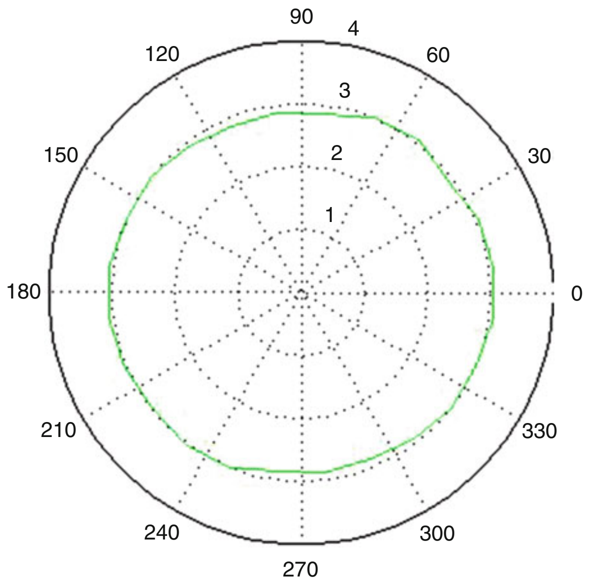

Fig. 10.7 Polar plot of the fractal dimension of the wall image of Fig. 10.6b

goodness-of-fit for the test image is 0.9063, indicating that it is probably an image of a wall too with the characteristic texture of a wall.

The radial power spectrum averages out any angular anisotropy of the Fourier power spectrum. It is possible to retain the angular information, and display a polar plot of the fractal dimension as a function of angle (Fig. 10.7). (A MatLab m-file. fracdim.m, to do this is available for downloading from the book Web site.) With some thought a compact feature (e.g., the circularity of the polar plot) to capture the angular anisotropy could be proposed, and added to the goodness-of-fit feature to improve classification.

In order to apply these methods to segmenting images, it would be important to determine the smallest region of interest (RoI) within an image that captures the essential features of the radial power spectrum. Overlapping windows of this size could then be used to compute local fractal dimensions throughout the image, and their values used to draw boundaries based on texture.

10.3 Biometric Systems

Biometric systems are used to recognize and/or identify a person using some specific physiological or behavioral characteristics. Depending on the application context, they can either be used for verification (a one-to-one comparison to authenticate a person by comparing the captured characteristic feature with his/her own template) or matching (a one-to-many comparison to establish the identity of an individual by searching a database for the best match).

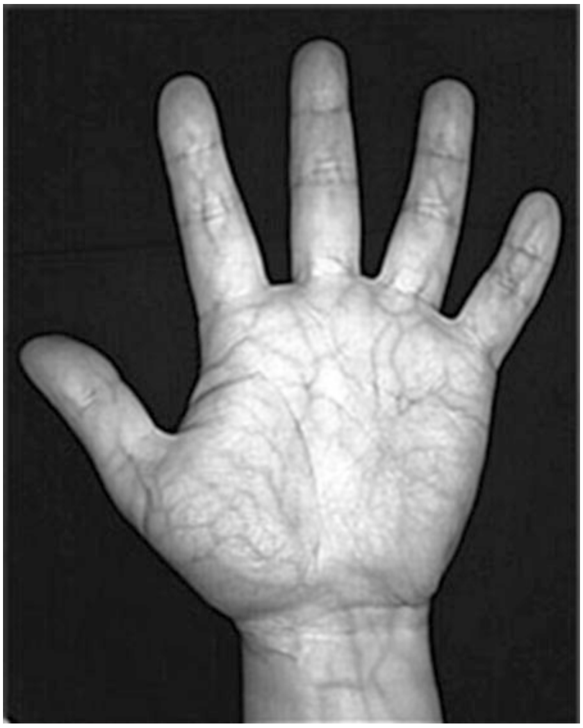
Fig. 10.8 An infrared scan of a hand

Table 10.2 A comparison of biometric systems

	Fingerprint	Face	Iris	Voice	Vein
Easy to use	•	•		•	•
Cheap	•	•		•	•
Accurate	•		•		•
Secure			•		•

A number of biometric technologies have been developed and are in use in a variety of applications. Among these, fingerprints, face, iris, speech, gait, and hand and finger geometry are the most commonly used. Recently hand and finger vein scans (Fig. 10.8), using infrared sensors, have been employed to authenticate ATM (automated teller machine) customers. Table 10.2 compares some of the technologies in terms of cost, accuracy, and security.

10.3.1 Fingerprint Recognition

Fingerprints are the oldest and most widely used form of biometric identification. However, fingerprints are rarely of perfect quality as they are often corrupted due to variations in skin and impression conditions. Consequently, fingerprint recognition

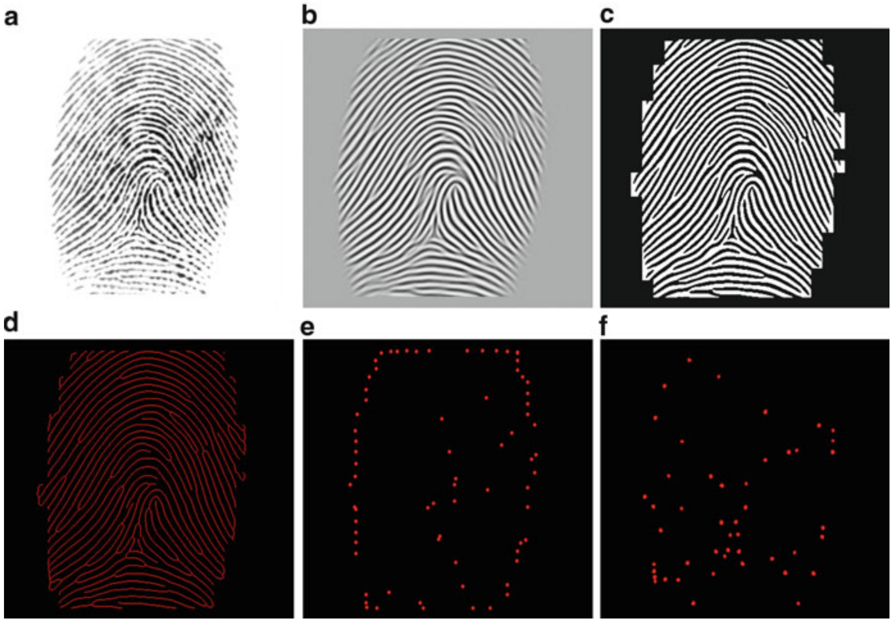

Fig. 10.9 (**a**) Original fingerprint image, (**b**) normalized image, (**c**) segmented (binarized) image, (**d**) skeletonized image, (**e**) end points (before deletion of spurious points), (**f**) branch points (before deletion of spurious points)

remains a challenging problem and image enhancement techniques used for reliable extraction of features from fingerprint images are a critical step in fingerprint matching. FVC-onGoing (https://biolab.csr.unibo.it/FVCOnGoing) provides extensive fingerprint databases as benchmarks to unambiguously compare the performance of different algorithms.

A fingerprint is the pattern of ridges and valleys on each finger tip (Fig. 10.9a). Minutiae points are the local ridge characteristics that occur either at a ridge ending (the point where the ridge ends abruptly) or a ridge bifurcation (the point where the ridge splits into two or more branches). The distinctiveness of a fingerprint is based on the unique spatial relationships between the two types of minutiae. Unfortunately, degraded fingerprint images can result in a significant number of spurious minutiae being created and genuine minutiae being ignored. A critical step in studying the statistics of fingerprint minutiae is to reliably extract minutiae from fingerprint images. Image enhancement techniques need to be employed prior to minutiae extraction to obtain a more reliable estimate of minutiae locations.

Typical preprocessing involves subtraction of any nonuniform background and contrast enhancement, possibly by histogram equalization, and produces a normalized fingerprint (Fig. 10.9b). This is followed by extraction of the minutiae: segmentation (Fig. 10.9c, e.g., by adaptive thresholding), skeletonization (Fig. 10.9d, to show ridges one pixel wide), and then selection of end point minutiae

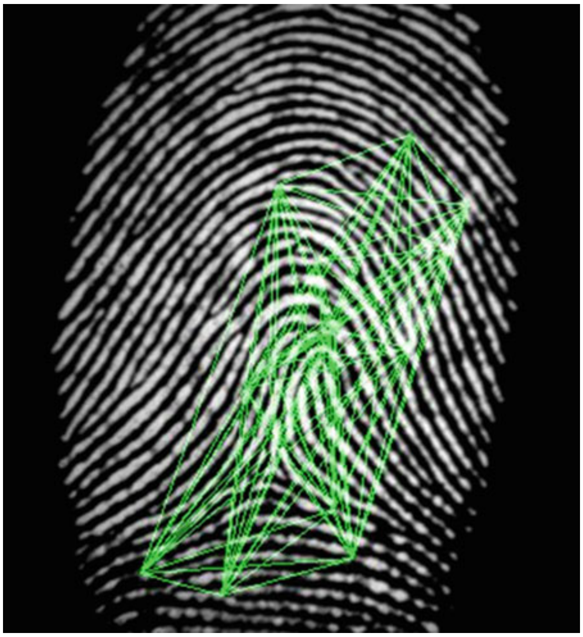

Fig. 10.10 *Triangles* formed from branch points (after elimination of spurious points)

[with only one neighbor (Fig. 10.9e)] and bifurcation minutiae [with three neighbors (Fig. 10.9f)]. False minutiae at the edges of the fingerprint are deleted using a mask created during segmentation. Many spurious end point minutiae resulting from ridge breaks due to degraded images can also be deleted by checking the distance between these minutiae. This results in two sets of minutiae, one comprising the end points and the other the bifurcations or branch points, with each minutia characterized by its coordinates (x, y). (The minutia angle, θ, the angle that the ridge makes at each position could also be considered.) The problem is then one of *point pattern matching*, which can be approached in a number of ways including relaxation methods, algebraic and operational research solutions, tree-pruning approaches, energy-minimization methods and the Hough transform (Maltoni et al. 2003).

An alternative approach is to form two sets of triangles from the two sets of minutiae, and then to compare the angles of the triangles in the test image (Fig. 10.10) with the angles of the triangles in the standard image(s). This eliminates the need for scaling and aligning the images, which saves a considerable computational cost. It does increase the size of the feature database. For N minutia [each characterized by (x, y)], we now have $\binom{N}{3}$ triangles, each characterized by three angles; triangles with very small sides should be eliminated. This may still correspond to a computational saving, depending on the search algorithm employed for comparing the data. The comparison of the angles can be organized to deliver a score indicating the goodness of a match between images.

10.3.2 Face Recognition

The face is the primary focus in everyday social interactions and plays a significant role in conveying identity and emotion. Our brain's ability to recognize faces is incredible; we are able to recognize and identify thousands of faces seen throughout our lifetime. Automated face recognition systems try to emulate the neurological thought processes of the human visual system, but developing such a system is a daunting task because our faces are extremely complex, multidimensional visual stimuli. It is very challenging to develop face recognition techniques that can tolerate the effects of aging, facial expressions, and variations in lighting and pose. However, once developed, they have numerous applications, for example in security systems, criminal identification, and human–computer interaction.

There are a number of models that have been used; some models measure the characteristics of informative landmarks from images of the face, using for example elastic bunch graphs (Campadelli and Lanzarotti 2005) or Gabor wavelets (Gokberk et al. 2005), while others, such as the *Eigenfaces* and *Fisherfaces* approaches, consider the salient features as combinations of a basis set of standardized faces derived from the statistical analysis of many pictures of faces. There are many databases available (http://www.face-rec.org/databases/) to benchmark algorithms. The Eigenfaces model is based on linearly projecting a high-dimensional image space to a low-dimensional feature space (face space), using Principle Component Analysis (PCA). The principle components are calculated from the covariance matrix of the probability distribution of the high-dimensional vector space of possible faces of common resolution, with the eyes and mouth approximately aligned across all the images, from an initial training set. These principle components, also known as eigenfaces, are the eigenvectors of the covariance matrix and they represent the basis features of all the faces. The principle components represent the projection directions that maximize the total spread or scatter of all the features in the images, regardless of class (identity). This differs from the Fisherfaces method which uses discriminant analysis to project the initial high-dimensional image space into the (canonical) directions that best separate the classes, by maximizing the ratio of between-class scatter to that of within-class scatter. Since face recognition is essentially a classification task, Fisherfaces is preferred method although the Eigenfaces method has been widely used (Belhumeur et al. 1997).

References

Belhumeur, P.N., Hespanha, J.P., Kriegman, D.J.: Eigenfaces vs. Fisherfaces: recognition using class specific linear projection. IEEE Trans. Pattern Anal. Mach. Intell. **19**, 711–720 (1997)

Campadelli, P., Lanzarotti, R.: A face recognition system based on local feature characterization. In: Tistarelli, M., Bigun, J., Grosso, E. (eds.) Advanced Studies in Biometrics. Springer, Berlin (2005)

Dougherty, G., Henebry, G.M.: Fractal signature and lacunarity in the measurement of the texture of trabecular bone in CT images. Med. Biol. Eng. Comput. **23**, 369–380 (2001)

Dougherty, G., Johnson, M.J., Wiers, M.D.: Measurement of retinal vascular tortuosity and its application to retinal pathologies. Med. Biol. Eng. Comput. **48**, 87–95 (2010)

Fan, J., Zhou, X., Dy, J.G., et al.: An automated pipeline for dendrite spine detection and tracking of 3D optical microscopy neuron images of in vivo mouse models. Neuroinformatics **7**, 113–130 (2009)

Gokberk, B., Irfanoglu, M.O., Akarun, L., Alpaydin, E.: Selection of location, frequency, and orientation parameters of 2D Gabor wavelets for face recognition. In: Tistarelli, M., Bigun, J., Grosso, E. (eds.) Advanced Studies in Biometrics. Springer, Berlin (2005)

Iorga, M., Dougherty, G.: Tortuosity as an indicator of the severity of diabetic retinopathy. In: Dougherty, G. (ed.) Medical Image Processing: Techniques and Applications. Springer, Berlin (2011)

Johnson, M.J., Dougherty, G.: Robust measures of three-dimensional vascular tortuosity based on the minimum curvature of approximating polynomial spline fits to the vessel mid-line. Med. Eng. Phys. **29**, 677–690 (2007)

Maltoni, D., Maio, D., Jain, A.K., Prabhakar, S.: Handbook of Fingerprint Recognition, p. 145. Springer, New York (2003)

Niemeijer, M., Staal, J.S., van Ginneken, B., et al.: Comparative study of retinal vessel segmentation on a new publicly available database. Proceedings of the SPIE 5370-5379 (2004)

Sofka, M., Stewart, C.V.: Retinal vessel centerline extraction using multiscale matched filters, confidence and edge measures. IEEE Trans. Med. Imaging **25**, 1531–1546 (2006)

Sun, C., Vallotton, P.: Fast linear feature detection using multiple directional non-maximum suppression. J. Microsc. **234**, 147–157 (2009)

Yuan, X., Trachtenberg, J.T., Potter, S.M., et al.: MDL constrained 3-D grayscale skeletonization algorithm for automated extraction of dendrites and spines from fluorescence confocal images. Neuroinformatics **7**, 213–232 (2009)

Index